



The
University
Of
Sheffield.

Investigating the Role of Tenascin-C and Extracellular Vesicles in Human Rhinovirus Induced Exacerbations of Asthma

By:

Jake Thomas Mills

A thesis submitted in partial fulfilment of the requirements for the
degree of
Doctor of Philosophy

The University of Sheffield
Faculty of Medicine, Dentistry and Health
Department of Infection, Immunity and Cardiovascular Disease

30th September 2018

Abstract

Introduction, Aims and Hypothesis: Viral infections are the cause of 75% of all asthma exacerbations, with human rhinovirus (RV) the most common trigger, but what happens during this process is not well understood. Tenascin-C (TN-C) is a large extracellular matrix protein that is present in small quantities in the airway of healthy individuals, but in high quantities in asthma sufferers. TN-C has been demonstrated to drive inflammation in diseases such as rheumatoid arthritis, but the inflammatory potential of TN-C in asthma has yet to be investigated. Furthermore, a subset of extracellular vesicles (EVs), known as exosomes, that are 50-120 nm in size, can contain TN-C and play role in airway inflammation. This study aimed to characterise the relationship between RV infection of airway epithelial cells (AECs) and TN-C expression and exosome release. It was hypothesised that RV infection of AECs promoted the release of TN-C and exosomes, leading to increased inflammatory cytokine and chemokine release in the airway and potentially contributing towards virally-induced exacerbations of asthma.

Methods: WT mice were treated with the viral mimic poly(I:C) and bronchoalveolar lavage fluid analysed for TN-C by western blotting. AECs from asthmatic and non-asthmatic donors were also stimulated with poly(I:C) or infected with RV and assayed for TN-C expression and release by qPCR and western blotting. Exosomes were then isolated by differential ultracentrifugation and analysed for TN-C expression by western blot. Finally, recombinant purified TN-C, and exosomes isolated with and without TN-C siRNA pre-treatment, were used to stimulate AECs and monocyte derived macrophages (MDMs). Cytokine and chemokine release was then measured by enzyme-linked immunosorbent assay (ELISA).

Results: It was determined that TN-C mRNA expression and cell-associated TN-C expression could be modulated in response to RV infection, ultimately leading to the significant release of TN-C from the cell. This pathway was demonstrated to be TLR3-dependent and independent of TLR7 and cell cytotoxicity. TN-C release following RV infection was more pronounced in asthmatics, potentially revealing why TN-C is expressed in higher quantities in the asthmatic airway. The study also revealed that viral TLR3-dependent stimulation induced significant exosomal release and TN-C was associated with these exosomes, with expression correlating with exosome number. RV-dependent TN-C release induced large inflammatory CXCL8 release from MDMs and moderate CXCL8 release from AECs. Also of note, exosomes from RV-infected AECs promoted significant inflammatory and anti-viral cytokine / chemokine release from AECs, whilst exosomes from non-virally cells did not, and both types of exosomes induced cytokine release from MDMs. The role of TN-C in RV-induced exosomal inflammation, however, is yet to be elucidated.

Conclusion: The results in this study reveal a pathway by which RV infection promotes the release of TN-C and exosomes that have the ability to induce inflammatory cytokine release in the airway. Further investigation is required to determine if TN-C or exosomes are viable therapeutic targets to modulate RV-induced asthma exacerbations in the future.

Contents

Abstract.....	ii
List of Abbreviations.....	i
List of Figures.....	viii
List of Tables.....	xi
Acknowledgements.....	xii
Chapter 1: Introduction.....	1
1.1. Asthma.....	1
1.1.1. Asthma Epidemiology.....	1
1.1.2. Asthma Pathophysiology.....	1
1.1.2.1. Characterisation and Phenotypes.....	1
1.1.2.2. Cytokines and Chemokines.....	2
1.1.2.3. Remodelling.....	4
1.1.3. Asthma Exacerbations.....	6
1.2. Human Rhinovirus.....	8
1.2.1. RV Structure and Serotypes.....	8
1.2.2. RV Epidemiology.....	8
1.2.3. RV and Asthma Exacerbations.....	9
1.2.4. RV Lifecycle and Signalling.....	10
1.2.4.1. Pattern Recognition Receptors (PRR) and RV TLR Activation.....	10
1.2.4.2. RV Signalling.....	13
1.2.4.3. Consequences of Pathway Activation in RV Infection.....	16
1.3. Tenascin-C.....	17
1.3.1. The Tenascin Family of Proteins.....	17
1.3.2. TN-C Structure and Function.....	18
1.3.2.1. TN-C Function.....	18
1.3.2.2. The Domains of TN-C.....	19
1.3.2.3. Alternative Splicing and Glycosylation.....	22
1.3.3. Pathways of Tenascin-C Upregulation.....	23
1.3.4. The Role of Tenascin-C in Disease and Chronic Inflammation.....	24
1.3.5. Tenascin-C and Viral Infections.....	26
1.3.6. Tenascin-C and Asthma Pathogenesis.....	26
1.4. The Role of Extracellular Vesicles (EV) in Asthma.....	29
1.4.1. EV Formation, Structure and Function.....	29

1.4.2. EV Isolation and Characterisation.....	31
1.4.3. The Roles of EVs in Enterovirus Infection.....	34
1.4.4. The Roles of EVs in Asthma and Airway Inflammation.....	34
1.5. Project Aims	36
Chapter 2: Materials and Methods	38
2.1. Materials.....	38
2.2. Cell Maintenance	49
2.2.1. BEAS-2B Cell Line Culture.....	49
2.2.2. PBEC Culture.....	50
2.2.3. HeLa-Ohio Cell Line Culture.....	50
2.2.4. HEK-293:pCEP-huTNC-his Cell Culture.....	50
2.2.5. Human Dermal Fibroblast Cell Culture.....	52
2.2.6. MDMs Cell Culture.....	52
2.3. Viral Culture	52
2.3.1. Viral Propagation.....	52
2.3.2. Viral Titration and Quantification.....	52
2.4. Stimulation and Infection of AECs	53
2.4.1. Stimulation of AECs.....	53
2.4.1.1. Polyinosinic:Polycytidylic Acid (Poly(I:C)) Stimulation	53
2.4.1.2. TNF α Stimulation	53
2.4.1.3. Gardiquimod Stimulation	53
2.4.1.4. Staurosporine Stimulation	54
2.4.1.5. LPS Stimulation.....	54
2.4.2. RV Infection of AECs.....	54
2.5. Harvesting Supernatant, mRNA and Protein	55
2.6. Obtaining External Asthmatic Samples and Mouse BALF	55
2.6.1. External Asthmatic Samples.....	55
2.6.2. Mouse BALF Samples and Neutrophil Counts.....	55
2.7. RT-qPCR.....	56
2.7.1. mRNA Extraction.....	56
2.7.2. Quantification of mRNA.....	56
2.7.3. cDNA Synthesis.....	56
2.7.4. Standard Creation for TaqMan and SYBR Green qPCR.....	57
2.7.5. TaqMan Sample Creation and Plate Loading.....	58
2.7.6. SYBR Sample Creation and Plate Loading.....	58
2.8. Western Blot	59

2.8.1. Making Gels.....	59
2.8.2. Processing and Loading Samples.....	59
2.8.3. Transfer of Protein.....	60
2.8.4. Addition of Antibodies.....	60
2.8.5. Imaging Blot.....	60
2.8.6. Calculating Protein Densitometry.....	60
2.9. Immunofluorescence Microscopy	61
2.9.1. Immunofluorescence Staining.....	61
2.9.2. Imaging by Immunofluorescence Microscopy.....	61
2.10. ELISA	62
2.10.1. Cytokine / Chemokine ELISA.....	62
2.10.2. N-Terminal TN-C ELISA.....	62
2.10.3. FNIII-B TN-C ELISA.....	63
2.11. Isolation of EVs from AECs.....	63
2.11.1. Removal of EVs from AEC Media.....	63
2.11.2. Stimulation or Infection of AECs.....	63
2.11.3. Isolation of EVs from AECs by Ultracentrifugation.....	63
2.11.5. Characterisation of EVs Following Isolation by NTA.....	65
2.11.6. Stimulation of AECs and MDMs with AEC Isolated Exosomes	65
2.12. Quantification of Protein by BCA	65
2.13. Quantification of Cell Viability	65
2.13.1. MTT Assay.....	66
2.13.2. Microscopy.....	66
2.14. TN-C Purification.....	66
2.14.1. Collection of HEK-293:pCEP-huTNC-his Cell TN-C Production.....	66
2.14.2. Treating the Conditioned Medium, FN Removal and Bead Incubation	66
2.14.3. Elution and Detection of TN-C.....	66
2.14.4. Quantification and Characterisation of TN-C.....	67
2.14.4.1. Quantification of TN-C by BCA and BSA Standard Curve	67
2.14.4.2. Circular Dichroism Spectra (CDS) Test	67
2.14.4.3. LAL Test	67
2.14.5. TN-C-FBG Purification.....	67
2.14.6. Purified Recombinant TN-C and FBG Stimulation of AECs.....	68
2.14.6.1. Purified Recombinant TN-C and FBG Stimulation of BEAS-2B Cells.....	68
2.14.6.2. Purified Recombinant TN-C and FBG Stimulation of MDMs	68

2.15. TN-C siRNA Treatment of AECs	68
2.16. Trichloroacetic Acid (TCA) Precipitation	68
2.17. Statistics	69
Chapter 3 – Results: The Relationship Between RV Infection and Tenascin-C Expression in AECs.....	70
3.1. Introduction	70
3.2. Hypothesis and Aims	71
3.3. Intranasal Poly(I:C) Administration of Mice Induces TN-C Expression in the BALF.....	72
3.4. Poly(I:C) Stimulation of BEAS-2B Cells Induces TN-C mRNA and Cell Associated Expression and Poly(I:C) Stimulation and RV-1B Infection Induces TN-C Release.	74
3.4.1. Poly(I:C) Stimulation of BEAS-2B Cells Induces TN-C mRNA Expression.....	74
3.4.2. Poly(I:C) Stimulation of BEAS-2B Cells Induces Cell-Associated TN-C Protein Expression.....	76
3.4.2.1. Poly(I:C) Stimulation of BEAS-2B Cells Induces Cell-Associated TN- C Protein as Measured by Western Blot	76
3.4.2.2. Poly(I:C) Stimulation of BEAS-2B Cells Induces Cell-Associated TN- C Protein as Visualised by Immunofluorescence	78
3.4.2.3. Poly(I:C) Stimulation of BEAS-2B Cells Induces Diffuse Cell- Associated TN-C Protein as Visualised by Confocal Imaging	78
3.4.3. Poly(I:C) Stimulation and RV-1B Infection of BEAS-2B Cells Induces TN- C Release.....	81
3.4.4. Poly(I:C) Stimulation and RV-1B Infection of BEAS-2B Cells Induces CXCL8 and CCL5 Production.....	83
3.5. Poly(I:C) Stimulation of PBECs Modulates TN-C mRNA Expression and Induces TN-C Release.....	85
3.5.1. Poly(I:C) Stimulation of PBECs Modulates TN-C mRNA Expression.....	85
3.5.2. Poly(I:C) Stimulation of PBECs does not Induce Cell-Associated TN-C Expression.....	87
3.5.3. Poly(I:C) Stimulation of PBECs Induces TN-C Protein Release.....	89
3.5.4. Poly(I:C) Stimulation of PBECs Induces Significant CXCL8 & CCL5 Release.....	89
3.6. RV-1B Infection of PBECs Induces TN-C Splice mRNA Expression and RV- 1B and RV-16 induced Significant TN-C Release.	92
3.6.1. RV-1B Infection of PBECs Induces Splice Variant Specific Expression of TN-C.....	92
3.6.2. RV-1B and RV-16 Infection of PBECs does not Induce TN-C Cell Associated Protein Expression.....	94
3.6.3. RV-1B and RV-16 Infection of PBECs Induces the Release of TN-C.....	96

3.6.3.1. RV-1B and RV-16 Infection of PBECs Induces the Release of TN-C as Measured by Western Blot.....	96
3.6.3.2. RV-1B and RV-16 Infection of PBECs Induces the Release of TN-C as Measured by ELISA.....	96
3.6.4. RV-1B and RV-16 Infection of PBECs Induces Significant Production of CXCL8 and CCL5.....	99
3.6.5. Basal Levels of TN-C mRNA and Cell-Associated Protein is Increased in PBECs Compared to BEAS-2B Cells.....	99
3.7. TN-C Expression and Release at Basal Levels and in Response to RV is More Pronounced in Atopic Asthmatic PBECs	102
3.8. Summary and Discussion	104
3.8.1. Summary.....	104
3.8.2. The Roles of the Splice Variants Identified in Mouse BALF and AECs..	105
3.8.3. TN-C was Significantly Upregulated in Response to Poly(I:C) <i>In Vivo</i> and May Play a Protective Role.....	107
3.8.4. AEC Response to RV is TLR3 and not TLR7 Dependent in AECs.....	108
3.8.5. TN-C mRNA is Modulated in Response to TLR3 Stimulation and RV Infection.....	109
3.8.5.1. Total TN-C mRNA is Upregulated in Response to Poly(I:C) and RV-1B in AECs, but may be Donor Specific	109
3.8.5.2. TN-C Splice Specific mRNA Expression is Upregulated in Response to RV Infection in AECs	110
3.8.6. TN-C Cell-Associated Protein Expression Induction in Response to RV.....	111
3.8.6.1. Total TN-C Protein is Upregulated in Response to Poly(I:C) in BEAS-2B Cells but not in Response to Poly(I:C) and RV infection PBECs.....	111
3.8.6.2. Large and Small Splice Variants of Cell-Associated TN-C Are Equally Expressed in BEAS-2B Cells, whilst the Larger Variant Predominates in PBECs.....	113
3.8.7. TN-C Release in Response to RV is a Novel Mechanism Following Viral Infection and the Large TN-C Protein Splice Variant is the Main Variant Released.....	113
3.8.8. Atopic Asthmatics Have Higher TN-C mRNA Expression and TN-C Release than Non-Atopic Non-Asthmatics.....	114
3.8.9. Conclusion.....	115
Chapter 4 – Results: The Mechanisms of RV-Induced TN-C and Exosome Release in AECs	118
4.1. Introduction.....	118
4.2. Hypothesis and Aims	119
4.3. Poly(I:C) and RV Induces Significantly More TN-C Release in AECs than Staurosporine-Induced Apoptosis, Indicating a Viral Specific Mechanism	120

4.3.1. RV Reduces Cell Viability in BEAS-2B Cells but Poly(I:C) has no Cytotoxic Effect.....	120
4.3.2. Poly(I:C) does not Affect BEAS-2B Cell Viability (as Measured by Cell Metabolic Activity) and Induces Significantly More TN-C Release than Staurosporine.....	122
4.3.3. Poly(I:C) does not Affect PBEC Cell Viability (as Measured by Cell Metabolic Activity) and Poly(I:C) and RV Induces Significantly More TN-C Release than Staurosporine.....	124
4.4. Poly(I:C) Stimulation and RV Infection of BEAS-2B Cells Induces Overall Exosome Release and Exosome-Associated TN-C Expression.....	126
4.4.1. AECs Grow and Respond to Poly(I:C) in EV-Depleted Media, Despite a Loss in Cell Viability.....	126
4.4.2. Poly(I:C) Stimulation of BEAS-2B Cells and PBECs Induces the Release of EVs with the Size-Range and Protein Composition of Exosomes.....	128
4.4.3. Poly(I:C) Stimulation of BEAS-2B Cells Induces Exosome-Associated-TN-C Expression.....	130
4.4.4. RV Infection of BEAS-2B Cells Induces Exosome-Enriched Protein Expression and Exosome-Associated-TN-C Expression.....	130
4.4.5. Exosome-Associated TN-C Release is an Abundant Pathway of Release Following Viral Stimulation / Infection.....	133
4.5. Summary and Discussion	135
4.5.1. Summary.....	135
4.5.2. TN-C Release is Viral Specific and Not Induced in Response to Non-Viral Cell Death.....	135
4.5.2.1. RV and Staurosporine Reduces Cell Viability in AECs, but Poly(I:C) Does Not.....	135
4.5.2.2. RV and Poly(I:C) Induces Significant TN-C Release in AECs, but Staurosporine Does Not.....	136
4.5.3. Poly(I:C) and RV Induce Exosome Release in AECs.....	137
4.5.3.1. Characterisation of the EVs Released by AECs Following Viral Stimulation Allow the EV Population to be Defined as Primarily Containing Exosomes.....	137
4.5.3.2. Poly(I:C) and RV Induces the Overall Concentration of Exosome Release in AECs	138
4.5.4. TN-C Release is Associated with Exosomes and is Induced in Response to Poly(I:C) Stimulation and RV Infection.....	140
4.5.5. Conclusion.....	141
Chapter 5 – Results: The Function of TN-C and Exosomes in the Airway Following RV Infection	142
5.1. Introduction	142
5.2. Hypothesis	143

5.3. Knockdown of TN-C by siRNA Prior to Poly(I:C) Stimulation of AECs may Modulate the Inflammatory and Anti-Viral Response.....	144
5.3.1. No Significant Changes in CXCL8 and CCL5 Release were Observed in BEAS-2B Cells Following TN-C siRNA Knockdown and Poly(I:C) Stimulation.....	144
5.3.2. Knockdown of TN-C by siRNA Prior to Poly(I:C) Stimulation of PBECs Successfully Reduced TN-C Expression, but the Knockdown of TN-C Prior to RV-1B Infection of PBECs was Unable to be Measured.....	146
5.3.3. Knockdown of TN-C by siRNA Prior to Poly(I:C) Stimulation of PBECs has No Impact on CXCL8 Release but may Modulate the Initial CCL5 Response.....	148
5.4. Recombinant TN-C Induced CXCL8 Release from Primary Human MDMs..	148
5.4.1. Recombinant Full-Length TN-C was Purified from HEK-293 Supernatant.....	148
5.4.2. Recombinant Full-Length TN-C, Recombinant FBG-TN-C and LPS Induce CXCL8 Release from MDMs.....	151
5.5. LPS and Recombinant TN-C-FBG Induced Moderate CXCL8 Release from BEAS-2B Cells	151
5.5.1. Smooth (but not Rough) LPS Induce CXCL8 Release from BEAS-2B Cells.....	151
5.5.2. Recombinant FBG-TN-C Induces Moderate CXCL8 Release from BEAS-2B Cells.....	154
5.6. Exosomes from Virally Stimulated BEAS-2B Cells Induces Inflammatory Cytokine and Chemokine Release from BEAS-2B Cells	154
5.7. TN-C Induces a Greater Fold-Induction of CXCL8 Release from MDMs, Whilst Exosomes Induce Greater CXCL8 Release from BEAS-2B Cells.....	157
5.8. TN-C Knockdown in BEAS-2B Isolated Exosomes did not Affect Exosome-Induced CXCL8 Release from AECs.....	157
5.8.1. Knockdown of TN-C in BEAS-2B Exosomes Was Successful Following Poly(I:C) Stimulation.....	157
5.8.2. TN-C Knockdown did not Impact Exosome-Induced CXCL8 Release from AECs.....	160
5.9. Summary and Discussion	162
5.9.1. Summary.....	162
5.9.2. TN-C Induces Inflammatory CXCL8 Release from MDMs.....	162
5.9.3. AECs Have the Ability to Respond to Smooth-LPS Stimulation.....	164
5.9.4. TN-C Induces Moderate Inflammatory CXCL8 Release from AECs and May Help Dampen the Initial Anti-Viral Response.....	165
5.9.4.1. FBG-TN-C Stimulation of AECs Induces CXCL8 Release	165
5.9.4.2. Knockdown of TN-C Prior to RV Infection has no Significant Effect on CXCL8 Release but may Affect the Initial Anti-Viral Response	167

5.9.5. Exosomes from Virally Stimulated AECs Induce Inflammatory and Anti-Viral Cytokine / Chemokine Release from BEAS-2B Cells.....	168
5.9.6. Exosomes from Control and Virally Stimulated AECs Induce CXCL8 Release from MDMs.....	170
5.9.7. Initial Results Indicate TN-C May Not Play a Role in Exosome-Induced AEC CXCL8 and CCL5 Release, but Further Investigation is Required.....	171
Chapter 6 – Overall Discussion and Conclusions.....	174
6.1. A Proposed Model of RV-Induced TN-C and Exosome Release in AECs Leading to Increased Airway Inflammation	174
6.1.1. RV-Induced TN-C Expression and Release is TLR3 Dependent, TLR7 Independent and a Viral Specific Mechanism.....	174
6.1.2. Intracellular TN-C Expression Following RV Infection is Dependent on a Number of Factors, can be Controlled by Alternative Splicing and may be More Pronounced in Asthmatics.....	176
6.1.3. RV Infection Induces Exosome Release in AECs.....	176
6.1.4. RV Infection Induces TN-C Release in AECs, is More Pronounced in Asthmatics and a Large Proportion is Associated with Exosomes.....	177
6.1.5. The Proposed Functional Reasons for RV-Induced Tenascin-C and Exosomal Release.....	177
6.1.6. The Proposed Detrimental Inflammatory Implications of RV-Induced TN-C and Exosome Release in the Airway.....	179
6.1.7. Clinical Implications of RV-Induced TN-C and Exosome Release.....	181
6.2. Limitations and Future Plans.....	182
6.3. Conclusion.....	184
References	185

List of Abbreviations

2-5A	5'-Triphosphorylated, 2',5'-Phosphodiester-Linked Oligoadenylates
α-SMA	Alpha Smooth Muscle Actin
AA	Atopic-Asthmatic
AD	Additional Domain
ADB	Antibody Dilution Buffer
ADP	Adenosine Diphosphate
AEC	Airway Epithelial Cell
AHR	Airway Hyperresponsiveness
Akt	Protein Kinase B
ALG-2	Alpha-1,3-Mannosyltransferase
ALI	Air Liquid Interface
ALIX	ALG-2 Interacting Protein X
Ang	Angiopoietin
ANOVA	Analysis of Variance
AP-1	Activator Protein-1
AP-2	Activator Protein-2
APS	Ammonium Persulfate
ARF6	ADP-Ribosylation Factor 6
ATF	Activating Transcription Factors
BALF	Brochoalveolar Lavage Fluid
BB	Basic Buffer
BCA	Bicinchoninic Acid Assay
BMDM	Bone Marrow-Derived Macrophage
BSA	Bovine Serum Albumin
cAMP	Cyclic Adenosine Monophosphate
CBP	CREB-Binding Protein
CD	Cluster of Differentiation

CDS	Circular Dichroism Spectra
CDHR3	Cadherin Related Family Member 3
cDNA	Complementary Deoxyribonucleic Acid
C/EBP	CCAAT-Enhancer-Binding Proteins
CHMP	Charged Multivesicular Body Protein
CM	Conditioned Medium
CNS	Central Nervous System
CREB	cAMP Response Element-Binding Protein
CRISPR	Clustered Regularly Interspaced Short Palindromic Repeats
CVD	Cardiovascular Disease
CVB	Coxsackievirus B
CXCL	C-X-C Motif Ligand
CysLTs	Cysteinyl Leukotrienes
DALY	Disability-Adjusted Life Year
DAMP	Danger Associated Molecular Pattern
DAPI	4',6-Diamino-2-Phenylindole
DMEM	Dulbecco's Modified Eagle Medium
dsRNA	Double Stranded RNA
ECM	Extracellular Matrix
EGF	Epidermal Growth Factor
ELISA	Enzyme-Linked Immunosorbent Assay
eIF2	E74-Like E26 Transcription Factor 2
EMT	Epithelial Mesenchymal Transition
Env	Envelope Protein
EQB	Equilibration Buffer
ER	Endoplasmic Reticulum
ERK	Extracellular Signal Regulated Kinases
ERJ	Endoplasmic Reticulum Resident J-Domain Protein
ESCRT	Endosomal Sorting Complex Required for Transport

ETS	E26 Transformation-Specific
EU	Endotoxin Units
EV	Extracellular Vesicle
FAK	Focal Adhesion Kinase
FBG	Fibrinogen Globe Like
FCϵRI	High-Affinity IgE Receptor
FCS	Fetal Calf Serum
FEV₁	Forced Expiratory Volume
FNIII	Fibronectin Type III
GAPDH	Glyceraldehyde 3-Phosphate Dehydrogenase
GDP	Guanosine Diphosphate
GRP94	Glucose Regulated Protein 94
GM-CSF	Granulocyte-Macrophage Colony-Stimulating Factor
GPCR	G-Protein-Coupled Receptor
GTP	Guanosine Triphosphate
HeLa	Henrietta Lacks
His	Polyhistidine
HIV-1	Human Immunodeficiency Virus 1
HLM	Human Lung Macrophages
HRP	Horseradish-Peroxidase
HRS	Hepatocyte Growth Factor-Regulated Tyrosine Kinase Substrate
IBD	Inflammatory Bowel Disease
ICAM-1	Intracellular Adhesion Molecule 1
IFN	Interferon
Ig	Immunoglobulin
IKK	I κ B Kinase
IL	Interleukin
iNOS	Inducible Nitric Oxide Synthase
IRAK	Interleukin-1 Receptor–Associated Kinase

IRF	Interferon Regulatory Factor
IκB	Nuclear Factor of Kappa Light Polypeptide Gene Enhancer in B-Cells Inhibitor
JAK-STAT	Janus Kinase-Signal Transducer and Activator of Transcription
JNK	c-Jun N-terminal Kinases
KC	Keratinocyte-Derived Cytokine
LAL	Limulus Amebocyte Lysate
LDLR	Low Density Lipoprotein Receptor
LGP2	Laboratory of Genetics and Physiology 2
LPS	Lipopolysaccharide
LT	Leukotriene
MAPK	Mitogen-Activated Protein Kinase
MAVS	Mitochondrial Antiviral-Signalling Protein
MCP	Monocyte Chemoattractant Protein
M-CSF	Macrophage Colony-Stimulating Factor
MD2	Myeloid Differentiation Factor 2
MDA5	Melanoma Differentiation-Associated Protein 5
MDM	Monocyte Derived Macrophages
MFI	Mean Fluorescence Intensity
MHC	Major Histocompatibility Complex
miRNA	microRNA
MMP	Matrix Metalloproteinase
MOI	Multiplicity of Infection
mRNA	Messenger RNA
MSK	Mitogen and Stress Activated Kinases
MTT	MTT 3-(4,5-Dimethylthiazol-2yl)-2,5-Diphenyltetrazolium Bromide
MUC	Mucin
MV	Microvesicle
MVB	Multivesicular Bodies
MyD88	Myeloid Differentiation Primary Response 88

NADPH	Nicotinamide Adenine Dinucleotide Phosphate
NANA	Non-Atopic Non-Asthmatic
NAP1	Nucleosome Assembly Protein 1
NEMO	NF- κ B Essential Modulator
NF-κB	Nuclear Factor Kappa-Light-Chain-Enhancer of Activated B Cells
NK	Natural Killer
NLF	Nasal Lavage Fluid
NLR	Nod-Like Receptor
NTA	Nanoparticle Tracking Analysis
OA	Osteoarthritis
OAS1	2'-5'-Oligoadenylate Synthetase 1
Ova	Ovalbumin
PAMP	Pathogen-Associated Molecular Pattern
PBEC	Primary Bronchial Epithelial Cells
PCR	Polymerase Chain Reaction
PDK1	Phosphoinositide-Dependent Protein Kinase-1
Pen-Strep	Penicillin-Streptomycin
PFU	Plaque Forming Units
PG	Prostaglandin
PBS	Phosphate Buffered Saline
PFA	Paraformaldehyde
PI3K	Phosphatidylinositol-4,5-Bisphosphate 3-Kinase
PIP₂	Phosphatidylinositol 4,5-Bisphosphate
PIP₃	Phosphatidylinositol (3,4,5)-Trisphosphate
PKR	Protein Kinase R
PM	Plasma Membrane
PMB	Polymyxin B
Poly(I:C)	Polyinosinic:Polycytidylic Acid
PRR	Pattern Recognition Receptors

PS	Phosphatidylserine
qPCR	Quantitative Polymerase Chain Reaction
RA	Rheumatoid Arthritis
RANTES	Regulated on Activation, Normal T-Cell Expressed and Secreted
RBM	Reticular Basement Membrane
RCF	Relative Centrifugal Force
RIG-I	Retinoic Acid-Inducible Gene I
RIP-1	Receptor-Interacting Serine/Threonine-Protein Kinase 1
RLR	RIG-I-Like Receptor
RNA	Ribonucleic Acid
RPMI	Roswell Park Memorial Institute Medium
RSV	Respiratory Syncytial Virus
RT	Room Temperature
RTK	Receptor Tyrosine Kinase
RV	Human Rhinovirus
SC	Standard Curve
SDS	Sodium Dodecyl Sulphate
SDS-PAGE	SDS-Polyacrylamide Gel Electrophoresis
SEM	Standard Error of the Mean
siRNA	Small Interfering RNA
SMAD	Mothers Against Decapentaplegic Homolog
SNP	Single Nucleotide Polymorphisms
Src	Proto-Oncogene Tyrosine-Protein Kinase Src
ssRNA	Single-Stranded RNA
STAM	Signal Transducing Adaptor Molecule 1
Syk	Spleen Tyrosine Kinase
TA	Tenascin Assembly
TAK1	Mitogen-Activated Protein Kinase Kinase Kinase
TBS	Tris Buffered Saline

TEMED	Tetramethylethylenediamine
TGFβ	Transforming Growth Factor β
TCA	Trichloroacetic Acid
Th2	T Helper Cell 2
TIMP	Tissue Inhibitor of Metalloproteinase
TIRAP	Toll-Interleukin 1 Receptor Domain Containing Adaptor Protein
TLR	Toll-Like Receptor
TN	Tenascin
TN-C	Tenascin-C
TNFα	Tumour Necrosis Factor alpha
TP	Thromboxane Receptor
t-PA	Tissue Plasminogen Activator
TRADD	Tumour Necrosis Factor Receptor Type 1-Associated DEATH Domain Protein
TRAF	TNF Receptor Associated Factors
TRAM	Translocating Chain-Associated Membrane Protein
TRIF	Toll-Interleukin Receptor-Domain-Containing Adapter-Inducing Interferon- β
TSG-101	Tumour Susceptibility Gene 101
TUNEL	Terminal Deoxynucleotidyl Transferase dUTP Nick End Labelling
UBAP1	Ubiquitin Associated Protein 1
V	Volts
VEGF	Vascular Endothelial Growth Factor
VP	Viral Protein
VPS	Vacuolar Protein Sorting

List of Figures

Figure 1.1. Asthma Pathophysiology

Figure 1.2. The PRRs and Signalling Pathways Involved in RV Infection of AECs

Figure 1.3. The Structure of Tenascin-C

Figure 1.4. TN-C Domains and Binding Partners Involved in Signalling

Figure 1.5. The TLR4 Signalling Pathway

Figure 1.6. The Classification of Exosomes and MVs

Figure 2.1. Images of BEAS-2B Cells and PBECs in Culture

Figure 2.2. The Isolation of MVs and Exosomes from AEC Supernatants Following Poly(I:C) Stimulation and RV Infection

Figure 3.1. Intranasal Poly(I:C) Stimulation of Wild-Type C57BL/6 Mice Induces TN-C Expression in the BALF

Figure 3.2. Poly(I:C) and TNF α Stimulation of BEAS-2B Cells Increases TN-C mRNA Expression

Figure 3.3. Poly(I:C) Stimulation of BEAS-2B Cells Induces Cell-Associated TN-C Expression and an Equal Ratio of Large and Small Variants was Present.

Figure 3.4. Poly(I:C) Stimulation of BEAS-2B Cells Induces Cell Associated TN-C as Visualised by Immunofluorescence

Figure 3.5. Poly(I:C) Stimulation of BEAS-2B Cells Induces Diffuse Cell-Associated TN-C Expression as Visualised by Confocal Imaging

Figure 3.6. Poly(I:C) Stimulation and RV-1B Infection of BEAS-2B Cells Induces the Release of TN-C, with the Large Variant Being the Main Variant Released

Figure 3.7. Poly(I:C) / TNF α Stimulation and RV Infection of BEAS-2B Cells Induces CXCL8 and CCL5 Production

Figure 3.8. Poly(I:C) Stimulation of PBECs Modulates TN-C mRNA Expression

Figure 3.9. Poly(I:C) Stimulation of PBECs does not Induce TN-C Protein Expression

Figure 3.10. Poly(I:C) Stimulation of PBECs Induces the Release of TN-C, with the Large Splice Variant Being the Main Variant Released

Figure 3.11. Poly(I:C) Stimulation of PBECs Induces CXCL8 and CCL5 Production

Figure 3.12. RV Infection of PBECs Induces TN-C FNIII-C Domain mRNA Expression

Figure 3.13. RV Infection of PBECs Does Not Induce Significant Cell-Associated TN-C Expression

Figure 3.14. RV Infection of PBECs Induces Significant TN-C Release as Measured by Western Blot and the Larger Splice Variant is the Main Variant Released

Figure 3.15. RV Infection of PBECs Induces Significant TN-C Release as Measured by ELISA

Figure 3.16. RV Infection of PBECs Induces CXCL8 and CCL5 Production in PBECs

Figure 3.17. Basal TN-C mRNA and Cell-Associated Protein Expression is Significantly Higher in PBECs Compared to BEAS-2B Cells

Figure 3.18. RV Infection of NANA PBECs Induces TN-C mRNA Expression and RV Infection of AA PBECs Induces Greater TN-C Release

Figure 4.1. RV Reduces Cell Viability in BEAS-2B Cells but Poly(I:C) has no Cytotoxic Effect

Figure 4.2. Poly(I:C) does not Affect BEAS-2B Cell Viability (as Measured by Cell Metabolic Activity) and Induces Significantly More TN-C Release than Staurosporine

Figure 4.3. Poly(I:C) does not Affect PBEC Cell Viability (as Measured by Cell Metabolic Activity) and Poly(I:C) and RV Induces Significantly More TN-C Release than Staurosporine

Figure 4.4. AECs Grow to Confluence and Respond to Poly(I:C) in EV-Depleted Media

Figure 4.5. Poly(I:C) Stimulation of AECs Induces the Expression of Exosome-Enriched Proteins and EV Release Within the Size Range of Exosomes

Figure 4.6. Poly(I:C) Stimulation of BEAS-2B Cells Induces Significant Exosome-Associated TN-C Release

Figure 4.7. RV Infection of BEAS-2B Cells Induces Exosome-Enriched Proteins and Exosome-Associated TN-C Release

Figure 4.8. Exosome-Associated TN-C Release is an Abundant Pathway Following Viral Stimulation

Figure 5.1. No Significant Changes in CXCL8 and CCL5 Release Occurred in BEAS-2B Cells Following TN-C siRNA Knockdown and Poly(I:C) Stimulation

Figure 5.2. siRNA Knockdown of TN-C Reduced Cell-Associated TN-C Expression and TN-C Release in PBECs

Figure 5.3. Knockdown of TN-C by siRNA Prior to Poly(I:C) Stimulation of PBECs had No Impact on Inflammatory Cytokine and Chemokine Release but May Modulate the Initial CCL5 Response

Figure 5.4. LPS-Free Full-Length Recombinant TN-C with His-tag was Purified, Concentrated and Quantified from HEK-293-pCEP-huTNChis Cells

Figure 5.5. Recombinant Full-Length TN-C and Recombinant FBG-TN-C Stimulation Induced CXCL8 Expression from Primary Human MDMs

Figure 5.6. Smooth LPS Stimulation Induced CXCL8 Expression from BEAS-2B Cells

Figure 5.7. Recombinant FBG-TN-C Stimulation Induced CXCL8 Expression from BEAS-2B Cells

Figure 5.8. Exosomes Isolated from Virally-Stimulated BEAS-2B Cells Induced Cytokine and Chemokine Release from BEAS-2B Cells

Figure 5.9. LPS, TN-C and TN-C-FBG Induced Greater CXCL8 Release in MDMs, Whilst Poly(I:C) Stimulated BEAS-2B Derived Exosomes Induced Greater CXCL8 Release from BEAS-2B Cells

Figure 5.10. siRNA Knockdown of TN-C Reduced Cell-Associated TN-C Expression, TN-C Release and Exosome-Associated TN-C in BEAS-2B Following Poly(I:C) Stimulation

Figure 5.11. TN-C Knockdown did not Impact on Exosome-Induced BEAS-2B Cell CXCL8 and CCL5 Release

Figure 6.1. The Proposed Mechanism of TN-C Release Following RV Infection in AECs

Figure 6.2. The Proposed Inflammatory and Anti-Viral Implications of RV-Induced TN-C and Exosome Release in the Airway

List of Tables

Table 1.1. Summary of Human TLRs

Table 1.2. Summary of Human Tenascins

Table 1.3. Proteins Involved in the ESCRT Pathway

Table 1.4. EV Isolation Methods

Table 1.5. EV Characterisation Methods

Table 2.1. Cells

Table 2.2. Cell Culture (Non-Viral Work)

Table 2.3. Cell Culture Media (Viral Work)

Table 2.4a. Buffers

Table 2.4b. Buffers Continued

Table 2.5. SDS-PAGE Gels

Table 2.6. Commercially Available Kits

Table 2.7. TaqMan RT qPCR Primer Probes

Table 2.8. SYBR Green Primers

Table 2.9a. ELISA and Western Blot Antibodies

Table 2.9b. ELISA and Western Blot Antibodies (Continued)

Table 2.9c. Immunofluorescence Antibodies

Table 2.10a. Machines (University of Sheffield)

Table 2.10b. Machines (University of Oxford)

Table 2.11. Reagents Required for cDNA Synthesis

Table 2.12. Composition of TaqMan qPCR cDNA Samples

Table 2.13. Composition of SYBR Green qPCR cDNA Samples

Table 3.1. Summary of TN-C Expression and Release in Response to Poly(I:C) and RV

Table 3.2. Summary of Specific PBEC Donors Used

Acknowledgements

First and foremost, I would like to thank my supervisors at the University of Sheffield, Dr Lisa Parker and Professor Ian Sabroe, and my Supervisor at the University of Oxford, Professor Kim Midwood, for all the support and care they have provided throughout this project. Without their patience, understanding and drive to help me improve as a scientist, I wouldn't be where I am today. Lisa has not only given me the knowledge and skills required to complete this work, she has also shown a great deal of patience, compassion and understanding that has allowed me to achieve something that I am very proud of, so thank you very much Lisa, I couldn't have asked for a better PI. Throughout the four years, Ian has been a constant provider of knowledge and his drive to help me develop has enabled me to improve as a research scientist, a writer, and an all-round person, thank you Ian. I would like to thank Kim for allowing me to spend a year in her lab in the University of Oxford, I truly felt at home there and it was a great privilege. Under Kim's supervision, I was able to learn a great deal and develop my project significantly, and I feel the year I spent under your direct supervision was invaluable. The constant support you also provided when I was at Sheffield was a huge help, so thank you for everything Kim.

There are a large number of people to thank who have helped me at the University of Sheffield and University of Oxford during this project. I would like first to thank the original members of the Sabroe group, who kept me sane throughout these four long years in the lab, and who I am proud to class as great friends. Dr Clare Stokes, thank you so much for the help and patience you provided at the start of the PhD, and the support and care you showed at the end, and Dr Grace Manley, I would like to thank you for all the help and guidance provided during the four years. I couldn't have done this without both Clare's and Grace's help. Liz Prestwich and Dr Elizabeth Marsh, the immeasurable help, advice and laughs you provided were invaluable, so thank you very much. Kirsty, thank you for also believing that England could win the World Cup, which helped me to get through the final summer of intense work! I would also like to thank the Midwood group at the University of Oxford, whose kindness and eagerness to help allowed me to settle into life at Oxford very quickly. I would especially like to thank Dr Anja Schwenzer and Dr Sean Giblin, not only for the technical help and knowledge you provided, but the effort you both showed to make sure I felt at home was beyond what I expected, and it is great to have become personal friends with you both. To Anna, Susan, Claire and my other friends I met in Oxford, I would like to thank you also, the friendly nature and drive for your own research you displayed made me feel part of the team straight away and enabled me to thrive, so thank you very much for that. Furthermore, I would like to thank Elizabeth for the providing the mouse samples and to Dr Michael Edwards for providing the asthmatic samples, which helped to dramatically improve the quality of my work and thanks to everyone else who assisted me during my studies.

To Dr Josh Casulli, Dr Will Finley, Dr Ben Ward and Dr Hannah Murray, I would like to thank you for the advice, compassion and most importantly for the times we have spent outside of the lab together over the years. To say we've come far from the fresh faced graduates we were four years ago is an understatement, and I am very proud of everything we've achieved together.

Without my family I would not be where I am today and I am constantly thankful for the love provided by you all. To Nana Pat, Nana Kath and Grandad Bob I would like to thank you so much for the lessons I have learnt from you and I love you all dearly. I would also like to thank Grandad for helping to move in and out of my accommodation every year, I couldn't have done it without you! To my brother Kane, I am very proud of your achievements and the passion you show for your own work has inspired me greatly, and I hope you continue to excel and thrive in your career. To my Mum and Dad, Darren and Kirsti, the support and advice you have given me throughout my life and in particular these four years has been priceless, and your kindness, self-sacrifice and love you have provided has enabled me to finish this project. Despite illness, my mother is the kindest and most selfless person I know and I am truly grateful for everything you and dad have done for me and I would like to thank you both from the bottom of my heart. Despite sounding trite, I couldn't have completed these four years without Sascha, my dog, and I would like to thank her for allowing me to forget about the stresses of work instantly by going home to see her, you are the best friend a person could wish for.

My largest thanks are reserved for my partner Georgia Unsworth, who was a pillar of support during the completion of my studies and I am eternally grateful to her for the emotional support she has provided. There are too many things you have done to thank you for, but to name a few: the countless trips to Oxford and Sheffield you have made, the holidays we have been on, the planning for the future, and the dedication to the development of your own career and your own hard work whilst helping me with mine, I am so thankful for everything you have done. I truly would not have been able to complete this work without you.

Finally, I would like to dedicate this thesis to both Mary 'Mama' Thornton and Glynn 'Pops' Mills, who I loved dearly, provided me with great inspiration and who both passed away during the completion of my studies.

Jake Mills

Chapter 1: Introduction

1.1. Asthma

1.1.1. Asthma Epidemiology

In the UK, it is estimated that 18.3% of the population (approximately 11 million people) suffer from asthma (To et al. 2012). The latest Global Asthma Report in 2014 estimated that the worldwide prevalence of asthma was in the region of 334 million people (Becker and Abrams 2017). The age of the individual does not affect the incidence of asthma, with 1 in 11 children, and 1 in 12 adults suffering from asthma in the UK (Bloom et al. 2018). Prevalence of the disease, however, does differ depending on the gender of the individual; for example, boys have a higher risk pre-puberty, but girls have a higher incidence following adolescence. Furthermore, a study showed that females were 20% more likely to have asthmatic symptoms compared to males in those over 35 years of age (Leynaert et al. 2012). Whilst asthma was initially a disease associated with developed countries, prevalence in English speaking countries is slowly decreasing over time (-0.51% decrease in prevalence in 13-14 year olds over a 12 month period), with substantial increases in countries in Latin America (+0.32%), Eastern Europe (+0.26%), Africa (+0.16%) and the Indian subcontinent (+0.06%; Pearce et al. 2007). At least 22 million disability-adjusted life years (DALY; number of years lost to ill health or disability) are lost to asthma annually (Becker and Abrams 2017), and the most recent studies estimate that the economic burden is approximately \$56 billion in the US (Barnett and Nurmagambetov 2011), €19.3 billion in Europe (Accordini et al. 2013) and £1.1 billion in the UK (Mukherjee et al. 2016). The global incidence of the disease is expected to increase to 400 million by 2025 (To et al. 2012); indicating that asthma is a prevalent, widespread and growing problem that needs to be addressed.

1.1.2. Asthma Pathophysiology

1.1.2.1. Characterisation and Phenotypes

Asthma is a chronic inflammatory disease characterised by wheezing, reversible airflow obstruction and chest tightness. The disease is driven by airway inflammation and airway remodelling, resulting in airway hyperresponsiveness (AHR). AHR is the greater susceptibility to the closing of the airway due to heightened sensitivity to inhaled constrictor agonists, with the severity of AHR correlating with the severity of asthma (O'Byrne and Inman 2003). There are a number of different phenotypes of asthma, however they are yet to be fully defined (Wenzel 2012). The underlying pathogenesis of asthma is a prolonged, chronic inflammation of the airway, and atopic asthma can be identified as being due to an eosinophil dominated and skewed T-helper type 2 (Th2) immune response towards usually non-harmful airborne agents (Murdoch and Lloyd 2010). Atopic asthmatic symptoms are induced by a common respiratory allergen and the genetic predisposition to mount an inappropriate antibody immunoglobulin (Ig

type E response (Pillai, Corrigan and Ying 2011). Non-atopic asthma also has a Th2 skewed response, may also involve IgE production (although less pronounced than the atopic form), has less goblet cell hyperplasia, less reticular basement membrane (RBM) thickening and more eosinophil infiltration (Pillai et al. 2011). Despite this, the defining cause of this form of the disease is not fully understood (Murdoch and Lloyd 2010). It is also clear that non-Th2 forms of asthma are present, which are associated with late-onset asthma and neutrophilic asthma (Wenzel 2012). There is currently no cure for asthma, with the standard therapeutics aiming to reduce inflammation, control symptoms in order to prevent asthma exacerbations from occurring and improving quality of life. The most common forms of treatment are β_2 -agonists (usually administered in the form of reliever inhalers) and glucocorticoids (usually administered in the form of preventer inhalers, in tablet form, or as an injection). β_2 -agonists are short-acting and bind to the β_2 -adrenergic receptor, causing relaxation of the airway smooth muscle and opening of the airway (Subbarao and Ratjen 2006), whereas corticosteroids are used to suppress Th2 cytokines and dampen inflammation in the airway over a longer period of time (Dunican and Fahy 2017). Furthermore, it is estimated that around 5-10% of asthmatics in Europe (with unknown percentages around the rest of the world) have severe asthma (Sears 2014). Severe asthma is defined as – ‘when adequate control of asthma cannot be achieved by high-dose treatment with inhaled corticosteroids and additional controllers, or by oral corticoid treatment, or is lost when treatment is reduced’ (Lommatzsch 2016). The large percentage of severe asthma sufferers makes it clear that alternative therapeutics are needed to help treat the pathogenesis of the disease.

1.1.2.2. Cytokines and Chemokines

Raised inflammatory cytokine and chemokine expression in the airway of asthmatics contributes to the pathogenesis of asthma in a large number of ways. One of the main cytokines implicated in asthma is transforming growth factor beta (TGF- β ; Duvernelle et al., 2003). The TGF- β family comprises of TGF- β 1, TGF- β 2 and TGF- β 3 which have an amino acid similarity of around 80% and induce similar responses. Eosinophilic infiltration in the airway is a presenting factor in asthma, and this cell type releases large amounts of TGF- β following activation (Duvernelle et al., 2003). TGF- β 1 is the main type of TGF- β associated with asthma, with expression present in higher quantities in the bronchoalveolar lavage fluid (BALF), lung biopsies and lung fibroblasts, and expression correlates with disease severity (Redington et al., 1997). Prior to activation, TGF- β is produced and secreted as latent TGF- β , through either association with latency associated protein or latent TGF- β binding protein interactions (Saharinen et al., 1999). Following activation, these proteins are sequestered from TGF- β , allowing the cytokine to become active, leading to the activation of mothers against decapentaplegic homolog (SMAD)3 and 4 receptors (Saharinen et al., 1999). The activation of these pathways induces a number of transcription factors, including c-Jun, CREB and NF- κ B (see Figures 1.2. and 1.5. for more information). TGF- β activation drives airway remodelling (section 1.2.2.3) by promoting the deposition of extracellular matrix (ECM) proteins, inducing smooth muscle proliferation, promoting angiogenesis and playing an important role in fibrosis (Duvernelle et al., 2003).

Furthermore it can promote apoptosis of healthy lung epithelial cells and increase ICAM-1 expression, which is important in viral infection, and ultimately asthma exacerbations (see Figure 1.2.), TGF- β also is a chemotactic agent for eosinophils, macrophages, neutrophils and mast cells, meaning once activated in the asthmatic airway, large recruitment of immune cells occurs, contributing further to the enhanced inflammatory environment (Duvernelle et al., 2003).

TNF α is a cytokine that is produced before activation as a membrane bound pre-cursor protein, which is then cleaved by TNF α converting enzyme prior to activation and this cytokine is produced by a number of cells, with macrophages the most prominent (Vanoverveld et al. 1991, Lukacs et al. 1995, Thomas and Heywood 2002, Berry et al. 2007). Upon activation TNF α exerts its effects via TNF α R1 and TNF α R2, leading to NF- κ B phosphorylation and activation (See Figure 1.2.). TNF α can lead to the transcription of CXCL8 and IL-6, can form a feedback loop that induces more TNF α expression, and contribute towards asthma pathogenesis in a number of ways. The cytokine is increased in the airways of asthmatics, and has been demonstrated to correlate with, and contribute towards AHR. This is due to TNF α inducing histamine release from mast cells, recruiting neutrophils, T-cells and eosinophils to the airway, induces contraction of airway smooth muscle, promotes glucocorticoid resistance and upregulates ICAM-1 (Berry et al. 2007). Anti-TNF α therapy has been somewhat effective in treating AHR, but this seems to be limited to a relatively small proportion of asthmatic patients, and has safety issues such as increased risk of pneumonia and cancer (Berry et al. 2007).

CXCL8 is a chemokine that is produced in response to NF- κ B signalling and is implicit in the increased inflammatory environment present in the airway of asthmatics (John et al., 2009). CXCL8 can be produced from a number of cells present in the airway, such as airway smooth muscle cells, airway epithelial cells, macrophages and neutrophils. It is present in higher quantities in the BALF of asthmatic patients, and following activation of the chemokine, CXCL8 is a potent recruiter of neutrophils and mast cells to the lung. (John et al., 2009)

A large number of other cytokines and chemokines play a role in asthma pathogenesis, are described in vast detail in Kips, 2001 and are briefly summarised below. Interleukin (IL)-4, IL-5 and IL-13 are present in higher quantities in the airways of asthmatics, recruiting a number of different inflammatory cells such as eosinophils, mast cells, neutrophils, basophils and macrophages (Corry et al. 1998, Hamid et al. 2003). Upon recognition of an allergen, IL-4 and IL-13, in the presence of T-cells, induce B cell antigen-specific-IgE production, which then activates the high-affinity receptor (Fc ϵ R1) on mast cells and basophils (Gauchat et al. 1993, Galli and Tsai 2012). Crosslinking of Fc ϵ R1 upon re-exposure to the allergen induces a hypersensitivity response in basophils and mast cells. This includes the initial release of histamine, serotonin, prostaglandins (PG) and leukotrienes (LT) and the secretion of cytokines, chemokines and growth factors over a longer period of time (Galli and Tsai 2012). PGs, such as PGD₂ can induce mucus hypersecretion and also bind to the thromboxane receptor (TP) on airway smooth muscle to induce bronchoconstriction (Johnston et al. 1995a). There is also contrasting evidence on whether PGD₂ causes bronchoconstriction through the PG receptor, as it has previously been shown to cause bronchodilation (Johnston et al. 1995a,

Hall 2000, Hata and Breyer 2004). LTs such as cysteinyl LTs (cysLTs) can induce bronchoconstriction and mucus secretion, but also recruit eosinophils to the airway through binding to the cysLT1 receptor and subsequent generation of IL-5 (Saito et al. 2004). Histamine elicits its effects through binding to the histamine H₁ and H₂ receptors, inducing bronchospasm, mucus hypersecretion and vasodilation, as well as inducing cytokine release from macrophages and T-cells (White 1990, Yamashita et al. 1991). Eosinophilia in the lungs is a hallmark of atopic asthma. IL-5 is required for eosinophil production and they secrete inflammatory cytokines (such as IL-5 and IL-13), chemokines, granule mediators and LTs, and can act as antigen presentation cells (Corry et al. 1998). Mast cells produce histamine, PGD₂ and inflammatory cytokines such as IL-3, IL-4, IL-5, IL-6 and tumour necrosis factor α (TNF α), whilst basophils release histamine, IL-13 and IL-4 (Hamid et al. 2003). In addition, macrophages are antigen presenting cells and release IL-1, TNF α , IL-6, granulocyte-macrophage colony-stimulating factor (GM-CSF) and LTs (Hamid et al. 2003). Nuclear factor kappa-light-chain-enhancer of activated B cells (NF- κ B) signalling is also increased in asthma patients (due to higher p65 protein expression) and a quicker p65 translocation to the nucleus is observed in mice that have induced asthma-like symptoms, leading to transcription of inflammatory cytokines such as TNF α (Poynter et al. 2002, Gagliardo et al. 2003, Edwards et al. 2009).

1.1.2.3. Remodelling

Airway remodelling in asthma involves a number of different processes that change the overall structure of the airway, including: fibrosis of the RBM, increased thickness of airway smooth muscle, goblet cell hyperplasia and bronchial vascularisation (Al-Muhsen et al. 2013). Airway smooth muscle cells surround the lumen of the bronchi, and control the opening and closing of the airway through bronchoconstriction and bronchodilation. They are plentiful cell in the upper airway (approximately a quarter of all cells are ASM) and decrease throughout the lower airway (around 5%; Doeing and Solway, 2013). The increase in airway smooth muscle (both in number of cells and thickness) compounds the narrowing of the airway, reducing peak expiratory flow and thus contributing to the breathing difficulties seen in asthma (Bergeron, Tulic and Hamid 2010). Eosinophils are purported to play a role in airway smooth muscle cell proliferation and thickness through the release of TNF α and IL-1 β (Halwani et al. 2013, Khan 2013). This eosinophil-derived TNF α and IL-1 β release cause contraction of airway smooth muscle by inducing the expression of G α_q and G α_i proteins, which induce cyclic adenosine monophosphate (cAMP) production in response to increased G protein-coupled receptor (GPCR) activation (Khan 2013). In asthmatics, airway smooth muscle cell relaxation is also impaired, due to gained tolerance to β -agonist treatment, obstructing airway flow even further (Doeing and Solway, 2013). This tolerance can also be potentiated by IL-1 β and IL-13, which are increased in asthma. Airway smooth muscle cells are not only impacted by the heightened inflammatory response in the asthmatic airway, they also contribute towards it, by the release of IL-5, IL-13, eotaxin and TGF- β (functions described in Section 1.1.2.2; Doeing and Solway, 2013)

Goblet cell hyperplasia is a vital part of the airway remodelling process, leading to mucus hypersecretion and therefore airflow obstruction, and can even lead to asphyxiation in extreme cases during asthma exacerbations (Ordonez et al. 2001, Rogers 2002). It is thought that IL-4, IL-9 and IL-13 are important in the induction of goblet cell hyperplasia. IL-4 and IL-9 can induce the differentiation of epithelial cells into mucin (MUC)5AC+ goblet cells, and epidermal growth factor (EGF)-receptor activation is required for IL-13-induced goblet cell hyperplasia, leading to the activation of receptor tyrosine kinase (RTK) and mitogen-activated protein kinases (MAPK; Rogers 2002, Vermeer et al. 2003, Scudieri et al. 2012).

Bronchial vessels cover the whole bronchial area, including the terminal bronchioles where they join and form pulmonary vessels (Zanini et al. 2010). During airway remodelling, increased bronchial vascularisation occurs, including angiogenesis of new bronchial vessels, vasodilation of existing vessels, decreased blood flow and increased permeability of vessels, leading to airway wall thickening and reduction of airflow through the lumen (Bailey et al. 2009, Zanini et al. 2010). Bronchial vascularisation also leads to oedema in the airway and can result in the failure to clear mucus secretions, which has been a common feature noted in fatal asthmatic cases (Dunnill 1960, Zanini et al. 2010). Many factors are important in the process of bronchial vascularisation, such as vascular endothelial growth factor (VEGF), matrix metalloproteinase (MMP)-9 and angiopoietin (Ang)-1 and 2, although the definitive roles of each are not clear (Zanini et al. 2010).

Fibrosis is perhaps the most important contributor of airway remodelling. Fibrosis of the RBM contributes to both the increased thickness of the airway and decreased airflow observed in airway remodelling, and occurs when loose collagen fibrils within the RBM are replaced by a dense cluster of ECM proteins, including fibrinogen, collagen and tenascin (TN; Royce et al. 2012). A number of cytokines play a role in this mechanism, including TGF- β , IL-4, IL-5, and IL-17. IL-5 is vital in eosinophil recruitment and is therefore indirectly involved in fibrosis, as eosinophils are an important producer of TGF- β (GharaeeKermani and Phan 1997, Al-Muhsen et al. 2013, Borthwick et al. 2013). TGF- β promotes the transcription and accumulation of ECM proteins alongside the reduction of matrix degrading proteases and their inhibitors such as tissue plasminogen activator (t-PA), MMP-1, MMP-9 and tissue inhibitor of metalloproteinase (TIMP)-1, 2 and 3 (Border and Noble 1994, Branton and Kopp 1999). TGF- β and IL-4 also drives the differentiation to fibroblasts to myofibroblasts during airway remodelling, which promotes the deposition of collagen and other ECM proteins (Brewster et al. 1990). Epithelial-mesenchymal transition (EMT) of epithelial cells (the reversion of epithelial cells back to mesenchymal stem cells and then to another cell type) is a vital mechanism involved in fibrosis and airway remodelling during atopic asthma (Hackett et al. 2009). This process is driven by TGF- β , which induces the EMT of airway epithelial cells (AEC) to myofibroblasts in a Smad3 transcriptional modulator dependent manner (Hackett et al. 2009). During EMT, cells become motile, elongated fibroblast like cells, which results in the recruitment of eosinophils. This drives ECM deposition and fibrosis, and induces the loss of adherens junctions, mucosal barrier deterioration and disrupts signalling pathways. Further work also revealed that stimulation of eosinophils with Th17 cytokines (such as IL-17F, which has been demonstrated to be increased

in the lung tissue of asthmatics) induces TGF- β expression, potentially through p38 MAPK activation (Al-Muhsen et al. 2013). The pathophysiology of asthma is summarised in Figure 1.1.

1.1.3. Asthma Exacerbations

In asthma sufferers, symptoms can suddenly worsen and lead to an asthma exacerbation (also known as an 'asthma attack'), which is the mass release of inflammatory cytokines, chemokines and mucus, triggering bronchospasm and therefore obstruction of the airway (Aikawa et al. 1992). Asthma exacerbations are surprisingly common in asthmatic patients, with a US study finding that approximately half of all American suffers experienced at least one exacerbation per year (Pollart, Compton and Elward 2011). Symptoms before respiratory arrest include: breathlessness, increased respiratory rate, wheezing, bradycardia, lowered lung function and drowsiness (Krishnan et al., 2006). Rapid care is vital, and according to the World Health Organisation, in the most severe cases, around 250,000 people per year die from asthma exacerbations, whilst many more are hospitalised (Bousquet et al. 2010). There are a number of risk factors that contribute towards the increased risk of death following an asthma exacerbation, including: the number of previous severe exacerbations, the number of annual hospitalisations to asthma, low socio-economic status, drug use, and mental health difficulties (Denlinger et al., 2014). When respiratory arrest occurs, it is vital that intravenous administration of β_2 -agonists occurs, rather than oral administration, in order to quickly induce bronchodilation (Krishnan et al., 2006). Intravenous magnesium sulphate treatment may also be beneficial in inducing bronchodilation (Krishnan et al., 2006). One of the main causes of asthma exacerbations are respiratory viruses, including human rhinovirus (RV).

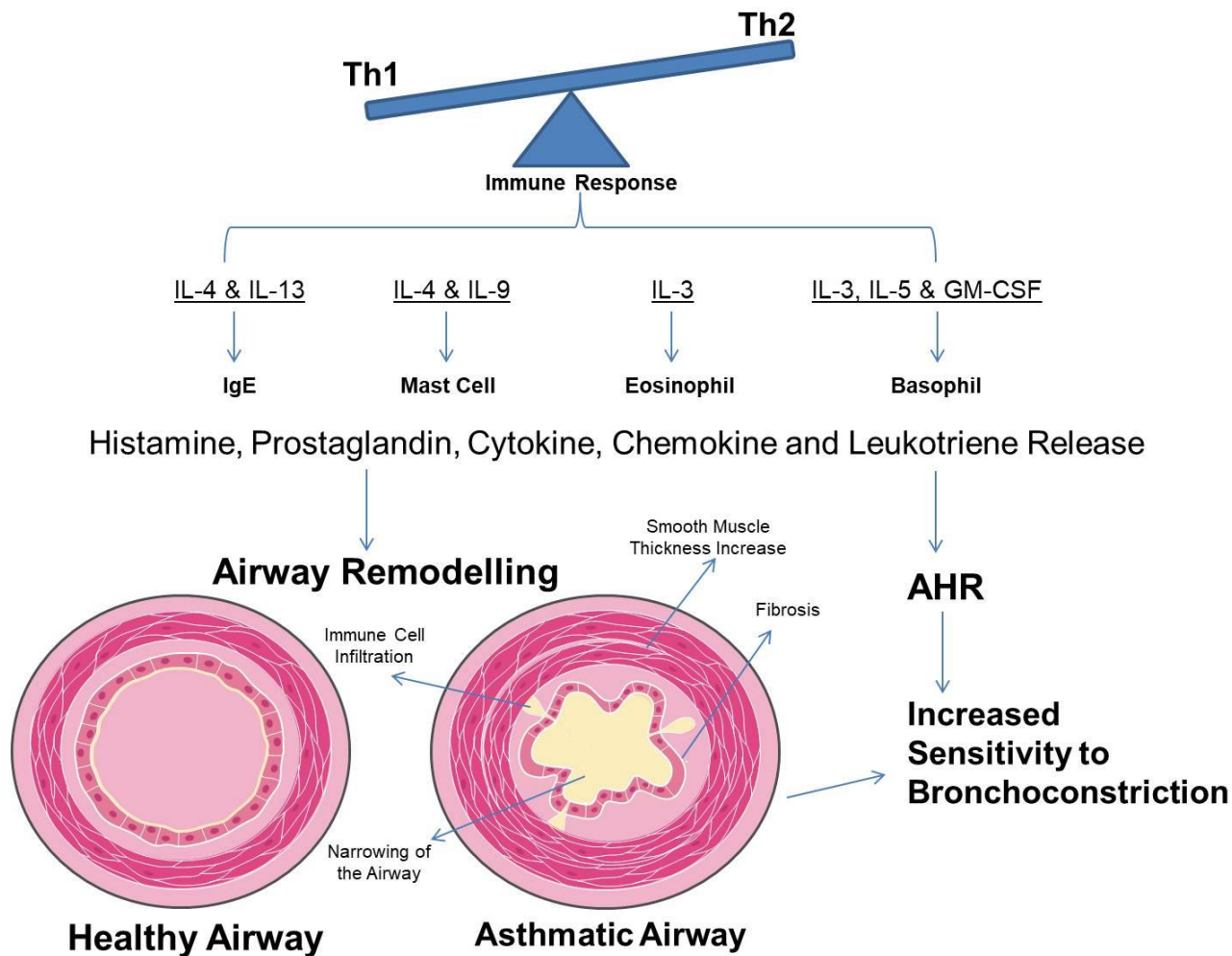


Figure 1.1. Asthma Pathophysiology

Asthma is a Th2 skewed immune response that involves a large number of cytokines and immune cells. The chronic and heightened immune response leads to airway remodelling, due to immune cell infiltration, narrowing of the airway, fibrosis, smooth muscle thickness increase, and goblet cell hyperplasia. Airway remodelling and inflammation leads to AHR, leading to increases sensitivity to bronchoconstriction during asthma exacerbations.

1.2. Human Rhinovirus

1.2.1. RV Structure and Serotypes

RV is one cause of the common cold and is a member of the *Enterovirus* genus in the *Picornaviridae* family of viruses, which also includes Coxsackievirus B (CVB) and Poliovirus (L'Huillier et al. 2015). The virus has single stranded ribonucleic acid (ssRNA) and is comprised of around 7000 bases with no envelope (Fuchs and Blaas 2012). RV infects the epithelial cells in both the upper and lower airway and there are around 148 serotypes which can be grouped into two classification systems (Mosser et al. 2002, Harvala et al. 2012, McIntyre, Knowles and Simmonds 2013). The A-B-C classification system is based on the similarity in the ribonucleic acid (RNA) sequences of the viral protein (VP)1, whereas the major-minor-C classification system is based on the entry receptor used by the virus to enter the cell (McIntyre et al. 2013, Schuler et al. 2014). Major serotypes bind to intracellular adhesion molecule (ICAM-1) on the cell surface, whilst minor serotypes use various low density lipoprotein receptors (LDLRs) – low density lipoprotein receptor, very low density lipoprotein receptor and low density lipoprotein receptor-related protein 1 (Schuler et al. 2014). All RV-B and around 80% of RV-A use the adhesion molecule ICAM-1 as the receptor for entry so hence are major, whilst the other 20% of RV-A use LDLRs and so are minor (Greve et al. 1989, Hofer et al. 1994, Slater et al. 2010, Schuler et al. 2014). RV-C was only identified in 2006 and uses cadherin-related family member 3 (CDHR3) for binding and replication, with domains 1 and 2 in the transmembrane protein shown to interact with the RV-C viral capsid (Bochkov et al. 2015).

1.2.2. RV Epidemiology

RV infections tend to predominate in the spring, summer and autumn months, with influenza and respiratory syncytial virus (RSV) becoming more prevalent in the winter (Jacobs et al. 2013). The geographical distribution of RV-A, RV-B and RV-C is not restricted to particular regions, and although particular serotypes are more prevalent in certain places (RV-B69 is most prevalent in Asia for example), the most common types of RV circulate worldwide (McIntyre et al. 2013). Most RV infections lead to exhibition of no symptoms at all or only mild clinical symptoms associated with the common cold, such as nasal irritation, mucus production and blocked sinuses, with approximately 10-33% of infections thought to be completely asymptomatic in children (Singeton et al. 2010). Symptoms can worsen however, with a sore throat, cough, headache, fevers and malaise lasting between 7-14 days, and in extreme cases, even possible mortality in the elderly. Despite the majority of these symptoms not being harmful or life-threatening, they are of huge economic burden, with estimated costs of respiratory viral infection (which RV is a large part of) in the UK totalling over £27 million per annum, contributing towards 16% of the overall outlay for respiratory conditions (Truman et al. 2017). RV is also involved in the development of acute otitis media, rhinosinusitis, croup and community acquired pneumonia (Jacobs et al. 2013). There are no approved antiviral agents for the treatment of RV infection currently on the market, primarily due to issues such as drug

toxicity and lack of efficacy (Jacobs et al. 2013). Furthermore, despite the recognition of a need for a RV vaccine, there is currently none available on the market and there are a vast number of challenges, such as a lack of *in vivo* models and difficulty in creating cross-serotype specificity, that need to be overcome to make a vaccine a possibility (Katpally et al. 2009, Edlmayr et al. 2011, McLean 2014).

1.2.3. RV and Asthma Exacerbations

There are many triggers of asthma exacerbations, such as pollution and allergens, but the most common cause are respiratory viral infections, with many studies demonstrating a direct association in asthmatic patients between exacerbations and respiratory viral infection of the airway (Johnston et al. 1995b, Freymuth et al. 1999, Wark et al. 2002, Chauhan et al. 2003, Johnston 2005). In multiple studies investigating exacerbations in children, respiratory viruses were detected in 71.9% (Freymuth et al. 1999), 78% (Chauhan et al. 2003) and 80% (Johnston et al. 1995b) of cases and whilst less clear in adults, one study showed a viral detection rate of 76%, with the presence of the virus associated with acute asthma symptoms (Wark et al. 2002). Respiratory viral infections detected in asthma exacerbations include respiratory syncytial virus and influenza virus, however the most common virus implicated is RV, which is detectable in approximately 60-70% of all virally-induced exacerbations (Garbino et al. 2004, Johnston 2005).

RV infection in children under 3 highly predisposed children to the development of asthma by 6 years of age, and RV had a greater risk factor compared to RSV (Jackson et al. 2008). One study attempted to detect the presence of respiratory viral infections in children aged 9-11 following an asthma exacerbation by polymerase chain reaction (PCR) and culture of the viruses from nasal aspirates. Of the 296 cases, respiratory viruses were present in 226 cases and RV was present in 84 of these (confirmed by PCR), with a further 62 cases also thought to be due to RV. RV is difficult to culture, whereas other respiratory viruses aren't, so those that weren't able to be cultured were assumed to also be RV (Johnston et al. 1995b). There may also be a seasonal influence on the effects of RV-induced asthma exacerbations, as a study demonstrated RV was significantly associated with asthma exacerbations in children in the winter, spring and summer, but not in autumn (Rawlinson et al. 2003). RV-C infection correlates with the most severe forms of asthma, with one study revealing the virus being present in 59.4% of children hospitalised for the acute form of the disease (Bizzintino et al. 2011). Furthermore, in children, boys under the age of 5 are the most susceptible to moderate / severe asthma exacerbations and the most common classification of RV identified in this group is RV-C (Lambert et al. 2017). A study identifying respiratory viruses in adults with asthma identified the presence of respiratory viruses in 114 of 229 nasal or throat swabs taken following an exacerbation, with RV present in 67% of these cases (Nicholson, Kent and Ireland 1993). Another study analysed sputum and nasal lavage fluid (NLF) in adults following the first symptoms of a cold. 52 asthmatic patients were enrolled and of these, 25 suffered an asthma exacerbation, with RV present in 19 of these patients (Denlinger et al. 2011). Although children infected with RV-C more likely to require additional oxygen and to have wheezing symptoms

(Miller et al. 2009), another study determined that RV-A had the highest risk factor of inducing an asthma exacerbation (Denlinger et al. 2011), and thus the severity of symptoms may also be based on other factors independent of RV serotype. A coding single nucleotide polymorphism (SNP; rs6967330, C₅₂₉Y) in the CDHR3 receptor was demonstrated to increase cell surface expression of the receptor, resulting in increased RV-C infection and viral replication in Henrietta Lacks (HeLa) cells (Bochkov et al. 2015), and this epitope has also been linked to recent lethal RV-C outbreak in Ugandan chimpanzees (Scully et al. 2018).

Whilst asthmatic patients are not at a greater risk of respiratory viral infection compared to non-asthmatics, those with the disease do suffer from longer, more persistent infections and have more severe symptoms (Corne et al. 2002). It is still not entirely clear as to why RV infection can induce mass cytokine responses and ultimately asthma exacerbations in asthmatics, whilst in non-asthmatics, RV infections are usually asymptomatic or only produce unremarkable 'cold-like' symptoms. A number of factors could play a role in this, such as inadequate interferon (IFN) production following RV infection; however this is a controversial topic. Primary bronchial epithelial cells (PBECs) from asthmatic patients was revealed to produce less IFN- β messenger RNA (mRNA) at 8 hours and 2.5 times less IFN- β protein at 48 hours post RV-16 infection, compared to that from non-asthmatic controls (Wark et al. 2005). Viral titre released into the supernatant was also significantly increased, resulting in decreased asthmatic cell viability (Wark et al. 2005). IFN- λ was also confirmed to be deficient in PBECs from asthmatic patients at 48 hours, again correlating with increased viral titre and severity of symptoms (Contoli et al. 2006). Interestingly, deficient IFN- α and IFN- β responses to RV-16 seem to not be due to deficiencies in signalling, with no reduction in myeloid differentiation primary response 88 (MyD88), IFN regulatory factor (IRF)3, IRF7 or NF- κ B protein expression observed between asthmatics and non-asthmatics (Sykes et al. 2012). Despite this information suggesting that asthmatics have an IFN deficient response to RV, there is also evidence to the contrary. Bronchial epithelial cells cultured into air liquid interface (ALI) from asthmatics did not display any differences in IFN- β production compared to non-asthmatic controls, following 48 hours RV-16 infection (Lopez-Souza et al. 2009) and PBECs from asthmatic and non-asthmatic individuals displayed no differences in IFN- β mRNA expression 16 hours post-RV-1A infection (Bochkov et al. 2010). It was also demonstrated that no IFN differences were observed in response to RV-1B and RV-16 infection in PBECs from patients with well controlled asthma (Sykes et al. 2014). Whilst IFN deficiencies may exist in asthmatic patients, this may be RV serotype specific and asthma severity specific, among other unknown factors, and needs to be investigated further.

1.2.4. RV Lifecycle and Signalling

1.2.4.1. Pattern Recognition Receptors (PRR) and RV TLR Activation

The main site of RV infection is the bronchus, where the virus encounters AECs. AECs have large amount of pattern recognition receptors (PRRs), including Toll-like receptors (TLRs),

retinoic acid-inducible gene 1 (RIG-I)-like receptors (RLRs) and Nod-like receptors (NLRs) in order to detect pathogens and trigger signalling cascades to provide an immune response (Slater et al. 2010).

TLRs are type 1 transmembrane proteins that contain leucine rich repeats, with 10 types of TLRs described in humans so far (Kawai and Akira 2010). TLRs can be present on the cell surface, (TLR4, TLR5 or a heterodimer of TLR2-TLR1/TLR2-TLR6) or can be expressed in intracellular vesicles, (TLR3, TLR7, TLR8 and TLR9), and as a general rule, cell surface TLRs recognise lipids, lipoproteins or proteins, whereas intracellular TLRs recognise RNA or DNA (Kawai and Akira 2010). Within cell surface or intracellular TLR subclasses, TLRs recognise different pathogen-associated molecular patterns (PAMPs) - for example, TLR4 recognises LPS, whilst TLR5 recognises flagellin (Kawai and Akira 2010). Upon recognition of these ligands (which may require activation of additional co-receptors, such as MD2 for LPS-TLR4 activation), TLRs use their Toll-IL1 receptor domains to initiate downstream signalling pathways. Different TLRs induce different signalling pathways, usually through the activation of NF- κ B or IRF3/7 (Kawai and Akira 2010), described in more detail in Section 1.2.4.2. Human TLRs are summarised in Table 1.1.

Table 1.1. Summary of Human TLRs (Kawai and Akira 2010)

Receptor	Location	Ligands	Signalling Pathways Induced
TLR1	Endoplasmic Reticulum (ER), PM (Heterodimer with TLR2)	Lipoproteins	NF- κ B
TLR2	PM (Heterodimer with TLR1 or 6), Endosome	Lipoproteins, Viral Capsid, Zymosan	NF- κ B, IRF3, IRF7
TLR3	Endosome, ER	Viral RNA	NF- κ B, IRF3
TLR4	PM, ER	LPS, Viral Protein	NF- κ B, IRF3
TLR5	PM	Flagellin	NF- κ B
TLR6	PM (Heterodimer with TLR2)	Lipoproteins	NF- κ B
TLR7	Endosome	Bacterial RNA, Viral RNA	NF- κ B, IRF7
TLR8	Endosome	Viral RNA	NF- κ B, IRF7
TLR9	Endosome	Bacterial DNA, Viral DNA, Parasite DNA	NF- κ B, IRF7
TLR10	Spleen, Lymph Nodes	No Known Ligand	Anti-Inflammatory, Exact Pathway Unknown

RLRs are a family of RNA helicases that function as recognition receptors for viral RNA, and are made up of three receptors, RIG-I, melanoma differentiation-associated protein 5 (MDA5) and laboratory of genetics and physiology 2 (LGP2; Loo and Gale, 2011). They have similar structures, which include caspase activation and recruitment domains, a RNA helicase domain and repressor domains. The receptors are expressed in the cytosol of a large number of cell types (such as AECs), and are usually only expressed in low levels at basal, before being dramatically upregulated in response to viral infection (Loo and Gale, 2011). Upon activation, RLRs specifically induce the expression of anti-viral IFNs in order to help combat viral infection (see Section 1.2.4.2. and 1.2.4.3.). Furthermore, there are 23 NLR human receptors, which primarily recognise bacterial infection and therefore are expressed in a wide range of immune cells, such as macrophages and neutrophils (Franchi et al., 2009). These cells induce the transcription of antimicrobial peptides and inflammatory cytokines, but will not be discussed further as they do not play a role in RV infection.

Many of these PRRs play an important role in recognising RV upon viral entry of the upper or lower airway. RV initially binds to the AECs via ICAM-1, LDLRs or CDHR3 (depending on the serotype of the RV, see Section 1.2.1). Binding to ICAM-1 is thought to induce a conformational change in major type RV, allowing the virus to be internalised (Fuchs and Blaas 2012). TLR2 (associated with TLR1 or TLR6 in a heterodimer) is present on the cell surface and recognises the viral capsid of RV (Triantafilou et al. 2011). Following binding to the cell surface receptors, clathrin mediated endocytosis is most the common route of internalisation in RV infection, but caveolae-dependent and clathrin/caveolae-independent endocytosis also occurs (Snyers, Zwickl and Blaas 2003, Fuchs and Blaas 2012). In clathrin mediated endocytosis, clathrin scaffold protein is assembled alongside other membrane factors such as activator protein-2 (AP-2), which leads the formation of clathrin-coated vesicles (Takei and Haucke 2001, Snyers et al. 2003). Upon internalisation into the cell, the virus is trafficked into the early endosome, where the low pH leads to the uncoating of the virus (Fuchs and Blaas 2012). Once uncoating has occurred, the RNA of the virus is released, host cell transcription is turned off, viral translation occurs and the viral polypeptide is processed rapidly (Whitton, Cornell and Feuer 2005). During this replication, the ssRNA forms a temporary double stranded RNA (dsRNA) intermediate, which can be recognised by TLR3 (Wang et al. 2009). Recently, the endosomal PRRs TLR7 and TLR8 have been suggested to potentially play a role in the recognition of RV in the endosome through recognition of ssRNA, but evidence is currently contradictory (see Section 1.2.3.2.; Parker et al. 2008, Slater et al. 2010, Triantafilou et al. 2011, Hatchwell et al. 2015). Upon exiting the endosome and entering the cell cytoplasm, the RLRMDA5) can detect the dsRNA of RV, whilst another RLR, RIG-I, can detect short dsRNA strands and ssRNA (Slater et al. 2010, Triantafilou et al. 2011).

It is also hypothesised that autophagy may play a vital role in detection and processing of the virus by the innate immune system. Autophagy is the process by which the cell encapsulates its own cytosolic components by autophagosome organelles, in order to be targeted for degradation by hydrolase containing autolysosomes (Parker et al. 2014). There is evidence that

RVs can regulate autophagy in a serotype specific manner that does not distinguish between major and minor type groups, for example, RV-2 (minor) and RV-14 (major) can induce autophagosome formation but RV-1A (minor) cannot (Jackson et al. 2005, Klein and Jackson 2011, Parker et al. 2014). Whilst research using HeLa cells has determined that RV-2 can use autophagy to modulate viral replication and release, evidence of this in human AECs is less clear (Klein and Jackson 2011). Work within our lab demonstrated that autophagy plays next to no role in the cytokine response to RV-1B and RV-16, or viral replication itself in the BEAS-2B cell line, whilst the autophagic pathway may play a role in RV-16 replication and infection in the NCI-H292 cell line and PBECs (Wu et al. 2013, Ismail et al. 2014, Parker et al. 2014, Wu et al. 2015).

1.2.4.2. RV Signalling

The PRRs activated and signalling pathways induced by RV in the airway are summarised in Figure 1.2. The TLR3 pathway is considered to be a primary mechanism of recognising RV and generating an immune response to the virus. TLR3 signalling is Toll-IL receptor domain-containing adapter-inducing IFN- β (TRIF)-dependent; TRIF binds directly to TNF receptor associated factor (TRAF)6, which then activates mitogen-activated protein kinase kinase kinase (TAK1). TRIF also recruits receptor-interacting protein 1 (RIP-1) through tumour necrosis factor receptor type 1-associated death domain protein (TRADD), which then forms a NF- κ B activation complex with TRAF6, TAK1 and Pellino-1 (Kawai and Akira 2010). Pellino-1 is an E3 ubiquitin ligase that is vital for the formation of the activation complex, which then phosphorylates the NF- κ B inhibitor (I κ B) kinase (IKK) complex (Chang, Jin and Sun 2009, Lawrence 2009). As Pellino-1 is independent of IL-1 receptor-associated kinase (IRAK) signalling and is vital for the formation of the IKK complex, it may represent a future therapeutic target, with Pellino-1 knockdown by small interfering RNA (siRNA) able to control harmful inflammation whilst not affecting anti-viral responses (Bennett et al. 2012). The IKK complex comprises of the NF- κ B essential modulator (NEMO), IKK α and IKK β proteins and phosphorylation of NEMO enables IKK β to phosphorylate I κ B (Lawrence 2009). The phosphorylation of I κ B enables the activation of the classic conical p50 and p65 NF- κ B subunits which translocate to the nucleus, inducing both pro and anti-inflammatory cytokines and chemokines such as TNF α , GM-CSF, IL-1 β , IL-6, C-X-C Motif Ligand (CXCL)8, IL-10 and IL-4 (Zhu et al. 1996, Kim et al. 2000, Alexopoulou et al. 2001). The alternative non-conical RelB and p50 subunits are phosphorylated by IKK α , activating genes required for B-cell activation and so is not relevant to RV infection (Senftleben et al. 2001, Lawrence 2009). TLR3 signalling is also responsible for the production of anti-viral IFNs. TRIF and phosphatidylinositol-4,5-bisphosphate-3-kinase (PI3K) are recruited and PI3K phosphorylation assists in the recruitment of TRAF3 and nucleosome assembly protein 1 (NAP1), causing IRF3 activation and type I IFN generation (Matsumoto and Seya 2008).

Upon major-type RV binding to ICAM-1, proto-oncogene tyrosine-protein kinase Src (Src) is activated and spleen tyrosine kinase (Syk) is phosphorylated, inducing clathrin mediated RV endocytosis (Lau et al. 2008). Furthermore, PI3K is activated, converting phosphatidylinositol (3,4)-bisphosphate (PIP₂) lipids to phosphatidylinositol (3,4,5)-trisphosphate (PIP₃). This

conversion allows protein kinase B (Akt) activation by phosphoinositide-dependent kinase-1 (PKD1), inducing NF- κ B signalling and inflammatory cytokine release (Lau et al. 2008, Hemmings and Restuccia 2015). Evidence documenting the signalling pathways induced by minor group RV following binding to LDLRs is not yet complete, but it has been ascertained that the virus has the ability to induce PI3K and Akt to activate NF- κ B signalling (Newcomb et al. 2008). Due to the recent discovery of RV-C, it is currently not yet known if and how CDHR3 initiates signalling pathways following the binding of the virus.

TLR2 stimulation leads to signalling through Toll-IL1 receptor domain containing adaptor protein (TIRAP), recruiting MyD88, a crucial adaptor protein in the production of inflammatory cytokines (Kawai and Akira 2010). MyD88 recruits IRAK4 for initial NF- κ B activation, with IRAK1 and IRAK2 potentiating a longer, more robust activation. IRAK activation then activates TRAF6 and thus TAK1, activating the NF- κ B pathway as described in TLR3 signalling. TAK1 can also activate the MAPK kinases such as extracellular signal regulated kinases (ERK), p38 and c-Jun N-terminal kinases (JNK), activating the transcription factor activator protein 1 (AP-1), which induces cytokines such as IL-2 and TGF- β (Kawai and Akira 2010). TLR2 can also recruit translocating chain-associated membrane protein (TRAM) alongside MyD88 to induce IRF7 and the production of type 1 IFNs (Stack et al. 2014).

TLR7 and TLR8 are phylogenetically similar and both can be expressed in the endosome. When stimulated, TLR7 can recruit MyD88 along with IRAK4 and TRAF6, inducing NF- κ B activation for inflammatory cytokine release and IRF7 activation for IFN release (Kawai and Akira 2010). There is some debate, however, as to whether TLR7/8 is involved in RV recognition and signalling. Studies have demonstrated a decrease in cytokine and chemokine secretion following RV infection when TLR7/8 was silenced in PBECs, and TLR7^{-/-} mice displayed impaired release upon RV-1B infection (Triantafilou et al. 2011, Hatchwell et al. 2015). Despite this, other studies found no evidence of a role for TLR7/8 in RV infection (Parker et al. 2008, Slater et al. 2010) and so whilst Triantafilou's and Hatchwell's findings fits with the knowledge of ssRNA being a natural ligand of TLR7/8 (Kawai and Akira 2010), more investigation is required.

RIG-I and MDA5 trigger downstream signalling through the mitochondrial antiviral-signalling protein (MAVS) which results in IRF3 activation and NF- κ B activation (Seth et al. 2005, Varelle et al. 2011). Studies have begun to reveal the role of these RLRs in RV infection, with both needing to be required in conjunction with TLR3 for maximal IFN- β production, whilst MDA5 activation is required for the production of IFN- λ (Slater et al. 2010). RIG-I and MDA5 are also required in conjunction with TLR3 for maximal inflammatory and anti-viral cytokine and chemokine expression, such as CCL5 and CXCL8 (Slater et al. 2010). MDA5 and RIG-I signalling in response to RV was found to be TLR3/TRIF dependent and this, alongside the fact that MDA5 and RIG-I are not constitutively expressed in PBECs, indicates that they are upregulated on the cells when TLR3 signalling is induced (Slater et al. 2010).

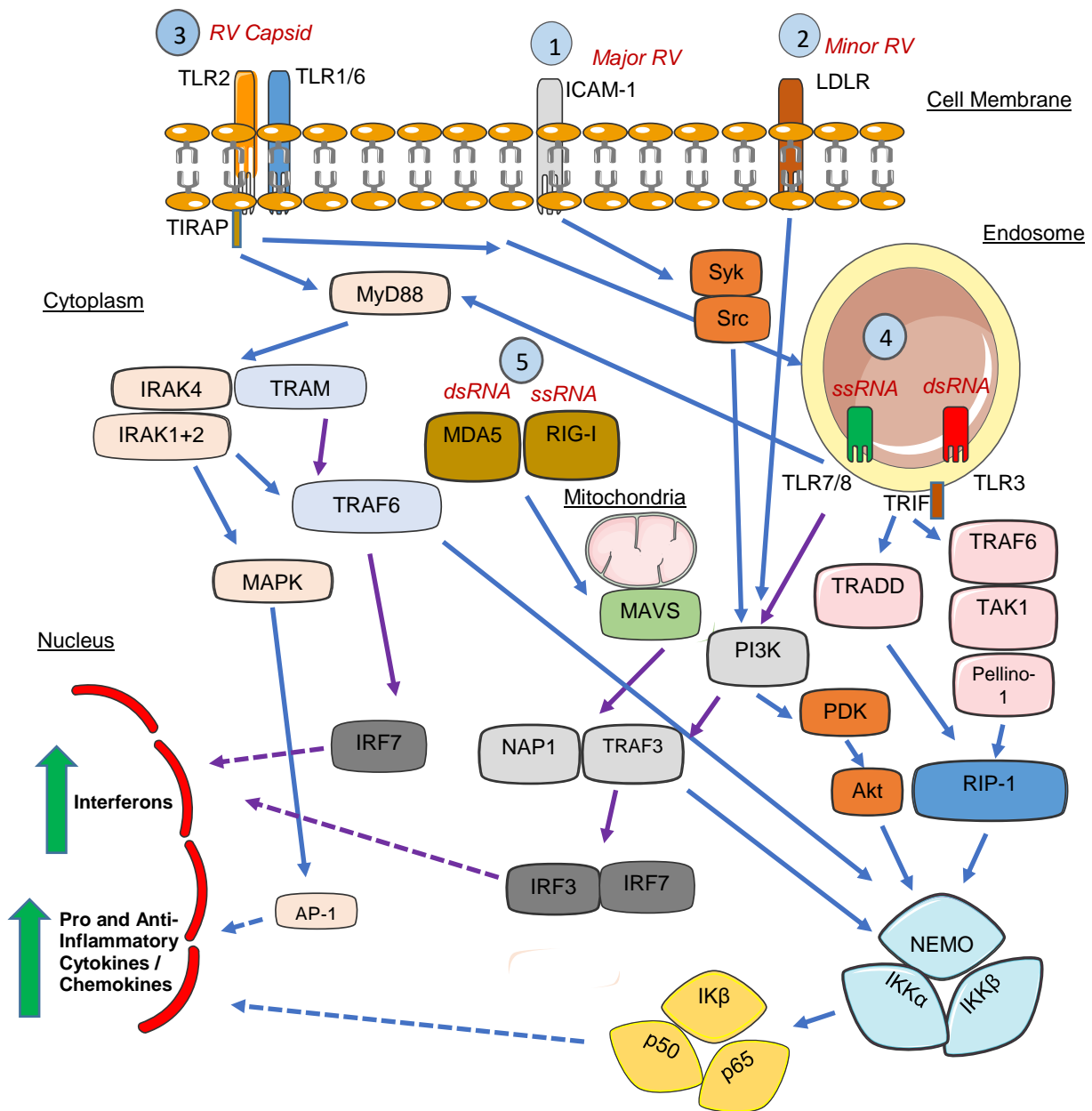


Figure 1.2. The PRRs and Signalling Pathways Involved in RV Infection of AECs.

Major RV bind to ICAM-1 (1) receptors on the cell surface and minor RV bind to LDLRs (2), which can signal through PI3K to induce anti-viral IFNs through IRF3/7 and pro and anti-inflammatory cytokines / chemokines through NF- κ B signalling. TLR2 (3) on the cell surface can recognise the RV capsid and signals through MyD88 to activate the MAPK pathway for AP-1-induced IFN production; TRAF6 for IRF7 induced IFN production or TRAF6-induced NF- κ B signalling. TLR7/8 and TLR3 (4) are located within the endosome and bind to ssRNA and dsRNA respectively, but there is contrasting evidence about whether TLR7/8 play a role in RV infection of PBECs. TL7/8 signals though PI3K for IRF3/7 IFN production and NF- κ B signalling, whilst TLR3 activates RIP-1 through TRADD-TRAF6-TAK1, inducing NF- κ B signalling. The final receptors involved in RV recognition are in the cytoplasm, with MDA5 primarily recognising dsRNA and RIG-I ssRNA (5). These receptors then signal through MAVS, activating NAP1 and TRAF3 for IRF3/7 IFN production and NF- κ B signalling. RV-C signals through the CDHR3 receptor, but as the signalling pathway is unknown, it has not been included. Blue arrows denote cytokine pathways, purple arrows denote IFN pathways and dotted arrows denote translocation to the nucleus. Adapted from Kawai and Akira (2010).

1.2.4.3. Consequences of Pathway Activation in RV Infection

It is also important to note however, that another study indicates that whilst TLR3 and MDA5 have a role in RV signalling, RIG-I does not, as RIG-1 knockdown by siRNA did not decrease cytokines produced in the signalling pathway (Wang et al. 2009). Both studies used the RV-1B serotype, but whilst BEAS-2B cells were used in the Wang study to look at RIG-I signalling, the Slater study used PBECs from healthy non-smokers (Wang et al. 2009, Slater et al. 2010), which could account for the differences in the observed signalling pathways. Furthermore, it cannot be ruled out that there may be a compensatory mechanism that occurs when RIG-I was knocked down in the Wang study, as MDA5 can recognise dsRNA and so could theoretically still produce a sufficient response to RV.

The inflammatory cytokines / chemokines produced through RV-induced signalling pathways have profound effects on the airway, primarily the increased recruitment of inflammatory cells to the airway, and activation of these in order to remove RV (Papi and Johnston 1999, Wark et al. 2005). IL-6 activates T-lymphocytes and augments Ig release (Zhu et al. 1996), whilst CXCL8 is known to recruit neutrophils and eosinophils and can also promote neutrophil degranulation (Johnston et al. 1997). IL-1 β is also produced in response to RV-induced caspase 1 activation and is required for RV-induced CXCL8 and IL-6 release (Piper et al. 2013). CCL5, also known as 'regulated on activation, normal T-cell expressed and secreted' (RANTES), promotes the recruitment of Th2 cells and eosinophils (Chun et al. 2013) and GM-CSF is required for proliferation, activation and differentiation of macrophages and dendritic cells (Francisco-Cruz et al. 2014). IL-33 recruits Th2 cells and innate lymphoid cells; IL-13 regulates monocyte and B-cell maturation and proliferation, and IL-17 is a chemotactic agent for monocytes and neutrophils (McKenzie et al. 1993, Aggarwal and Gurney 2002, Jackson 2014). Furthermore, many of these cytokines can have anti-inflammatory roles, and specific anti-inflammatory cytokines are also released. IL-4 can inhibit TNF α , IL-6, CXCL8 release, whilst IL-6 also downregulates TNF α (Libert et al. 1994, Wang et al. 1995, Opal and DePalo 2000). IL-10 is an anti-inflammatory cytokine which can inhibit cytokine release in neutrophils and natural killer (NK) cells, p50/p65 translocation to the nucleus, TNF α receptor function and the transcription of pro-inflammatory cytokines (Joyce et al. 1994, Clarke et al. 1998, Opal and DePalo 2000).

There are 3 types of IFNs: IFN-I, IFN-II and IFN-III (Levy, Marie and Durbin 2011). IFN- α and IFN- β are type I IFNs, IFN- γ is a type II IFN and IFN- λ 1, IFN- λ 2 and IFN- λ 3 are type III (Cakebread et al. 2011). Once activated by respiratory viruses (including RV), they induce the janus kinase-signal transducer and activator of transcription (JAK/STAT) pathway, inducing a number of processes that are vital for the anti-viral response, which is primarily focused on the inhibition of viral polypeptides (Samuel 2001, Cakebread et al. 2011, Levy et al. 2011). Protein Kinase R (PKR) is an anti-viral RNA dependent protein kinase that is upregulated by IFN- α and IFN- β and also has a role in stabilising IFN- α and IFN- β expression following infection (Kuhlen and Samuel 1999, Williams 1999, Williams 2001, Schulz et al. 2010). The main role of PKR is to phosphorylate eukaryotic initiation factor 2 (eIF2), blocking guanosine diphosphate (GDP) to guanosine triphosphate (GTP) exchange, which is vital for mRNA synthesis and therefore viral

replication is inhibited (Gale and Katze 1998). 2',5' oligoadenylate synthetase 1 (OAS1) can be induced by IFNs (including IFN- α) and generates 2',5'-linked oligoadenylate (2-5A), activating RNase L, which has the ability to degrade viral RNA and stop viral protein synthesis (Rutherford, Hannigan and Williams 1988, Choi et al. 2015). Inducible nitric oxide synthase (iNOS) is induced by IFNs (including IFN- γ) and can inhibit cytokines generated by respiratory viral infection, as well as limiting viral replication (Karupiah et al. 1993, Sanders et al. 1998). The mechanism behind the anti-viral properties of iNOS varies depending on the virus type, but has been demonstrated in enteroviruses to inhibit the viral cysteine protease (Saura et al. 1999). It should be noted however, that IFN-inducible proteins can also be modulated by viruses (for example RV has the ability to downregulate OAS1 gene expression following infection) and can be potentially harmful in response to viral infections, with PKR found to be vital in the induction of pro-inflammatory cytokines following RV infection (Edwards et al. 2007, Graser et al. 2016).

RV has also been implicated with the deposition of ECM proteins important in airway remodelling. RV-2 and RV-16 infection of PBECs and fibroblasts induced perlecan and collagen V protein deposition, and was demonstrated to be TLR3 and TLR7 dependent in fibroblasts (with TLR7 stimulation inducing the most deposition) and TLR3 dependent in PBECs (Kuo et al. 2012). Furthermore, RV-1B infection of C57BL/6 mice induced lung FN mRNA expression between 24-96 hours and collagen I at 48 hours. RV-72 infection of A549 cells (a human alveolar basal epithelial cell line) also induced mRNA expression of a number of ECM proteins such as fibrinogen, transferrin, VEGF, thrombomodulin, matrix metalloproteinase and complement factor H (Etemadi et al. 2017). Despite no observed change in tenascin-C (TN-C) protein expression in PBECs in response to RV (Kuo et al. 2012), gene array analysis was carried out on nasal scrapings from adults infected with RV-16, revealing a 2.8-fold increase in TN-C mRNA (Proud et al. 2008).

1.3. Tenascin-C

1.3.1. The Tenascin Family of Proteins

The human TN family are ECM proteins that are distinct to vertebrates and made up of four proteins – TN-C, TN-R, TN-W and TN-X (Jones and Jones 2000a, Hsia and Schwarzbauer 2005). The TN family of proteins were first shown to modulate the adhesive properties of the target molecules they bind to, but since then have been revealed to be involved in a number of other functions such as cell signalling and disease (Jones and Jones 2000b, Midwood et al. 2016). Table 1.2. summarises the alternate names, cellular localisation, chromosome number located on, and diseases that the human TN proteins are implicated in (Chiquet-Ehrismann and Tucker 2004, Midwood and Orend 2009, Merke et al. 2013, Morawski et al. 2014).

Table 1.2. Summary of Human Tenascins

Protein	Alternate Names	Localisation of Protein Expression	Human Chromosome Located On	Diseases Implicated In
Tenascin-C	Cytotactin, Glioma associated ECM antigen, J1 220/200, Neuronectin, Hexabrachion	Bones, Cartilage, Nervous System, Tendon, airway smooth muscle, Tumours, Wounds	9 (9q33)	Asthma, Cancer, Rheumatoid Arthritis (RA) Inflammatory Bowel Disease (IBD), Chronic Inflammation, Atherosclerosis
Tenascin-R	Janusin, Restrictin	Nervous System	1	Potential Role in Neurological Disorders Such as Epilepsy, Schizophrenia, Addiction
Tenascin-W	Tenascin-N	Bones, airway smooth muscle	1	Cancer, Osteogenesis
Tenascin-X	N/A	Skeletal Muscle	6	Ehlers-Danlos Syndrome

There is strong evidence that TN-C is implicated in the pathogenesis of asthma and is therefore of primary interest for my PhD. As such, this study will now focus on TN-C only.

1.3.2. TN-C Structure and Function

1.3.2.1. TN-C Function

TN-C is an ECM protein that was first identified in 1983 when it was found to be associated with gliomas and other cancerous cell types (Bourdon et al. 1983). The protein is named after two of the main sites where it is expressed, tendons (Latin – *tenure*, meaning to hold) and the embryo (Latin – *nasci*, meaning to be born; Chiquet-Ehrismann et al. 1986, Midwood et al. 2016). As TN-C is a large, multi-domain glycoprotein, it has the ability to interact with a vast number of targets through a myriad of different mechanisms, and therefore the protein does not in theory have one primary function. TN-C modulates the adhesive properties of the target cells (including fibroblasts, FN and keratinocytes), through a number of different interactions: such as cell adhesion molecule interactions and syndecan binding (Tan et al. 1987, Jones and Jones

2000b). For example, TN-C can modulate the adhesion of FN by binding to the proteoglycan syndecan-4 through its glycosaminoglycan chains. This inhibits co-receptor function of syndecan-4 in FN-induced integrin signalling, and FN loses its adhesive properties. Furthermore, TN-C FNIII domain-dependent inhibition of syndecan-4 has also been implicated in inducing tumour cell proliferation and metastasis, highlighting the importance of these interactions in cancer (Huang et al 2001). TN-C is highly expressed in the embryo and is involved in embryonic development (Midwood and Orend 2009). TN-C knockdown in chick embryos (using antisense oligonucleotides) abrogates normal neural crest development and TN-C KO mice displayed myelin degradation but enhanced growth of axons, thus indicating the importance of TN-C in a functional and organised neuronal pathway (Cifuentes-Diaz et al. 1998, Tucker 2001). TN-C is also important in skeletogenesis. For example, in cartilage, a TN-C layer lies directly below syndecan-3 (a cell surface heparin sulphate proteoglycan)-rich chondrocytes, with this interaction vital in cartilage development and integrity (Koyama et al. 1995). The quantity of TN-C drops dramatically during adulthood and has the primary function of being involved in wound healing and repair, with the initial work demonstrating that TN-C becomes abundant in the affected tissue just 24 hours after the initial wound (Mackie, Halfter and Liverani 1988). During this process, the protein aids in the recruitment of endothelial cells, keratinocytes and fibroblasts that control the wound healing by inducing the migration of these cells (Midwood and Orend 2009). TN-C null mice have defects in wound healing, exhibiting lower FN levels and keratinocyte numbers in corneal tissue in response to both linear perforation wounds and nylon suture wounds (Matsuda et al. 1999). Another important role of TN-C is in tissue neovascularisation, where it modulates endothelial cell shape and migration (Chung, Murphy-Ullrich and Erickson 1996, Carmeliet 2000). TN-C can also induce different signalling pathways involved in cell proliferation, cell survival, cellular recruitment and inflammation through binding to TLRs, integrins and other receptors (Midwood et al. 2016). There is vast evidence documenting that the function of TN-C differs depending on a number of factors, including: the tissue the protein is expressed in, the disease state of the tissue and which domain TN-C is signalling through.

1.3.2.2. The Domains of TN-C

The size of the TN-C protein ranges between 180-330 kDa and is composed of four main domains: tenascin assembly (TA) domain, EGF-like repeats, fibronectin type III (FNIII)-like repeats and fibrinogen-like globe (FBG) domain (Figure 1.3). Individual TN-C polypeptides can form a hexabrachion (a six armed structure which enables enhanced protein stability and allows the protein to interact with more molecules), with the TA domain facilitating this interaction through terminal cysteine residues (forming disulphide bonds) and heptad repeats (forming hydrophobic interactions; Conway and Parry 1991, Jones and Jones 2000b, Giblin and Midwood 2015). The 14.5 EGF-like repeats contain six cysteine residues which form disulphide bonds with target molecules.

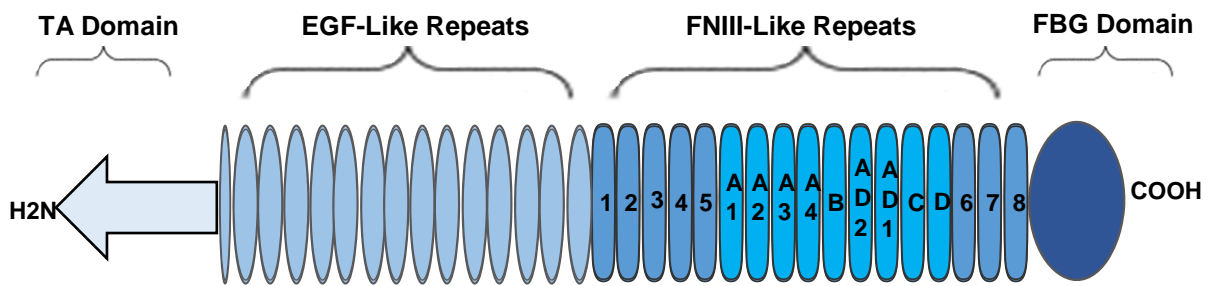


Figure 1.3. The Structure of Tenascin-C

The human form of the TN-C can range from 180 kDa to 330 kDa and is comprised of different distinct domains: the TA domain, EGF-like repeats, FNIII-like repeats and a FBG domain (Midwood and Orend 2009). There are 14.5 EGF-like repeats which are each around 30-50 amino acids in length (and are stabilised by disulphide bonds between cysteine residues) and the FBG domain is a large single protein of around 210 amino acids (Bonizzi and Karin 2004, Midwood and Orend 2009). There can be up to 17 FNIII domains (determined by alternative splicing) which are made of anti-parallel beta strands (90 amino acids long). FNIII-A1–FNIII-D are the alternatively spliced domains, with FNIII-1–FNIII-5 and FNIII-6–FNIII-8 being the constant domains. The alternative splicing in the FNIII domains is extremely important on protein function and varies depending on the localisation of the protein; it is thought TN-C can vary by the size of up to nine domains (Latijnhouwers et al. 2000, Matsuda et al. 2005, Midwood and Orend 2009). The size and function of TN-C can also be modified by glycosylation, with 26 N-linked and 34 O-linked glycosylation sites present. Adapted from Midwood and Orend (2009).

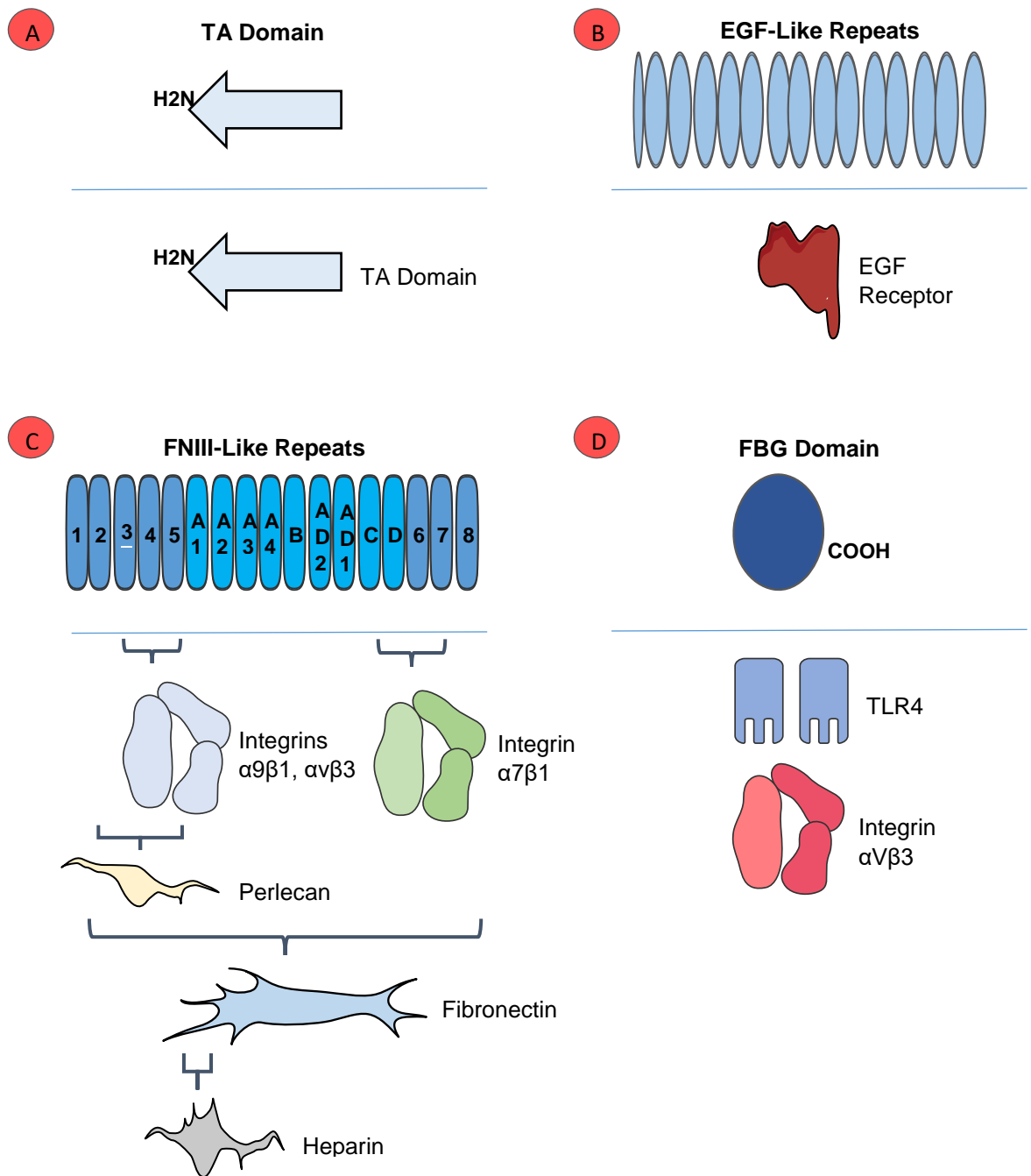


Figure 1.4. TN-C Domains and Binding Partners Involved in Signalling

TN-C is a large multi-domain glycoprotein that has the ability to bind to and induce signalling pathways through a large number of targets. The N-terminal TA domain **(A)** binds to another five TA domains, forming a six-armed oligomer called a hexabrachion. The EGF-like repeats **(B)** have the ability to bind to EGF receptor, inducing a range of responses in multiple cell types, including inducing cell migration in melanoma cells by modulating cell adhesion. The FNIII-like **(C)** domains can bind to multiple integrins, including $\alpha 9 \beta 1$, $\alpha v \beta 3$ and $\alpha 7 \beta 1$, inducing inflammatory pathways and adhesion modulation. The FNIII-like domains can also bind to a number of proteins including perlecan, FN and heparin and modulate the function and adhesion of these proteins. Finally, the FBG domain **(D)** binds to TLR4 and integrins such as $\alpha v \beta 3$, inducing inflammation and cell proliferation.

These repeats can bind to, and induce anti-adhesive properties in, fibroblasts, neurons and glia and therefore this interaction is assumed to be vital in the development of the central nervous system (CNS; Prieto, Anderssonfison and Crossin 1992, Fischer et al. 1997, Jones and Jones 2000b). The FNIII-like repeats are an extended beta structure that are highly elastic, and this elasticity is purported to allow the revealing and hiding of domains allowing interactions with ligands such as integrins (Erickson 1994, Oberhauser et al. 1998, Jones and Jones 2000b). The FBG domain has a calcium binding loop and a globular fibrinogen-like domain and has been demonstrated to bind to a large number of different molecules, such as TLR4, integrins, collagen and other ECM proteins (Jones and Jones 2000b, Midwood et al. 2009, Midwood and Orend 2009). The binding partners of each TN-C domain are summarised in Figure 1.4.

1.3.2.3. Alternative Splicing and Glycosylation

TN-C can differ by a size of approximately 140 kDa due to two main mechanisms, alternative splicing and glycosylation, and these are vital to both the structure and function of TN-C. Alternative splicing of TN-C was first discovered in the late 1980s (Jones et al. 1988, Gulcher et al. 1989), and this has since been expanded much further – the FNIII repeats contain eight ‘constant’ repeats which are always present in the TN-C protein and nine ‘splice’ repeats which can be present or absent, depending on the post-translational alternative splicing of the protein (Giblin and Midwood 2015). Up to 95% of protein coding genes in humans are alternatively spliced and the mechanism of alternative splicing occurs in two main steps (Wang et al. 2015). First, a spliceosome forms following signalling pathway activation that consists of small nuclear ribonucleic proteins, exonic splicing enhancers and intronic splicing enhancers. Secondly, depending on the enhancers recruited to the spliceosome, certain introns are then excised from the RNA and exons ligated to form pre-mRNA with particular TN-C domains included or omitted (Wang et al 2015).

The eight constant repeats are FNIII-1, FNIII-2, FNIII-3, FNIII-4, FNIII-5, FNIII-6, FNIII-7 and FNIII-8 and the nine splice repeats are FNIII-A1, FNIII-A2, FNIII-A3, FNIII-A4, FNIII-B, FNIII-additional domain (AD)-2, FNIII-AD1, FNIII-C and FNIII-D. There are theoretically 511 possible human splice variants of TN-C, but currently only approximately 100 have been discovered, potentially due to certain ‘rules’ of expression, including AD2 only being expressed alongside AD1, FNIII-C only alongside FNIII-D, and there is no documentation of FNIII-A4 and C being linked together (Mighell et al. 1997, Joester and Faissner 2001, Giblin and Midwood 2015). Alternative splicing can lead to variations in the molecular weight of the TN-C protein (each FNIII domain is approximately 10 kDa), which can lead to expression of distinct small and large variants. The definition of small and large variants can differ depending on the study and so for the purpose of this study, small variants will be defined as approximately 180-250 kDa and large as transcripts above 250 kDa.

The specific variants and splice domains expressed in different tissues are too vast to fully explain in this study but are summarised in Giblin and Midwood (2015). As a general rule (there

are exceptions however), small variants of TN-C are predisposed towards modulating adhesion during embryogenesis (in rats and mice, there is limited evidence in humans) and are involved in the wound healing response, whereas larger isoforms are thought to be associated in diseases such as RA, malignant tumours and inflammation (Borsi et al. 1992, Ghert et al. 2001b, Page et al. 2012). The smallest TN-C variant (with no alternatively spliced domains) has been demonstrated to bind strongly to FN and induce cell adhesion through the formation of focal adhesions, whereas the larger variants have been revealed to be anti-adhesive (Zisch et al. 1992, Ghert et al. 2001b, Giblin and Midwood 2015). Furthermore, FNIII-B, FNIII-D and FNIII-AD2 and FNIII-AD1 are associated with breast cancer malignancy, and the quantity of FNIII-AD2 and FNIII-AD1 may be a predictor of tamoxifen resistant tumours (Guttery et al. 2010). The FNIII-C domain also has a strong association with poor disease prognosis; it is linked with high grade (III) astrocytoma and glioblastoma tumours, thyroid carcinomas, proliferating cells and is absent in healthy tissues (Carnemolla et al. 1999, Tseleni-Balafouta et al. 2006).

Both experimental evidence and predictive software analysis of the protein has indicated that TN-C has 26 putative *N*-linked and 34 *O*-linked glycosylation sites present (Taylor et al. 1989, Gulcher et al. 1990, Steentoft et al. 2013, Giblin and Midwood 2015). Evidence on the functions of the extensive glycosylation of the protein is currently sparse, with current studies focused on one glycosylation epitope only, human-NK-1 (Yagi et al. 2010, Giblin and Midwood 2015). The human NK-1 epitope is present on many glycosylated proteins and is present on TN-C variants containing the splice domains FNIII-A1, FNIII-A2, FNIII-A4, FNIII-B, FNIII-C and FNIII-D, where it was demonstrated to regulate the proliferation of neural stem cells (Yagi et al. 2010). Further roles of glycosylation on TN-C have been predicted through the investigation of the effects glycosylation has on FN, an ECM protein that closely associated with TN-C *in vivo*. Glycosylation was demonstrated to protect FN from proteolytic degradation, as well as modulating the adhesive properties of the protein, potentially by masking the domains and making them unable to bind to target cells or proteins (Sano et al. 2007, Giblin and Midwood 2015). Further investigation is needed, but it can be predicted that the glycosylation of TN-C is a nuanced mechanism that allows greater control over the function of the protein (Giblin and Midwood 2015) and may explain why TN-C is differentially glycosylated depending on the location of expression.

1.3.3. Pathways of Tenascin-C Upregulation

TN-C is upregulated in tissues via a number of different pathways. The protein has a TATA box promoter that has a number of binding sites for transcription factors such as E26 transformation-specific (ETS), focal adhesion kinase (FAK) and Smad2/3 (Chiquet-Ehrismann et al. 1994, Watanabe et al. 2003, Tucker and Chiquet-Ehrismann 2009). TN-C can also be upregulated by mechanotransduction and hemodynamic stress, but the two most well established inducers of TN-C are the cytokines TGF- β 1 and TNF α (Goh et al. 2010, Imanaka-Yoshida and Aoki 2014).

TGF- β 1 is secreted as an inactive precursor by immune cells such as eosinophils, macrophages and mast cells and it is then activated by the removal of latency associated peptide 1 by proteins such as MMP-9 (Makinde et al. 2007). Once activated, TGF- β 1 can induce TN-C expression either through the MAPK / ERK pathway (binding to ETS on the promoter) or through the Smad2/3 binding sites (Makinde et al. 2007). In the latter pathway, further work revealed that the Smad3/4, specificity protein 1, ETS1 and cAMP-binding protein (CBP)/p300 are also involved in this upregulation (Jinnin et al. 2004). TNF α has been demonstrated to induce TN-C expression through ETS1 promoter activation by the NF- κ B / p65 pathway. A number of studies identified this mechanism through abolishment of ETS1 activation in chondrocytes, and by both bacterial lipopolysaccharide (LPS) stimulation and TNF α stimulation of primary human myeloid cells (Nakamura et al. 2004, Nakoshi et al. 2008, Goh et al. 2010). Furthermore, TN-C has the ability to induce TNF α expression in synovial membrane cells and thus TN-C expression can be regulated by an autocrine inflammatory loop pathway, with the protein itself acting as a danger associated molecular pattern (DAMP) at its focal point (Midwood et al. 2009, Goh et al. 2010). The upregulation of specific variants of TN-C depends on a large number of factors such as cell type, tissue location and disease state but it seems that cytokines are an integral part of this mechanism. TGF- β 1, for example, has been demonstrated to induce small variants of TN-C (with no alternatively spliced domains) in endometrial adenocarcinoma cells, but can also induce large variants (Vollmer et al. 1997). In human skin cells, TNF α induced smaller TN-C variants, IL-4 induced equal amounts of small and large variants, whereas IFN- γ preferentially induced large variants of the protein (Latijnhouwers et al. 2000).

As previously mentioned, despite the important roles of TN-C in development and tissue regulation, the upregulation of the protein is also implicated in a large number of disease states.

1.3.4. The Role of Tenascin-C in Disease and Chronic Inflammation

TN-C has been demonstrated to be vital in the metastatic niche in cancers such as breast and lung cancer, where it is thought to assist with tumour survival and metastasis through adhesion modulation (Minn et al. 2005, Matei, Ghajar and Lyden 2011). TN-C is also implicated in the pathogenesis of IBD, atherosclerosis and cardiovascular disease (CVD; Riedl et al. 2001, Minear et al. 2011, Machino-Ohtsuka et al. 2014), but this study will focus on the role of TN-C in inflammation and asthma, which is most pertinent to the research aim.

The inflammatory role of TN-C has been extensively researched in RA, where it has been demonstrated to be expressed in areas of tissue damage in the rheumatoid joints (such as the synovial membrane) and play a vital role in joint inflammation. Exogenously added recombinant TN-C induced CXCL8 and TNF α in primary human synovial membrane cells, with the FBG domain of the protein potentiating the inflammatory response through the TLR4-MyD88 pathway (Midwood et al. 2009). In addition, TN-C KO mice were protected from sustained inflammation following injection with zymosan (an inducer of acute synovitis), with no cell aggregates present or proteoglycan loss (Midwood et al. 2009). One study investigating the presence of TN-C in the

joints of RA patients revealed that there was raised levels of circulating TN-C compared to non-RA controls, significantly more TN-C in late stage RA samples compared to the early stages of the disease, and that levels of TN-C expression correlated with joint erosion (Page et al. 2012). Furthermore, RA patients with high TN-C levels of expression in the joint were predicted to respond poorly to infliximab treatment, with unresolved joint tenderness (Page et al. 2012). It also seems that citrullinated residues in the FBG domain (conversion of arginine into citrulline) correlates with RA pathogenesis, with between 40-50% of RA patients having anti-citrullinated FBG antibodies compared to 3-6% of patients with non-RA arthritis or patients who recovered from their symptoms (Raza et al. 2016, Schwenger et al. 2016). This biomarker can also be detected years prior to RA diagnosis (18% detection rate in pre-RA sera) and therefore could be a useful biomarker to predict the onset of the disease (Schwenger et al. 2016). TN-C is also important in the regulation of pathogen induced TLR4 inflammation, with TN-C^{-/-} mice displaying no symptoms 1.5 hours after LPS infection, compared to sepsis, weight loss and diarrhoea in the WT control (Piccinini and Midwood 2012). TNF α was significantly reduced in these TN-C^{-/-} mice, and a bone marrow engraftment from WT mice rescued synthesis of this cytokine. Furthermore, *in vivo* LPS stimulation of bone-marrow-derived macrophages (BMDMs) from TN-C^{-/-} mice released significantly less TNF α , IL-6 and CXCL1 and more of the anti-inflammatory cytokine IL-10. It was determined that TN-C mediates the transcription of these cytokines through inducing microRNA (mir)-155 expression, as mir-155 was inhibited in TN-C^{-/-} BMDMs in response to LPS and overexpression of mir-155 in these cells rescued the TNF α response (Piccinini and Midwood 2012).

The TLR4 signalling pathway has been previously well described in response to LPS stimulation (Kawai and Akira 2010), but the TLR4 pathway in response to FBG is not fully understood, and may differ from the LPS-TLR4 pathway. For example, the co-receptor MD2 is vital for LPS-TLR4 stimulation, whilst it is not required for FBG-TLR4 stimulation (Midwood et al. 2009). FBG-TLR4 signalling has been determined to be MyD88 dependent (Midwood et al. 2009), induce JNK and p38 MAPKs (Piccinini et al. 2016) and cause nuclear translocation of the NF- κ B p65 protein (Nakoshi et al. 2008). As the full downstream effects of FBG-TLR4 stimulation is not yet known, the main LPS-TLR4 pathway is described in Figure 1.5., with the current knowledge of the FBG pathway highlighted within this.

TN-C can also induce inflammatory cytokine release, cellular recruitment and cellular proliferation through binding to integrins, such as α 9 β 1, α 4 β 1, α 5 β 1 and α v β 3. A gene expression study of synovial tissues from murine arthritic joints following LPS stimulation revealed an increase in the α 9 integrin and TN-C (Kanayama et al. 2009). Addition of TN-C to murine synovial fibroblasts and macrophages induced a large range of cytokines, including IL-6, TNF α , MMP-9 and IL-1 α , and these effects were ablated with either addition of an anti- α 9 antibody, or by stimulation with a recombinant TN-C that was unable to bind to the α 9 integrin (Kanayama et al. 2009). α 9 integrin mediated signalling is thought to be vital in Th17 cell generation, recruitment of the cells to synovial tissues and development of arthritis (Kanayama et al. 2011), and therefore TN-C is integral in this mechanism. Another study revealed that TN-C and the integrin α 9 β 1 are significantly increased in synovial fibroblasts and macrophages in RA

patients compared to patients with osteoarthritis (OA). Additionally, the stimulation of these cells with all the FNIII domains of TN-C induced significant fibroblast proliferation and significant induction of MMP-1, MMP-3, MMP-13 and IL-6, and blockade of the $\alpha 9$ integrin ablated this effect (Asano et al. 2014). Depletion of TN-C or $\alpha 9$ from fibroblast-like synoviocytes from RA patients also suppressed the pro-inflammatory phenotype of the tissues, blocking the phosphorylation of FAK and decreased MMP-1, MMP-3 and IL-6 (Emori et al. 2017). TN-C can also bind to the $\beta 1$ integrin through FNIII-1-5 (and not through FNIII-A-D and 6-8), inhibiting $\alpha 4\beta 1$ and $\alpha 5\beta 1$ mediated T-cell binding to FN, and thus modulating T-cell adhesion, migration and activation (Hauzenberger et al. 1999). Finally, TN-C can bind to $\alpha v\beta 3$ through the FBG domain, inducing IL-6 and TNF α release (Shimojo et al. 2015), as well as inducing tyrosine kinase phosphorylation and therefore target cell proliferation, which is an important feature in the immune response (Jones and Jones 2000b).

1.3.5. Tenascin-C and Viral Infections

More recently, TN-C has been documented to be a human immunodeficiency virus-1 (HIV-1) neutralising agent, reducing viral transmission to children in the breast milk of infected mothers (Fouda et al. 2013). It was demonstrated that TN-C binds to the cluster of differentiation (CD)4 epitope on the V3 loop of the gp120 envelope (Env) protein of the HIV-1 virus, which is vital for the virus to bind to the CD4 receptor on CD4+ T-cells (Ivanoff et al. 1992). The ability of TN-C to block this epitope therefore means HIV-1 infectivity is reduced, blocking infectivity *in vitro* by up to 66% (Fouda et al. 2013). It was also demonstrated that this neutralising interaction occurs in an electrostatically charged manner (as adding sodium chloride significantly reduced binding) and that the neutralising site may overlap a chemokine co-receptor (Fouda et al. 2013). Further investigations into TN-C and other viruses have observed no relationships or interactions, however.

1.3.6. Tenascin-C and Asthma Pathogenesis

Airway remodelling is a mechanism that contributes towards the pathogenesis of asthma (see Section 1.1.2), with the thickening of RBM and airway smooth muscle, leading to reduced airflow and difficulty in breathing (Roche et al. 1989). A vital part of this process is fibrosis of the RBM, with ECM proteins such as collagen, FN and TN-C deposited and contributing towards the thickening of the airway (Royce et al. 2012). An important study by Laitinen et al. (1997) demonstrated that the presence of TN-C in the RBM of asthmatics was significantly increased compared to non-asthmatic controls. Furthermore, the severity of asthma correlated with TN-C thickness in the RBM: those with chronic asthma had greater TN-C thickness than patients with seasonal asthma. Interestingly, six weeks budesonide treatment (a commonly used inhaled asthmatic treatment) significantly reduced the presence of TN-C compared to the placebo control treatment (Laitinen et al. 1997). Further investigation of bronchial biopsies revealed that the presence of TN-C was present in greater quantities in atopic asthmatic patients compared to non-atopic asthmatic patients and non-asthmatic controls (Amin et al. 2000), with similar results also demonstrated by Karjalainen et al (2003).

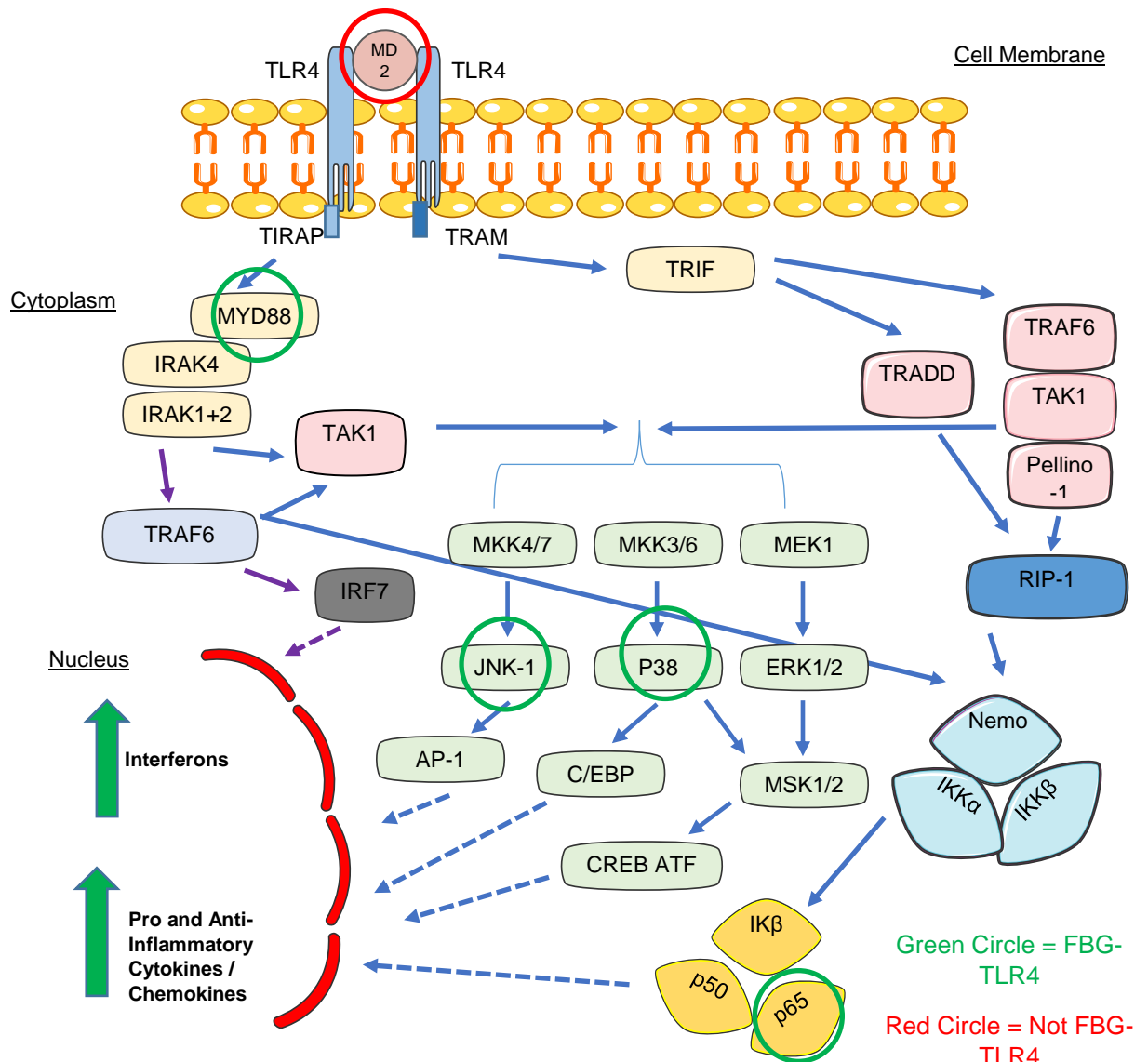


Figure 1.5. The TLR4 Signalling Pathway

FBG binds to the TLR4 PRR independent of the MD2 co-receptor (Midwood et al. 2009), whilst LPS requires MD2 for TLR4 activation. The downstream pathways following FBG-TLR4 activation are not fully known, so the LPS-TLR4 pathway is described. TIRAP, MyD88, TRAM and TRIF are recruited, inducing both the MyD88 and TRIF-dependent pathways. In the MyD88 pathway, IRAK1, 2 and 4 are recruited, activating TRAF6 and generating IRF7 IFN production and NF- κ B signalling. The MAPK pathway is also induced by TAK-1, with the MAPKs endoplasmic reticulum resident J-domain protein (ERJ) 1/2, p38 and JNK activated by phosphorylation of MAPK kinases. These then activate AP-1, CCAAT-enhancer-binding proteins (C/EBP), mitogen and stress activated kinases (MSK)1/2 and cAMP Response Element-Binding Protein (CREB) activating transcription factors (ATF) transcription factors, inducing IFN and cytokine / chemokine production. The TRIF-dependent pathway also induces the MAPK pathway, as well as NF- κ B signalling through the TRADD-TRAF6-TAK1-RIP-1 complex. Whilst the FBG pathway is not fully described, it is known to be MyD88 dependent (Midwood et al. 2009) and induce MAPK (Piccinini et al. 2016) and NF- κ B p65 signalling (Nakoshi et al. 2008). Those circled in red do not occur in FBG-TLR4 signalling and those circled in green have been confirmed to occur in FBG-TLR4 signalling. Adapted from Kawai and Akira (2010).

TN-C expression was revealed to be upregulated in the RBM in atopic asthmatics 24 hours after challenge with methacholine (a bronchospasm inducer), before decreasing back to basal levels at day 7 (Kariyawasam et al. 2007). A Japanese case-control study of 12 adult asthmatic patients and 12 non-asthmatic controls investigated the SNPs of TN-C, revealing 62 genetic polymorphisms within the TN-C region (Matsuda et al. 2005). Further investigation using computational modelling revealed a substitution of the 1677th amino acid in the FNIII-D domain from leucine in the non-asthmatics to isoleucine in the asthmatic population. This isoleucine is located in the beta sheet of the FNIII-D domain, and the substitution is hypothesised to result in steric hindrance and an increase in the stiffness of the protein and thus the asthmatic airway. Furthermore, Th2 airway remodelling cytokines such as IL-4 and IL-13 were demonstrated to upregulate TN-C expression in human lung fibroblasts (Matsuda et al. 2005).

Despite the evidence implicating TN-C in the process of airway remodelling, there is much less direct research describing the role of TN-C as an inducer of inflammation in the airway. The most prominent study in this area compared the airway inflammatory phenotype of TN-C^{-/-} mice (generated by lacZ gene insertion) sensitised to ovalbumin (Ova; an *in vivo* model of allergic asthma) and WT Ova mice (Nakahara et al. 2006). The TN-C^{-/-} Ova mice had significantly lower airway hyperresponsiveness as measured by both Penh value and airway pressure, and when investigated further, it was determined these mice had decreased total cell counts and eosinophil counts in the BALF and less cellular infiltrate in the peribronchial areas. Furthermore, the TN-C^{-/-} Ova mice had decreased goblet cells and there was significant decrease in monocyte chemoattractant protein (MCP)-1, MMP-9, IL-5, IL-13 and IgE in the BALF. In the same study, recombinant TN-C was added to mouse splenic lymphocytes, inducing IL-5, IL-13, IFN- γ and IgE (Nakahara et al. 2006), however crucially, TN-C was not added to any epithelial cells or immune cells originating from the mouse airway. A study investigating the presence of TN-C in the airway of asthmatics revealed a positive correlation between the thickness of TN-C and the number of mast cells present in bronchial biopsies, but only in atopic asthmatic patients and not non-atopic asthmatics (Amin et al. 2000). An additional study investigated bronchial biopsies taken from 63 asthmatic patients, revealing that RBM TN-C thickness correlated positively with the presence of activated eosinophils, macrophages, CD3⁺, CD4⁺ (in atopic asthmatics only) and CD8⁺ T-cells (in atopic and non-atopic asthmatics), but not mast cells or neutrophils (Karjalainen et al. 2003). A correlation was also revealed between TN-C expression in atopic asthmatics following allergen challenge with cellular inflammation, but, despite this, there was no correlation between TN-C expression and AHR (Kariyawasam et al. 2007). Finally, it was demonstrated that reducing eosinophils by treatment with IL-5 inhibitor mepolizumab also reduced TN-C expression in the RBM (Lambrecht and Hammad 2012). Although it is known that inflammatory cells (such as eosinophils) can cause deposition of TN-C, and that TN-C can also induce the recruitment of inflammatory cells, it is not clear whether TN-C is primarily a driver or consequence of inflammation in the airway in asthma.

Thus, there is detailed evidence implicating TN-C as a contributor towards the thickening of the airway in the airway remodelling phase of asthma. TN-C is also a known inducer of chronic inflammation (in other diseases such as RA) and the presence of TN-C correlates with the

presence of inflammatory cells in the airway of asthmatics. However, despite this, direct and causal evidence of TN-C inducing inflammation in the human airway is currently unavailable, and it is therefore important that further research investigating the ability of TN-C to induce inflammation in the airway is undertaken.

1.4. The Role of Extracellular Vesicles (EV) in Asthma

1.4.1. EV Formation, Structure and Function

As the research into the mechanisms responsible for the pathogenesis of asthma progresses, it is becoming clear that EVs may also have an integral role. There are three main classifications of EVs: exosomes, microvesicles (MVs) and apoptotic bodies, with exosomes and MVs the most pertinent to this project (Figure 1.6.). The endosomal sorting complex required for transport (ESCRT) is the mechanism behind EV formation (Budnik et al. 2016). The ESCRT is required for transporting proteins for degradation to the lysosome and EVs (known as intraluminal vesicles whilst intracellular) are formed by inward budding during this process. Over 30 proteins comprise the ESCRT complex such as ESCRT-0, which starts a recruitment cascade - ESCRT-I is recruited to the endosome, recruiting ESCRT-II and ESCRT-III. ESCRT-III assembles into a long protein that coils around the budding vesicle and causes the pinching and budding from the endosome, and vacuolar protein sorting-associated protein-4 (VPS4) and alpha-1,3-mannosyltransferase (ALG-2) interacting protein x (ALIX) causes the disassembly and degradation of ESCRT-III (Budnik et al. 2016). All four ESCRT protein complexes consist of a number of proteins with a number of different function and these are summarised in Table 1.3.

Table 1.3. Proteins Involved in the ESCRT Pathway (Budnik et al. 2016)

Complex	Comprised Of:	Role
ESCRT-0	Hepatocyte growth factor-regulated tyrosine kinase substrate (HRS), signal transducing adaptor molecule (STAM)	Clusters proteins for ubiquitination, binds to PIP ₃ and recruits ESCRT-I
ESCRT-I	Tumour susceptibility gene 101 (TSG-101), (VPS)37, VPS28, ubiquitin associated protein 1 (UBAP1)	Clusters ubiquitylated proteins, establishes binding between ESCRT-0 and ESCRT-II, remodels membranes and recruits ESCRT-III
ESCRT-II	VPSNF8, VPS26, VPS36	Establishes binding of ESCRT-0 and ESCRT-I to ESCRT-III
ESCRT-III	Charged multivesicular body proteins (CHMP) 2, CHMP7, VPS-IST1	Causes vesicle formation and budding by causing pinch of membrane

It has been recently proposed that EVs can also form due to lipid-dependent mechanisms, which are independent of the ESCRT complexes (Budnik et al. 2016). Sphingomyelin (catalysed

into sphingomyelin synthase), ceramide and sphingosine-1 phosphate are thought to be vital in this process, with sphingosine and phosphatidylcholine metabolism implicated in initiating changes in membrane curvature (Budnik et al. 2016). Furthermore, it has been demonstrated that upon EVs leaving the cell and reaching a target cell, they are internalised by macropinocytosis and clathrin-independent endocytosis (Verdera et al. 2017).

Exosomes and MVs have the role of delivering contents, including mRNA proteins and lipids, to surrounding cells, which is vital for cell homeostasis and communication (Valadi et al. 2007, Bakhti, Winter and Simons 2011, Raposo and Stoorvogel 2013). Apoptotic bodies differ from exosomes and MVs in that they form to allow phagocytosis and removal of pathogens, DAMPs and other material during apoptosis (El Andaloussi et al. 2013). The research field of EVs is particularly dynamic, with the criteria for EV classification constantly changing, but currently, EVs are classified based on their cellular origin, size and/or function (El Andaloussi et al. 2013). Exosomes can range from 30-120 nm in size and originate from the endocytosis pathway. They form multi-vesicular bodies (MVBs) from endosomes, which then fuse with the plasma membrane (PM), and are actively released in a process that is dependent on GTPases (Raposo et al. 1996, Hsu et al. 2010, Vlassov et al. 2012, El Andaloussi et al. 2013). Due to being of endosomal origin, exosomes contain tetraspanins (such as CD9 and CD63), exosomal protein trafficking proteins (such as ALIX and TSG-101), GTPases, flotillin-1 and lipids (Conde-Vancells et al. 2008, Vlassov et al. 2012), however, the composition of exosomes can differ depending on cell type and location in the body. MVs range in size between 100-1000 nm and are formed when they bud directly from the PM, which may be controlled by adenosine diphosphate (ADP)-ribosylation factor 6 (ARF6; Muralidharan-Chari et al. 2009, El Andaloussi et al. 2013, Raposo and Stoorvogel 2013). The composition of MVs is dependent on the PM they arise from and thus there are currently no commonly accepted markers, although CD40-L can be present (Cantaluppi et al. 2012, El Andaloussi et al. 2013). Apoptotic bodies can range in size from 500-2000 nm, contain a large presence of phosphatidylserine, have a permeable membrane and are produced in response to controlled cell death by apoptosis (El Andaloussi et al. 2013). Whilst exosomes, MVs and apoptotic bodies are essential for maintaining cell homeostasis and communication, they are also implicated in a vast range of diseases. Exosomes are involved in cancer (Ji et al. 2013, Greening et al. 2016), diseases of the CNS such as Parkinson's (Kong et al. 2014) and asthma (Sastre et al. 2017), MVs in CVD (Jansen et al. 2014), cancer (Al-Nedawi et al. 2009) and lung epithelial inflammation (Lee et al. 2016) and apoptotic bodies in IBD (Araki et al. 2010) and prostate cancer (Aihara et al. 1994).

Furthermore, TN-C has been previously demonstrated to present in exosomes isolated from colorectal cancer cell lines (Ji et al. 2013), in TIMPless exosomes produced from cancer-associated fibroblasts (Ferrari and Calvo 2014) and from malignant mesothelioma cell-derived exosomes (Greening et al. 2016), with the theory that TN-C-rich EVs contribute to the metastatic phenotype of these cells.

1.4.2. EV Isolation and Characterisation

EV biology is a new and dynamic field that is constantly being revised as novel information is being uncovered. As such, the standards and practices employed in this study affirm to the current guidelines set out by the Journal of Extracellular Vesicles (Lotvall et al. 2014) and responses from other scientists prominent in the field (Witwer et al. 2017). There are currently four main established methods of EV isolation from blood, serum or supernatant, each that come with their own advantages and disadvantages and are summarised in Table 1.4.

Table 1.4. EV Isolation Methods (Konoshenko et al. 2018)

Type of Isolation	Description	Advantages	Disadvantages
Differential Ultracentrifugation	Exosome containing liquid is differentially centrifuged four times, with each pellet containing a different fraction (described in Figure 2.2.).	Large yield, large sample capacity, reduced cost (if ultracentrifuge is already present) , no contamination with other reagents, good for EV functional assays.	Purity is questionable, exosome damage can occur, variability in yield, poorer for EV characterisation, ultracentrifuge is expensive if have to purchase.
Size Exclusion Chromatography	Molecules, including EVs, are separated by chromatography based on size	Higher purity than ultracentrifugation, good reproducibility.	Moderate purity overall, shear stress induces EV deterioration, small yields and loss of yields common, needs dedicated equipment.
Precipitation	Addition of precipitation reagents such as Exoquick aim to pellet exosomes only	Easy to use, large sample capacity.	Poor purity as other proteins and contaminants are co-precipitated.
Immunoaffinity Capture	Anti-epithelial cell adhesion molecule-coated magnetic beads bind to exosomes and 'capture' them from the suspension and can then be eluted from the beads	Highly purified.	High cost, low capacity and yield, hampers immune recognition.

As with EV isolation, EV characterisation is also a complicated topic. Firstly, exosomes and MVs have a size crossover, and thus a distinction between these two vesicle subsets cannot be

determined by size analysis only. Furthermore, exosomes are composed of a number of proteins, but specific exosome composition depends on a number of factors such as cell type and disease setting, and so are said to be exosome enriched proteins, rather than markers. MVs may also contain proteins that are present in exosomes and have no definitive markers, thus it is difficult to definitively distinguish between the two subsets on protein composition alone. It is therefore standard to characterise EVs by two methods, one that characterises by size, and one that characterises by protein composition. EV characterisation methods are summarised in Table 1.5.

Table 1.5. EV Characterisation (Szatanek et al. 2017)

Method	Description	Advantages	Disadvantages
Nanoparticle Tracking Analysis (NTA)	Uses light scattering and Brownian motion to calculate EV size in nm	Accurate measurement of the concentration and size of EVs, small amounts of sample needed	Groups vesicles into set nm sizes for ease of displaying the data, machines are expensive, time consuming
Western Blot	Detects specific protein presence in a EV suspension (e.g. CD9)	Can detect specific protein content, can check for intracellular protein contamination	Cannot distinguish between membrane associated and internal proteins, limited amount of protein per sample can be measured
Flow Cytometry	Fluorescently labelled proteins can be detected and analysed by using a laser to emit light at varying wavelengths. Vesicle size can also be measured	Large number of proteins per sample can be measured, can potentially distinguish between internal and membrane associated proteins	Less accurate for calculating size than NTA, larger sample size required,
Tunable Resistive Pulse Sensing	Similar to NTA, but allows EVs one at a time through a nm specific pore to calculate size	More accurate than NTA at determining EV size	Very expensive, time consuming, larger amount of sample required

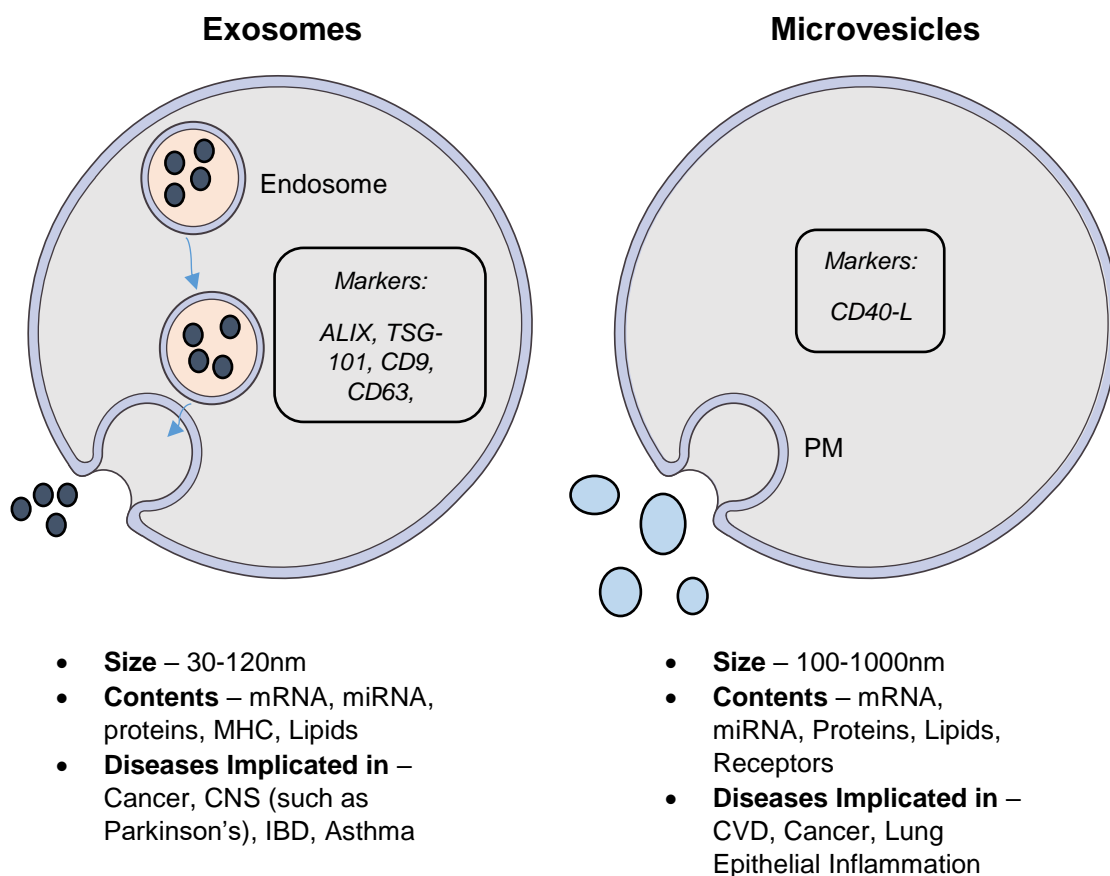


Figure 1.6. The Classification of Exosomes and MVs

The two main subsets of EVs are exosomes and MVs. Exosomes are between 30-120 nm in size and originate from the endosomal pathway, where they fuse with the PM and are released. ALIX, TSG-101, CD9, CD63 and flotillin-1 are all commonly accepted markers of exosomes, which carry and deliver mRNA, miRNA, proteins (including viral proteins), major histocompatibility complex (MHC) and lipids to surrounding cells and tissues. MVs are formed directly from the PM, where the vesicles form and bleb away from the membrane. MVs range from 100-1000 nm in size and there are no commonly accepted markers, although CD40-L is thought to be present. MVs have a similar role to exosomes, delivering mRNA, miRNA, proteins, lipids and receptors to surrounding cells during cell signalling and homeostasis. Exosomes are implicated in cancer, CNS diseases, IBD and asthma, whereas MVs are implicated in cardiovascular disease, cancer and lung epithelial inflammation. Adapted from El Andaloussi et al. 2013 and Raposo and Stoorvogel (2013)

1.4.3. The Roles of EVs in Enterovirus Infection

It is clear that despite the extensive evidence uncovered from *in vitro* studies of RV replication, there is still a lot of information left to uncover about the RV lifecycle. For example, despite viral egress during *in vitro* RV infection inducing cell cytotoxicity through cell lysis, RV infection of the AECs of patients *in vivo* does not always lead to loss of cell viability (Blaas and Fuchs 2016). Further research into enteroviral infection has revealed EVs as a potential candidate in facilitating this non-lytic viral spread (Robinson et al. 2014, Chen et al. 2015, Altan-Bonnet 2016). CVB infection of neural stem/progenitor cells and C2C12 myoblast cells induced the release of fluorescently tagged viral proteins in EVs, and some of these EVs attached to neighbouring uninfected cells. Furthermore, the EVs were found to harbour virus that had the ability to be infectious (rather than non-infectious viral proteins), EV-associated CVB was more infectious than non-EV-associated CVB, and transmission electron microscopy revealed an EV size of between 100-150 nm, the size of exosomes / small MVs (Robinson et al. 2014). Another study investigated both the efflux of poliovirus and CBV following infection of HeLa cells and it was revealed that 7 hours post-poliovirus infection, 85% of viral capsid proteins had co-localised with LC3-II and been released non-lytically from cells within phosphatidylserine (PS) lipid enriched vesicles (Chen et al. 2015). Interestingly, the vesicular size differed from the previous study with a size of 250-350 nm, but this difference could be due to the different cell types infected. Fluorescent microscopy revealed the presence of mature poliovirus and CVB viral proteins following infection, as did analysis of the vesicles for the poliovirus VP2 protein by western blot. Additionally, comparison of the infectivity of EV-associated poliovirus and non-EV-associated poliovirus revealed that there was a 40% increase in viral proteins present in the cell in response to EV-associated poliovirus infection. Finally, viral RNA was transferred into the cell via EVs, suggesting that the virus had the ability to replicate inside the new target cell (Chen et al. 2015).

Whilst investigated much less extensively than CVB and PV infection, the RV protein VP2 was also demonstrated to be present (by western blot) in PS lipid enriched vesicles following 8 hours RV infection of HeLa cells (Chen et al. 2015). As RV particles are approximately 30 nm in size and EVs can range between 50-1000 nm, it is feasible that EVs theoretically can contain hundreds of viral particles each (Altan-Bonnet 2016, Raab-Traub and Dittmer 2017). As EVs are internalised and used to deliver contents to surrounding cells, hijacking of the host EV system would be an effective transmission pathway.

1.4.4. The Roles of EVs in Asthma and Airway Inflammation

There is growing evidence that exosomes are a key player in airway inflammation and asthma pathogenesis. A comparison of BALF taken from patients with mild allergic asthma or non-asthmatic controls, revealed that exosomes from asthmatic patients had significantly increased enzymes for LT biosynthesis (important in bronchoconstriction and mucus secretion), such as LTA₄H (Paredes et al. 2012). Furthermore, *in vivo* mouse studies revealed that the BALF of

Ova-sensitised mice contained significantly more exosomes than sham mice controls, and that reduction of exosome secretion by the inhibitor GW4869 reduced airway hyperresponsiveness, serum IgE levels and cytokines such as IL-4, IL-5 and IL-13 (Kulshreshtha et al. 2013). Another study isolated and analysed exosomes obtained from the BALF of patients with mild asthma and non-asthmatic controls, and revealed substantial differences in the miRNA profile of the exosomes between the two groups, with 24 differentially regulated miRNAs identified (Levanen et al. 2013). For example, there was a 1.9-fold increase in miR-200b in exosomes isolated from asthmatic patients, which has been implicated in EMT (Gregory et al. 2008, Levanen et al. 2013). Furthermore, miR-let7b and miE-let7c regulate IL-13 expression (implicated in airway inflammation, fibrosis and mucus metaplasia), and were both increased 1.5-fold in asthmatic exosomes (Kumar et al. 2011, Levanen et al. 2013). Other miRNAs identified are involved in the regulation of IL-10, CXCL8 and IL-6, as well as regulation of the MAPK/ERK and JAK-STAT pathways, thus implicating exosomes in contributing to the upregulation of the inflammatory signalling pathways in asthma. Infiltration of eosinophils in the lungs and the release of eosinophilic inflammatory mediators occurs in the chronic phase of asthma pathogenesis, and recent research has attributed roles for exosomes in these processes (Mazzeo et al. 2015). IFN- γ stimulation of eosinophils *in vitro* induced exosome production, and eosinophils from asthmatic patients produced significantly more exosomes than healthy controls, suggesting that eosinophils contribute to the production of pro-inflammatory exosomes in the lung (Mazzeo et al. 2015). Furthermore, exosomes from the NLF of asthmatic patients contained increased biologically active iNOS (which is a vital enzyme upregulated during inflammation of the airway epithelium) and MUC5B and MUC57 (vital proteins in mucus hypersecretion), as well as filaggrin and hornerin (vital for the epithelium integrity and function; Lasser et al. 2016).

MVs have also recently been implicated in lung epithelial inflammation. Hyperoxia-induced oxidative stress (an established model of lung injury in mice) induced MV release into the BALF of mice and analysis of the MVs revealed that miR-320a and miR-221 were upregulated (Lee et al. 2016). MVs isolated from mouse primary lung epithelial cells that were directly transfected with miR-320a and 221 and then used to stimulate THP1 macrophages were found to induce TNF α and MMP9 release and cell migration. Furthermore, BEAS-2B MVs isolated following hyperoxia damage induced TNF α and IL-1 β release in THP1 macrophages, as well as cell migration (Lee et al. 2016).

The study of the effects of EVs on the pathogenesis of asthma is a dynamic field, with it becoming clear that EVs, particularly exosomes, have an important role in potentiating airway inflammation in asthmatic patients. Subtle changes to the miRNA profile and composition of cargo within exosomes can lead to upregulation of inflammatory cytokines and inflammatory cell chemotactic agents, as well as a decrease in proteins that protect airway epithelium cell integrity. Exosomes, therefore, must be considered as a potential therapeutic target in the treatment of asthma and airway inflammation, and the relationship between RV infection and EVs needs to be investigated further.

1.5. Project Aims

RV-induced exacerbations of asthma are poorly understood and further research is required to elicit the underlying mechanisms in order to help combat this phenomenon. Furthermore, the fact that 5-10% of patients with asthma have severe, untreatable asthma highlights the lack of effectiveness of current asthma medication, and therefore there is a high priority need for the development of new medicines for novel targets.

TN-C is an ECM protein that is already established in the pathogenesis of asthma, having an integral role in the process of airway remodelling, with the thickness of TN-C correlating with the severity of the disease. In diseases such as RA, TN-C is a DAMP, inducing inflammatory cytokines (such as TNF α and IL-6), and a study of TN-C in a mouse model of asthma highlighted that TN-C KO mice sensitised to Ova had reduced airway hyperresponsiveness compared to WT sensitised mice. Despite this, there are no studies that have directly investigated the inflammatory potential of human TN-C in the airway. TN-C has also previously been shown to associate with HIV-1, reducing the infectivity of the virus, but there is no further evidence of TN-C interacting or being involved with other types of viral infection. Furthermore, despite the fact that RV induces cytokines vital in asthma pathogenesis such as TGF- β 1 (involved in airway remodelling) and TNF α (involved in inflammation), and that these cytokines are known transcriptional regulators of TN-C, there has been a lack of research examining the direct relationship between TN-C expression and RV infection in the airway. Currently, the only indication of a relationship between TN-C and RV is from the Proud et al. (2008) study, which indicated a 2.8-fold upregulation in TN-C mRNA expression in nasal scrapings taken from adults infected with RV-16.

Furthermore, EVs and in particular exosomes are also known to contribute towards inflammation in asthma, may be vital in the infectivity of RV and have been demonstrated to contain TN-C in other diseases such as cancer. Despite this, there is no currently scant information on the quantity, composition and function of AEC exosomes following RV infection.

My hypothesis is that RV infection of AECs induces the expression and release of TN-C. I further hypothesise that the over-expression of this protein contributes towards the increased inflammatory cytokine and chemokine released observed during RV-induced exacerbations of asthma. Furthermore, I hypothesise that RV infection induces AEC exosomal release that has the capacity to induce inflammation in the airway, due to RV-induced changes in exosomal composition, such as TN-C.

This study will aim to answer 4 main questions:

- How is TN-C expression and release regulated by RV infection of AECs from both non-asthmatic and asthmatic patients?
- What are the mechanisms behind RV-induced TN-C expression and release?
- How is AEC EV release regulated by RV infection?

- What is the role of TN-C and RV-induced EVs in the consequent inflammation and anti-viral response?

The aims of this study will be answered by the following objectives:

- Measuring overall and splice specific TN-C mRNA and protein expression by qPCR and western blot following RV infection of non-asthmatic and asthmatic AECs.
- Measuring overall and splice specific TN-C release by ELISA and western blot following RV infection of non-asthmatic and asthmatic AECs.
- Investigating whether non-specific cell death can induce TN-C release in AECs
- Measuring EV concentration, size and protein composition (including TN-C) by western blot and NTA analysis following viral stimulation of AECs
- Stimulation of AECs and macrophages with full length TN-C, TN-C-FBG and virally stimulated EVs both high and low in TN-C expression.

The data generated will potentially provide evidence of a novel mechanism between TN-C expression in the airway and RV infection. The study will also determine whether TN-C and RV induced EVs have the capacity to induce inflammatory cytokine / chemokine release in the airway, which would identify the protein or EV pathway as a future therapeutic target in the treatment of asthma.

Chapter 2: Materials and Methods

2.1. Materials

Table 2.1. Cells

Name (Supplier)	Species / Disease State	Seeding Density ($\times 10^6/\text{ml}$)	Doubling Time (Hours)
BEAS-2B Cells (ATCC)	Human / Healthy	1.0-1.5	18-24
PBECs (ATCC) PBECs (Imperial College London)	Human / Healthy Human / Atopic Asthmatic (AA)	0.75-1 0.75-1	24-26
HeLa-Ohio (ATCC)	Human / Healthy	0.05-0.5	23
Human Dermal Fibroblasts (ATCC)	Human / Healthy	0.05-0.5	18-24
Human Embryonic Kidney (HEK)-293:pCEP-huTNC-his (University of Strasbourg)	Human / Healthy	0.05-0.5	34
Human Peripheral Blood Monocyte-Derived Macrophages (MDMs)	Human / Healthy	0.3-1	18-22

Table 2.2. Cell Culture (Non-Viral Work)

Name	Composition (Supplier)	Application
Fibroblast Culture Media	Roswell Park Memorial Institute medium (RPMI; Gibco), Supplemented with 10% Fetal Calf Serum (FCS; PromoCell),	Fibroblast Culture
HEK-293 Culture Media	Dulbecco's Modified Eagle Media (DMEM; Thermo Fisher Scientific), Supplemented with 10% FCS and 2.5 $\mu\text{g}/\text{ml}$ Puromycin (Sigma-Aldrich)	HEK-293 Culture
HEK-293 Collection Media	DMEM and 2.5 $\mu\text{g}/\text{ml}$ Puromycin	HEK-293 Collection
MDM Culture Media	RPMI Supplemented with 3-5% FCS and 1% Penicillin-Streptomycin (Pen-Strep; Sigma-Aldrich)	MDM Culture

Table 2.3. Cell Culture Media (Viral Work)

Name	Composition (Supplier)	Application
BEAS-2B Complete Media / EV-Depleted Complete Media*	RPMI, Supplemented with 10% FCS and 1% Pen-Strep	BEAS-2B Cell Culture
BEAS-2B Basal Media / EV-Depleted BEAS-2B Basal Media*	RPMI, Supplemented with 2% FCS and 1% Pen-Strep	BEAS-2B Serum Starve
PBEC Basal Media	Airway Epithelium Cell Basal Medium (PromoCell) Supplemented with 1% Pen-Strep	PBEC Serum Starve
PBEC Complete Media / EV-Depleted PBEC Complete Media**	Airway Epithelium Cell Basal Medium Supplemented with 1% Pen-Strep, 0.004 ng/ml Bovine Pituitary Extract (PromoCell), 10 ng/ml Recombinant Human EGF (PromoCell), 5 µg/ml Recombinant Human Insulin (PromoCell), 0.5 µg/ml Hydrocortisone Epinephrine (PromoCell), 6.7 ng/ml Triiodo-L-Thyronine (PromoCell), 10 µg/ml Transferrin Holo (PromoCell) and 0.1 ng/ml Retinoic Acid (PromoCell)	PBEC Cell Culture
PBEC Recovery Media / EV-Depleted PBEC Recovery Media**	Airway Epithelium Cell Basal Medium Supplemented with 1% Pen-Strep, 10 ng/ml Recombinant Human EGF, 5 µg/ml Recombinant Human Insulin, 0.5 µg/ml Hydrocortisone Epinephrine, 6.7 ng/ml Triiodo-L-Thyronine 10 µg/ml, Transferrin Holo, and 0.1 ng/ml Retinoic Acid (PromoCell).	PBEC Culture After RV Infection
HeLa-Ohio Complete Media	DMEM (Gibco) Supplemented with 10% FCS, 1% Pen-Strep, 1% Non-Essential Amino Acids and 1% L-Glutamine (Gibco).	HeLa Cell Maintenance
HeLa-Ohio Infection Media	DMEM, Supplemented with 2% Hepes, 1% Bicarbonate (Gibco), 2% FCS and 1% Pen-Strep	HeLa Cell Infection

* - Centrifuge and filter FCS prior to use (see Section 2.11.)

** - Centrifuge Media prior to use (see Section 2.11)

Table 2.4a. Buffers

Name	Composition (Supplier)	Application
Enzyme-Linked Immunosorbent Assay (ELISA) Coating Buffer (pH 7.2-7.4)	0.14 M NaCl (VWR), 2.7 mM KCl (Sigma-Aldrich), 1.5 mM KH ₂ PO ₄ (BDH) and 8.1 mM Na ₂ HPO ₄ (VWR)	ELISA
Cytokine / Chemokine ELISA Wash Buffer (pH 7.2)	0.5 M NaCl, 2.5 mM NaH ₂ PO ₄ (VWR), 7.5 mM Na ₂ HPO ₄ , 0.1% Tween-20 (Fisher Scientific) and pH to 7.2 with NaOH (Thermo Fisher Scientific)	ELISA
Running Buffer 10x	30.3 g Tris/Trizma Base (Thermo Fisher Scientific), 144 g Glycine (Thermo Fisher Scientific), 10 g Sodium Dodecyl Sulphate, (SDS; Sigma-Aldrich) and 1 L H ₂ O (MilliQ)	Western Blot
Running Buffer 1x	100 ml of 10x Stock and 900 ml H ₂ O	Western Blot
Transfer Buffer 10x	29 g Tris/Trizma Base, 145 g Glycine and 1 L H ₂ O	Western Blot
Transfer Buffer 1x	80 ml of 10x Stock, 200 ml Methanol (VWR) and 720 ml H ₂ O	Western Blot
Phosphate Buffered Saline (PBS)-0.1 / 0.5% Tween-20	10 PBS Tablets (Oxoid), 1 L of H ₂ O and 1 ml / 5 ml Tween-20	Western Blot
5% Bovine Serum Albumin (BSA)/Tris Buffered Saline (TBS)-0.1% Tween-20	0.5 g BSA (Sigma-Aldrich), 50 ml TBS (Sigma-Aldrich) and 1 ml Tween-20	Western Blot
Phosphatase Lysis Buffer	50 mM Tris/Trizma Base, 1% Triton x-100 (Sigma-Aldrich), 50 mM NaF (Sigma-Aldrich), 1 mM Phenylmethylsulfonyl Fluoride (PMSF; Sigma-Aldrich), 50 mM β-Glycerophosphate (Sigma-Aldrich), 10 mM Sodium Orthovanadate (Sigma-Aldrich) and 1% Protease Inhibitor (Calbiochem)	Harvesting Protein
4x Sample Buffer	4% SDS, 0.1 M Dithiothreitol (Sigma-Aldrich), 20% Glycerol (VWR), 0.0625 M Tris-Cl (Baxter), 0.004% Bromophenol Blue (Baxter) and 2.175 ml H ₂ O	Protein Extraction & Western Blot

Table 2.4b. Buffers (continued)

Name	Composition (Supplier)	Application
3.8% Paraformaldehyde (PFA)	360 ml dH ₂ O, 40 ml 10x PBS (Heat to Boiling) and 15.2 g PFA (Sigma-Aldrich; Adjust to pH 6.9)	Microscopy
0.2% Triton X-100	1x PBS and 0.2% Triton X-100 (VWR)	Microscopy
Blocking Buffer	1x PBS, 5% Goat Serum (Sigma-Aldrich) and 1% BSA	Microscopy
4',6-Diamino-2-Phenylindole (DAPI)	1x PBS, DAPI (1:200; Thermo Fisher Scientific) and 2% BSA	Microscopy
Antibody Dilution Buffer (ADB)	1x PBS and 1% BSA	Microscopy
MTT	5 mg MTT (Thermo Fisher Scientific) in PBS (Sterile and Filtered)	Cell Viability
Solubilising Solution	10% SDS and 0.01 M Hydrochloric Acid (Thermo Fisher Scientific)	Cell Viability
2x Basic Buffer (BB)	500 mM Na Phosphate pH 7.4, 900 mM NaCl and 0.02% Tween	Purification
1x BB	500 ml 2x BB and 500 ml H ₂ O	Purification
Washing Buffer	1x BB and 20 mM Imidazole pH 7.0 (Thermo Fisher Scientific)	Purification
Equilibration Buffer (EQB)	1x BB, 20 mM Imidazole pH 7.0 and 500 mM Urea in H ₂ O	Purification
Washing Buffer 0.1% Triton-X114	100 ml Washing Buffer and 100 µl Triton-X114 (Sigma-Aldrich)	Purification
Elution A	1x BB and 300 mM Imidazole pH 7.0	Purification
Elution B	1 x BB and 500 mM Imidazole 7.0	Purification
5 x Storage Buffer	250 mM Boric Acid pH 8.0 (Sigma-Aldrich) and 750 mM NaCl	Purification
10x TN Buffer	0.5 M Tris pH 8 and 1.5 M NaCl	Purification
1 x TN Buffer	100 ml 10x TN Buffer and 900 ml H ₂ O	Purification

Table 2.5. SDS-Polyacrylamide Gel Electrophoresis (PAGE) Gels

Reagent (Supplier)	Amount (ml) 10% Resolving Gel (15ml)	Amount (ml) 6% Resolving Gel (15ml)	Amount (ml) 5% Stacking Gel (4ml)
H ₂ O (MilliQ)	5.9	7.9	2.7
30% Acrylamide Mix (GeneFlow)	5.0	3.0	0.67
1.5mM Tris (pH 8.8; Bio-Rad)	3.8	3.8	N/A
1.0mM Tris (pH 6.8; Bio-Rad)	N/A	N/A	0.5
SDS (Panreac)	0.15	0.15	0.04
10% Ammonium Persulfate (APS; Fluka)	0.15	0.15	0.04
Tetramethylethylenediamine (TEMED; Sigma Aldrich)	0.006	0.012	0.004

Table 2.6. Commercially Available Kits

Name	Components (Supplier)	Application
DNA-Free DNase Treatment & Removal	10x DNase I Buffer, rDNase I, DNase Inactivation Reagent (Ambion)	mRNA Extraction
High Capacity Complementary Deoxyribonucleic Acid (cDNA) Reverse Transcription Kit	10x Reverse Transcriptase Buffer, 25x Deoxyribonucleotide Triphosphate Mix (100mM), 10x Reverse Transcriptase Random Primers, MultiScribe Reverse Transcriptase, RNase Inhibitor, Nuclease-Free Water (Applied Biosystems)	cDNA Synthesis
Quantitative PCR (qPCR) 2x Master Mix Plus	qPCR Master Mix (Eurogentec)	TaqMan RT-qPCR
Power SYBR Green PCR Master Mix	SYBR Green qPCR Master Mix (Thermo Fisher Scientific)	SYBR Green RT-qPCR
Bicinchoninic Acid Assay (BCA)	BCA Standard and Working Reagent (WR; Bio-Rad)	Protein Concentration
ELISA Kit for TN-C (N-Terminal TN-C)	ELISA Plate Coated with Anti-TN-C Antibody and Secondary Anti Mouse TN-C Antibody (Cloud Corp)	Overall TN-C ELISA
TN-C Large (FNIII-B) ELISA	ELISA Plate Coated with Anti-TN-C Antibody (FNIII-B) and Secondary Anti Mouse TN-C Antibody (IBL)	FNIII-B ELISA
Limulus Amebocyte Lysate (LAL) Test	LAL Standard, LAL Test Substrate and Stop Solution (Lonza)	Test For LPS Concentration

Table 2.7. TaqMan RT qPCR Primer Probes

Name	Sequence 5'-3'	Supplier (Code)
Glyceraldehyde 3-Phosphate Dehydrogenase (GAPDH) Forward	ACTTTGGTATCGTGGAAGGAC	Applied Biosystems (Hs02758991_g1)
GAPDH Reverse	TGGTCGTTGAGGGCAATG	Applied Biosystems (Hs02758991_g1)
TN-C Forward	GCAAATGGGTTCCCTCCCTGGCCGA	Applied Biosystems (Hs01115663_m1)
TN-C Reverse	AAGGATGTCTGGAGGCGAGGCGT	Applied Biosystems (Hs01115663_m1)

Table 2.8. SYBR Green Primers

mRNA Target	Primer Name	Primer Sequence 5'-3'	Primer Length (BP)	Product Size (BP)
A1	SG.SYBR-A1F	GCCGAGAAAGGCAGACACAAG	21	92
	SG.SYBR-A1R	ACGGTGAGGTTTTCCAGCTCAG	22	
A2	SG.SYBR-A2F	CCCAGAACCTCACCGTCCCA	20	105
	SG.SYBR-A2R	TGAAGTCCTGAGTGACCCCGC	21	
A3	SG.SYBR-A3F	GAGGCTCACAATCTCACGGT	20	80
	SG.SYBR-A3R	ACTGTGTAAGGAGTGCCAGC	20	
A4	SG.SYBR-A4F	ACAGCTGGGAGATTTAGCCG	20	108
	SG.SYBR-A4R	ACCTCCTGCACCTGAATGAC	20	
B	SG.SYBR-BF	TGCTGAACGAACTGCCATA	20	96
	SG.SYBR-BR	ATGGTTTTGGTCCGGATGCT	20	
AD2	SG.SYBR-AD2F	GTCCATCTCGTGGGAAGCTC	20	85
AD1	SG.SYBR-AD1F	CACAGTTGGGCACGCTAATC	20	73
	SG.SYBR-AD1R	CCAGCTTGAGTGGTCCATGA	20	
C	SG.SYBR-CF	AGTTTCCTGGATGGCATCGG	20	72
	SG.SYBR-CR	AGCAGCTTCCCAGAATCCAC	20	
D	SG.SYBR-DF	AGCTGATGAAGGGGTCTTCG	20	94
	SG.SYBR-DR	TTCGGGGGCAAGTAGGGTTA	20	
7-8	SG.SYBR-Fn7,8F	CCCCAGAAGAGCTCAACCAT	20	99
	SG.SYBR-Fn7,8R	AAGGAGGGCAGTTTCCGACT	20	
GAPDH	SG.SYBR-GAPDHf	ATCCCTGAGCTGAACGGGAA	20	89
	SG.SYBR-GAPDhr	TCTAGACGGCAGGTCAGGTC	20	

Table 2.9a. ELISA and Western Blot Antibodies

Name	Isotype	Experiment	Supplier (Code)
Capture Antibody, Anti-Human CXCL8	Mouse IgG ₁	ELISA	R&D Systems (MAB208)
Detection Antibody, Anti-Human CXCL8	Biotinylated Goat IgG	ELISA	R&D Systems (BAF208)
Capture Antibody, Anti-Human CCL5	Mouse IgG ₁	ELISA	R&D Systems (MAB678)
Detection Antibody, Anti-Human CCL5	Biotinylated Goat IgG	ELISA	R&D Systems (BAF278)
Capture Antibody, Anti Human IL-6	Mouse IgG ₁	ELISA	R&D Systems (MAB206)
Detection Antibody, Anti Human IL-6	Biotinylated Goat IgG	ELISA	R&D Systems (BAF206)
Capture Antibody, Anti Human TNF α	Mouse IgG ₁	ELISA	R&D Systems (MAB610)
Detection Antibody, Anti Human TNF α	Biotinylated Goat IgG	ELISA	R&D Systems (BAF210)
B-actin Primary Antibody	Rabbit (Affinity Isolated)	Western Blot	Sigma-Aldrich (A2066)
Anti-Human TN-C N-Terminal Region Monoclonal Antibody	Mouse IgG ₁	Western Blot	Millipore (MAB1908)
Anti-Mouse TN-C Antibody	Rabbit (Affinity Isolated)	Western Blot	Abcam (Ab108930)
Anti-Rabbit Secondary Antibody	Polyclonal Goat Anti-Rabbit Ig/ Horseradish-Peroxidase (HRP)	Western Blot	Dako (P0449)
Anti-Mouse Secondary Antibody	Polyclonal Goat Anti-Mouse Ig/ HRP	Western Blot	Dako (P0447)

Table 2.9b. ELISA and Western Blot Antibodies (Continued)

Name	Isotype	Experiment	Supplier (Code)
Anti-Fibronectin Antibody	Polyclonal Rabbit	Western Blot	Abcam (ab2413)
Anti-CD9 Antibody (C-4)	Mouse IgG ₁	Western Blot	Santa-Cruz (sc-13118)
Anti-Flotillin-1 Antibody	Polyclonal Rabbit	Western Blot	Abcam (ab41927)
Anti-GAPDH Antibody	Polyclonal Rabbit	Western Blot	Abcam (ab9485)
Anti-KDEL Antibody (Glucose Regulated Protein 94; GRP94)	Monoclonal Mouse	Western Blot	Abcam (ab12223)

Table 2.9c. Immunofluorescence Antibodies

Name	Isotype	Supplier (Code)
Anti-TN-C Antibody (EGF-Like)	Mouse IgG ₁ (Clone BC-24)	Sigma-Aldrich (T2551)
Anti-Fibronectin Antibody	Polyclonal Rabbit	Sigma-Aldrich (F3648)
Anti-Mouse Secondary Antibody Alexa Fluor 488	Polyclonal Goat	Thermo Fisher Scientific (A-11001)
Anti-Rabbit Secondary Antibody Alexa Fluor 568	Polyclonal Goat	Thermo Fisher Scientific (A-11011)
Anti-Neutrophil Antibody (NIMP-R14)	Rat Monoclonal	Abcam (ab2557)

Table 2.10a. Machines (University of Sheffield)

Name	Supplier	Application
Nano-Drop ND100 Spectrophotometer	Lab Tech	mRNA Quantification
PTC-200 Peltier Thermal Cycler	MJ Research	cDNA Synthesis
7900HT Fast RT-PCR System	Applied Biosystems	RT-qPCR
Chemidoc XRS+ Machine	Bio-Rad	Western Blot Imaging
Plate Washer	Lab Tech	Wash ELISA Plate
MultiSkan Ex Plate Reader	Thermo Fisher Scientific	Optical Density Reader for ELISA and Cell Viability Assays
ZetaView NTA	Particle Metrix	NTA of EVs

Table 2.10b. Machines (University of Oxford)

Name	Supplier	Application
Nano-Drop ND100 Spectrophotometer	Lab Tech	mRNA Quantification
ViiA 7 RT-PCR System	Thermo Fisher Scientific	RT-qPCR and SYBR Green qPCR
G:BOX Chemi XX6	Syngene	Western Blot Imaging
Varioskan LUX Multimode Reader	Thermo Fisher Scientific	Optical Density Reader for ELISA, Cell Viability Assays and BCA
NanoSight NTA Machine	Malvern Instruments	NTA of EVs
BX51 Fluorescent Microscope	Olympus	Immunofluorescence Microscopy
FV-1200 Confocal With Imaris Software	Olympus	Immunofluorescence Confocal Microscopy
CKX41 Microscope with U-TVO-5XC-3 Lens	Olympus	Cell Culture Images
J-1110 Circular Dichroism Spectrophotometer	Jasco	Measure Folding of Protein

2.2. Cell Maintenance

2.2.1. BEAS-2B Cell Line Culture

BEAS-2Bs are lung bronchial epithelial cells that are isolated from healthy volunteers and immortalised by transformation with an AD12-SV40 virus. They have been established by the supplier to undergo squamous differentiation, be suitable for screening biological agents and pathogenic infection, are able to form colonies and are not tumorigenic. They have been established in our lab for over a decade, with published material demonstrating that RV viral replication and response to infection (determined by CXCL8 release) is similar between the cell line and PBECs (Stokes et al. 2016). They are therefore deemed to be a suitable cell model for use in preliminary experiments, before transitioning into primary cells. They are more robust

than PBECs, with a quicker doubling time, and this allowed efficient optimisation of the RV MOI required to investigate the experimental aims (such as TN-C expression).

BEAS-2B lung epithelial cells (Table 2.1.) were maintained in 75 cm² flasks (Thermo Fisher Scientific) in BEAS-2B Complete Media (Table 2.3.) at 37°C and 5% CO₂. The cells were maintained by replacing Complete Media every 3-4 days and the cells were passaged when the cells had reached 80-90% confluency with cell dissociation fluid (Sigma-Aldrich). Cells were plated for stimulation or infection (Section 2.4.) in 12 or 96 well plates (Corning) after passage 6, and the flask was passaged until passage 16.

2.2.2. PBEC Culture

PBECs are primary bronchial epithelial cells taken from healthy volunteers by bronchoscopy and are batch specific for age and gender. They have a packed cuboidal morphology, are adherent, and are suitable for viral infection, as determined by the supplier and our previous work (Stokes et al. 2016). Both PBECs and BEAS-2B's were grown in submerged cultures, with the advantages and disadvantages of this described in Section 6.2.

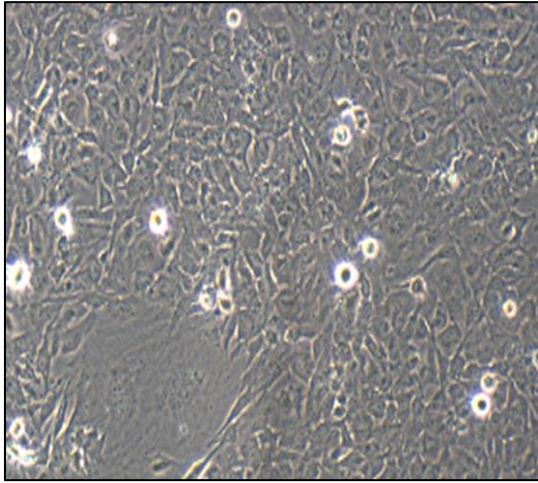
PBECs (Table 2.1.) isolated from healthy volunteers were purchased from the manufacturer and then grown and maintained in 75 cm² flasks in PBEC Complete Media (Table 2.3.) at 37°C and 5% CO₂. Every 2-3 days the media was removed and replaced with fresh Complete Media. The cells were passaged every 7-9 days when the cells had reached 80-90% confluency by first washing with PBS (Table 2.4a.) and HEPES, then adding 2 ml of Trypsin-EDTA (PromoCell) for detachment. The cells were then seeded in a new flask with Complete Media at the required density. At passage 5 or 6 the cells were seeded on 12 well or 96 well plates, stored in an incubator (37°C and 5% CO₂) and then stimulated or infected (Section 2.4.). Images of BEAS-2B and PBECs in culture are displayed in Figure 2.1.

2.2.3. HeLa-Ohio Cell Line Culture

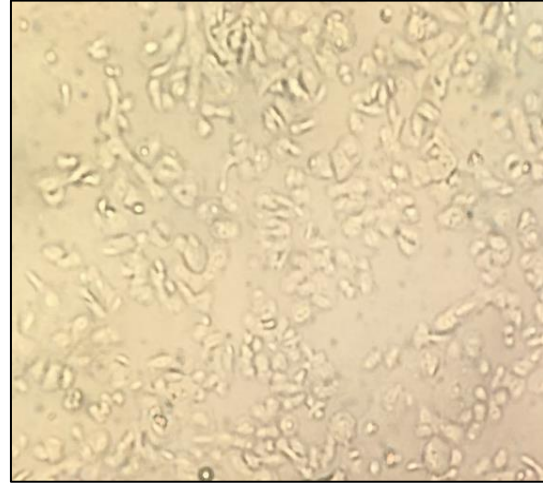
HeLa-Ohio cells (Table 2.1.) were maintained in 75 cm² flasks in HeLa-Ohio Complete Media (Table 2.3.) at 37°C and 5% CO₂. The cells were maintained by replacing the Complete Media every 3-4 days and cells were passaged when the cells had reached 80-90% confluency with cell dissociation fluid (Sigma-Aldrich).

2.2.4. HEK-293:pCEP-huTNC-his Cell Culture

HEK-293 cells transfected with the cDNA encoding human tenascin-C (HxBL.pBS) encompassing all alternative FNIII repeats, sub-cloned into the pCEP-Pu vector with a polyhistidine (his)-tag (HEK-293:pCEP-huTNC-his cells; Table 2.1.) was acquired from the University of Strasbourg (Lange et al, 2017). The cells were maintained in 75 cm² flasks in HEK-293 Culture Media (Table 2.2.) at 37°C and 5% CO₂.



BEAS-2B Cells



PBECs

Figure 2.1. Images of BEAS-2B Cells and PBECs in Culture

BEAS-2B cells and PBECs were seeded at the 1×10^6 and 0.75×10^6 respectively in BEAS-2B Complete Media and PBEC Complete Media and left to grow to confluency. Cell cultures were imaged (40x magnification) with an Olympus U-TVO-5XC-3 Lens (Olympus CKX41 microscope).

2.2.5. Human Dermal Fibroblast Cell Culture

Human Dermal Fibroblasts (Table 2.1.) were purchased and then grown and maintained in 75 cm² flasks in Fibroblast Cell Culture Media (Table 2.2.) at 37°C and 5% CO₂. The cells were maintained by replacing Fibroblast Cell Culture Media every 3-4 days and the cells were passaged when the cells had reached 80-90% confluency by Trypsin-EDTA treatment and seeded at 40,000 cells per ml onto coverslips when required.

2.2.6. MDMs Cell Culture

All blood from healthy volunteers was taken by a trained phlebotomist with written informed consent, under a protocol approved by the South Yorkshire Research Ethics Committee (reference number: 05/Q2305/4). Monocytes were then isolated from peripheral blood by Ficoll gradient and counterflow centrifugation. One million monocytes per ml were then plated in MDMs Culture Media (Table 2.2.) and differentiated into MDMs (Table 2.1.) for 7 days by stimulation with 100 ng/ml macrophage colony-stimulating factor (M-CSF). MDMs were then plated at 100,000 cells/well in 96 well plates for 24 hours before stimulation.

2.3. Viral Culture

2.3.1. Viral Propagation

RV serotypes 1B and 16 (ATTC) were cultured in the HeLa-Ohio cell line in 175 cm² flasks. The HeLa-Ohio Complete Media (Table 2.3.) was removed and the cells were washed twice in 10 ml of HeLa-Ohio Infection Media (Table 2.3.). 5 ml of the virus was added per flask and placed in the incubator (37°C and 5% CO₂) for an hour with a gentle rotation every 15 minutes. A further 12.5 ml of Infection Media was then added per flask and this was placed in the viral incubator overnight at 37°C & 5% CO₂ (by at which point 90% cytopathic effect should be observed). The cells were freeze-thawed (defrosted in incubator and frozen at -80°C for an hour) 3 times and then centrifuged at 4000 relative centrifugal force (rcf) for 15 minutes. The supernatant was then placed into a syringe and filtered 0.2 µm filter (Millipore) into Falcon tubes (Sarstedt) where it was stored at -80°C.

2.3.2. Viral Titration and Quantification

Titration of the virus was carried out. 200 µl of virus was used to create a serial dilution from 10⁻⁹ to 10⁻¹. 50 µl of this was then added to the appropriate wells in a 96 well plate, with 50 µl virus added directly to the no dilution wells. Control wells were included which was media only. HeLa-Ohio cells were dissociated, split, re-suspended in HeLa-Ohio Infection Media and seeded at required density. 150 µl of cells were then added to each well of the viral titration plate and incubated in the viral incubator at 37°C & 5% CO₂ for 4-5 days. The cytopathic effect was then determined and the TCID₅₀ was determined using the Spearman Karber Formula:

$$= xk + d [0.5 - (1/n) (r)]$$

xk = dose of the highest dilution.

r = sum of the number of wells that have cell death

d = spacing between dilutions.

n = wells per dilution

Next, plaque forming units (PFU) was calculated ($0.7 \times \text{TCID}_{50}$) and then finally, multiplicity of infection (MOI) could be calculated ($\text{PFU} \div \text{number of cells}$). BEAS-2Bs and PBECs were infected with RV-1B and RV-16 at multiple MOIs (such as 5, 3, 1.5 and 0.6) and suitable MOIs that induced cytokine release but did not promote large amounts of cell death were used in this study.

2.4. Stimulation and Infection of AECs

2.4.1. Stimulation of AECs

2.4.1.1. Polyinosinic:Polycytidylic Acid (Poly(I:C)) Stimulation

Poly(I:C) stimulation was used for TLR3 stimulation of AECs. For poly(I:C) stimulation of BEAS-2B cells, the cells were serum starved overnight (in 12 well plates) before stimulation by removing BEAS-2B Complete Media and replacing with 1 ml of BEAS-2B Basal Media (Table 2.3.) per well. At time of stimulation, the media was removed, then 1 ml of fresh Basal Media was added to the control wells and 990 μl was added to the stimulated cells. 10 μl of 25 $\mu\text{g/ml}$ poly(I:C) (Invivogen) was added to the media in the wells of the stimulated cells and the cells were placed in the incubator at 37°C & 5% CO_2 . For poly(I:C) stimulation of PBECs, the same protocol as for stimulation of BEAS-2B cells was carried out, with the only difference being cells were removed from PBEC Complete Media and placed in PBEC Basal Media (Table 2.3.) before stimulation.

2.4.1.2. TNF α Stimulation

TNF α stimulation was used as a positive control for TN-C expression, as TNF α is a transcriptional regulator of TN-C. For TNF α stimulation of BEAS-2B cells, the cells were serum starved overnight (in 12 well plates) before stimulation by removing BEAS-2B Complete Media and replacing with 1 ml of BEAS-2B Basal Media per well. At time of stimulation, the media was removed, replaced with 1 ml of fresh Basal Media and 100 ng/ml TNF α (Invivogen) was added. For TNF α stimulation of PBECs, the same protocol as for stimulation of BEAS-2B cells was carried out with the only difference being cells were removed from PBEC Complete Media and placed in PBEC Basal Media before stimulation.

2.4.1.3. Gardiquimod Stimulation

Gardiquimod stimulation was used for TLR7 stimulation of AECs. For gardiquimod stimulation of BEAS-2B cells, the cells were serum starved overnight (in 12 well plates) before stimulation by

removing BEAS-2B Complete Media and replacing with 1 ml of BEAS-2B Basal Media per well. At time of stimulation, the media was removed, then 1 ml of fresh Basal Media was added to the control wells and 990 μ l was added to the stimulated cells. 10 μ l of 1 μ g/ml gardiquimod (Invivogen) was added to the media in the wells of the stimulated cells and the cells were placed in the incubator at 37°C & 5% CO₂. For gardiquimod stimulation of PBECs, the same protocol as for stimulation of BEAS-2B cells was carried out, with the only difference being cells were removed from PBEC Complete Media and placed in PBEC Basal Media (Table 2.3.) before stimulation.

2.4.1.4. Staurosporine Stimulation

Staurosporine was used to induce apoptosis in AECs and thus was used as a positive control for cell death, For staurosporine stimulation of BEAS-2B cells, the cells were serum starved overnight (in 12 well plates) before stimulation by removing BEAS-2B Complete Media and replacing with 1 ml of BEAS-2B Basal Media per well. At time of stimulation, the media was removed, then 1 ml of fresh Basal Media was added to the control wells and 998 μ l was added to the stimulated cells. 4.6 μ g/ml staurosporine (Sigma-Aldrich) was added to the media in the wells of the stimulated cells and the cells were placed in the incubator at 37°C & 5% CO₂. For staurosporine stimulation of PBECs, the same protocol as for stimulation of BEAS-2B cells was carried out, with the only difference being cells were removed from PBEC Complete Media and placed in PBEC Basal Media (Table 2.3.) before stimulation.

2.4.1.5. LPS Stimulation

LPS stimulation was used as a positive control for TLR4 stimulation. For LPS stimulation of BEAS-2B cells, the cells were serum starved overnight (in 96 well plates) before stimulation by removing BEAS-2B Complete media and replacing with 1 ml of BEAS-2B Basal Media per well. At time of stimulation, the media was removed, replaced with 1 ml of fresh Basal Media and 0.1-10 μ g/ml LPS strain 0111:B4 (smooth serotype; Sigma-Aldrich) or EH100 (rough strain; Enzo Life Sciences) was added. The LPS was vortexed for 3-5 minutes before use. 15 μ g/ml Polymyxin B (PMB; Sigma-Aldrich) was also added to some wells prior to LPS stimulation as an inhibitor of LPS and a negative control.

2.4.2. RV Infection of AECs

For RV infection of BEAS-2B cells, the cells were serum starved overnight (in 12 well plates) before infection by removing BEAS-2B Complete Media and replacing with 1 ml of BEAS-2B Basal Media per well. At time of infection, the media was removed and 250 μ l of BEAS-2B Basal Media was added to the control wells and 250 μ l of RV-1B or RV-16 (multiplicity of infection of either 0.6 or 1.5) was added to the wells to be infected. The plate was placed in the viral incubator at 37°C & 5% CO₂ for an hour (plate rotated every 15 minutes) and after an hour the media from the wells was removed. The cells were washed twice in 1 ml of PBS to remove excess bound RV, then 1 ml of BEAS-2B Complete Media was added to each well and the cells were stored in the viral incubator 37°C & 5% CO₂.

For RV infection of PBECs, the same protocol as for infection of BEAS-2B cells was carried out, with the only difference being cells were removed from PBEC Complete Media, placed in PBEC Basal Media before infection and placed in PBEC Recovery Media (Table 2.3.) after infection.

2.5. Harvesting Supernatant, mRNA and Protein

To collect supernatant, the cells were removed from the incubator at the required time point and placed on ice. The supernatant was collected and placed in an Eppendorf (Sarstedt) before being centrifuged (Sigma-Aldrich) at 1,000 rcf for 2-3 minutes. The supernatant was then placed in a new Eppendorf and stored at -80°C.

To collect mRNA, the media was removed from the well and 1 ml of Tri-Reagent (Sigma-Aldrich) was added. The well was then scraped and the Tri-Reagent was pipetted up and down 3 times. The Tri-Reagent was then removed, placed in an Eppendorf and stored at -80°C.

To collect protein, 75 µl of Phosphate Lysis Buffer (Table 2.4a.) was added to each well and left for 15 minutes. The well was then scraped with a pipette tip and the lysate collected and placed in an Eppendorf. The samples were centrifuged at 9,000 rcf for 1 minute and the supernatant was then transferred to another tube. 25 µl of 4x Sample Buffer (Table 2.4a.) was then added to each of the samples and stored at -80°C.

2.6. Obtaining External Asthmatic Samples and Mouse BALF

2.6.1. External Asthmatic Samples

PBECs from atopic-asthmatic (AA) and non-atopic non-asthmatic (NANA) patients were obtained by collaboration with Dr Mike Edwards from Imperial College London. Bronchoscopy was performed on AA and NANA patients as part of the ALLIANCE study (following the correct ethics and approval codes and practices), and PBECs were obtained, plated in PBEC Complete Media and grown to confluence. The PBECs were then infected with RV-1B and RV-16 at Imperial College London as per Section 2.4.2. and mRNA and supernatant was collected as per Section 2.5. Further analysis by qPCR (Section 2.7) and western blot (Section 2.8) was then carried out by Jake Mills at the University of Sheffield.

2.6.2. Mouse BALF Samples and Neutrophil Counts

The mouse work involved in this study had ethical approval and was licensed and regulated by the Home Office under the Animals (Scientific Procedures) Act 1986. The University of Sheffield also abides by the Concordat on Openness in Animal Research and Animal Research: Reporting of *In Vivo* Experiments guidelines, developed as part of a National Centre for the Replacement, Refinement and Reduction of Animals in Research initiative. All mouse breeding, handling, stimulation, culling and sample collection was carried out by Dr Elizabeth Marsh and Dr Helen Marriott in the Animal Research Department at the University of Sheffield (project license code 40/3726 and establishment license code 50/2509). Under sedation, adult C57BL/6 WT mice were stimulated intranasally with either 50 µl sterile PBS or 100 µg poly(I:C) in 50 µl

PBS for up to 48 hours (n=3 for PBS controls and 6-7 for Poly(I:C) stimulation). At time of collection, the mice were culled and BALF fluid was collected by lavaging the mouse lungs 3 times with 1 ml sterile PBS. Next, neutrophils were isolated by dextran (Sigma-Aldrich) sedimentation and Ficoll (Sigma-Aldrich)-density gradient separation, concentrated by cytopsin (Thermo Fisher), before being added to sterile slides coated in fibrinogen (Sigma). The cells were then stained with NIMP-R14 (Abcam) and counted by immunofluorescence microscopy. BALF samples were then analysed KC and CCL5 by ELISA (Section 2.10). Cytokine and chemokine ELISAs and neutrophils counts were carried out by Dr Elizabeth Marsh and western blot (Section 2.8) analysis for TN-C was then carried out by Jake Mills at the University of Sheffield.

2.7. RT-qPCR

2.7.1. mRNA Extraction

The mRNA samples were removed from the -80°C freezer and defrosted. 0.2 ml of Chloroform (Sigma-Aldrich) was added to the samples and shaken vigorously for 15 seconds, before standing at room temperature (RT) for 10 minutes. The samples were then centrifuged at 12,000 rcf for 15 minutes at 4°C in the temperature controlled centrifuge (Phillip Harris). The aqueous phase of the sample was then transferred to a fresh Eppendorf tube. 0.5 ml Isopropanol (Fisher Scientific) was added to the aqueous phase before being mixed and left to stand for 10 minutes at RT. The samples were then centrifuged at 12,000 rcf for 10 minutes at 4°C and the supernatant carefully removed and discarded. The pellet was then washed in 75% Ethanol (Fisher Scientific) and centrifuged at 7,500 rcf for 5 minutes at 4°C. The supernatant was next removed and discarded; the pellets were left to air dry for around 15-25 minutes (until the pellet was glassy) and then 20 µl of sterile water for injections (B Braun) was added to each sample. 10x DNase I Buffer and rDNase I from DNA-Free™ DNase Treatment & Removal kit (Table 2.6.) was added to the RNA and mixed gently, before being incubated at 37°C for 20-30 minutes. DNase Inactivation Reagent (from DNA-Free™ DNase Treatment & Removal Kit) was then added, mixed well and left for 2 minutes at RT. Finally, the samples were centrifuged at 10,000 rcf for 90 seconds, transferred to fresh tubes and stored at -80°C.

2.7.2. Quantification of mRNA

The Nano-Drop ND100 Spectrophotometer (Table 2.10a. and b.) was blanked and prepared for quantification of RNA as per manufacturer's instructions. 1 µl of sample was added to the ND100 Spectrophotometer, and the ng/µl, 260/280 and 260/230 readings were noted.

2.7.3. cDNA Synthesis

The High Capacity cDNA Reverse Transcription Kit (Table 2.6.) was made up as follows in Table 2.11. The volume of sample required for 500 µg of mRNA was combined with water to make up 20 µl, before being combined with the amounts in the table below.

Table 2.11. Reagents Required for cDNA Synthesis

Component	Volume Per Sample (µl)
10x Reverse Transcriptase Buffer	4
25x Deoxyribonucleotide Triphosphate Mix (200mM)	1.6
10x Reverse Transcriptase Random Primers	4
MultiScribe Reverse Transcriptase	2
RNase Inhibitor	2
Nuclease-Free Water	6.4
Template RNA	20

A control with no enzyme present (MultiScribe negative control) and a control with no sample present (sample negative control) was also made up. The samples were analysed on the PCR machine (Peltier ThermoCycle) using the following protocol:

- 25°C for 10 minutes
- 37°C for 2 hours
- 85°C for 5 minutes

The samples were then stored at -80°C.

2.7.4. Standard Creation for TaqMan and SYBR Green qPCR

cDNA created from the FBG domain of the TN-C incorporated into a Pet32B vector was used for the TN-C standard. The following calculation was carried out to calculate the number of copies of cDNA per µl:

$$\text{Number of copies} = (\text{amount} \times 6.022 \times 10^{23}) \div (\text{length} \times 1 \times 10^9 \times 650)$$

The amount was 297 ng/µl and the length was 6586 so the cDNA had 4.18×10^{10} copies per µl.

Separate standard curve (SC) dilutions were made, one for GAPDH (control) and one for TN-C. The GAPDH standard curve was a 1:10 dilution from 10^8 to 10^0 (actual amount varied between standards used) and the TN-C SC was a 1:10 SC dilution from 4.18×10^8 to 4.18×10^0 .

2.7.5. TaqMan Sample Creation and Plate Loading

The amount of cDNA-TaqMan Master Mix Sample (Table 2.6.) needed was next calculated (Table 2.12).

Table 2.12. Composition of TaqMan qPCR cDNA Samples

Reagent	Amount per Sample (µl)
Primer/Probes (Table 2.7.)	1
qPCR 2x Master Mix (Table 2.6.)	10
H ₂ O	8
Standard (Applied Biosciences) or Sample	1
Total	20

Next two controls were made up, an enzyme negative sample (19 µl of Master Mix & 1 µl of enzyme negative sample) and a water negative sample (19 µl Master Mix & 1 µl of water sample). The plate was then loaded with the samples, sealed tightly, centrifuged for 2 minutes at 8,900 rcf and placed on the 7900HT Fast RT-qPCR machine (Table 2.10a.) using the following protocol:

- 50°C for 2 minutes
- 95°C for 10 minutes
- 95°C for 15 seconds*
- 60°C for 1 minute*

*for 40 cycles

2.7.6. SYBR Sample Creation and Plate Loading

The amount of cDNA-SYBR Green Master Mix Sample (Table 2.6.) needed for each FNIII domain was next calculated (Table 2.13).

Table 2.13. Composition of SYBR Green qPCR cDNA Samples

Reagent	Amount Per Sample (µl)
FNIII Domain Forward and Reverse Primers (Table 2.8.)	1 (of each; Diluted 1:10 in H ₂ O)
SYBR Green Master Mix (Table 2.6.)	5
Standard (Applied Biosciences) or Sample	3 (Diluted 1:10 in H ₂ O)
Total	9

Next, a sample negative control for each FNIII domain was created and loaded onto the plate. The plate was then loaded with the samples, sealed tightly, centrifuged for 2 minutes at 8,900 rcf and placed on the ViiA 7 RT-PCR System (Table 2.10b.) using the following protocol:

- 50°C for 2 minutes
- 95°C for 10 minutes
- 95°C for 15 seconds*
- 60°C for 1 minute*

*for 40 cycles

2.8. Western Blot

2.8.1. Making Gels

The SDS-PAGE gel apparatus was assembled according to the manufacturers (Bio-Rad) instructions. 10% and 6% resolving gel mixes were created (Table 2.5.), 10% gels were required for the β-actin, and 6% for TN-C. The running gel was loaded to around 1-2 cm from the top of the glass mould, and the 5% stacking gel was created (Table 2.5). The stacking gel was added to the top of the mould followed by a 10 or 15 well comb. After allowing 15 minutes for the gel to set, the gel was placed in the Mini Protean Tetra Cell running chamber (Bio-Rad) with the required amount of 1x Running Buffer (Table 2.4a.) derived from 10x Running Buffer (Table 2.4a.).

2.8.2. Processing and Loading Samples

For supernatant western blots, 5 µl of Sample Buffer was added to the 15 µl of cell free supernatant before the samples were boiled for 5 minutes at 97°C in the heating block. For protein lysate western blots, the collected protein samples (Section 2.5.1.) were boiled for 5 minutes at 97°C in the heating block.

5 µl of Blue Protein Ladder (New England Biolabs) was added to the first well in the gel (left hand side) and then 10 µl of the protein samples or 20 µl of the supernatant sample was added to the following wells. The gel was run at 100 Volts (V) through the stacking gel and then increased to 200 V to allow full separation of the proteins to occur.

2.8.3. Transfer of Protein

Filter paper (4 per gel; Whatman) and nitrocellulose membrane (1 per gel; Pall Life Sciences) were soaked in 1x Transfer Buffer (Table 2.4a.) derived from 10x Transfer Buffer (Table 2.4a.) for 5 minutes, along with sponges (2 per gel). The transfer cassette (Bio-Rad) was assembled as per manufacturer's instructions and was then loaded into the transfer tank alongside an icepack and ran at 100 V for 70 minutes. After the time elapsed, the nitrocellulose membrane was covered with Ponceau Stain (Sigma-Aldrich) to check the quality of the transfer. The Ponceau was then washed off with PBS-0.1% Tween-20 (Table 2.4a.; Fisher Scientific) and blocked for an hour in 5% Milk / PBS-0.1% Tween (Table 2.4a.) at RT on the shaking platform.

2.8.4. Addition of Antibodies

After an hour the primary antibodies were added to the blots in Falcon tubes. The β-actin antibody (10% gel; Table 2.9a.) was added to 5% Milk / PBS-0.1% Tween at a 0.08 µg/ml and the TN-C antibody (6% gel; Table 2.9a.) was added to 5% BSA / TBS-0.1% Tween at 1 µg/ml. These were then placed on a shaking platform overnight at 4°C.

The blots were rinsed 3 times in PBS-0.1% Tween for 10 minutes. Then the secondary antibody was added to the blots and incubated on a plate shaker for one hour. For β-actin this was Polyclonal Goat Anti-Rabbit Ig / HRP (Table 2.9a.) and for TN-C this was Polyclonal Goat Anti-Mouse Ig / HRP (Table 2.9a.) at 0.025 µg/ml.

2.8.5. Imaging Blot

The blots were again rinsed 3 times in PBS-0.1% Tween for 10 minutes and then 2.5 ml of both Clarity Western Enhanced Chemiluminescence Substrate (Bio-Rad) A and B was added to the blots and incubated for 5 minutes. The blot was then imaged via the Image Lab Software on the Chemidoc XRS+ machine (Table 2.10a.) or G:BOX Chemi XX6 (Table 2.10b.).

2.8.6. Calculating Protein Densitometry

To calculate protein densitometry, ImageJ software v1.48 was used. When calculating the overall TN-C expression, densitometry was performed on the dominantly expressed band, which was the ~250 kDa in the mouse samples, and the larger >250 kDa in the human samples.

2.9. Immunofluorescence Microscopy

2.9.1. Immunofluorescence Staining

First, 18 mm circular coverslips were autoclaved and washed in ethanol (R&D) before placing in a 12 well plate. Cells were plated as required and placed in the incubator at 4°C and 5% CO₂ until confluent. The cells were then stimulated or infected (Section 2.4) for the desired time and human dermal fibroblasts were used for positive controls, cultured onto coverslips for 24 hours prior to staining. Next, the coverslips were removed and rinsed in 1x PBS twice, before the cells were fixed in 0.5 ml 3.8% PFA (Table 2.4b.) for 15 minutes. The fixative was aspirated before the cover slip was washed four times in 1 ml of 1x PBS. For samples that required intracellular antibody staining, the cells were permeabilised by the addition of 0.5 ml 0.2% Triton X-100 (Table 2.4b) for 10 minutes at RT. Next the coverslips were placed (cell side up) on parafilm inside a plastic tray, and 200 µl blocking buffer was added (Table 2.4b.) for 1 hour at room temperature.

The blocking buffer was aspirated and 150 µl of the relevant primary antibody (1:500 for TN-C and 1:200 for FN; Table 2.9b.) in ADB (Table 2.4b) was added and incubated for 2 hours at RT, free from light. A no primary antibody control was also created by incubating coverslips containing cells in ADB alone with no primary antibody. Next the coverslips were washed in 1x PBS-0.5% Tween-20 five times, and excess water was blotted away with tissue. Anti-Mouse Secondary Antibody Alexa Fluor 488 was added to TN-C stained samples or Anti-Rabbit Secondary Antibody Alexa Fluor 568 was added to FN stained samples (Table 2.9b.), and incubate for 1 hour at RT, free from light. Cells were washed in 1xPBS-Tween20 as previously described and once in distilled water, and remaining liquid was blotted away. One drop (5-15ul) of ProLong Gold Antifade Reagent (Thermo Fisher Scientific) was added onto a clean glass slide using a top-cut p200 tip and the immunostained coverslip was placed on top of droplet, with cells facing down. The coverslip as gently pressed down and excessed Prolong gold was blotted away. The coverslips were left to dry for 2-3 minutes and then the edges of the glass slide were coated with nail varnish to secure the coverslip and prevent drying. The slides were then stored at 4°C in dark covered in aluminium foil until use.

2.9.2. Imaging by Immunofluorescence Microscopy

To analyse the images by immunofluorescence microscopy, a BX51 Olympus Immunofluorescence Microscope was used (Table 2.10b), and for immunofluorescence confocal microscopy, a FV-1200 Olympus Confocal Microscopy was used (Table 2.10b). ImageJ and Imaris (Bitplane) software was then used to analyse the images.

2.10. ELISA

2.10.1. Cytokine / Chemokine ELISA

First, the coating antibody (Table 2.9a) was diluted in the ELISA Coating Buffer (Table 2.4a.). For CCL5, IL-6, TNF α and IL-5 this was 2 μ g/ml and for CXCL8 this was 0.32 μ g/ml. 100 μ l was added to each well of a 96-well microtiter-plate (Costar) and the plate was sealed and incubated overnight at RT. The next day the plate was placed in the plate washer (Table 2.10a., or washed by hand), washed with ELISA Wash Buffer (Table 2.4a.; washed four times) and the plate was blotted on blue roll to remove any remaining buffer. The plates were then blocked for 1 hour by adding 100 μ l of BSA diluted in ELISA Coating Buffer (0.2 g in 20 ml; Sigma-Aldrich) to each well and placed on the rotating platform at RT. The plates were then washed as described previously.

100 μ l of standard (ranging from 19.6-5,000 pg/ml for CXCL8, 39-10,000 pg/ml for CCL5 and 13-10,000 pg/ml for IL-6, TNF α and IL-5), or sample was added to each well (duplicate wells) and incubated for 1.5 hours on the rotating platform (200 rpm) at RT. The wash step was then repeated and 100 μ l of the Biotinylated Antibody (Table 2.9a.) diluted in Wash Buffer (CCL5 – 0.08 μ g/ml, CXCL8 – 0.32 μ g/ml and IL-6 and TNF α – 0.1 μ g/ml) was added to each well before being incubated for 1.5 hours at RT on a shaker. The wash step was again repeated before 100 μ l of Streptavidin-HRP (50 μ l in 10 ml of Wash Buffer; R&D Systems) was added to each well. The plate was covered in foil and incubated for 20 minutes on a shaker at RT.

The plate was then washed for a final time following the protocol and 100 μ l of substrate solution (5 ml of A & 5 ml of B; R&D Systems) was added to each well and incubated for 20-30 minutes at RT on a shaker. When the colour change was sufficient, 50 μ l of 1M Sulphuric Acid (Fisher Scientific) was added per well to stop the reaction. The optical density of each well was then determined immediately on the plate reader (Table 2.10a and b.) at a 450 nm absorbance wavelength.

2.10.2. N-Terminal TN-C ELISA

First, the 96-well plate pre-coated with Anti-TN-C (N-Terminal) Mouse IgG antibody was brought to room temperature. 100 μ l of standard (ranging from 31.2-2000 pg/ml) or sample was added to each well (duplicate wells) and incubated for 1 hour at 37°C. Next, Detection Reagent A was added, and again incubated for 1 hour at 37°C, before this was aspirated and washed as per Section 2.9.1. three times. 100 μ l of Detection Reagent B was then added and incubated at 37°C for 30 minutes, before this was aspirated and washed five times. 90 μ l of Substrate Solution was next added for 10-20 minutes at 37°C, before 50 μ l of Stop Solution was added and read at 450 nm immediately on the plate reader.

2.10.3. FNIII-B TN-C ELISA

First, the 96-well plate pre-coated with Anti-TN-C (FNIII-B) Mouse IgG antibody was brought to room temperature. 100 µl of standard (ranging from 200-12,500 pg/ml) or sample was added to each well (duplicate wells) and incubated for 1 hour at 37°C. Next, the wells were washed vigorously seven times as described in Section 2.9.1., 100 µl of the detection antibody (HRP conjugated Anti-Tenascin-C Mouse IgG) was added per well and the plate was incubated for 30 minutes at 4°C. The plate was washed nine times and 100 µl of chromogen was added and incubated for 30 minutes at RT (covered in foil). The Stop Solution was then added and the optical density of each well was then determined immediately on the plate reader at a 450 nm absorbance wavelength.

2.11. Isolation of EVs from AECs

2.11.1. Removal of EVs from AEC Media

First, EVs were removed from FCS and PBEC Basal Media in order to ensure that bovine EVs did not contaminate AEC EV analysis. The FCS and bovine pituitary extract was placed in thick walled ultracentrifuge tubes (Hitachi), centrifuged at 120,000 rcf for 18 hours at 4°C in a ultracentrifuge (Sorvall Discovery M150 SE) and the supernatant was taken. The FCS or bovine pituitary extract was then filtered through a 0.22 µm filter to purify the supernatant, creating EV-Depleted BEAS-2B Basal Media and EV-Depleted PBEC Basal Media.

2.11.2. Stimulation or Infection of AECs

BEAS-2B cells and PBECs cultured in EV-Depleted Media was then stimulated with poly(I:C) or infected with RV as per Section 2.4.1. and 2.4.2., using the relevant EV-Depleted Media.

2.11.3. Isolation of EVs from AECs by Ultracentrifugation

Following stimulation or infection, the supernatant was collected and both MVs and exosomes were then isolated by ultracentrifugation, as described in Figure 2.2. To summarise, the supernatant was collected and centrifuged at 300 rcf for 5 minutes to remove dead cells. Next, the cells were centrifuged at 3,000 rcf for 5 minutes to remove cell debris, and then MVs were pelleted by centrifugation at 10,000 rcf for 30 minutes and re-suspended in 100 µl sterile PBS. Exosomes were next pelleted by centrifugation in an ultracentrifuge at 100,000 rcf for 120 minutes, before the pellet was re-suspended in sterile PBS and centrifuged again at 100,000 rcf for 120 minutes in order to remove contaminant proteins from the exosome isolates. Finally, the exosomes were re-suspended in 100 µl of sterile filtered PBS.

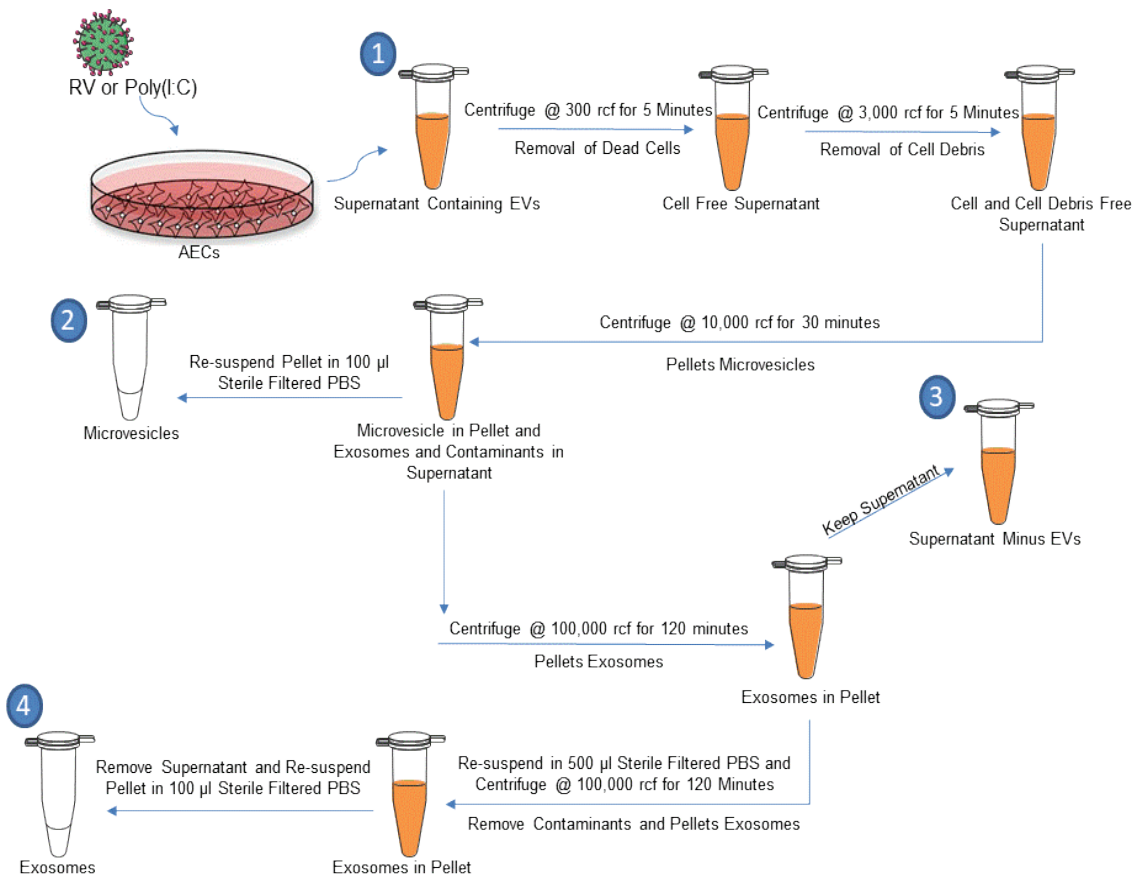


Figure 2.2. The Isolation of MVs and Exosomes from AEC Supernatants Following Poly(I:C) Stimulation and RV Infection

Following poly(I:C) stimulation or RV infection, the supernatant (**fraction 1**) was collected and both MVs and exosomes were then isolated by ultracentrifugation. First, the supernatant was centrifuged at 300 rcf for 5 minutes at 4°C in order to remove dead cells and the supernatant was collected. Next, the supernatant was centrifuged at 3,000 rcf for 5 minutes at 4°C in order to remove cell debris. The supernatant was then centrifuged at 10,000 rcf for 30 minutes at 4°C in order to isolate MVs and re-suspended in 100 µl sterile PBS and stored at 4°C (**fraction 2**). The supernatant was next centrifuged in an ultracentrifuge at 120,000 rcf for 2 hours at 4°C to pellet exosomes, and the supernatant was kept and stored at 4°C (**fraction 3**). The pellet was re-suspended in 500 µl sterile PBS, spun at 120,000 rcf for 2 hours at 4°C to re-pellet exosomes and remove contaminants, the supernatant was discarded, and the pellet was re-suspended in 100 µl sterile PBS and stored at 4°C (**fraction 4**).

2.11.4. Characterisation of EVs Following Isolation by Western Blotting

Following the EV isolation protocol, western blotting was used to analyse for the presence of exosome-enriched proteins (Section 2.7). The primary antibodies CD9, β -actin and KDEL (10% gel Table 2.9) was added to 5% Milk / PBS-0.1% Tween at 1 $\mu\text{g}/\text{ml}$ and the flotillin-1 antibody (10% gel; Table 2.9a.) was added to 5% Milk / PBS-0.1% Tween at 1 $\mu\text{g}/\text{ml}$. These were then placed on a shaking platform overnight at 4°C. The Anti-Rabbit Secondary Antibody was used for flotillin-1 and β -actin and Anti-Mouse Secondary Antibody was used for CD9 and KDEL at the appropriate concentrations.

2.11.5. Characterisation of EVs Following Isolation by NTA

Exosomes were also analysed for concentration (particles per ml) and size (nm) by NTA. The NanoSight NTA machine (Table 2.10a) was used in the University of Oxford to analyse BEAS-2B cell exosomes and the ZetaView NTA machine (Table 2.10a) was used in the University of Sheffield for both BEAS-2B and PBEC exosome analysis.

Exosomes were diluted as required to provide 100-1000 particles per μl , ran through the machine for analysis 3-5 times, and the average concentration and size was calculated. NTA uses a laser, light dispersion and Brownian motion to track EVs in a liquid suspension and through this, the translation diffusion constant is calculated, by which then size and concentration can be measured. NTA can measure vesicles between 10–3000 nm and able to handle concentrations between 10^5 - 10^{10} particles per cm^3 .

2.11.6. Stimulation of AECs and MDMs with AEC Isolated Exosomes

Following exosome calculation by NTA, exosomes were added exogenously to confluent BEAS-2B cells, PBECs or MDMs at concentrations between 10,000-20,000 particles per μl (200 μl overall), following the stimulation protocol described in Section 2.4.

2.12. Quantification of Protein by BCA

The BCA (Table 2.4b.) was used to calculate protein concentration. A standard curve ranging from 0-2000 $\mu\text{g}/\text{mL}$ was first prepared and 25 μl was loaded into a 96 well plate alongside samples requiring quantification. 200 μl of the Bicinchoninic acid assay (BCA) working reagent (VWR) was added to each well and mixed on a plate shaker for 30 seconds, before being incubated at 37°C for 30 minutes. The plate was then left to reach room temperature before being read on the plate reader at 562 nm. The standard curve was generated and the unknown samples were interpolated onto the curve and quantified.

2.13. Quantification of Cell Viability

Cell viability was quantified by in two experiments: A MTT 3-(4,5-Dimethylthiazol-2yl)-2,5-Diphenyltetrazolium Bromide (MTT) assay measuring cell metabolic activity by NADPH (nicotinamide adenine dinucleotide phosphate) activity (Table 2.6b.) and by microscopy to view

cell viability. First, cells were maintained and stimulated or infected as per Section 2.4.

2.13.1. MTT Assay

At the required time, fresh media was replaced on the cells, and then MTT solution (10% of total well volume; Table 2.4b.) was added and incubated for 2 hours at 37°C. Next, 100 µl of Solubilising Solution (Table 2.4b.) was added and then incubated overnight. The plate was then placed on the plate reader and read at 620 nm.

2.13.2. Microscopy

At the time of the assay, images of the cell cultures were taken at 40x magnification by an Olympus U-TVO-5XC-3 Lens on an Olympus CKX41 microscope and then were cropped to highlight areas of interest on ImageJ software.

2.14. TN-C Purification

2.14.1. Collection of HEK-293:pCEP-huTNC-his Cell TN-C Production

HEK-293:pCEP-huTNC-his cells were grown to confluency (Section 2.2.4) and then were washed with PBS before being placed in HEK-293 Collection Medium (Table 2.2) for two days. The conditioned medium (CM) was then collected and stored at -80°C, before cells were recovered in HEK-293 Complete Media for one day and then transferred back to Collection Medium. This cycle was repeated up to eight times.

2.14.2. Treating the Conditioned Medium, FN Removal and Bead Incubation

The CM was first filtered over a 0.45 µm filter and then precipitated with ammonium sulphate (291 g per 1 L of CM; Sigma-Aldrich) for 2 hours at 4°C. Next, the CM was centrifuged at 12,000 rcf for 20 minutes at 4°C, before being re-suspended in 1xPBS / 0.01% Tween-20 (50 ml for 1 L CM). The CM was then dialysed against 1xPBS / 0.01% Tween-20 for 2 hours in 50 times volume at 4°C. This was repeated further two times. The dialysed protein was then centrifuged at 12,000 rcf for 10 minutes at 4°C (Sorvall RC6 centrifuge) and the supernatant was collected. A column containing 15 ml of gelatin-agarose beads (Sigma-Aldrich) was next equilibrated with 50 ml MilliQ water and then 50 ml 1xPBS / 0.01% Tween-20. The dialysed protein was then passed over the agarose column using a peristaltic pump (VWR) to remove FN, and the supernatant was collected. The protein sample was next adjusted to the same concentration as the EQB (Table 2.4b.) by adding the appropriate concentrations of the EQB reagents, and then incubated overnight with 20 ml Ni²⁺ column resin beads (Thermo Fisher Scientific) at 4°C.

2.14.3. Elution and Detection of TN-C

The bead-protein sample was next loaded into a column and the flow through was collected, before the flow through was again passed through the column by a peristaltic pump and

collected. The beads were washed with 50 ml EQB, 50 ml Washing Buffer (Table 2.4b.), 100 ml ice cold Washing Buffer 0.1% Triton-X114 and then 100 ml ice cold Washing Buffer. TN-C was next eluted from the beads by washing with 50 ml Elution Buffer A (collected in 5 ml fractions; Table 2.4b.), and then 20 ml Elution Buffer B (Table 2.4b.). Next, the presence of TN-C and his-tag was measured by western blot (as per Section 2.7.).

2.14.4. Quantification and Characterisation of TN-C

2.14.4.1. Quantification of TN-C by BCA and BSA Standard Curve

Following positive detection of TN-C, protein concentration was determined. BCA test was first performed as per Section 2.11. and to confirm this concentration, quantification by BSA standard curve was also performed. A BSA standard curve was generated (ranging from 2 µg to 0.1 µg) and ran on a gel alongside the purified TN-C fractions. Coomassie Brilliant Blue (Thermo Fisher) staining was performed and quantified by densitometry by ImageJ. The BSA standard curve was then generated, and the TN-C fractions were interloped onto the curve. The µg concentration of the protein was then converted into µM concentrations for use in stimulations.

2.14.4.2. Circular Dichroism Spectra (CDS) Test

Next, CDS was used to determine whether the protein was folded or not. 200 µl of protein, diluted to 0.2 mg/ml in TN buffer was loaded into the Jasco J-815 CDS Spectrometer (Table 2.10b.). The CDS of the TN-C was measured 5 times by Jasco CDS Manager at the 250-190 nm wavelength. Following CDS analysis, the sample was heated for 15 min at 80°C before being analysed again. CDS analysis determined the alpha helix (peak at 222-208 nm), beta sheet (peak at 215 nm) and random coil (negative at 195 nm) of the full-length TN-C protein.

2.14.4.3. LAL Test

Finally, the presence of LPS in the TN-C sample was quantified using the LAL test (Table 2.6). First, a standard curve ranging from 0.05-1 Endotoxin Units (EU) was prepared and 50 µl was loaded into a 96 well plate alongside the TN-C protein samples (in duplicates). 50 µl Lysate Solution was added and incubated at 37°C for 10 minutes, before Chromophore was added and incubated for a further 7 minutes. 25% acetic acid was then added and then the plate was read on the plate reader at 340 nm. The samples were interpolated onto the standard curve, with an LPS concentration of less than 0.1 EU deemed acceptable (as this is below the limit of detection). The TN-C samples were then snap-frozen with liquid nitrogen and stored at -80°C.

2.14.5. TN-C-FBG Purification

Recombinant LPS-free TN-C-FBG was purified by Dr Anja Schwenzer at the University of Oxford (as per Midwood et al. 2009) and donated for the use in this study. To summarise, FBG DNA was cloned into a PCR Blunt vector and inserted into a pET32b plasmid, before being transformed into cultured in 3 L of Luria-Bertani medium containing 50 µg ml⁻¹ carbenicillin and

induced with 1 mM isopropyl-D-thiogalactopyranoside. After 3 hours, the media was collected and FBG was purified by Ni²⁺ chromatography (as per Section 2.14), and quality checks such as LAL testing, CDS and determining the concentration by BCA was performed as per Section 2.14. The FBG was then used for stimulation experiments by Jake Mills.

2.14.6. Purified Recombinant TN-C and FBG Stimulation of AECs

2.14.6.1. Purified Recombinant TN-C and FBG Stimulation of BEAS-2B Cells

For purified recombinant TN-C and FBG stimulation of BEAS-2B cells, the cells were serum starved overnight (in 96 well plates) before stimulation by removing BEAS-2B Complete Media and replacing with 200 µl of BEAS-2B Basal Media (Table 2) per well. At time of stimulation, the media was replaced with fresh Basal Media, before 0.1-2 µM purified recombinant TN-C or FBG was exogenously added.

2.14.6.2. Purified Recombinant TN-C and FBG Stimulation of MDMs

For purified recombinant TN-C and FBG stimulation of MDMs, the same protocol as for stimulation of BEAS-2B cells was carried out (Section 2.4.5.1), with the only difference being cells were cultured in MDM media. MDMs were also stimulated with a LPS TLR4 positive control as per Section 2.4.

2.15. TN-C siRNA Treatment of AECs

TN-C siRNA (Dharmacon) and Scrambled siRNA (Dharmacon) was re-suspended in nuclease-free water to make 20 µM stocks, and 100 nM of siRNA was used per well, diluted in Opti-MEM (Thermo Fisher Scientific). The 100 nM siRNA-Opti-MEM mix was added to a lipofectamine (Thermo Fisher Scientific) Opti-MEM mix (1:40 lipofectamine-Opti-MEM dilution) and left at RT for 20 minutes.

Next, cell media was removed, washed with 1 ml PBS and 800 µl BEAS-2B Basal Media or PBEC Basal Media was added per well. 200 µl of TN-C siRNA-lipofectamine-Opti-MEM or Scrambled siRNA-lipofectamine-Opti-MEM was added to the relevant well in a small dropping motion, moving the pipette around the well to cover all the area, and left to incubate for 4 hours. The media was next removed, washed in 1 ml PBS and 1 ml BEAS-2B Complete Media or PBEC Recovery Media per well, depending on the cell type. A mock control with water replacing the 100nM siRNA and an untransfected Opti-MEM only control was also used. The cells were left for 24 hours, before stimulation or infection was carried out as per Section 2.4.

2.16. Trichloroacetic Acid (TCA) Precipitation

Mouse BALF samples were concentrated by TCA precipitation. 1 part of cold 10% TCA (Sigma-Aldrich) was added to 3 part BALF sample, mixed thoroughly and placed on ice for 10 minutes. The sample was then centrifuged at 14,000 rcf for 5 minutes and the supernatant was removed,

leaving the sample pellet. This was then washed with 200 μ l of cold acetone (Sigma-Aldrich), and this was repeated 3 times. The pellet was then dried by placing in the heat block at 95°C for 10 minutes, and then the sample was suspended in 4x sample buffer.

2.17. Statistics

Data was analysed and presented via GraphPad Prism v7.0 as mean \pm standard error of the mean (SEM). D'Agostino-Pearson omnibus tests were carried out on the data sets for Figure 3.2., 3.12, 3.13, 3.15 and 3.18., and normal distribution of the data was determined, which also correlated with previous calculations in our lab that used the same cells (Parker et al. 2008, Stokes et al. 2016, Manley et al. 2018). Appropriate statistical tests were carried out, including paired T-test, One Way ANOVA with Dunnett's post-hoc test and Two Way ANOVA with Dunnett's post-hoc test and p values of <0.05 (*), <0.01 (**), <0.001 (***) and <0.0001 (****) were considered statistically significant.

Chapter 3 – Results: The Relationship Between RV Infection and Tenascin-C Expression in AECs

3.1. Introduction

There is a direct association between the presence of respiratory viruses and asthma exacerbations in asthma patients. One study found that respiratory viruses were detected in 80% of wheezing episodes and 85% of upper respiratory symptoms in 108 children aged 9-11 (Johnston et al. 1995b). The evidence is less clear in adults, but one study showed a detection rate of 76% (via PCR) in 49 adults, and the viral infection was associated with acute asthma symptoms (Wark et al. 2002). RV were found to be the most common virus detected in the studies mentioned above, being present in approximately 66% of cases, implicating RV as the major cause of asthma exacerbations with regards to respiratory viruses (Johnston 2005).

TN-C is implicitly linked to the pathogenesis of asthma. TN-C is present in higher quantities in the bronchial sub-epithelial RBM in patients with asthma when compared to non-asthmatic controls, and TN-C levels correlate positively with the severity of the disease (Laitinen et al. 1997). Furthermore, when patients with asthma were treated with a corticosteroid twice daily for 4 to 6 weeks, TN-C levels in the RBM decreased (Laitinen et al. 1997); but work in this study did not investigate whether this correlated with a decrease in disease specific symptoms. An increase in TN-C expression in the RBM of asthmatics also occurs during airway hyperresponsiveness (increased sensitivity to a constrictor agonist; Kariyawasam et al. 2007). Following allergen challenge of patients with mild-moderate asthma (house dust mites, grass, cat dander), TN-C expression was increased at 24 hours in the RBM of bronchial epithelial cells, before falling to basal levels at 7 days. The increase of TN-C was accompanied by the increase of eosinophil, macrophage, neutrophil, and CD3⁺ T cells (Kariyawasam et al. 2007). The role of TN-C in asthma has also been investigated in a knockout murine model. In this model, airway inflammation was induced in TN-C KO BALB/C mice by sensitisation and challenge with Ova. As measured by Penh value (airflow measured by a plethysmography), airway hyperresponsiveness was significantly lower in the TN-C KO mice compared to the wild type (Nakahara et al. 2006). Furthermore, a genetic polymorphism study in Japan revealed an SNP that strongly associated with adult bronchial asthma (Matsuda et al. 2005). This SNP affects the beta sheet of the FNIII-D domain, causing a loss in elasticity and airway integrity (Matsuda et al. 2005).

TN-C has also been demonstrated to play a role in viral / pathogenic infection. In a study by Fouda et al (2013), TN-C was implicated in the role of neutralisation of HIV-1 transmission in the breast milk of infected mothers. Purified TN-C (22-200 µg/ml) had the capacity to bind and neutralise the infectivity of HIV-1 by binding to the CD4 receptor of the virus and depletion of TN-C from breast milk ablated the neutralising effect (Fouda et al. 2013). Finally TN-C plays a vital role in the TLR4-dependent inflammatory response to LPS, with TN-C^{-/-} macrophages unable to transcribe mir-155 and consequently TNFα (Piccinini and Midwood 2012).

RV infection of AECs induces cytokine, chemokine and IFN production by binding to a large range of receptors, including TLR3 (as summarised in in Section 1.2.). A number of these cytokines have previously been demonstrated to be transcriptional regulators of TN-C; but crucially not in the context of RV infection. TGF- β can induce TN-C expression, by binding to Smad2/3 on the promoter (Tucker and Chiquet-Ehrismann 2009, Akhurst et al. 1990, Soini et al. 1993), whilst IL-4, IFN and TNF α can also induce TN-C expression (Latijnhouwers et al. 2000). Importantly, a study conducted by Proud et al (2008) measured the gene expression profile from nasal scrapings following a 2 day inoculation of RV-16 in healthy human individuals, and this revealed TN-C mRNA was upregulated nearly 3-fold compared to non-infected individuals (Proud et al. 2008), however, this finding was not further investigated.

Despite the fact that TN-C and RV are both linked to the pathogenesis of asthma, TN-C has previously been demonstrated to have differing roles in the response to pathogenic infection and TN-C mRNA has been shown to be induced in response to RV in a human infection study, the relationship between the two has yet to be investigated.

3.2. Hypothesis and Aims

It was hypothesised that RV infection induces TN-C mRNA expression, protein expression and protein release in the airway, in a RV serotype (i.e. major or minor group) independent manner.

The specific aims of this chapter were to investigate:

1. TN-C expression *in vivo* in the BALF of mice following nasal administration of the viral mimic poly(I:C).
2. Whether TN-C mRNA expression, cell-associated TN-C protein expression and TN-C protein release are modulated in response to stimulation with poly(I:C) or RV infection (major and minor serotypes) *in vitro* in human AECs.
3. The specific splice domains and variant size of TN-C present basally in human AECs and induced by stimulation with poly(I:C) and RV infection *in vitro*.
4. Potential differences in RV-induced TN-C mRNA expression and TN-C release in PBECs from asthmatic patients compared to PBECs from non-asthmatic patients.

3.3. Intranasal Poly(I:C) Administration of Mice Induces TN-C Expression in the BALF

The first aim was to investigate whether nasal administration of the TLR3 ligand and viral mimic poly(I:C) induced TN-C expression *in vivo* in the BALF of C57BL/6 mice. Under recovery anaesthesia, adult C57BL/6 mice were treated intranasally with 50 μ l PBS or 100 μ g poly(I:C) in 50 μ l PBS for up to 48 hours. The mice were then sacrificed, and BALF was collected by washing the lungs with 3 ml of PBS. The expression of BALF keratinocyte-derived cytokine (KC) was measured by ELISA. BALF was also concentrated by TCA precipitation and the presence of TN-C was analysed by western blotting and expression was normalised to neutrophil cell count. To analyse the TN-C variant expression, densitometry was performed at 48 hours in ImageJ software, and a ratio of small to large variants was calculated. In this study, small variants were defined as 250 kDa or below, with large variants as >250 kDa. The correlation between TN-C expression and KC release was also calculated.

In response to poly(I:C), no significant change was observed in KC expression at 24 and 48 hours (; Figure 3.1A). At 24 hours post stimulation, there was no visible expression of TN-C in the PBS control samples and only negligible TN-C expression was observed in response to poly(I:C (data not shown), whilst at 48 hours, there was a low level of TN-C expression in the PBS control samples, and upregulation occurred in response to poly(I:C) (Figure 3.1B). There were two clear variants present in response to 48 hours of poly(I:C) stimulation, one 'small' ~250 kDa variant and one 'large' variant at >250 kDa. The induction of TN-C at 24 hours was not statistically significant, however at 48 hours TN-C expression was significantly induced in response to poly(I:C) compared to PBS controls ($p < 0.05$), as measured by densitometry and normalised to neutrophil cell count (Figure 3.1C). There was no correlation between KC production and TN-C expression ($R^2 = 0.09722$) however, if Mouse 3 was treated as an anomaly and removed, a positive correlation was observed (Figure 3.1D; $p < 0.01$; $R^2 = 0.8985$). The smaller variant was the predominantly expressed TN-C variant in the media controls and in response to poly(I:C), with a 4:1 and 3:1 ratio of expression between the smaller ~250 kDa and larger >250 kDa variant (Figure 3.1E).

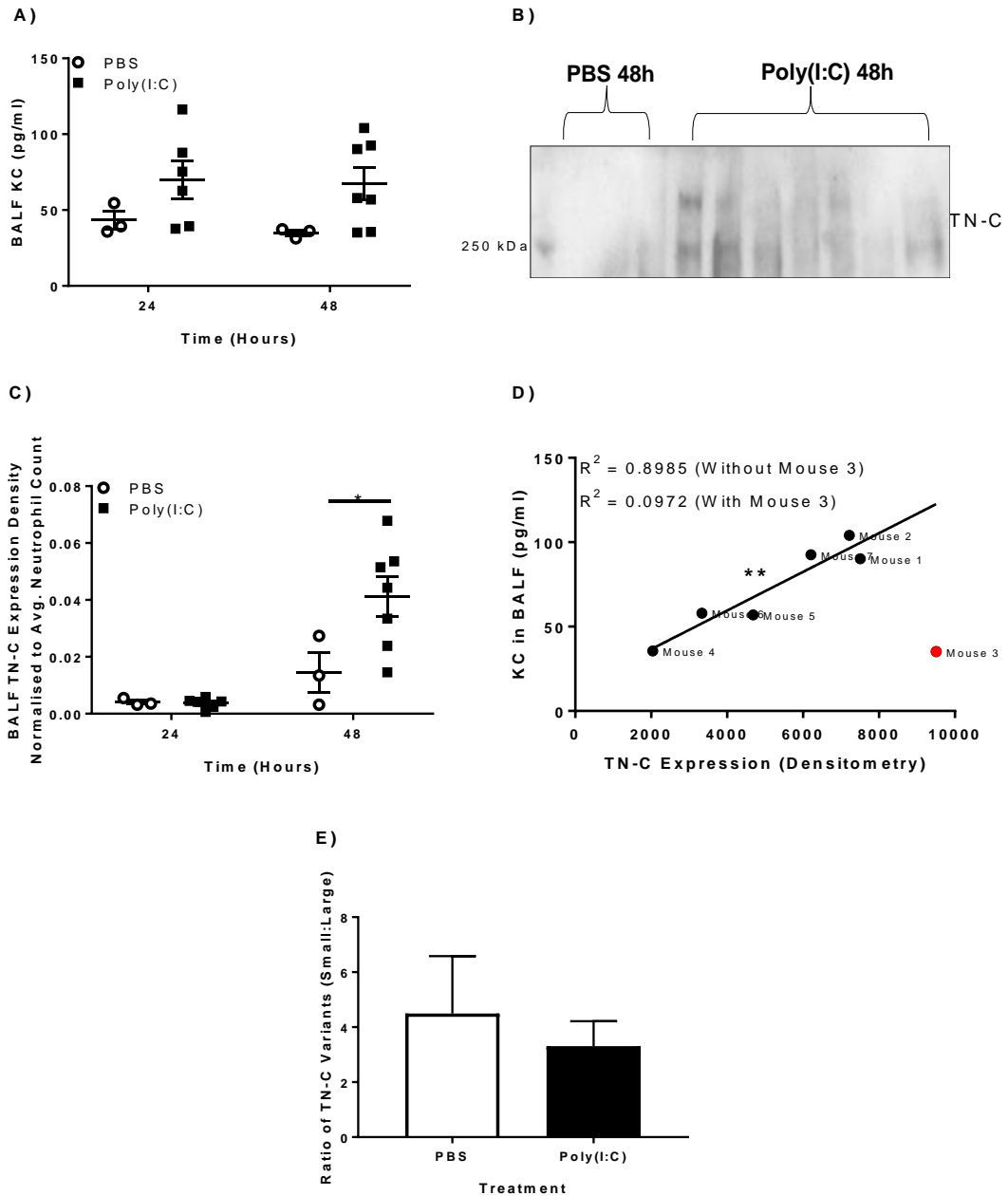


Figure 3.1. Intranasal Poly(I:C) Stimulation of Wild-Type C57BL/6 Mice Induces TN-C Expression in the BALF

Under recovery anaesthesia, adult C57BL/6 mice were treated intranasally with 50 μ l PBS or 100 μ g poly(I:C) in 50 μ l PBS for up to 48 hours. The mice were then sacrificed, and BALF was collected by washing the lungs with 3 ml of PBS. BALF KC was measured by ELISA (A). 150 μ l of BALF was TCA precipitated to 20 μ l, the presence of TN-C at 24 and 48 hours was analysed by western blotting (B; representative 48-hour blot shown) and densitometry of the bottom band was performed using ImageJ software and normalised to neutrophil cell count (C). Correlation of TN-C expression to KC production was plotted (D) and densitometry was performed on both bands at 72 hours in ImageJ software, and a ratio of small to large variants was calculated (E). Data shown are mean \pm SEM, with each replicate representing a separate mouse (N=3 for PBS controls, N=6 for poly(I:C) 24 Hours and N=7 for poly(I:C) 48 hours). Significant differences in TN-C expression are indicated by * $p < 0.05$; ** $p < 0.01$, analysed by two way analysis of variance (ANOVA) with Tukey's post hoc test, paired T-test or Pearson correlation coefficient.

3.4. Poly(I:C) Stimulation of BEAS-2B Cells Induces TN-C mRNA and Cell Associated Expression and Poly(I:C) Stimulation and RV-1B Infection Induces TN-C Release.

The next aim was to assess human TN-C expression *in vitro* in AECs. TN-C mRNA and cell-associated TN-C expression in response to poly(I:C) and TN-C release in response to poly(I:C) and RV-1B (a minor group RV) was investigated in the BEAS-2B cell line.

3.4.1. Poly(I:C) Stimulation of BEAS-2B Cells Induces TN-C mRNA Expression

To quantify total TN-C mRNA expression, BEAS-2B cells were left unstimulated, or stimulated with poly(I:C) (25 µg/ml) or TNFα (100 ng/ml) for up to 72 hours. The concentration of Poly(I:C) used to stimulate AECs was based on previous established protocols used in our lab (Stokes et al. 2016, Manley et al. 2018). To determine the appropriate concentration of TNFα to use as a positive control, a dose response experiment was carried out, with 100 ng/ml determined to induce TN-C mRNA expression (data not shown). Cells were then lysed, mRNA extracted, converted to cDNA and TaqMan real time quantitative PCR was performed for TN-C (FBG domain) and GAPDH expression, with TN-C levels normalised to the GAPDH control. The relative abundance of TN-C normalised to GAPDH samples was analysed by using absolute quantification by standard curve. As two timecourse experiments were performed separately, 1-8 hours (no TNFα stimulation) and 24-72 hours data were placed on separate graphs and analysed independently. To quantify the splice variants of TN-C present, a SYBR Green real time quantitative PCR was performed for each of the alternative splice domains (A1-D) and total TN-C (7/8) in the 24 hour samples. The relative abundance of TN-C normalised to GAPDH samples was analysed by using relative fold change quantification.

TN-C mRNA was significantly increased at 4, 6, 8 and 24 hours in response to poly(I:C) compared to unstimulated media controls (Figure 3.2A and 3.2B). TN-C mRNA increased 5-fold at 4 hours ($p < 0.001$) and was maintained at 6 hours ($p < 0.0001$), before decreasing marginally at 8 hours ($p < 0.05$). The expression profiles of TN-C mRNA expression induced by poly(I:C) and TNFα post 24 hours appeared comparable, with a peak at 24 hours ($p < 0.01$), before returning close to basal levels at 48 and 72 hours. At 24 hours post stimulation, TN-C mRNA was increased around 8-fold compared to the media control. There was no significant expression of splice specific domains observed due to a large variation in response between the separate donors (Figure 3.2C), but some patterns observed that should be investigated further in the future. In response to TNFα, the domains FNIII-AD1, FNIII-C and FNII-D all increased compared to the media control, alongside a 3.5-fold increase in overall TN-C (FNIII-7/8). Furthermore, FNIII-A2, FNIII-A3, FNIII-A4 and FNIII-B were upregulated 4-8-fold in one donor, but not in the other two donors, so further investigation is needed. Although not statistically significant, there was a 3-fold increase in overall TN-C mRNA expression (FNIII-7/8) at 24 hours in response to poly(I:C) compared to media control. In addition, FNIII-B, FNIII-C and FNIII-D were again upregulated around 4-fold in one donor, but not the other two, and FNIII-AD2 was not expressed either basally or in response to poly(I:C) and TNFα.

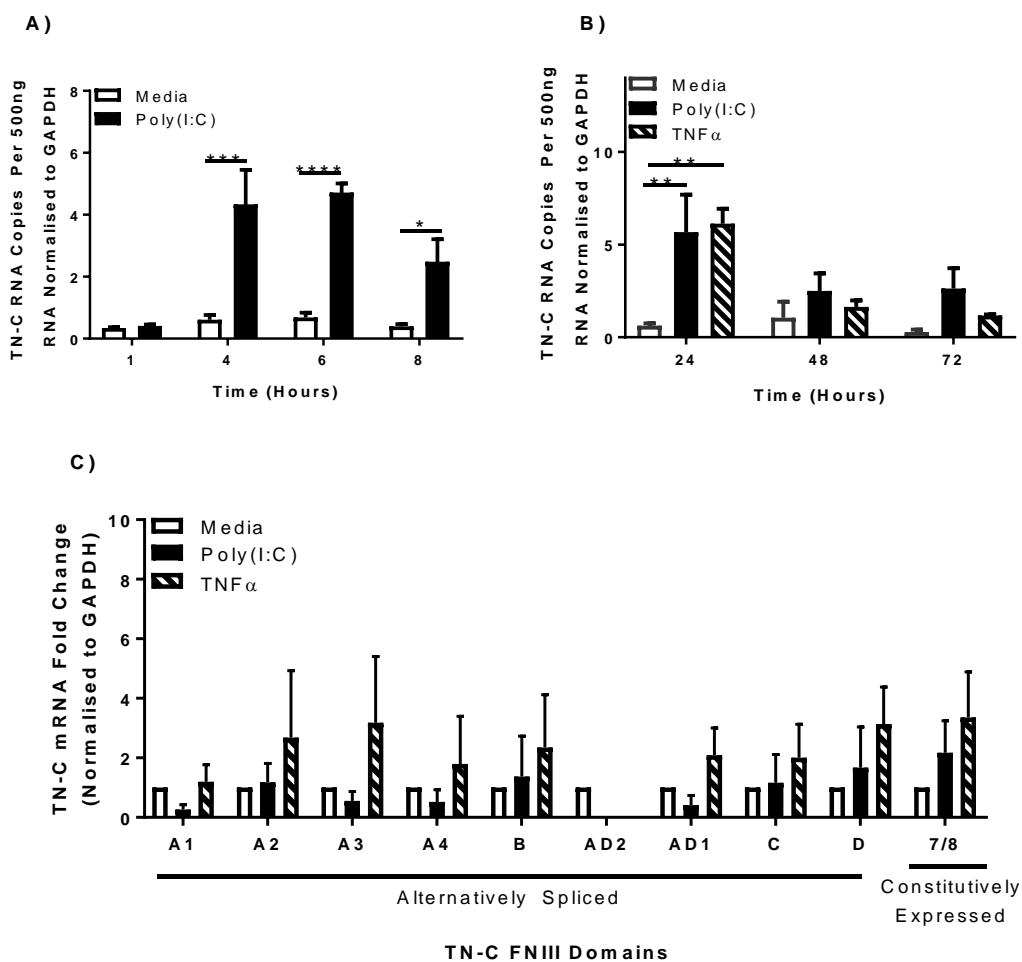


Figure 3.2. Poly(I:C) and TNF α Stimulation of BEAS-2B Cells Increases TN-C mRNA Expression

BEAS-2B cells were treated with poly(I:C) (25 μ g/ml) or TNF α (100 ng/ml) for the indicated times. RNA was extracted from cell lysates and total TN-C mRNA expression (FBG domain) was measured using TaqMan quantitative real time PCR, with data presented as the total RNA copies normalised to GAPDH control. 1-8 hours (**A**) and 24-72 hours (**B**) were performed as separate experiments. (**C**) RNA was extracted at 24 hours post stimulation and specific FNIII splice domain expression and total TN-C (7/8) expression was quantified using SYBR Green quantitative real time PCR. Data shown are mean \pm SEM, with each replicate representing a separate cell passage (N=3). Significant differences in TN-C mRNA copies are indicated by * $p < 0.05$; ** $p < 0.01$; *** $p < 0.001$; **** $p < 0.0001$, analysed by two way repeated measures ANOVA with Tukey's or Dunnett's post hoc test.

3.4.2. Poly(I:C) Stimulation of BEAS-2B Cells Induces Cell-Associated TN-C Protein Expression

3.4.2.1. Poly(I:C) Stimulation of BEAS-2B Cells Induces Cell-Associated TN-C Protein as Measured by Western Blot

Having observed significant TN-C mRNA induction in response to poly(I:C) stimulation (Figure 3.2), TN-C protein expression following poly(I:C) stimulation was next investigated. BEAS-2B cells were left unstimulated or stimulated with poly(I:C) (25 µg/ml) or TNFα (100 ng/ml) for up to 72 hours. Cells were then lysed and the protein was extracted and analysed for TN-C and β-actin by western blot. Cell-associated TN-C expression was analysed by densitometry using ImageJ software, and normalised to the β-actin control. As the two time-course experiments were performed separately, 1-8 hours and 24-72 hours data were placed on separate graphs and analysed independently. To analyse TN-C variant expression, densitometry was performed at 72 hours in ImageJ software, and a ratio of large to small variants was calculated. The larger variants were measured together, due to the close proximity of the two.

Analysis of the western blot data revealed that there were three clear variants of TN-C present, two large variants above 250 kDa and one small variant at ~250 kDa (Figure 3.3A). It is difficult to distinguish between the two large variants due to large expression of these bands, but they are more visible in the 8h TNFα sample. During the early 1-8 hour time points, there was no induction of TN-C expression (Figure 3.3B). TN-C protein expression was induced significantly at 24 and 48 hours ($p < 0.05$) however, before decreasing at 72 hours (Figure 3.3C). TNFα did not induce TN-C expression up to 8 hours post stimulation, but significant expression was observed at 24 ($p < 0.01$) and 72 hours ($p < 0.05$) post stimulation (Figure 3.3B and 3.3C). Induction of TN-C protein expression was also observed at 48 hours, but this was not statistically significant. Interestingly, the absolute amount of TN-C expression induced by poly(I:C) and the positive control TNFα were similar, with the peak induction of TN-C protein observed at 24 hours for TNFα and 48 hours for poly(I:C). The ratio of large to small TN-C variant expression in BEAS-2B cells at the media 72 hours control and in response to poly(I:C) was close to 1:1 (Figure 3.3D), differing from the small variant dominant expression observed in the BALF of mice administered with poly(I:C) (Figure 3.1C).

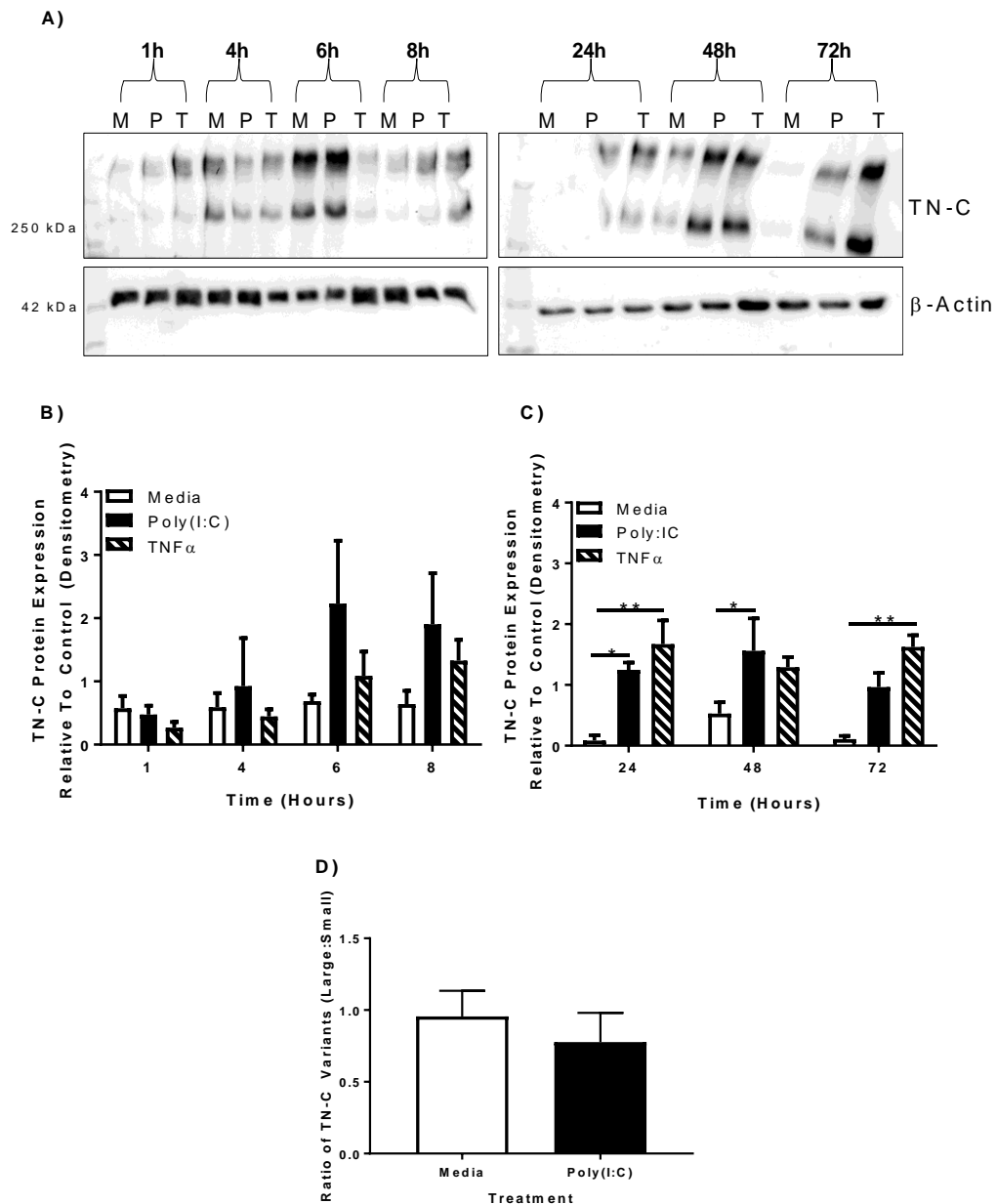


Figure 3.3. Poly(I:C) Stimulation of BEAS-2B Cells Induces Cell-Associated TN-C Expression and an Equal Ratio of Large and Small Variants was Present.

BEAS-2B cells were treated with poly(I:C) (25 μ g/ml) or TNF α (100 ng/ml) for the indicated times. 1-8 hours and 24-72 hours were conducted in separate experiments. Whole-cell lysates were analysed by western blotting using antibodies specific to TN-C (N-Terminal) and β -actin. **(A)** A representative image of three independent BEAS-2B colonies are shown, with media control samples indicated with M, poly(I:C) samples indicated with P and TNF α samples indicated with T. Densitometry of the top band on 1-8 hour blots **(B)** and 24-72 **(C)** was performed in ImageJ software with TN-C normalised to β -actin control. **(D)** Densitometry was performed on both bands at 72 hours in ImageJ software, and a ratio of large to small variants was calculated. Data shown are mean \pm SEM, with each replicate representing a separate cell passage (N=3). Significant differences in TN-C protein expression are indicated by * p<0.05, ** p<0.01; analysed by two way repeated measures ANOVA with Tukey's or Dunnett's post hoc test or paired T-test.

3.4.2.2. Poly(I:C) Stimulation of BEAS-2B Cells Induces Cell-Associated TN-C Protein as Visualised by Immunofluorescence

Cell-associated TN-C expression was also investigated by immunofluorescence. BEAS-2B cells were plated on coverslips and either left unstimulated or stimulated with poly(I:C) (25 µg/ml) for up to 24 hours. Cells were then fixed in 3.8% PFA and permeabilised (to permit intracellular staining) for 15 minutes with Triton-X100. The cells were then stained for TN-C (green) and FN (red) expression and the nucleus was stained with DAPI (blue). Finally, the coverslips were placed onto microscope slides, and fluorescent imaging was performed on the Olympus BX51 Ostometric Fluorescence microscope and Imaris Software. A 24 hour poly(I:C) stimulated no-primary antibody negative control and a fibroblast positive control were also generated. Mean TN-C fluorescence per cell was measured using ImageJ software.

Cell surface and intracellular TN-C expression was modest in the 1 hour unstimulated media control and poly(I:C) stimulated cohort (Figure 3.4A). TN-C expression began to increase intracellularly in response to poly(I:C) at 6 hours and a large increase in expression was observed at 24 hours, correlating with the western blot data (Figure 3.3). Furthermore, increased TN-C expression was observed on the cell surface at 6 and 24-hours post-stimulation. No TN-C or FN expression was observed in the no-primary antibody control and typical staining was observed in the fibroblast control, demonstrating the specificity of the immunofluorescence staining (Figure 3.4B). TN-C expression was significantly upregulated at 24 hours compared to the unstimulated media control ($p < 0.05$) when measured by mean TN-C fluorescence intensity per cell, with a statistically non-significant increase also observed at 6 hours (Figure 3.4C). Whilst TN-C and fibronectin seemed to be closely associated in the fibroblast control, there was no associated in the BEAS-2B samples.

3.4.2.3. Poly(I:C) Stimulation of BEAS-2B Cells Induces Diffuse Cell-Associated TN-C Protein as Visualised by Confocal Imaging

Following immunofluorescence microscopy, confocal imaging was performed on the same slides on the Olympus FV1200 Confocal System to further investigate the type and distribution of TN-C expression.

TN-C fluorescence was low in the unstimulated BEAS-2B cell media controls, with the expression clustered close to the nucleus, whilst FN expression was fibrillar and did not associate with TN-C expression (Figure 3.5A). In the unstimulated fibroblast control, TN-C expression was also grouped around the nucleus, but FN expression seemed to be more closely associated with TN-C (Figure 3.5B). In response to poly(I:C), TN-C expression was upregulated and the distribution changed from clustered around the nucleus to diffuse and distributed throughout the cell population (Figure 3.5A). There was no FN or TN-C expression in the no primary antibody control, antibodies (Figure 3.5B). Mean Fluorescence Intensity (MFI) per cell was measured, showing no significant induction of TN-C expression (Figure 3.5C). This lack of significant increase could be due to the low light setting use on the image exposure time, so as to not bleach the image.

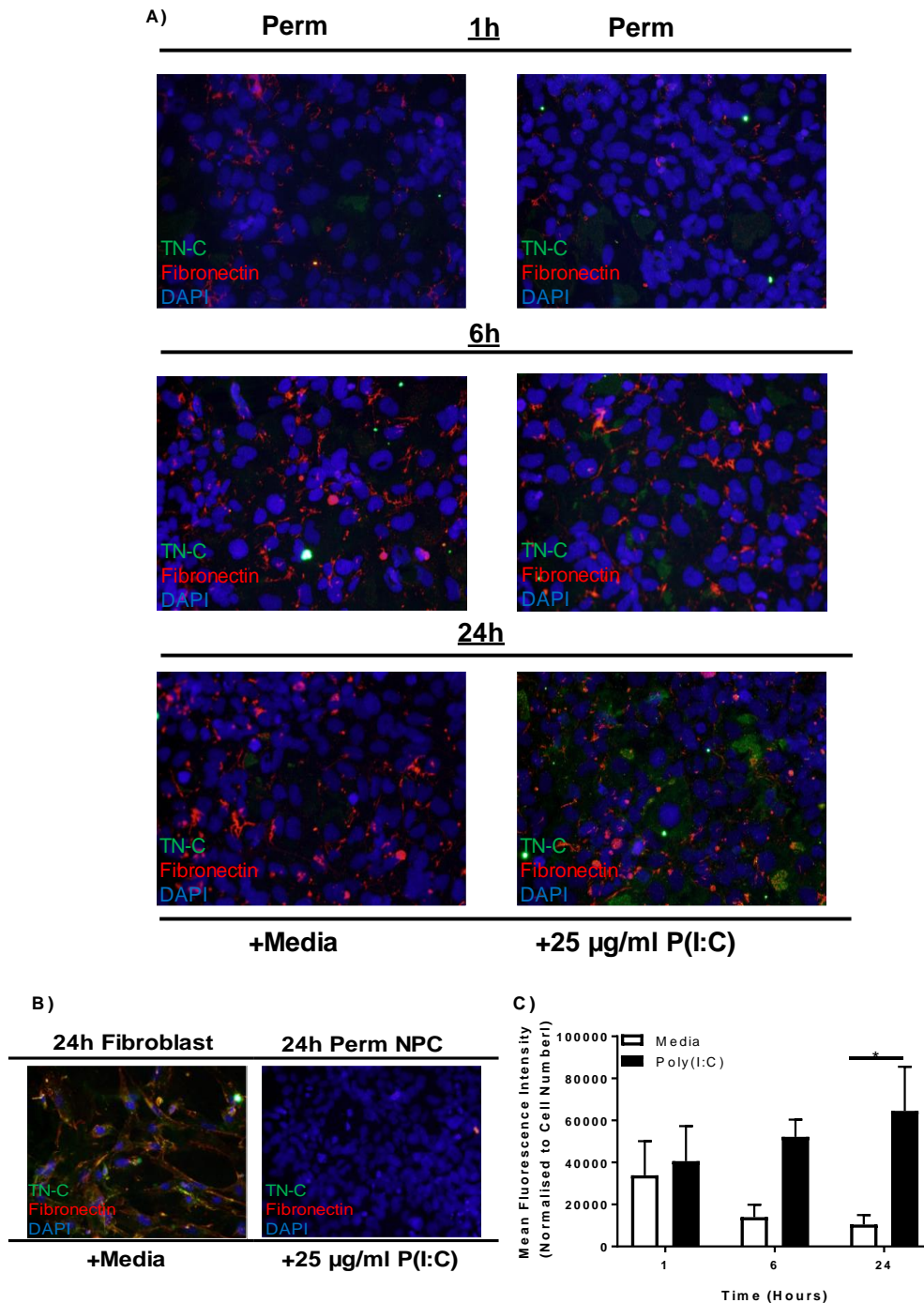


Figure 3.4. Poly(I:C) Stimulation of BEAS-2B Cells Induces Cell Associated TN-C as Visualised by Immunofluorescence

BEAS-2B cells were plated on coverslips and left unstimulated or stimulated with poly(I:C) (25 µg/ml) for up to 24 hours. Permeabilised cells were stained for TN-C (green) and fibronectin (red) and the nucleus was stained with DAPI (blue). **(A)** Fluorescent imaging was performed on the Olympus BX51 Ostometric Fluorescence microscope. A no-primary antibody negative control and a fibroblast positive control **(B)** were also imaged. TN-C MFI was also measured by ImageJ software. Images displayed are a representative time course and data shown are mean \pm SEM, with each replicate representing a separate cell passage (N=3). Significant differences in fluorescence are indicated by * $p < 0.05$; analysed by two way repeated measures ANOVA with Tukey's post hoc test.

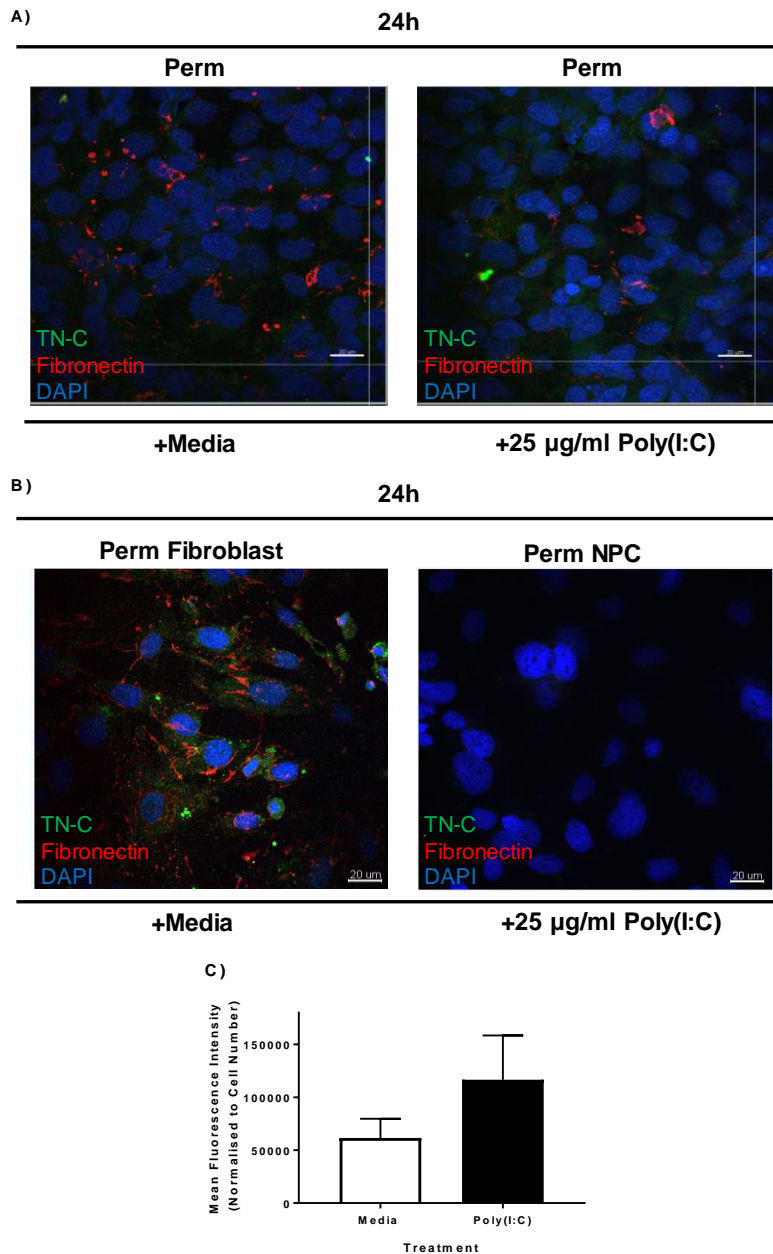


Figure 3.5. Poly(I:C) Stimulation of BEAS-2B Cells Induces Diffuse Cell-Associated TN-C Expression as Visualised by Confocal Imaging

BEAS-2B cells were plated on coverslips and left unstimulated or stimulated with poly(I:C) (25 µg/ml) for up to 24 hours. Permeabilised cells were stained for TN-C (green) and fibronectin (red) and the nucleus was stained with DAPI (blue). Confocal imaging was performed on the Olympus FV1200 Confocal System (A) and fibroblast and no primary control was also imaged by confocal microscopy (B). TN-C MFI per cell was calculated by ImageJ software (C). Images displayed are a representative time course and data shown are mean ± SEM, with each replicate representing a separate cell passage (N=3). Data analysed by paired T-test.

3.4.3. Poly(I:C) Stimulation and RV-1B Infection of BEAS-2B Cells Induces TN-C Release

TN-C release was next investigated in response to poly(I:C) stimulation, gardiquimod (TLR7 agonist) stimulation, TNF α stimulation and RV-1B infection of BEAS-2B cells. First, BEAS-2B cells were left unstimulated or stimulated with poly(I:C) (25 μ g/ml) or infected with RV-1B (MOI 1.5) for 72 hours. Cell free supernatants were then collected and TN-C expression was determined by western blot (analysed densitometrically using ImageJ software) and by TN-C N-terminal) ELISA. To analyse TN-C variant release, densitometry was performed at 72 hours using ImageJ software, and the ratio of large to small variants calculated. In an independent series of experiments, BEAS-2B cells were left unstimulated or stimulated with gardiquimod (10 μ g/ml) or TNF α (100 ng/ml) for 72 hours, and cell supernatants collected. The concentration of gardiquimod used was based on the supplier's instructions. TN-C expression was determined by western blot and analysed densitometrically using ImageJ software.

Analysis of the western blot data confirmed that the two TN-C variants identified in the cell associated data were also present in the supernatant – the large >250 kDa and small ~250 kDa variants (Figure 3.6A). Significant TN-C release was induced at 24, 48 and 72 hours post poly(I:C) stimulation as measured by western blot, when compared to the unstimulated media control (Figure 3.6B). At 24 hours post stimulation, TN-C release significantly increased 5-fold ($p < 0.05$) with peak TN-C release being observed at between 48 ($p < 0.01$) and 72 hours ($p < 0.01$). At these time points, TN-C release increased 4-fold when compared to the media controls. In response to poly(I:C) TN-C was significantly induced at 48 ($p < 0.01$) and 72 hours ($p < 0.0001$), whilst in response to RV-1B, TN-C was induced at 24 ($p < 0.0001$), 48 ($p < 0.0001$) and 72 hours ($p < 0.0001$) compared to unstimulated controls, as measured by ELISA (Figure 3.6C). TN-C release peaked at 72 hours, both in response to poly(I:C) and RV-1B, at 22 and 30 ng/ml respectively. Interestingly the large variant predominated in the supernatant from the 72-hour media control. Although this ratio reduced in response to poly(I:C), there was still a 4:1 ratio of large to small TN-C variant expression (Figure 3.6D). In response to gardiquimod, there was no induction of TN-C release (Figure 3.6E), whilst preliminary investigation (N=1) of TN-C release following TNF α seemed to indicate TN-C release from 24 hours post stimulation (Figure 3.6F).

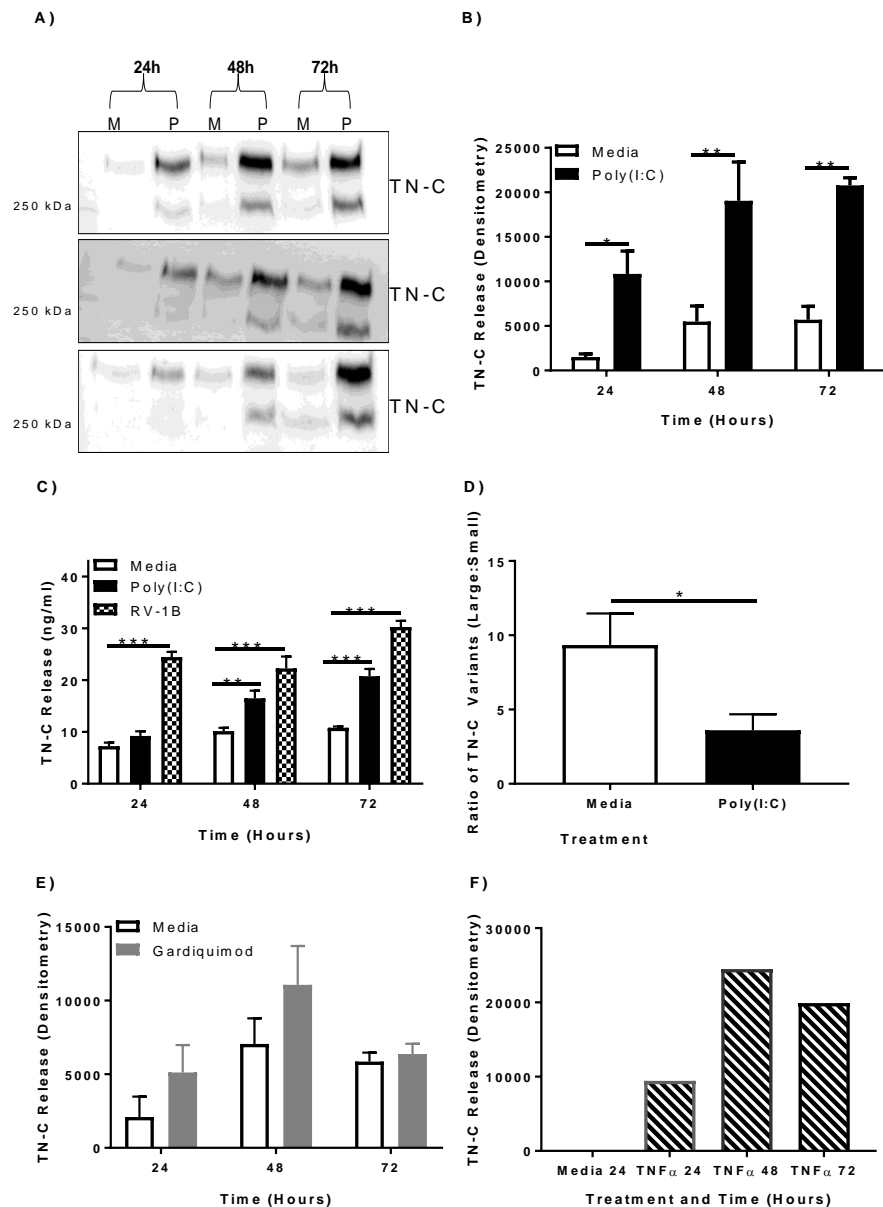


Figure 3.6. Poly(I:C) Stimulation and RV-1B Infection of BEAS-2B Cells Induces the Release of TN-C, with the Large Variant Being the Main Variant Released

BEAS-2B cells were treated with poly(I:C) (25 µg/ml) or RV-1B (MOI 1.5), gardiquimod (10 µg/ml) or TNFα (100 ng/ml) for the indicated times. Cell-free supernatants were prepared and analysed by western blotting using an antibody specific to TN-C. **(A)** All three western blots from the independent poly(I:C) BEAS-2B passages are shown, with media samples indicated with M and poly(I:C) samples indicated with P. **(B)** Densitometry of the top band on the poly(I:C) blots was performed in ImageJ software. **(C)** Cell free supernatants were analysed for the presence of TN-C by TN-C (N-Terminal) ELISA. **(D)** Densitometry was performed on both bands of the poly(I:C) blots at 72 hours using ImageJ software, and a ratio of large to small variants was calculated. Densitometry of the top band on the gardiquimod **(E)** and TNFα **(F)** blots was performed in ImageJ software. Data shown are mean ± SEM, with each replicate representing a separate cell passage (N=3, apart from TNFα, N=1). Significant differences in TN-C release are indicated by * p<0.05; ** p<0.01; *** p<0.001 analysed by two way repeated measures ANOVA with Tukey's, Dunnett's post hoc test or paired T-test.

3.4.4. Poly(I:C) Stimulation and RV-1B Infection of BEAS-2B Cells Induces CXCL8 and CCL5 Production

To confirm that poly(I:C) stimulation and RV infection of BEAS-2B cells was effective and in keeping with published literature (Morris et al. 2006, Parker et al. 2008, Stokes et al. 2011), CXCL8 and CCL5 release was measured over the 72 hour time course. CXCL8 and CCL5 ELISAs were performed for three separate experiments. BEAS-2B cells were (1) unstimulated or stimulated with poly(I:C) (25 µg/ml) or TNFα (100 ng/ml), or (2) unstimulated or stimulated with poly(I:C) (25 µg/ml) or infected with RV-1B MOI 1.5 for up to 72 hours. Due to contradictory evidence regarding TLR7 stimulation in AECs, BEAS-2B were (3) also left unstimulated or stimulated with gardiquimod (10 µg/ml) for 72 hours. Supernatants were then collected and CXCL8 and CCL5 production was measured by ELISA.

In the first stimulation experiment, poly(I:C) induced CXCL8 release at all the time points studied, with a maximal and statistically significant release attained at 48 hours and 72 hours post stimulation ($p < 0.05$; Figure 3.7A). A substantial induction was observed at 24 hours, but this was not statistically significant. CCL5 production also significantly increased in response to poly(I:C) at 24 hours ($p < 0.0001$), 48 hours ($p < 0.0001$) and maximal level of production at 72 hours post-stimulation ($p < 0.0001$; Figure 3.7B). TNFα also induced production of CXCL8 (Figure 3.7A) and CCL5 (Figure 3.7B). TNFα induced significant CXCL8 production at 24 hours ($p < 0.01$), 48 hours ($p < 0.0001$) and 72 hours ($p < 0.0001$). CCL5 production increased at 24 hours (not significant), and at 48 and 72 hours was induced significantly ($p < 0.01$ and $p < 0.01$ respectively). In keeping with the literature (Imaizumi et al. 2015, Matsuzaki et al. 2015), poly(I:C) induced less of the pro-inflammatory chemokine CXCL8 compared to TNFα, but higher levels of the anti-viral chemokine CCL5.

In the second stimulation/infection experiment, poly(I:C) induced significant CXCL8 production at 24 ($p < 0.0001$), 48 ($p < 0.0001$) and 72 hours ($p < 0.0001$) and significant CCL5 at 48 ($p < 0.01$) and 72 hours ($p < 0.05$; Figure 3.7C and D). RV-1B induced significant CXCL8 at 24 ($p < 0.01$), 48 ($p < 0.0001$) and 72 hours ($p < 0.0001$) and although not statistically significant, CCL5 was induced at 48 and 72 hours. Interestingly, poly(I:C) induced greater amounts of CXCL8 and CCL5 than RV-1B.

In response to gardiquimod, there was no induction of CXCL8 (Figure 3.7E) or CCL5 (Figure 3.7F) over the 72 hour period.

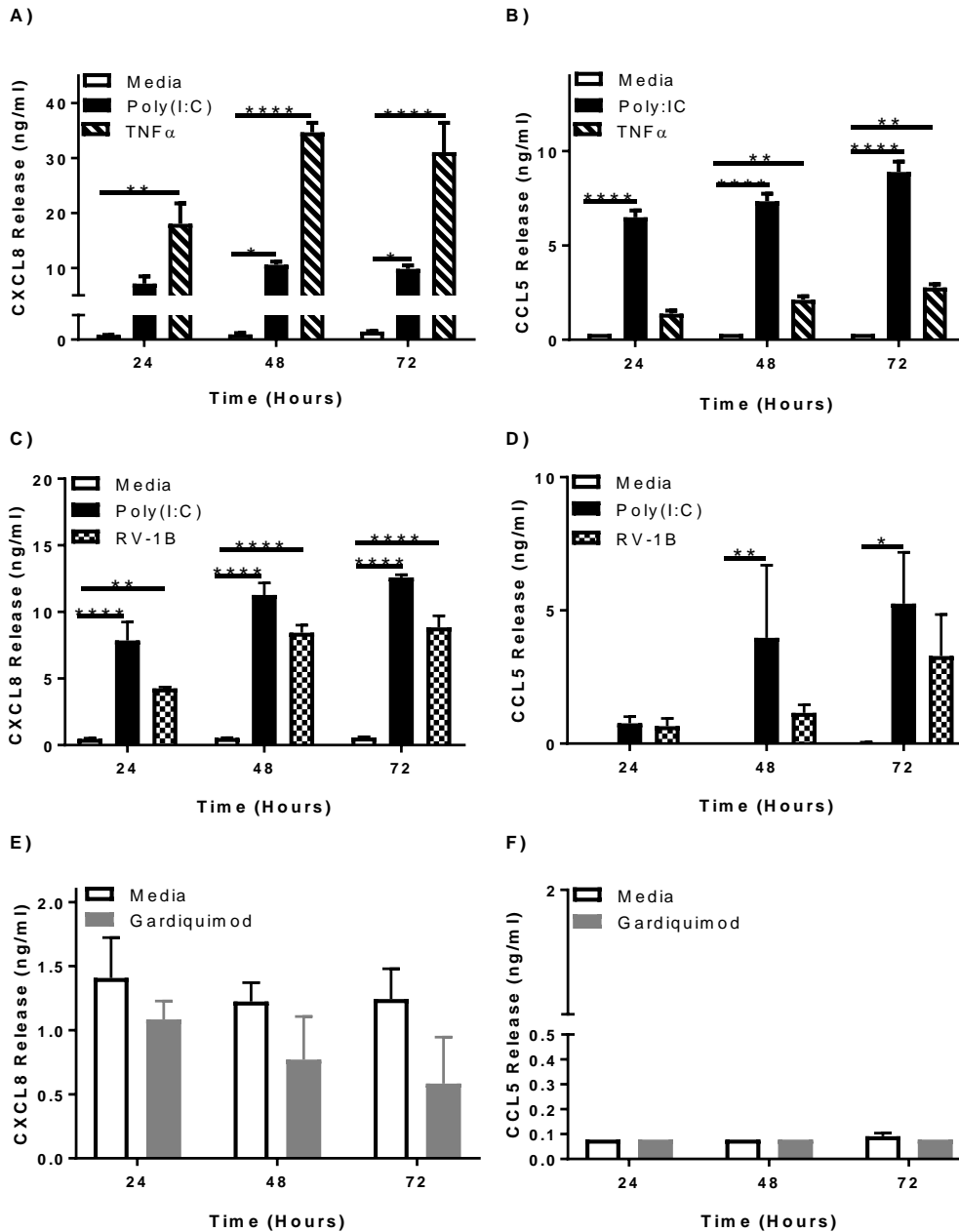


Figure 3.7. Poly(I:C) / TNF α Stimulation and RV Infection of BEAS-2B Cells Induces CXCL8 and CCL5 Production

BEAS-2B cells were stimulated with poly(I:C) (25 μ g/ml) or TNF α (100 ng/ml) or infected with RV-1B (MOI 1.5) for the indicated times. Cell-free supernatants were prepared and levels of CXCL8 and CCL5 was measured by ELISA. Poly(I:C)/TNF α stimulations (**A** and **B**) and poly(I:C)/RV-1B stimulations/infections (**C** and **D**) was performed separately and analysed independently. BEAS-2B cells were also stimulated with gardiquimod (10 μ g/ml) for the indicated times and CXCL8 (**E**) and CCL5 (**F**) was analysed by ELISA. Data shown are mean \pm SEM, with each replicate representing a separate cell passage (N=3). Significant differences in chemokine production are indicated by * p<0.05; ** p<0.01; **** p<0.0001, analysed by two way repeated measures ANOVA with Tukey's post hoc test.

3.5. Poly(I:C) Stimulation of PBECs Modulates TN-C mRNA Expression and Induces TN-C Release.

Following the demonstration of increased TN-C mRNA expression, TN-C cell associated expression and TN-C release in response to poly(I:C) (and release in response to RV) in the BEAS-2B cell line, the next objective of the study was to investigate how poly(I:C) stimulation modulated TN-C expression and release in primary cells – PBECs.

3.5.1. Poly(I:C) Stimulation of PBECs Modulates TN-C mRNA Expression

TN-C mRNA expression in PBECs in response to poly(I:C) was first investigated. To determine total overall TN-C mRNA expression and splice variants present in PBECs in response to poly(I:C), the experiments were carried out as detailed in Section 3.4.1.

In response to poly(I:C), TN-C mRNA expression increased at 6 hours post stimulation (more than 2-fold, as measured by TaqMan qPCR), although this did not reach statistical significance (Figure 3.8A). TN-C mRNA levels were also moderately increased compared to the media control at 24 hours (Figure 3.8B). However, overall TN-C expression (FNIII-7/8), as measured by SYBR Green qPCR, increased approximately 5-fold in response to poly(I:C) at 24 hours post stimulation (not statistically significant; Figure 3.8C). The donor variation is again large, with splice domains FNIII-A3, FNIII-A4 and FNIII-D upregulated 6-15 fold in one donor, marginally in another, and not at all in the final donor. Correlating with BEAS-2B data, the FNIII-AD2 domain was not present in PBECs at basal levels or in response to poly(I:C), but low expression of FNIII-ADI was observed.

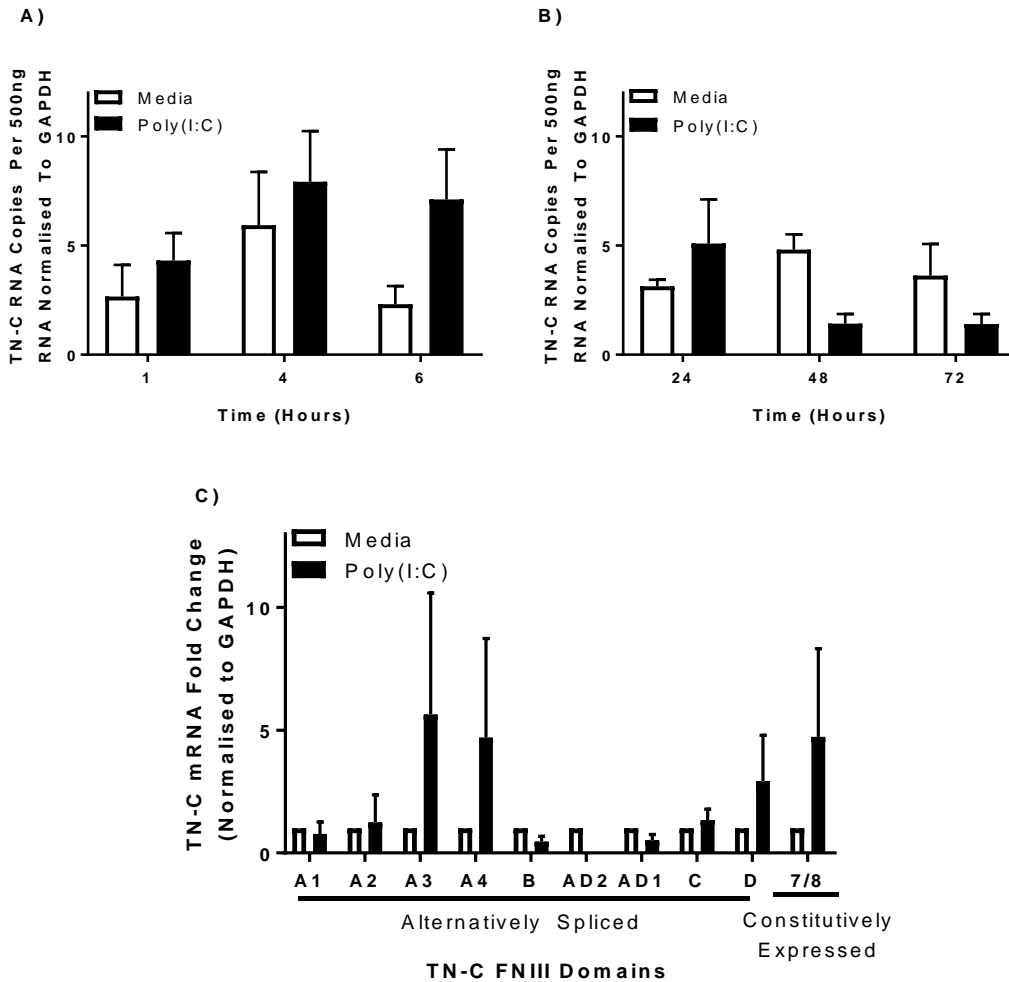


Figure 3.8. Poly(I:C) Stimulation of PBECs Modulates TN-C mRNA Expression

PBECs were treated with poly(I:C) (25 µg/ml) for the indicated times. RNA was extracted from cell lysates and TN-C mRNA expression was quantified using TaqMan quantitative real time PCR, with data presented as the total RNA copies normalised to GAPDH control. 1-6 hours **(A)** and 24-72 hours **(B)** were conducted in separate experiments and analysed independently. **(C)** RNA was extracted at 24 hours post stimulation and specific FNIII splice domain expression and total TN-C (7/8) expression was quantified using SYBR Green quantitative real time PCR. Data shown are mean ± SEM (N=3-4), with each replicate an independent PBEC donor. Data analysed by two way repeated measures ANOVA with Tukey's post hoc test.

3.5.2. Poly(I:C) Stimulation of PBECs does not Induce Cell-Associated TN-C Expression

To determine if cell-associated TN-C protein expression was induced in response to poly(I:C), PBECs were left unstimulated or stimulated with poly(I:C) (25 µg/ml) for up to 72 hours. To investigate total TN-C protein expression and TN-C variant expression in PBECs in response to poly(I:C), experiments were carried out as detailed in Section 3.4.2.1.

Analysis of the western blot data revealed large TN-C variants >250 kDa and a smaller variant at ~250 kDa (Figure 3.9A), correlating with the variants observed in BEAS-2B cells. Poly(I:C) stimulation of PBECs did not induce TN-C expression when compared to the media controls at up to 72 hours post-stimulation (Figure 3.9B and 3.9C). Between 1 and 72 hours, the expression of TN-C protein was unchanged in both the media control and poly(I:C) cohorts. Interestingly, the positive control TNF α did not induce TN-C protein expression, with levels similar to the media controls between 24 and 72 hours. Unlike BEAS-2B cells, there was dominance of larger variants of TN-C present compared to small variants in the media control at 72 hours, and this did not change in response to poly(I:C) (Figure 3.9D).

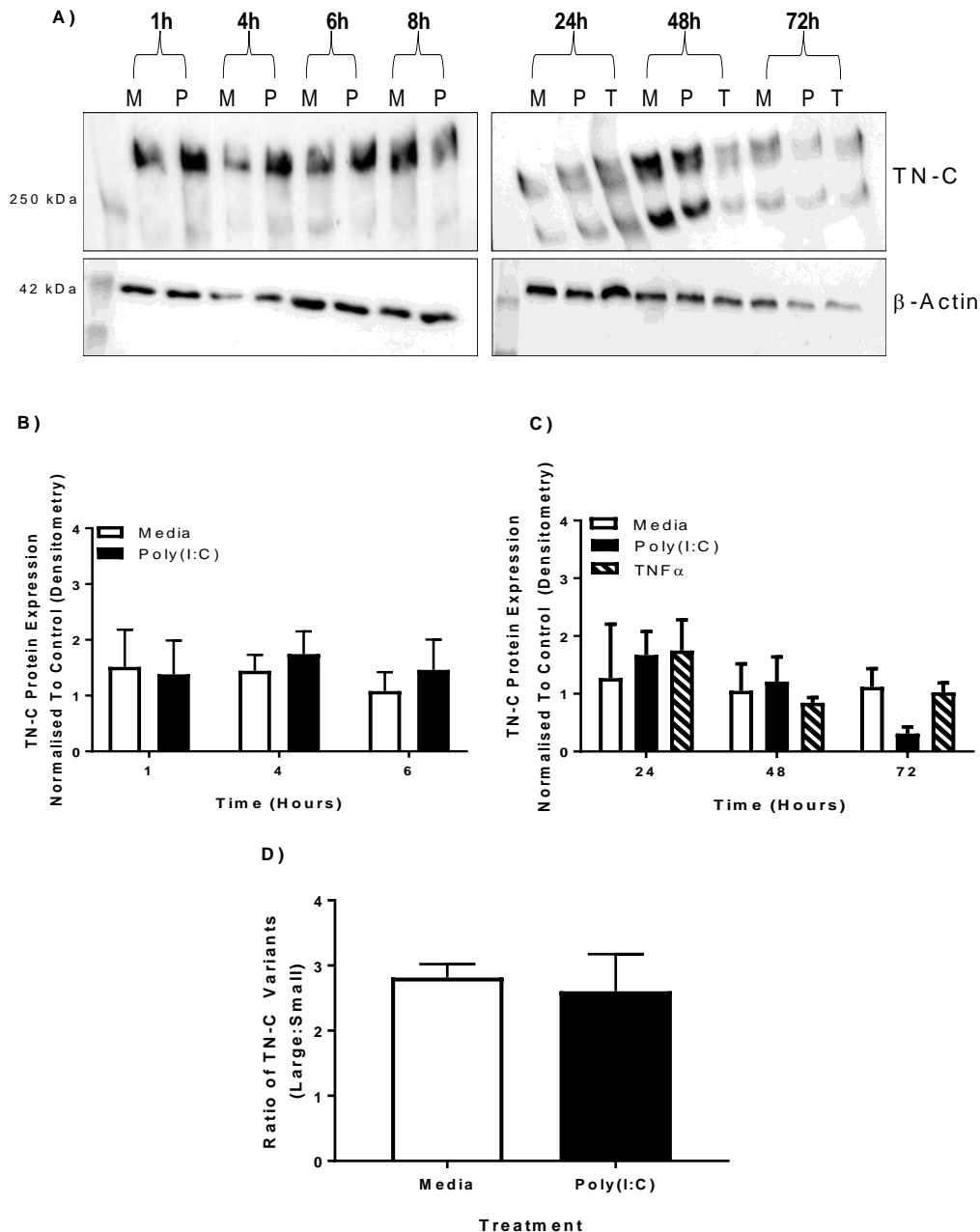


Figure 3.9. Poly(I:C) Stimulation of PBECs does not Induce TN-C Protein Expression

PBECs were treated with poly(I:C) (25 μ g/ml) for the indicated times. Whole-cell lysates were analysed by western blotting using antibodies specific to TN-C and β -actin. **(A)** A representative image of three independent PBEC donors are shown, with media samples indicated with M and poly(I:C) samples indicated with P. Densitometry of the top band of all 1-6 hour blots **(B)** and 24-72 hours **(C)** was performed in ImageJ software with TN-C normalised to β -actin control. **(D)** Densitometry was performed on both bands at 72 hours in ImageJ software, and a ratio of large to small variants was calculated. 1-6 hours and 24-72 hours were conducted in separate experiments and analysed separately. Data shown are mean \pm SEM (N=3-4) with each replicate an independent PBEC donor. Data analysed by two way repeated measures ANOVA with Tukey's post hoc test or paired T-test.

3.5.3. Poly(I:C) Stimulation of PBECs Induces TN-C Protein Release

The next aim was to investigate whether poly(I:C) stimulation of PBECs induced TN-C release into the supernatant. To analyse total and variant specific TN-C release in PBECs in response to poly(I:C), the experiments were carried out as detailed in Section 3.4.3, apart from that gardiquimod stimulation was not performed.

From analysis of the western blot data, the >250 kDa and ~250 kDa variants identified in the cell associated data were also present in the supernatant (Figure 3.10A). There may be two larger variants, but again it is difficult to distinguish due to their close proximity. Significant TN-C release was induced at 48 hours ($p < 0.05$) in response to poly(I:C) stimulation, as measured by western blotting (Figure 3.10B). TN-C was significantly upregulated in response to poly(I:C) at 48 and 72 hours ($p < 0.05$) post-stimulation as measured by TN-C ELISA, when compared to the unstimulated 72 hour media control (Figure 3.10C). TN-C release increased from 1 ng/ml to 4.5 ng/ml at 48 hours and 3.9 ng/ml at 72 hours. The large variant was the primary variant released in both the media control and poly(I:C) stimulated samples. The large to small variant ratio was 3:1 in the media controls, and this increased considerably to approximately 75:1 in the poly(I:C) stimulated samples (Figure 3.10D). Preliminary results indicate TNF α induced TN-C release (N=1; Figure 3.10E) but more replicates are needed.

3.5.4. Poly(I:C) Stimulation of PBECs Induces Significant CXCL8 & CCL5 Release

To confirm the poly(I:C) stimulation of PBECs was effective and in keeping with published literature (Bennett et al. 2012), the production of CXCL8 and CCL5 in response to poly(I:C) was analysed. The experiment was carried out as described in Section 3.4.4. PBECs and MDMs were also stimulated with gardiquimod as per Section 3.4.4. and supernatant analysed for CXCL8 (both cell types) and CCL5 (PBEC only).

Poly(I:C) stimulation induced significant CXCL8 (Figure 3.11A) and CCL5 (Figure 3.11B) production at 24 ($p < 0.01$), 48 hours ($p < 0.0001$) and 72 hours ($p < 0.0001$) post stimulation, compared to media controls. Compared to CXCL8 and CCL5 production in response to poly(I:C) in BEAS-2B cells, poly(I:C) induced greater amounts of CXCL8 release in PBECs (17 ng/ml at 72 hours compared to 10 ng/ml), and comparable CCL5 release (approximately 8-10 ng/ml). As in BEAS-2B cells, gardiquimod induced no CXCL8 (Figure 3.11C) or CCL5 (Figure 3.11D) release at any of the time points in PBECs, but induced significant CXCL8 release in MDM's ($p < 0.001$; Figure 3.11E), demonstrating the activity of the gardiquimod used.

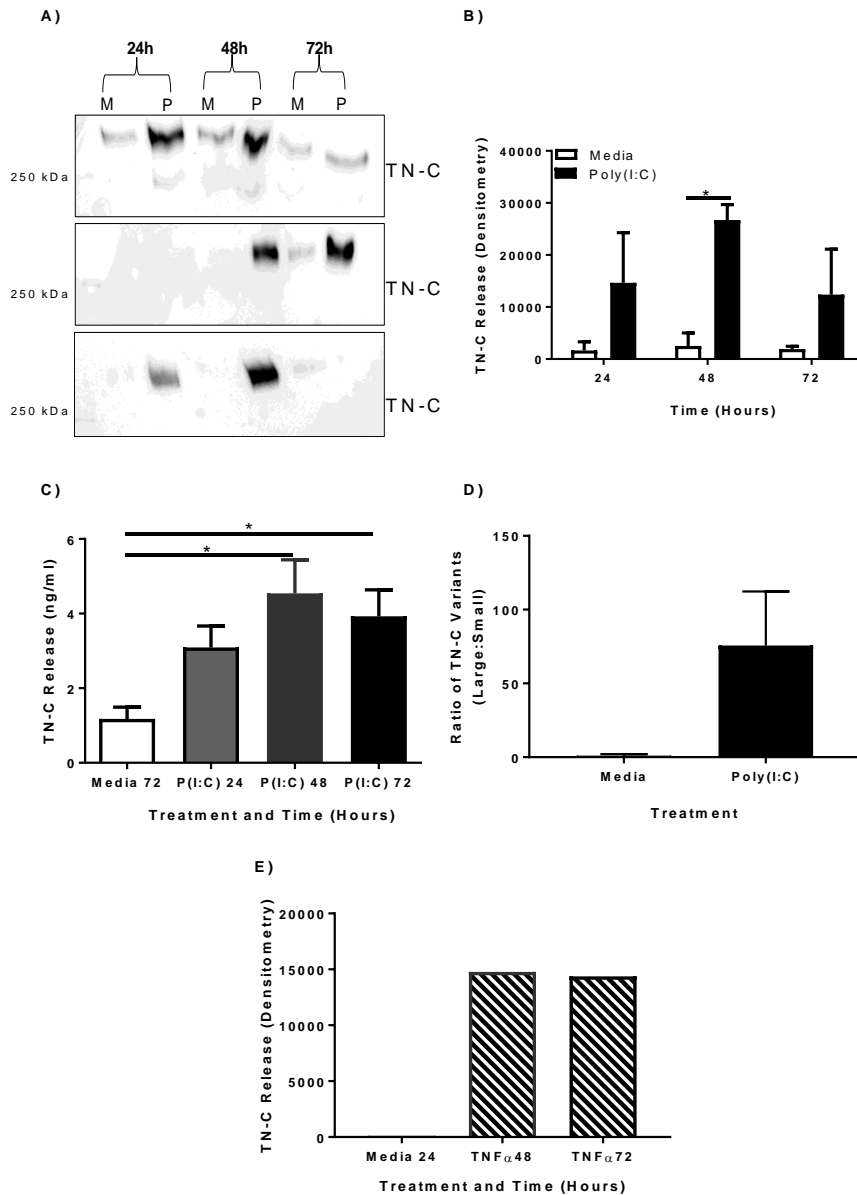


Figure 3.10. Poly(I:C) Stimulation of PBECs Induces the Release of TN-C, with the Large Splice Variant Being the Main Variant Released

PBECs were treated with poly(I:C) (25 µg/ml) or TNFα (100 ng/ml) for the indicated times. Cell-free supernatants analysed by western blotting using an antibody specific to TN-C. **(A)** All three independent poly(I:C) PBEC donors are shown, with media samples indicated with M and poly(I:C) samples indicated with P. **(B)** Densitometry of top band of all poly(I:C) blots was performed in ImageJ software. **(C)** Cell-free supernatants in response to poly(I:C) were prepared and levels of TN-C were measured by ELISA. **(D)** Densitometry was performed on both bands at 72 hours in ImageJ software, and a ratio of large to small variants was calculated. **(E)** Densitometry of top band of TNFα blot was performed in ImageJ software. Data shown are mean ± SEM with each replicate representing an independent PBEC donor (poly(I:C) experiments are N=3 with TNFα N=1). Significant differences in TN-C secretion are indicated by * p<0.05; analysed by two way repeated measures ANOVA with Tukey's post hoc test, one way ANOVA with Dunnett's post hoc test or paired T-test

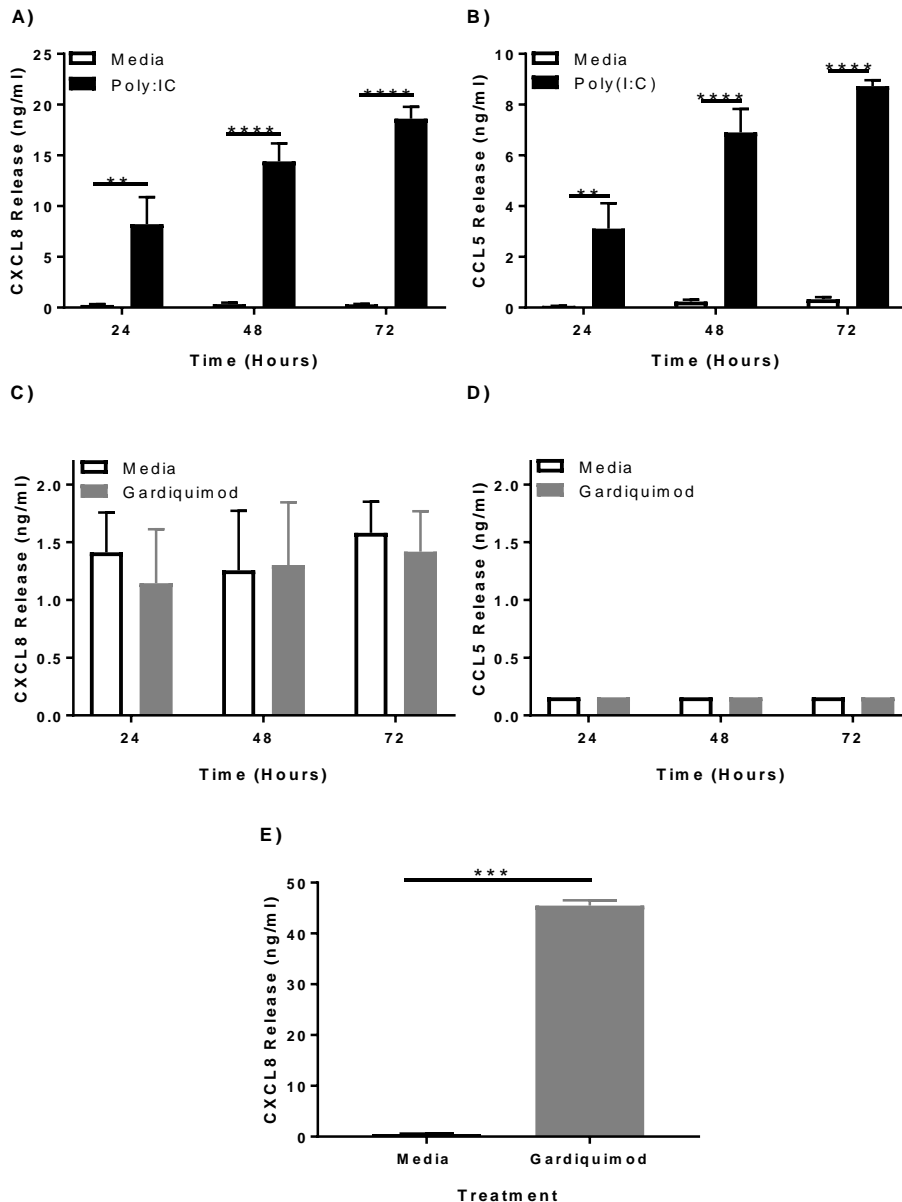


Figure 3.11. Poly(I:C) Stimulation of PBECs Induces CXCL8 and CCL5 Production

PBECs were treated with poly(I:C) (25 μ g/ml) for the indicated times. Cell-free supernatants were prepared and levels of CXCL8 **(A)** and CCL5 **(B)** measured by ELISA. PBECs were treated with gardiquimod (10 μ g/ml) for the indicated times. Cell-free supernatants were prepared and levels of CXCL8 **(C)** and CCL5 **(D)** measured by ELISA. MDM's were treated with gardiquimod (10 μ g/ml) for 24 hours, cell-free supernatants were prepared and levels of CXCL8 measured by ELISA. Data shown are mean \pm SEM, with each replicate an independent PBEC or MDM donor (N=3). Significant differences in chemokine production are indicated by ** $p < 0.01$; *** $p < 0.001$; **** $p < 0.0001$, analysed by two way repeated measures ANOVA with Tukey's post hoc test.

3.6. RV-1B Infection of PBECs Induces TN-C Splice mRNA Expression and RV-1B and RV-16 induced Significant TN-C Release.

Following confirmation that poly(I:C) induced TN-C mRNA expression, cell-associated TN-C protein expression in BEAS-2B cells and TN-C release in both BEAS-2B cells and PBECs, next, the ability of RV to induce TN-C expression was determined. TN-C mRNA expression, cell-associated TN-C expression and TN-C release in PBECs in response to the minor group RV, serotype RV-1B, and the major group RV, serotype RV-16, was assayed.

3.6.1. RV-1B Infection of PBECs Induces Splice Variant Specific Expression of TN-C

To investigate total TN-C mRNA and splice specific expression in PBECs in response to RV infection, cells were left uninfected or infected with RV-1B (MOI 0.6 and 1.5) for up to 72 hours or RV-16 (MOI 1.5) for up to 48 hours. The experiments were then carried out as detailed in Section 3.4.1., with the TaqMan qPCR carried out for all experiments, and the Splice SYBR Green qPCR carried out for RV-1B (MOI 0.6) only.

In response to RV-1B (MOI 0.6) infection (Figure 3.12A) and RV-1B (MOI 1.5) infection (Figure 3.12B), there was no change in overall TN-C mRNA expression throughout the timeline.). Furthermore, RV-16 also did not induce TN-C mRNA expression at 24 and 48 hours compared to the unstimulated media controls (Figure 3.12C). Investigation of splice domain expression in response to RV-1B (MOI 0.6) infection, however, revealed a 4-fold upregulation in the FNIII-C domain ($p < 0.0001$), despite no change in overall (FNIII-7/8) TN-C expression (Figure 3.12D).

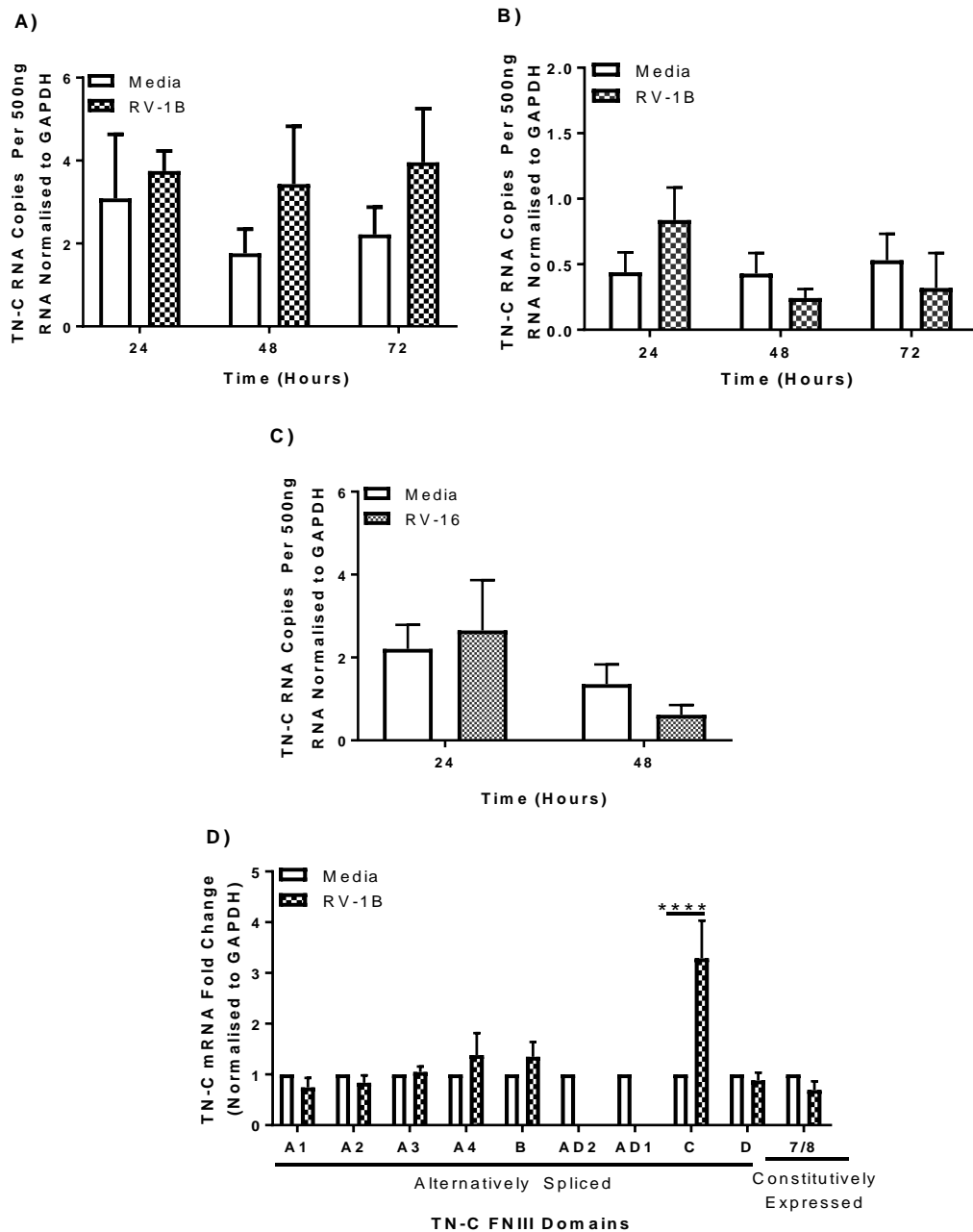


Figure 3.12. RV Infection of PBECs Induces TN-C FNIII-C Domain mRNA Expression

PBECs were treated with RV-1B (MOI 0.6) **(A)** or RV-1B (MOI 1.5) **(B)** or RV-16 (MOI 1.5) **(C)** for the indicated times. RNA was extracted from lysates and TN-C mRNA expression was quantified using a TaqMan quantitative real time PCR, with data presented as the total RNA copies normalised to GAPDH control. **(D)** RNA was extracted at 24 hours post infection (RV-1B MOI 0.6) and specific FNIII splice domain expression and total TN-C (7/8) expression was quantified using SYBR Green quantitative real time PCR. Data shown are mean \pm SEM, with each replicate representing an independent PBEC donor (N=3). Significant differences in TN-C mRNA copies are indicated by **** $p < 0.0001$, analysed by two way repeated measures ANOVA with Tukey's post hoc test.

3.6.2. RV-1B and RV-16 Infection of PBECs does not Induce TN-C Cell Associated Protein Expression

Next, the aim was to investigate total TN-C and variant specific expression in PBECs in response to RV-1B and RV-16 infection. Cells were left uninfected or infected with RV-1B (MOI 0.6 and 1.5) for up to 72 hours or RV-16 (MOI 1.5) for up to 48 hours. The experiments were then carried out as detailed in Section 3.4.2.1.

Analysis of the western blot data again revealed that three TN-C variants were present, two large variants at >250 kDa and a ~250 kDa TN-C variant (Figure 3.13A). TN-C expression in both the media controls and RV-1B infected samples increased over the 72 hour time course, but there were no significant differences between the two groups (Figure 3.13B).. Interestingly, TN-C expression in response to RV-1B (MOI 1.5) infection differed from RV-1B (MOI 0.6) infection. At 48 hours, TN-C protein expression was significantly decreased compared to the media control ($p < 0.05$) (Figure 3.13C). In response to RV-16 there was a 2-fold increase in TN-C protein expression at 24 hours and a small increase at 48 hours when measured by densitometry, however this did not reach statistical significance (Figure 3.13D). There was a dominance of the large variant of TN-C at basal levels (4:1 large to small variant ratio) and this increased to 6:1 in response to RV-1B (Figure 3.13E).

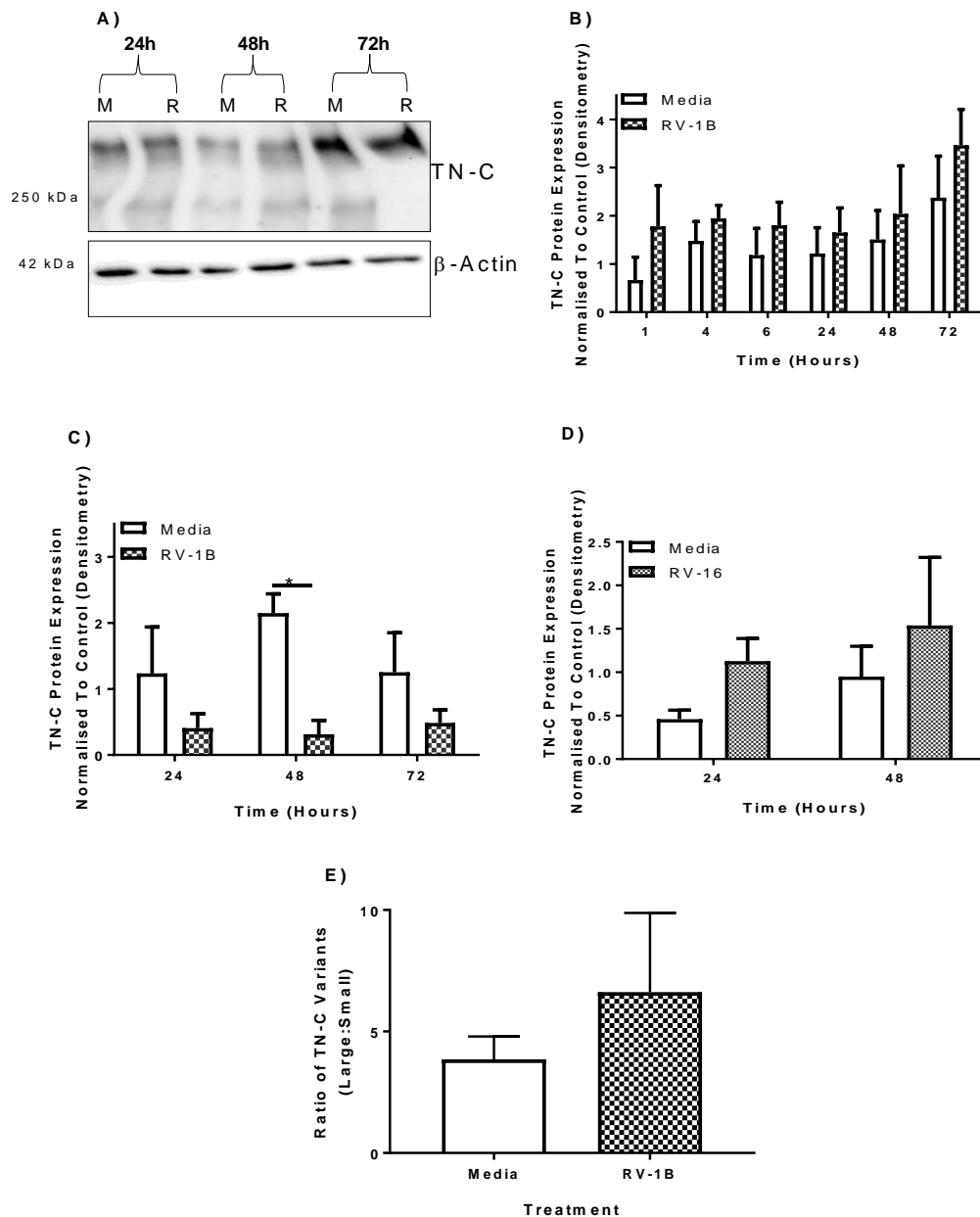


Figure 3.13. RV Infection of PBECs Does Not Induce Significant Cell-Associated TN-C Expression

PBECs were treated with RV-1B (MOI 0.6 or MOI 1.5) or RV-16 (MOI 1.5) for the indicated times. Whole-cell lysates were analysed by western blotting using antibodies specific to TN-C and β -actin. A representative image of three independent PBEC donors is shown, with media samples indicated with M and RV-1B (MOI 0.6) indicated with R (**A**). Densitometry of the top band of all RV-1B (MOI 0.6) (**B**) RV-1B (MOI 1.5) (**C**) and RV-16 (MOI 1.5) (**D**) blots was performed in ImageJ software with TN-C normalised to β -actin control. (**E**) Densitometry was performed on both bands at 72 hours of RV-1B (MOI 0.6) samples in ImageJ software, and a ratio of large to small variants was calculated. Data shown are mean \pm SEM (N=3-4) with each replicate an independent PBEC donor. Data analysed by two way repeated measures ANOVA with Tukey's post hoc test or paired T-test.

3.6.3. RV-1B and RV-16 Infection of PBECs Induces the Release of TN-C

3.6.3.1. RV-1B and RV-16 Infection of PBECs Induces the Release of TN-C as Measured by Western Blot

After confirming that RV-1B and RV-16 infection did not induce significant TN-C cell-associated protein expression, and may in fact decrease TN-C expression (Figure 3.13), the ability of RV-1B and RV-16 to induce the release of TN-C was investigated. Cells were left uninfected or infected with RV-1B (MOI 0.6 and 1.5) for up to 72 hours or RV-16 (MOI 1.5) for up to 48 hours. Western blot analysis was then carried out as detailed in Section 3.4.3.

Analysis of the western blot data revealed that the TN-C variants identified in the cell associated data was also present in the supernatant, however the large variant was the dominant variant (Figure 3.14A). Densitometry revealed that in response to RV-1B (MOI 0.6) infection, TN-C release was significantly increased at 48 ($p<0.05$) and 72 ($p<0.0001$) hours compared to the media controls (Figure 3.14B). In response to RV-1B (MOI 1.5), TN-C release was significantly increased at 48 hours ($p<0.05$) as measured by western blot densitometry (Figure 3.14C). In response to RV-16, TN-C release significantly increased in PBECs compared to the media control at 24 ($p<0.05$) and 48 ($p<0.01$) hours post infection (Figure 3.14D) and in response to RV-1B infection, the large to small variant ratio was approximately 12:1, with low small variant expression (Figure 3.14E).

3.6.3.2. RV-1B and RV-16 Infection of PBECs Induces the Release of TN-C as Measured by ELISA

Next, TN-C release following RV infection was measured by ELISA. Cells were left uninfected or infected with RV-1B (MOI 0.6 and 1.5) for up to 72 hours or RV-16 (MOI 1.5) for up to 48 hours. TN-C ELISA analysis was then carried out as detailed in Section 3.4.3.

When measured by ELISA, TN-C release was increased significantly in response to RV-1B (MOI 0.6) infection at 48 ($p<0.05$) hours, compared to the 72 hour media control (Figure 3.15A). TN-C release was increased from 0.5 ng/ml in the media control to 1 ng/ml at 48 and 72 hours post infection, although the 72 hour increase was not statistically significant. TN-C release in response to RV-1B (MOI 1.5) increased 3-fold (non-statistically significant) at 48 hours compared to media control when measured by ELISA (Figure 3.15B). In this experiment, quantities of TN-C release increased from 2 ng/ml to 6 ng/ml and 5 ng/ml at 48 and 72 hours post infection respectively. In response to RV-16, TN-C release significantly increased 5-fold at 48 hours, increasing from approximately 0.75 ng/ml to 3.75 ng/ml ($p<0.05$; Figure 3.15C).

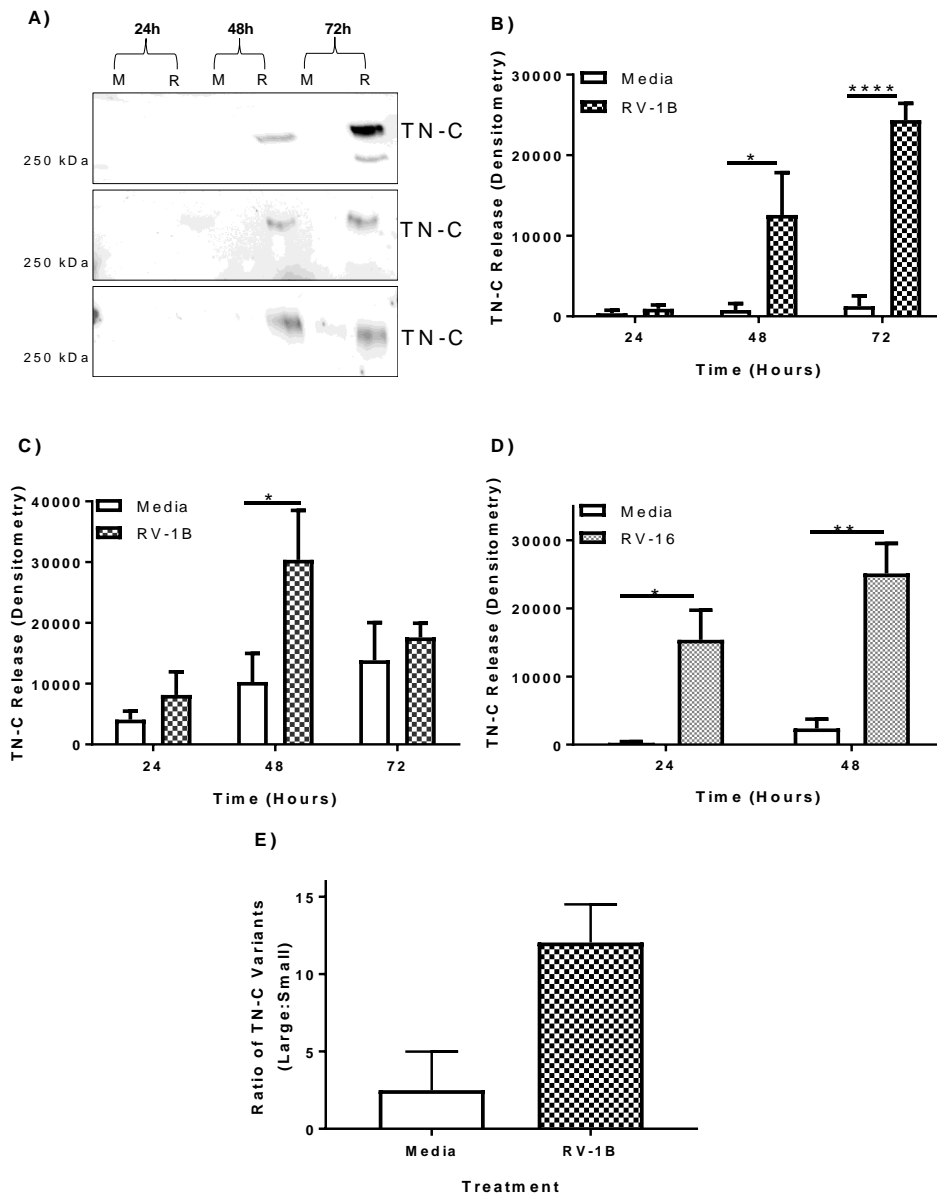


Figure 3.14. RV Infection of PBECs Induces Significant TN-C Release as Measured by Western Blot and the Larger Splice Variant is the Main Variant Released

PBECs were treated with RV-1B (MOI 0.6), RV-1B (MOI 1.5) or RV-16 (MOI 1.5) for the indicated times. Cell-free supernatants analysed by western blotting using an antibody specific to TN-C. **(A)** All three independent PBEC donors of the RV-1B MOI 0.6 experiment are shown, with media samples indicated with M and RV samples indicated with R. Densitometry of the large variant was performed in ImageJ software for the RV-1B (MOI 0.6) **(B)**, RV-1B (MOI 1.5) **(C)** and RV-16 (MOI 1.5) **(D)** experiments. Densitometry was performed on both variants in the 72 hour samples of the RV-1B (MOI 0.6) infection experiments in ImageJ software, and a ratio of large to small variants was calculated **(E)**. Data shown are mean \pm SEM (N=3) with each replicate an independent PBEC donor. Significant differences in TN-C secretion are indicated by * p<0.05; ** p<0.01; **** p<0.0001, analysed by two way repeated measures ANOVA with Tukey's post hoc test or paired T-test.

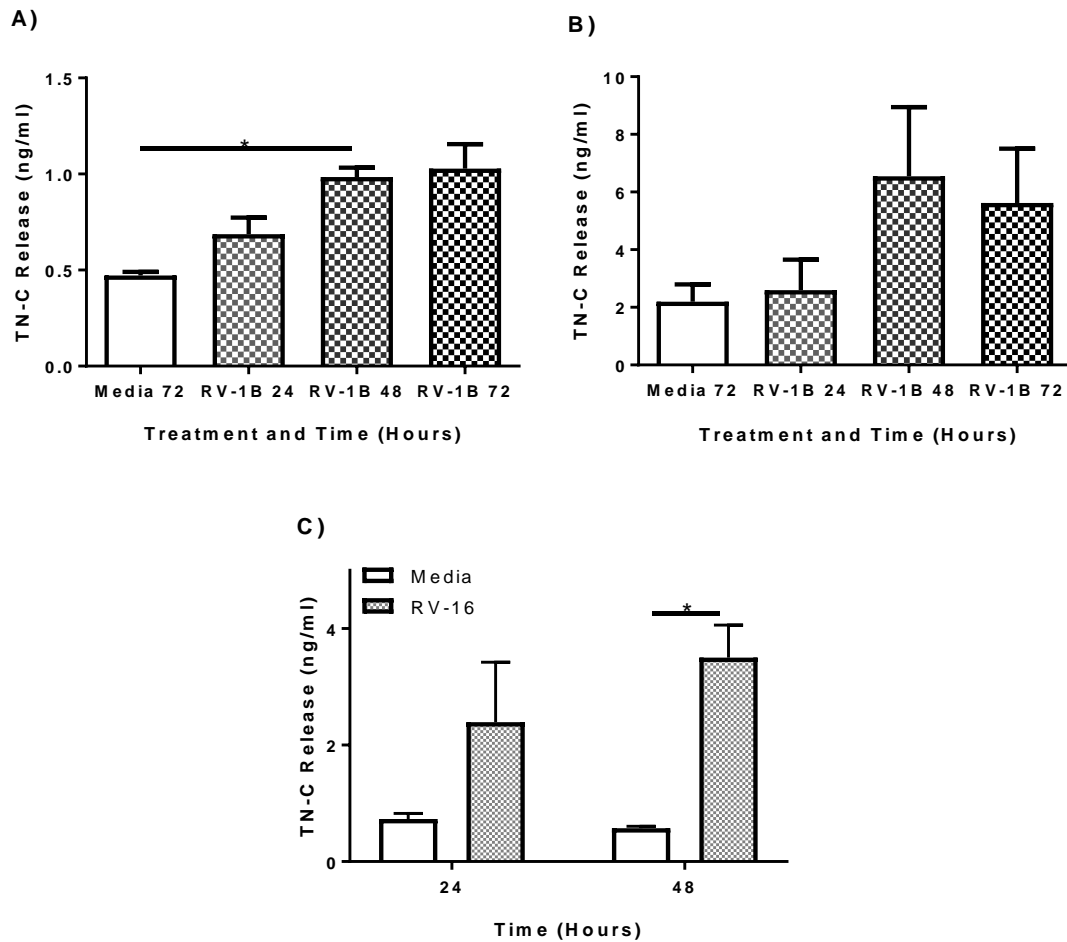


Figure 3.15. RV Infection of PBECs Induces Significant TN-C Release as Measured by ELISA

PBECs were treated with RV-1B (MOI 0.6), RV-1B (MOI 1.5) or RV-16 (MOI 1.5) for the indicated times. Cell-free supernatants were prepared and levels of TN-C produced in response to RV-1B (MOI 0.6) **(A)**, RV-1B (MOI 1.5) **(B)** and RV-16 (MOI 1.5) **(C)** were measured by ELISA. Data shown are mean \pm SEM (N=3) with each replicate an independent PBEC donor. Significant differences in TN-C secretion are indicated by * $p < 0.05$, analysed by one way Repeated Measures ANOVA with Dunnett's post hoc test or two way repeated measures ANOVA with Tukey's post hoc test.

3.6.4. RV-1B and RV-16 Infection of PBECs Induces Significant Production of CXCL8 and CCL5

To validate whether RV infection was successful, PBECs were infected with the RV and CXCL8 and CCL5 production was measured. PBECs were left uninfected or infected with RV-1B (MOI 1.5) for up to 72 hours or RV-16 (MOI 1.5) for up to 48 hours and experiments were carried out as described in Section 3.4.4.

RV-1B (MOI 1.5) induced significant CXCL8 induction at 72 hours ($p < 0.001$; Figure 3.16A) and significant CCL5 levels at 48 ($p < 0.01$) and 72 ($p < 0.05$) hours post infection. CXCL8 and CCL5 production at 24 hours in response to RV-16 was unchanged from the media control (Figure 3.16C and 3.16D). However, RV-16 induced both CXCL8 and CCL5 at 48 hours post infection, although this did not reach statistical significance.

3.6.5. Basal Levels of TN-C mRNA and Cell-Associated Protein is Increased in PBECs Compared to BEAS-2B Cells

To compare basal TN-C mRNA expression between BEAS-2B and PBECs, basal TN-C mRNA expression quantified from BEAS-2B and PBEC experiments (Figure 3.2B and 3.8B) were plotted on the same graph, and to compare basal cell associated TN-C expression between BEAS-2B and PBECs, basal TN-C protein expression data quantified from BEAS-2B and PBEC experiments (Figure 3.3C and Figure 3.13B) were plotted on the same graph.

Interestingly, basal TN-C mRNA levels were significantly greater in PBECs compared to BEAS-2B cells at 48 (3-fold; $p < 0.05$) and 72 hours (9-fold; $p < 0.05$), and although not significant, a 4-fold increase was observed at 24 hours (Figure 3.17A). Furthermore, the basal levels of TN-C cell-associated protein expression in PBECs was 3-fold greater compared to BEAS-2B cells at 48 hours ($p < 0.05$), with approximately 5-fold greater at 24 hours and 72 hours, although this did not reach statistical significance (Figure 3.17B).

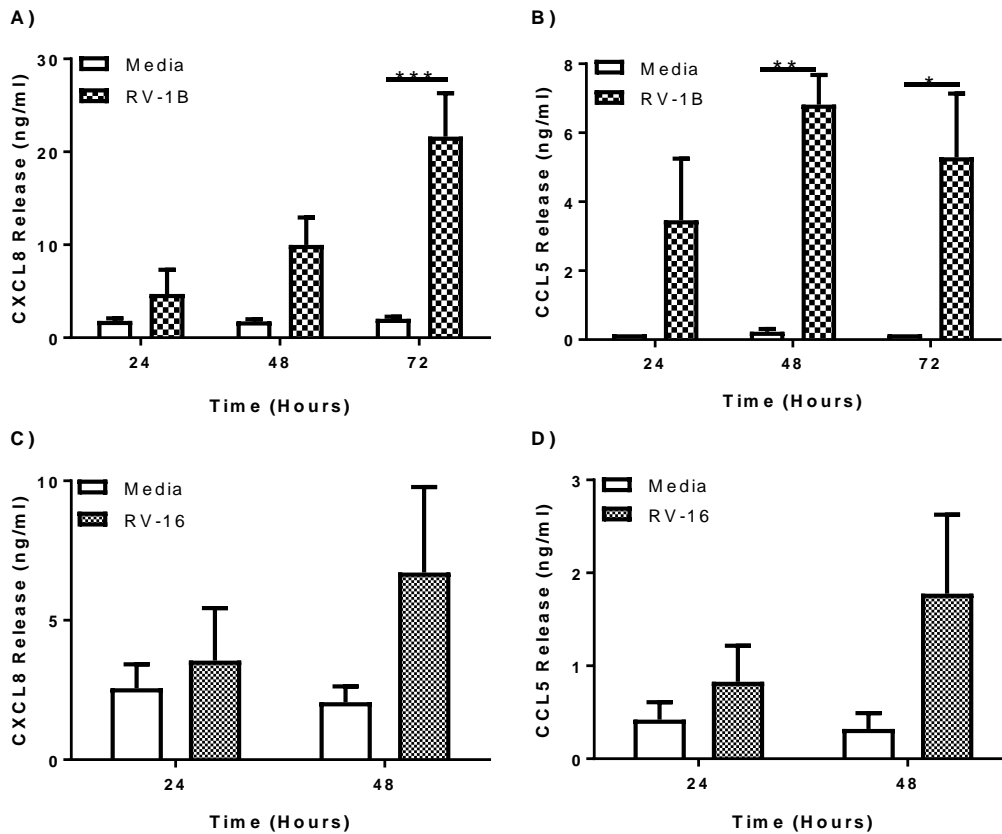


Figure 3.16. RV Infection of PBECs Induces CXCL8 and CCL5 Production in PBECs

PBECs were treated with RV-1B (MOI 1.5) or RV-16 (MOI 1.5) for the indicated times. Cell-free supernatants were prepared and levels of CXCL8 (A and C) and CCL5 (B and D) measured by ELISA. Data shown are mean \pm SEM, with each replicate an independent PBEC donor (N=3). Significant differences in chemokine production are indicated by * $p < 0.05$; ** $p < 0.01$; *** $p < 0.001$, analysed by two way repeated measures ANOVA with Tukey's post hoc test.

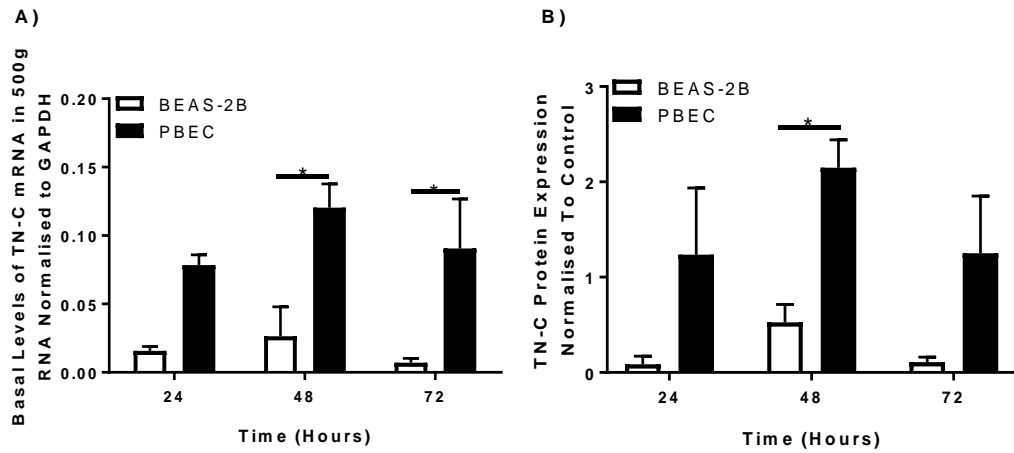


Figure 3.17. Basal TN-C mRNA and Cell-Associated Protein Expression is Significantly Higher in PBECs Compared to BEAS-2B Cells.

Basal TN-C mRNA expression quantified from BEAS-2B and PBEC experiments (Figures 3.2B and Figure 3.8B respectively) were compared **(A)** and basal cell-associated TN-C protein expression quantified from BEAS-2B and PBEC experiments (Figure 3.3B and Figure 3.13B respectively) were compared **(B)**. Data shown are mean \pm SEM (N=3) with each replicate an independent BEAS-2B cell passage or PBEC donor. Significant differences in TN-C expression are indicated by * $p < 0.05$, analysed by two way repeated measures ANOVA with Tukey's post hoc test.

3.7. TN-C Expression and Release at Basal Levels and in Response to RV is More Pronounced in Atopic Asthmatic PBECs

The final aim of the chapter was to investigate TN-C mRNA expression and TN-C protein release in response to RV infection in PBECs from AA patients, and whether RV induced greater TN-C expression and release in AA compared to NANA PBECs. To investigate total TN-C expression and release in NANA and AA PBECs, mRNA and supernatants were obtained from AA and NANA patient PBECs that had been infected with RV-1B and RV-16 (as part of the ALLIANCE study from Dr Mike Edwards at Imperial College London). The TaqMan qPCR and western blot experiments were then carried out as detailed in Section 3.4.1 and 3.4.3. Furthermore, a BCA was performed to analyse the overall protein concentration of the samples.

TN-C mRNA expression at the 6 hours unstimulated media control and in response to RV-1B and RV-16 was largely unchanged in the NANA PBECs (Figure 3.18A). In AA PBECs, there was an increase in TN-C mRNA expression (non-statistically significant) in the unstimulated media control and in response to both RV-1B ($p=0.08$) and RV-16 in the AA PBECs. There was a consistent pattern of three out of the five donors having increased TN-C expression in response to RV, with two donors at the same level as NANA PBECs. At 24 hours, there was again a trend of increased TN-C mRNA expression in the AA media control compared to NANA media control, but this was not statistically significant. In response to RV-1B and RV-16, there was similar induction of TN-C expression between NANA and AA samples. Of note, significant TN-C mRNA expression was observed in the NANA RV-1B samples compared to the NANA media control ($p<0.05$). When 6 and 24 hours TN-C mRNA were compared, AA samples had a consistently high TN-C expression, whilst NANA TN-C mRNA expression was initially low at 6 hours and increased at 24 hours in response to RV.

TN-C was released in response to RV-1B and 16, in both the NANA and AA PBECs (one representative blot shown; Figure 3.18B). Whilst there was a small increase in TN-C expression in NANA cells in response to RV-1B and RV-16 at 24 hours, it was not statistically significant (Figure 3.18C), however, TN-C was significantly induced compared to the unstimulated media control in response to RV-16 ($p<0.01$) in AA PBECs. In the unstimulated media controls, there was increased TN-C release in the AA cells compared to NANA cells, but this was not statistically significant. Importantly, however, AA cells released significantly more TN-C than NANA cells in RV-16 ($p<0.05$). It was also revealed that despite significantly increased TN-C release in AA cells, there was no significant difference between NANA and AA cells in the fold change induction of TN-C expression in response to RV-1B and RV-16 (Figure 3.18D). Finally, the large >250 variant was the main variant of TN-C released at basal levels, in response to RV-1B and in response to RV-16, both in NANA and AA cells (Figure 3.18E).

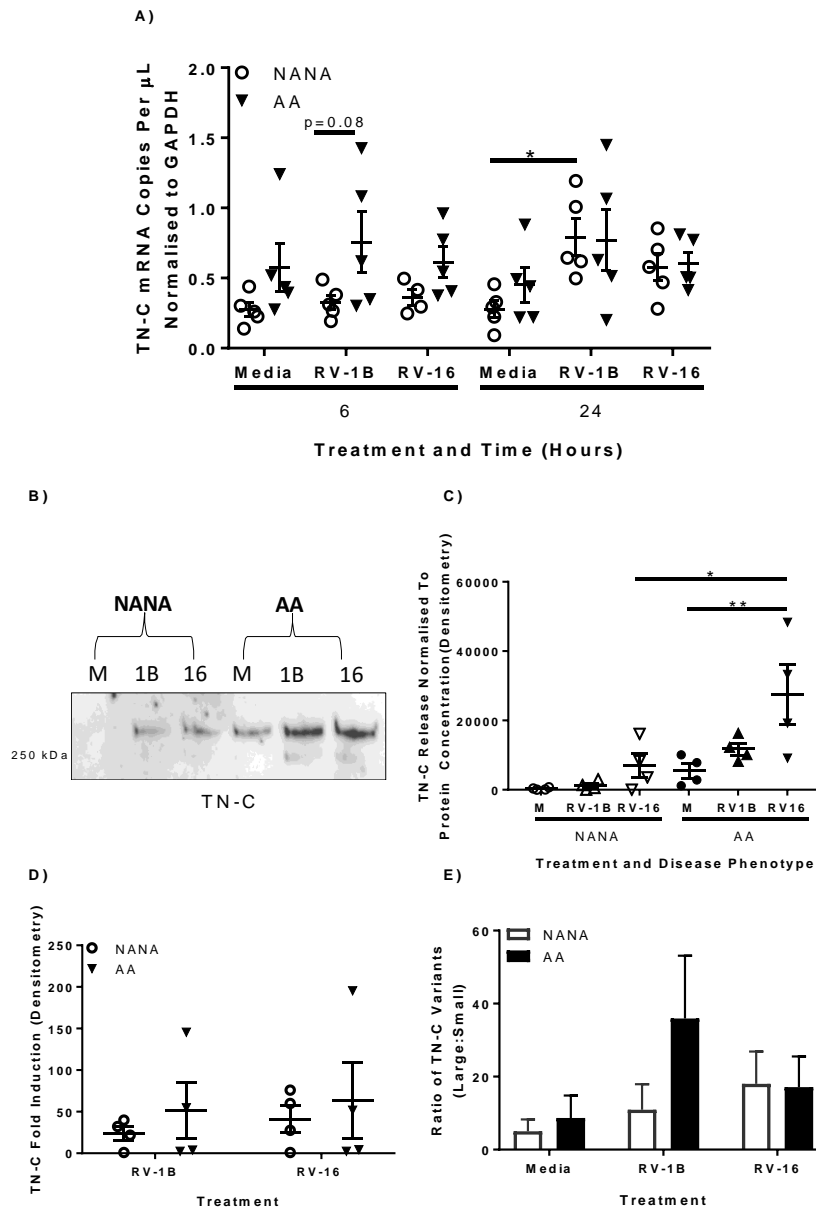


Figure 3.18. RV Infection of NANA PBECs Induces TN-C mRNA Expression and RV Infection of AA PBECs Induces Greater TN-C Release

mRNA and Cell-free supernatants from NANA and AA PBECs, infected with RV-1B and RV-16 for 6 and 24 hours were obtained from the ALLIANCE study. Total TN-C mRNA expression (FBG domain) was measured using TaqMan quantitative real time PCR, with data presented as the total RNA copies normalised to GAPDH control (**A**). Samples were analysed by western blotting using an antibody specific to TN-C (one representative blot shown), with media samples indicated with M, RV-1B samples indicated with 1B and RV-16 samples indicated with 16 (**B**). Densitometry of the top band of all blots were performed in ImageJ software, and normalised to overall protein concentration (**C**). The fold induction of TN-C expression in response to RV-1B and RV-16 was calculated (**D**). Densitometry was performed on both bands in ImageJ software, and a ratio of large to small variants was calculated (**E**). Data shown are mean \pm SEM (N=4-5) with each replicate an independent PBEC donor. Significant differences in TN-C secretion are indicated by * $p < 0.05$; ** $p < 0.01$; analysed by two way ANOVA with Tukey's post hoc test.

3.8. Summary and Discussion

3.8.1. Summary

The findings presented in this chapter revealed for the first time a relationship between RV infection and TN-C expression and release in the airway. This expression and release was demonstrated to be TLR3 dependent, TLR7 independent and not RV-serotype specific. The work demonstrated that nasal administration of poly(I:C) to an *in vivo* mouse model induced TN-C expression in the BALF, and that poly(I:C) stimulation and RV infection *in vitro* in AECs modulated TN-C mRNA expression, cell associated TN-C protein expression and TN-C protein release. Furthermore, it was demonstrated that both TN-C mRNA and TN-C protein release was increased in the AECs of asthmatics compared to non-asthmatics, both at basal levels and in response to RV-1B and RV-16. The results are summarised in Table 3.1.

Table 3.1. - Summary of TN-C Expression and Release in Response to Poly(I:C) and RV

Legend: ✓ = Induction of Expression / Release * = No Induction of Expression / Release

Figures	Sample Type (Species)	Stimulus	TN-C mRNA Increase	Cell-Associated TN-C Increase	TN-C Release Increase
3.1	BALF (Mouse)	Poly(I:C)	N/A	N/A	✓
3.2, 3.3, 3.4, 3.5, 3.6	BEAS-2B (Human)	Poly(I:C)	✓	✓	✓
3.8, 3.9, 3.10	PBECs (Human)	Poly(I:C)	*	*	✓
3.12, 3.13, 3.14, 3.15, 3.18	PBECs (Human)	RV-1B	✓	*	✓
3.12, 3.13, 3.14, 3.15	PBECs (Human)	RV-16	*	*	✓
3.18	PBECs (Human AA)	RV-1B and RV-16	✓	N/A	✓

3.8.2. The Roles of the Splice Variants Identified in Mouse BALF and AECs

The data in this chapter identified for the first time that poly(I:C) and RV induced subtle changes to the structure of the protein, with the predominance of certain alternatively spliced domains and isoform size following infection in AECs. Multiple splice variants of TN-C (both mRNA and protein) have been identified in mouse BALF and / or human bronchial epithelial cells in this chapter, with small ~250 kDa isoforms and larger >250 kDa isoforms present. In mice BALF, the smaller isoforms seemed to predominate, whilst there was a greater proportion of large isoforms present in AECs.

A number of caveats exist however, when using western blot molecular weight markers to measure the size of the TN-C protein. First, the large isoform could not be given a definite size, due to it being above the top molecular weight marker on the molecular weight ladder. Furthermore, unpublished work in the Midwood lab has also found that the molecular weight of TN-C can vary as much as 40 kDa, depending on a number of factors, such as the molecular weight ladder and type of gel (percentage of acrylamide, contents of the gel etc.) used. Nuclear magnetic resonance or single molecule spectroscopy can be used to calculate the molecular weight of proteins more accurately, but these are expensive, especially for large molecular weight proteins (Kleckner and Foster 2011, Tian et al. 2015). Due to these issues, the discussion will therefore cover a number of large isoforms from 280-330 kDa and it must be noted that it is difficult to directly compare between studies.

The ~250 kDa mouse variant has been previously been demonstrated to be present in the striated leg muscle, where it is dominantly expressed over the ~200 kDa variant (Fluck et al. 2008). It has also been demonstrated to be present in mouse embryonic fibroblasts, where it is upregulated in response to basic fibroblast growth factor and again predominates over a ~200 kDa splice variant (Tucker et al. 1993). Mouse embryonic fibroblasts that have higher percentage expression of the ~200 kDa variant are more strongly attached to the substratum, whereas those with a higher proportion of ~250 kDa variant expression are more rounded and are loosely attached (Tucker et al. 1993). As TN-C is vital for the movement of neuronal cell bodies in the embryo, it can be determined the ~250 kDa variant has the function of affecting cell adhesion and cell migration. In the mouse leg, the predominance of the ~250 kDa variant and induction in response to mechanical stress is thought to be vital in the wound healing response and regeneration of mouse muscle fibres, as TN-C KO mice do not initiate the repair system (Fluck et al. 2008). In humans, the ~250 kDa has previously been identified in airway RBM samples from asthmatic patients, alongside ~190 kDa variants (Laitinen et al. 1997) and in lung cancer tissues it is expressed less than ~190 kDa isoforms but more than ~220 kDa variants (Kusagawa et al. 1998). Additionally, in oesophageal carcinomas, the ~250 kDa variant is expressed alongside ~310 kDa isoforms (Yang et al. 2016). In the lung cancer study and oesophageal carcinoma study, the ~250 kDa isoform was weakly expressed in normal lungs and normal oesophageal tissue, leading to the conclusion that this isoform is vital for cancer cell metastasis and adhesion modulation (Kusagawa et al. 1998, Yang et al. 2016). Furthermore,

the presence of any TN-C isoform was unable to be detected in non-asthmatic airway RBM samples, leading to the conclusion that TN-C (including the ~250 kDa variant) is required for the constant wound healing response that occurs during airway remodelling in the airway of asthmatics.

In mice, large variants have been described previously in a number of locations, such as embryonic fibroblasts (Brellier et al. 2011) and in joint inflammation (Midwood et al. 2009). In humans, the FNIII-C domain of TN-C has been demonstrated to be absent from healthy tissues, present in proliferating cells and expressed in glioblastoma (Carnemolla et al. 1999), breast cancer (Tsunoda et al. 2003) and lung cancer (Silacci et al. 2006). This domain is therefore associated with cell migration, cell proliferation and cancer metastasis. A number of large protein isoforms exist, with the majority ~280 kDa, ~320 kDa and ~330 kDa in size. As a large proportion of TN-C research has been concerned with the role of the protein in cancer, this is where the bulk of the isoforms have been identified (see Table 3.1.). The most interesting isoform is perhaps the ~320 kDa isoform, which has been identified in the synovia of RA patients (Midwood et al. 2009, Goh et al. 2010, Page et al. 2012), is expressed in higher quantities in chondrosarcoma compared to healthy human chondrocytes (Ghert et al. 2001a) and is produced in human dermal fibroblasts in response to IL-13 (Jinnin et al. 2006). This isoform of TN-C is a potent inducer of inflammation (through FBG-TLR4 induced inflammation in synovial macrophages), is expressed in much higher quantities in the RA synovia compared to non-RA synovia and the protein's expression in RA synovia is controlled through an inflammatory autocrine transcription loop, meaning it is a biomarker of disease severity in RA (Midwood et al. 2009, Goh et al. 2010). The ~320 kDa variant may also be associated with inflammation in the cancer stroma (Ghert et al. 2001a, Ghert et al. 2001b). The ~280 kDa isoform has also been shown to be pro-apoptotic in myocytes, is present in carotid atheroma and may induce inflammation leading to the formation of atheroma, demonstrating that it is not just the ~320 kDa variant of TN-C that can drive inflammation (Wallner et al. 2004, Golledge et al. 2011). Furthermore, whilst TN-C was originally established to modulate the adhesive properties in tumour cells, it is now thought to also be an important driver in cancer-associated inflammation (demonstrated through its inflammatory potential in the RA synovia and other tissues), and thus further aiding metastasis and tumour progression (Midwood and Orend 2009).

The results from this study demonstrate that the large >250 kDa variant (a variant closely associated with inflammation) predominates in AECs. These results are also interesting as they demonstrate differences in TN-C splice variant expression between mice and humans. Despite homology of 72% (www.ncbi.nlm.nih.gov/homologene) between mouse and human TN-C, differences do exist that could affect the structure and function of the protein in the two species. For example, although mouse TN-C contain a TA, EGF-Like, FNIII-Like and FBG domains, human TN-C has 8 constitutive FNIII-domains, compared to 6 for mice (Joester and Faissner 1999, Giblin and Midwood 2015). Due to structural differences, expression differences and

potential functional differences, it can be concluded that extensive studies in human cells are required alongside mouse studies in order to fully reveal the function and expression profile of TN-C.

3.8.3. TN-C was Significantly Upregulated in Response to Poly(I:C) *In Vivo* and May Play a Protective Role

In response to poly(I:C) stimulation, significant TN-C expression was induced in the BALF of WT C57BL/6 mice at 48 hours and furthermore, this may correlate with KC production (Figure 3.1).

Whilst a previous study correlated TN-C expression and airway hyperresponsiveness in an asthmatic mouse model (Nakahara et al. 2006), there is currently a lack of evidence of TN-C expression in the airway of mice following RV infection. Although, RV infection of mice can induce cytokine and IFN release, MUC5B production, lung eosinophilia and virus specific antibodies (Bartlett et al. 2008, Nagarkar et al. 2010), RV-infection mouse models are currently limited (Jacobs et al. 2013). There are no murine-specific rhinoviruses and RV infection of mice requires an unnaturally high MOI during infection, with a steep decline in titre from 12 hours, meaning there is limited viral replication and subsequent viral response (Jacobs et al. 2013). Due to this, it was decided that the poly(I:C) intranasal stimulation of mice was the best model to investigate *in vivo* viral induced-TN-C expression.

TN-C expression in the BALF of WT C57BL/6 mice was present in low quantities in response to PBS (Figure 3.1). This low airway expression of TN-C is in keeping with mouse transcriptome data from healthy adult mouse lung (Yue et al. 2014) and immunohistochemical staining of mouse bronchus and lungs following inhaled saline or PBS treatment (Nakahara et al. 2006, Meuronen et al. 2011). TN-C expression remained low in response to poly(I:C) at 24 hours, however, there was a large and statistically significant upregulation of TN-C expression in response to 48-hour poly(I:C) stimulation (Figure 3.1). Of note, there seemed to be a large variation in the magnitude of TN-C upregulation in the poly(I:C) treated mice, with the largest TN-C expression five times greater than the lowest. The distinct bands observed on the western blot are determined to be different variants of TN-C due to the mouse TN-C antibody being targeted towards the N terminus region. The ~250 kDa isoform was the predominant splice variant expressed in response to both PBS and poly(I:C), with a 3-4:1 expression ratio over the larger >250 kDa variant (Figure 3.1E; Table 3.1). As described in Section 3.8.2, the ~250 kDa isoform has been demonstrated to be vital in wound healing, cell adhesion modulation and muscle repair. Hence, it can be postulated that the observed TN-C upregulation in this study following poly(I:C) stimulation may indicate a protective role for TN-C in response to RV infection, initiating the wound healing response to damage caused in the airway by infection. Furthermore, only two distinct mouse lung TN-C RNA isoforms have been previously described, 7 kilobase and 8 kilobase (Saga et al. 1991, Ocklind et al. 1993, Giblin and Midwood 2015), which could potentially correlate with the two protein isoforms described in this study.

The Pearson's correlation coefficient seems to indicate that there is no correlation between concentration of KC release and TN-C expression ($R^2=0.09722$; Figure 3.3C), with the highest quantity of TN-C expressed in the BALF associated with the lowest quantity of KC and CCL5 (Mouse 3). This may be an anomaly however, and if Mouse 3 is removed from the correlation calculation, TN-C expression in the BALF forms a positive correlation with KC expression ($R^2=0.895$). This therefore needs to be investigated further, with literature that demonstrates that inflammatory cytokines (such as TNF α and TGF- β) are transcriptional regulators of TN-C in rats and humans (Zhao and Young 1995, Nakamura et al. 2004) supporting this potential finding.

These results revealed for the first time, an *in vivo* link between TLR3 stimulation (and therefore viral infection) and TN-C expression in the airway. This data therefore provided a proof of principle before transitioning into *in vitro* human cell investigation. Unfortunately, only BALF could be obtained from the mice (due to the samples being donated from another study), and therefore it was not possible to perform immunohistochemistry on the lung and airway tissue, which would have allowed further investigation into TN-C expression in response to poly(I:C) *in vivo*.

3.8.4. AEC Response to RV is TLR3 and not TLR7 Dependent in AECs

Both BEAS-2B (Figure 3.7) and PBECs (Figure 3.11 and 3.16) responded to poly(I:C) stimulation and RV infection, but not gardiquimod stimulation, as measured by CXCL8 and CCL5 release. The gardiquimod used was determined to be active, with stimulation of MDMs inducing significant CXCL8 release (Figure 3.11E).

Upon RV infection, virions have the ability to interact with a myriad of TLRs and RLRs, including TLR3, TLR2, MDA5 and RIG-I. There is, however, conflicting evidence about whether TLR7 plays a role in RV infection of AECs (Section 1.2.4.). TLR7 has mainly been demonstrated to signal in response to RV infection in other cell types, such as mice *in vivo* (Hatchwell et al. 2015), human dendritic cells (Diebold et al. 2004, Heil et al. 2004) and human macrophage cells (Heil et al. 2004). Data from this chapter revealed that TLR3 stimulation by poly(I:C) induced significant CXCL8 and CCL5 release in BEAS-2B and PBECs, but TLR7 stimulation by gardiquimod did not, in keeping with multiple other studies in the field (Sha et al. 2004, Parker et al. 2008, Slater et al. 2010). These studies demonstrated either low TLR7 expression, or a lack of response to TLR7 agonists, in AECs. PBECs are the primary site for RV infection and replication in humans *in vivo*, and although TLR7 may elicit a response to RV in other cell types, this study correlates with the majority of the evidence in the field demonstrating no role for TLR7 in PBEC RV infection. The data in this chapter confirms that poly(I:C) stimulation and RV infection both induce significant CXCL8 and CCL5 release in AECs and therefore it can be concluded that TLR3 signalling is required for a sufficient response to RV infection, drawing a parallel with previous work demonstrating the requirement of TLR3 for a sufficient anti-viral

response to RV (Hewson et al. 2005). Furthermore, these results are of relevance and are important as they determine that the observed results described in the rest of this study are likely to be TLR3-dependent and TLR7-independent.

3.8.5. TN-C mRNA is Modulated in Response to TLR3 Stimulation and RV Infection

3.8.5.1. Total TN-C mRNA is Upregulated in Response to Poly(I:C) and RV-1B in AECs, but may be Donor Specific

In response to poly(I:C), TN-C mRNA was significantly upregulated at 4, 6, 8 and 24 hours in BEAS-2B cells, before falling to baseline at 48 and 72 hours (Figure 3.2). Interestingly, although this could not be replicated in PBECs in response to poly(I:C) (Figure 3.8) or RV infection experiments from PBECs obtained from the PromoCell (Figure 3.12), RV-1B did induce significant TN-C mRNA expression at 24 hours in the NANA PBECs obtained from the ALLIANCE study (Figure 3.18).

In BEAS-2B cells, the TN-C mRNA levels did not increase throughout the experiment timeline in the media controls and interestingly, poly(I:C) induced similar levels of upregulation as TNF α (a known transcriptional regulator of TN-C), with approximately a 6-fold induction of TN-C mRNA. The work in this study demonstrates a larger scale of TN-C mRNA upregulation (approximately 5-10-fold) than the Proud et al study, which described approximately 3-fold induction of TN-C mRNA in nasal scrapings taken following 3-4 week RV infection in human volunteers (Proud et al. 2008). This may demonstrate that greater upregulation occurs in AECs (the main site of RV replication) and that time of peak expression may be at the point of initial infection, rather than weeks after. Additionally, the timeline of TN-C mRNA upregulation following RV infection in BEAS-2B cells (upregulated from 4 hours, with the peak at 24 hours) fits with a number of studies investigating the upregulation of TN-C mRNA. For example, in airway fibroblasts treated with TGF- β , despite no observable induction of TN-C at 4 hours post stimulation, there was a large upregulation at 24 hours (Estany et al. 2014). TNF α treatment of airway fibroblasts also induced considerable TN-C expression from 3 hours onwards, with the largest upregulation at 24 hours (Nakamura et al. 2004).

There are a number of potential reasons that may explain the discrepancy in the qPCR results in this study, which describes TN-C mRNA upregulation in some experiments, but not in others. It is important to note that the basal levels of TN-C mRNA are approximately 2-5 times higher in PBECs compared to BEAS-2B cells throughout the experiment (Figure 3.17). It can be theorised, therefore, that this higher TN-C basal expression in PBECs means upregulation of TN-C mRNA in response to viral infection is either not required, or is not as pronounced as in the BEAS-2B cells. This is further evidenced by the results in Figure 3.18, which demonstrate that despite similar upregulation in TN-C mRNA in response to RV-1B in NANA and AA PBECs, only the induction in NANA samples was statistically significant, due to higher basal levels of

TN-C mRNA in the AA samples. There is large donor variability in PBECs to infection susceptibility, cytokine / chemokine release and cell cytotoxicity in response to RV and this may explain as to why total TN-C mRNA expression was induced in response to RV-1B in Figure 3.18 but not 3.12, as different donors were used. These two experiments also had different replicate numbers (N=3 and N=5), with a power calculation for Figure 3.12A revealing that an N of 3 only gave 20% power and that for a power of 80%, an N of 14 would be needed (which is not possible, due to the number of PBEC donors available). A feasible experiment in the future however, would be to boost N numbers to the maximum number of donors possible.

3.8.5.2. TN-C Splice Specific mRNA Expression is Upregulated in Response to RV Infection in AECs

TN-C is a large multi-domain ECM glycoprotein, with the expression of FNIII-domains controlled by alternative splicing (Midwood et al. 2016). The TaqMan qPCR data described in Section 3.8.4.1. is limited by the fact that the primers binds to the FBG domain only (which is constitutively expressed and therefore measures overall TN-C expression). This assay therefore cannot investigate any changes in the expression of TN-C FNIII splice domains. A SYBR Green qPCR was therefore performed in order to analyse the expression of every alternatively spliced domain (FNIII-A1-D) and overall TN-C (FNIII-7/8). The BEAS-2B SYBR green qPCR correlated with the TaqMan qPCR from the same experiment, with an upregulation of overall TN-C at 24 hours post poly(I:C) and TNF α stimulation. Furthermore, in response to poly(I:C), there is a potential upregulation of the FNIII-A2, FNIII-B, FNIII-C and FNIII-D domains. Interestingly, the splice domain expression profile in response to poly(I:C) is distinct from that induced by TNF α , which induced FNIII-AD1, FNIII-C and FNIII-D expression. The large error bars are a limitation of this experiment, and further donor numbers are required to elucidate more information. In PBECs, there is a disconnect between the SYBR green and TaqMan qPCR experiments, with the SYBR-Green experiment demonstrating a 5-fold increase in overall TN-C. Selective splice domain upregulation (FNIII-A3, FNIII-A4 and FNIII-D) was also observed in response to poly(I:C). Furthermore, in response to RV, despite no overall TN-C mRNA expression observed (correlating with the TaqMan experiment); there is a statistically significant 3-fold increase of the FNIII-C splice domain, as well as potential upregulation in FNIII-A4 and FNIII-B. Finally, FNIII-AD1 domain is present at only very low levels and is not upregulated in response to poly(I:C) and RV-1B, whilst FNIII-AD2 is not present at all.

Whilst it has previously been demonstrated that TGF- β , TNF α , IFN γ and IL-4 (among others) can induce the expression of TN-C FNIII domains (Latijnhouwers et al. 2000), these results demonstrate for the first time that RV infection can change the splice profile of the protein. The domains induced also give an indication of the function of the protein, based on previous studies analysing the effects of FNIII expression. A specific SNP in the FNIII-D domain strongly associates with the prevalence of asthma, potentially through reducing the elasticity of the protein, affecting the stiffness and integrity and contributing further to airway remodelling

(Matsuda et al. 2005). The specific upregulation of this domain in AECs in response to TLR3 stimulation / viral infection is therefore of importance, as it can be hypothesised that if asthmatics already have a genetic predisposition to FNIII-D expression, viral infection could further exacerbate this. Additionally, FNIII-D has previously been proven to induce phospholipase C expression in rats (Michele and Faissner 2009) and phospholipase C induces airway smooth muscle contraction through Ca^{2+} release (McGraw et al. 2003). More research is required, but FNIII-D upregulation in response to TLR3 stimulation may also impact upon this pathway, detrimentally affecting the asthmatic airway. As described in Section 3.8.2., the FNIII-C domain is strongly associated with proliferating cells and disease, mainly being described as being associated with cancers such as lung cancer and glioblastoma tumours, whilst being absent from healthy tissues (Carnemolla et al. 1999, Silacci et al. 2006, Giblin and Midwood 2015). Although the exact function of the FNIII-C domain is unclear, upregulation in response to RV infection seems to induce a disease splice specific variant of TN-C, which may lead to proliferation of cells during airway remodelling or migration of immune cells during airway hyperresponsiveness. Interestingly, work investigating TN-C splice domain expression reported that FNIII-C in mice was only expressed alongside FNIII-D (Joester and Faissner 1999, Giblin and Midwood 2015) and thus the results of the RV infection work may suggest differential regulation in humans. It must also be noted however, that as this assay measures fold change in mRNA, FNIII-D may already be expressed and therefore may not need to be upregulated in large amounts. The lack of upregulation of FNIII-AD1 in AECs is to be expected, due to its normal association with cancerous cells and absence in lung fibroblasts (Garwood et al. 2012) and the absence of FNIII-AD2 is explained as it is thought to be preferentially expressed alongside FNIII-AD1 (Mighell et al. 1997).

Importantly, this study reveals that poly(I:C) stimulation has the capacity in BEAS-2B cells to induce similar levels of TN-C mRNA expression as TNF α (a known transcriptional regulator of TN-C). Despite a lack of statistically significant overall TN-C mRNA upregulation in some PBECs in response to poly(I:C) and RV, there are nuanced changes to alternatively spliced domains, which have been demonstrated to have a profound effect on protein expression and function. This mechanism, therefore, could play a vital role in airway remodelling and airway hyperresponsiveness and future work analysing splice variants in depth will reveal the extent to which TN-C splice variants play a role in asthma pathogenesis and RV-induced exacerbations.

3.8.6. TN-C Cell-Associated Protein Expression Induction in Response to RV

3.8.6.1. Total TN-C Protein is Upregulated in Response to Poly(I:C) in BEAS-2B Cells but not in Response to Poly(I:C) and RV infection PBECs

In BEAS-2B cells, cell-associated TN-C protein was significantly upregulated in response to poly(I:C) (Figure 3.3 and 3.4) however in PBECs, poly(I:C) (Figure 3.9), RV-1B or RV-16 (Figure 3.13), did not induce any significant TN-C expression. To investigate these discrepancies, the

basal levels of TN-C in the BEAS-2B and PBEC experiments were compared. This revealed a much larger basal level of TN-C protein expression in PBECs compared to BEAS-2B cells, with significantly more expression at 48 hours post RV-1B infection (Figure 3.17).

Interestingly, the temporal upregulation of TN-C protein expression in BEAS-2B cells following poly(I:C) stimulation correlated with the timeline of expression following TGF- β and TNF α treatment of airway fibroblasts, with induction occurring between 24 and 48 hours (Nakamura et al. 2004, Estany et al. 2014). Additionally, IL-4 and IL-13 stimulation of dermal fibroblasts induced TN-C upregulation at 24 hours post stimulation (Jinnin et al. 2006). This may suggest that these cytokines generated following RV infection are responsible for the induction of TN-C expression, but more research is required. The immunofluorescence data (Figure 3.4. and 3.5.) also suggested that TN-C is present in the cytoplasm of AECs and is upregulated following RV-infection, with the location of expression (in the cytoplasm) correlating with data in other studies investigating TN-C expression in tumour cells (Brunner et al. 2004) and skin biopsies (Afsar, Aktas and Diniz 2011).

In this study, multiple differences have been described between BEAS-2B cells and PBECs regarding TN-C mRNA and protein expression. BEAS-2B cells are used in this study as they closely resemble PBECs, but there are differences between BEAS-2B cells and PBECs that could help to explain the variation in results. BEAS-2B cells are a bronchial epithelial cell line that is immortalised with AD12-SV40 virus, whereas PBECs are cells taken from the airway of healthy volunteers during biopsy (Reddel et al. 1988, Stewart et al. 2012). PBECs have a limited passage number but form monolayers, secrete cytokines and are also able to secrete MUC and form tight junctions. On the other hand, BEAS-2B cells are more resistant to cell death, can be passaged extensively, are able to form confluent monolayers and can express cytokines, but there is contrasting evidence as to whether they can form tight junctions and secrete MUCs (Reddel et al. 1988, Noah et al. 1995, BeruBe et al. 2010). This contrasting evidence may be because BEAS-2B are susceptible to physiological changes such as ATP production and oxygen consumption depending on culture conditions (Zhao and Klimecki 2015), and thus it can be postulated that this may impact tight junction formation, MUC secretion etc. BEAS-2B cells also produce more pro-inflammatory cytokines to the bacterial molecule LPS compared to primary PBECs (Mayer et al. 2007). Previous work from our lab has demonstrated that RV viral replication (quantified by concentration of intracellular viral RNA) and cytokine / chemokine release produced in response to infection is very similar between BEAS-2B and PBECs (Stokes et al. 2016) and thus the differences in TN-C expression may not be due to viral response but due to differences in cell culture between the two cell types. TN-C is known to be induced by mechanotransduction and cyclic strain (Fluck et al. 2008, Maier et al. 2008, Imanaka-Yoshida and Aoki 2014) and PBECs may therefore be more susceptible than BEAS-2B cells to mechanotransduction-induction of TN-C. Due to mechanotransduction, the act of plating the cells onto the culture plates may be enough to induce expression, and BEAS-2B are plated and left 1-4 days to grow to full confluency before use, whilst PBECs require 7-10 days to

reach confluency, which therefore may affect basal TN-C expression. Furthermore, rather than induction of overall TN-C expression, there may be induced changes to the TN-C FNIII domain expression (such as FNIII-C) in response to RV, which may not be detected by current commercially available antibodies. It should also be noted that the lack of upregulation of cell-associated TN-C in response to poly(I:C) and RV in PBECs correlates with data in airway smooth muscle cells, with the observation that an upregulation in perlecan and FN occurred, despite no induction of TN-C (Kuo et al. 2011).

3.8.6.2. Large and Small Splice Variants of Cell-Associated TN-C Are Equally Expressed in BEAS-2B Cells, whilst the Larger Variant Predominates in PBECs

The human TN-C antibody used in this study is targeted towards the N terminus region and thus the distinct bands observed on the western blot are determined to be different variants of TN-C (Jinnin et al. 2004, Hasegawa et al. 2007, Goh et al. 2010). Interestingly, the ratio between large (>250 kDa) and small variants (~250 kDa) of cell-associated TN-C differs between BEAS-2B and PBECs. In BEAS-2B cells, there is almost a 1:1 ratio during both basal conditions and in response to poly(I:C) (Figure 3.3D), however in PBECs the ratio was 3:1 during basal conditions and in response to poly(I:C) (Figure 3.9D) and 6:1 in response to RV (Figure 3.13E). Interestingly these also differ from the predominance of the small variant in mice (Figure 3.1E).

The increase in large:small variant ratio following RV infection indicates a change in the structure of the TN-C molecule, despite a lack of increase in overall TN-C expression. Each FNIII domain has a mass of 10 kDa (Giblin and Midwood 2015) and thus incorporation of added domains into the molecule would result in a change in the expression ratio from small to large variants (glycosylation can also add to the mass of the protein). This also correlates with the TN-C splice domain data qPCR data and it can be postulated that an induction in the FNIII-C domain (or other domains) occurs following infection. Unfortunately, the specific TN-C splice domains expressed following infection cannot be thoroughly investigated, as commercial TN-C western blot antibodies are currently targeted at the N-terminal, FBG domain, the constant FNIII domains or the FNIII-B domain, with no FNIII-C or other FNIII domain antibodies currently available.

3.8.7. TN-C Release in Response to RV is a Novel Mechanism Following Viral Infection and the Large TN-C Protein Splice Variant is the Main Variant Released

The results in this chapter demonstrated a novel pathway that has not been previously described. In BEAS-2B cells and PBECs, poly(I:C), RV-1B and RV-16 induced significant TN-C release as measured by western blot, ELISA, or both, between 24 and 72 hours (Figures 3.6, 3.10, 3.14 and 3.15).

In BEAS-2B cells, cell associated TN-C in unstimulated cells is low and thus TN-C mRNA and protein upregulation occur prior to TN-C release. However, the large release of TN-C in PBECs

in response to poly(I:C) and RV, despite a lack of induction (in some cases) in TN-C mRNA or TN-C cell associated protein is an observation that should not be overlooked. Basal levels of TN-C expression are higher in PBECs compared to BEAS-2B cells and therefore it can be hypothesised that TN-C may be stored within PBECs in higher quantities. This would then allow TN-C to be packaged and released quickly in response to infection, and thus less upregulation in intracellular TN-C expression is required. In addition, despite no induction of overall TN-C mRNA in PBECs, there is a change in the mRNA splice domain expression profile, with RV significantly inducing FNIII-C domain expression (Figure 3.3C) and poly(I:C) potentially inducing a number of FNIII domains (Figure 3.8C). This may translate to the protein level, as an increase in the ratio of large to small cell associated TN-C splice variant expression was observed in response to RV (Figure 3.13E). It is well documented that specific TN-C splice variants and FNIII domains have the ability to bind to different targets and thus the induced change in the structure would allow the TN-C protein to interact with more target molecules (Giblin and Midwood 2015). Therefore, it could be theorised that the incorporation of more FNIII domains following infection could allow already expressed cell-associated TN-C to be released from the cell. Current projects in the Midwood lab (Kennedy Institute of Rheumatology, University of Oxford) are focusing on cloning specific FNIII domains and creating recombinant FNIII proteins, which would allow for direct investigation into the function of these domains in AECs following RV infection.

The mechanisms behind this release will be investigated in Chapter 4 and the functions of TN-C release will be investigated in Chapter 5. As described in Section 3.8.2., whilst the smaller variants are associated with wound healing, the larger variants of TN-C are expressed at only low levels in healthy tissues and highly associated with inflammation and disease, such as inducing TLR4 inflammation in the synovium of RA. The fact that RV infection of AECs induces the release of specific large TN-C variants, that have a predisposition towards inflammation and disease in the airway, suggests this is a novel pathway of potential importance.

3.8.8. Atopic Asthmatics Have Higher TN-C mRNA Expression and TN-C Release than Non-Atopic Non-Asthmatics

In AA PBECs, there was an increase in TN-C mRNA (non-statistically significant) in the 6-hour media control and in response to RV-1B and RV-16 compared to NANA PBECs (Figure 3.18A). At 24 hours, significant TN-C induction was observed in response to RV-1B in NANA PBECs compared to the media control, but not in AA PBECs, despite a similar level of expression. This was due again to elevated levels of TN-C mRNA expression at the 24-hour media control in the AA samples compared to the NANA samples (not-statistically significant). Furthermore, RV-1B and RV-16 induced significant TN-C release compared to the unstimulated control at 24 hours post infection (Figure 3.18B). Another important observation was that the amount of TN-C released was also significantly higher than that induced by NANA PBECs in response to both

RV serotypes. There was also no significant difference in the fold induction of TN-C release in response to RV between AA and NANA samples (Figure 3.18D). Finally, the main isoform released was the large splice variant, with the ratio of large to small variants as high as 35:1 in AA samples (Figure 3.18E).

These results demonstrate for the first time that TN-C release in response to RV is greater in an asthmatic disease setting. Furthermore, this is the first confirmation that TN-C release in AA PBECs is greater at basal levels compared to NANA PBECs. The higher basal levels of TN-C release in AA PBECs compared with NANA PBECs in this study correlates with previous data investigating asthmatic TN-C expression, with cell associated TN-C expression increased in the basement membrane of asthmatic patients compared to non-asthmatic controls (Laitinen et al. 1997) and in the lungs of an Ova-sensitised mouse model of asthma compared to saline treated controls (Nakahara et al. 2006). The main TN-C isoform released at basal levels and TN-C was the large isoform associated with disease and inflammation (Section 3.8.2.) and RV-1B induced almost a 3-fold increase in the expression of large:small variant expression. This is important as it demonstrates that RV infection of AA PBECs can not only induce TN-C release, but can also induce the expression of a particularly pro-inflammatory variant of the protein. With the levels of TN-C protein expression increased in the RBM of asthmatics compared to non-asthmatics (Laitinen et al. 1997), potential increased mRNA expression in AA PBECs compared to NANA PBECs (Figure 3.18) and RV inducing greater TN-C release in AA PBECs (Figure 3.18), it could be theorised that AA PBECs have higher basal levels of TN-C present, leading to a more pronounced induction of TN-C release in response to RV infection. This theory is further bolstered by the observation of a similar fold in upregulation of TN-C release in NANA and AA PBECs in response to RV-1B and 16 compared to the respective media controls, suggesting that there is no increased sensitivity to RV induced TN-C release in AA PBECs, but further studies are required.

3.8.9. Conclusion

The results in this chapter demonstrate for the first time that poly(I:C) and/or RV infection induce the release of TN-C *in vivo* in a mouse model and *in vitro* in AECs (both BEAS-2B and PBECs). Furthermore, the amount of TN-C release at basal levels and in response to RV is increased in asthmatic AECs, a fact that could have potential pathogenic consequences in asthma. The results in this chapter also demonstrated two further types of regulation of TN-C following poly(I:C) stimulation and RV infection. First, overall TN-C mRNA and cell-associated upregulation occurs in BEAS-2B cells following viral infection. Secondly in PBECs, overall TN-C mRNA occurs in some donors, but in others, a more nuanced change to TN-C expression was observed, with the induction of specific FNIII domains occurring. The induction of these domains also lead to a change in the ratio of intracellular and released splice variant sizes of TN-C, with the larger splice variants closely linked to inflammation and disease being induced. Due to the

variation and donor specific responses observed in this chapter, the donors used in this chapter are summarised in Table 3.2.

This chapter demonstrates that specific TN-C splice variants pre-disposed to an inflammatory phenotype are released from AECs following RV infection, and that this mechanism is more pronounced in AECs from asthmatic patients. Next, the mechanisms behind RV-induced AEC TN-C release (primarily, release through cell cytotoxicity and EVs) are investigated and detailed in Chapter 4, in order to investigate this pathway further.

Table 3.2. Summary of Specific PBEC Donors Used

Experiment (Figure)	PBEC Donors Used	Origin of Donor	Experimental Outcome
Poly(I:C) TN-C mRNA(3.8)	D1.01, D4.08, D9	PromoCell	No Change in Expression
Poly(I:C) TN-C Cell-Associated (3.9)	D2, D8, D9	PromoCell	No Change in Expression
Poly(I:C) TN-C Release (3.10)	D2, D8, D9	PromoCell	Increase in Release
Poly(I:C) / Gardiquimod Cytokine / Chemokine Release (3.11)	D4.03, D4.08, D9	PromoCell	Increase in Release
RV TN-C mRNA (3.12)	D1.01, D3, D4.03, D4.08	PromoCell	Increase in FNIII-C Specific Expression
RV TN-C Cell-Associated (3.13)	D3, D4.03, D4.08, D9	PromoCell	No Change in Expression
RV TN-C Release (Western Blot; 3.14)	D3, D4.03, D4.08, D9	PromoCell	Increase in Release
RV TN-C release (ELISA; 3.15)	D3, D4.03, D4.08, D9	PromoCell	Increase in Release
RV Cytokine / Chemokine Release (3.16)	D1.01, D3, D4.03, D4.08, D9	PromoCell	Increase in Release
Basal TN-C Expression (3.17)	D1.01, D3, D4.03, D4.08, D9	PromoCell	Increased Basal mRNA and Cell-Associated Expression Compared to BEAS-2B Cells
RV NANA and AA TN-C Expression and Release (3.18)	qPCR: JD001, JD002, JD003, JD004, JD005, JD009, JD016, JD025, JD048, JD073 Western Blot: JD009, JDO50, JD073, JD080, JD095, JD110, JD133, JD145, JD156	ALLIANCE Study Donors	Increased mRNA Expression in NANA PBECs (Compared to NANA Control) and Increased TN-C Release in AA PBECs (Compared to AA Control and NANA RV Samples)

Chapter 4 – Results: The Mechanisms of RV-Induced TN-C and Exosome Release in AECs

4.1. Introduction

The novel results in Chapter 3 demonstrated TN-C upregulation and release in response to poly(I:C) stimulation and RV infection in an *in vivo* mouse model and *in vitro* in AECs, with this pathway more pronounced in asthmatic cells. However, the mechanism behind this phenomenon is unclear. TN-C is rapidly upregulated in the lungs and in other cells after injury (Midwood and Orend 2009), and poly(I:C) and RV have the capacity to induce cell cytotoxicity (Koizumi et al. 2016) in AECs (although not as much as, for example, staurosporine, which is an inducer of apoptosis), so therefore cell cytotoxicity may play a role in TN-C release. Furthermore, despite the release of TN-C being demonstrated in a plethora of different cell types during homeostasis (Nishio et al. 2003, Fluck et al. 2008) and in disease states such as cancer (Midwood and Orend 2009, Shao, Kirkwood and Wells 2015), the mechanisms leading to TN-C release are yet to be investigated in depth. One of the primary mechanisms of TN-C release described is via EV-associated release and in particular, exosomes. Proteomic analysis of exosomes from malignant colorectal and pleural tumours revealed the presence of tumour antigens and a number of metastatic and inflammatory factors, including TN-C (Ji et al. 2013, Greening et al. 2016). To demonstrate the metastatic potential of these exosomes, addition of exosomes from tumours to endothelial cells induced proliferation, whilst addition to fibroblasts and human umbilical vein endothelial cells induced significant cell migration (Ji et al. 2013, Greening et al. 2016). MVs are also implicated in disease pathogenesis (in particular CVD), but despite plentiful evidence that TN-C can associate with exosomes, it currently is not clear whether TN-C can associate with MVs.

There is growing evidence that EVs play a vital role in viral infection and in particular, enterovirus infection. For example CVB is a member for the *picornaviridae* family (which includes RV) that has six serotypes and is implicated in myocarditis and pancreatitis (Inal and Jorfi 2013). One of the ways viruses can egress without causing cell cytotoxicity is by EV release. CVB causes the depolymerisation of β -actin cytoskeleton, which induces EV release and the presence of CVB virions in EVs following infection of myoblast cells has also been observed (Inal and Jorfi 2013, Robinson et al. 2014). Autophagosomal markers such as LC3 protein were also present in the exosomes, leading to the hypothesis that EVs are released through the non-lytic autophagy pathway (Robinson et al. 2014). Alongside CVB, a wide range of viruses, including HIV, hepatitis C, Epstein Barr virus and herpes virus have been documented to utilise the host cells exosome machinery for virus particle egress, infectivity and modulation of host cell contents (Narayanan et al. 2013, Ramakrishnaiah et al. 2013, Petrik 2016). Furthermore, exosomes obtained from nasal samples of RV infected patients exhibited an increase in the miRNA hsa-mir-155, which was predicted by *in silico* screening to regulate

antiviral immunity, suggesting exosomes could also be vital in the antiviral response following infection (Gutierrez et al. 2016).

The mechanisms behind RV-induced TN-C release in AECs are currently unknown. TN-C is induced in response to cell damage in certain cells and both poly(I:C) and RV can induce cell cytotoxicity in AECs. Furthermore, evidence describing a role for EVs in viral infections, modulation of the host response, and carrying inflammatory mediators vital in disease pathogenesis is plentiful, but currently the evidence in relation to RV infection is sparse. Investigating the role of cell cytotoxicity and EVs in RV-induced TN-C release is yet to be studied, and may provide insight into the physiological relevance of TN-C release in response to RV infection of AECs.

4.2. Hypothesis and Aims

It was hypothesised that AEC TN-C release following RV infection is a specific response to RV infection and not solely a consequence of non-specific cell cytotoxicity. Furthermore, it was hypothesised that poly(I:C) stimulation and RV infection of AECs induces the release of EVs and that TN-C expression is associated with these vesicles.

The specific aims of this chapter were to investigate:

1. Whether poly(I:C), RV and staurosporine induce cell cytotoxicity in AECs.
2. Whether staurosporine induces AEC TN-C release and how this compares to poly(I:C) and RV-induced release.
3. The concentration and size of EVs produced by AECs at basal levels and in response to poly(I:C) stimulation and RV infection.
4. The presence and quantity of TN-C in AEC-derived EVs following poly(I:C) stimulation and RV infection.

4.3. Poly(I:C) and RV Induces Significantly More TN-C Release in AECs than Staurosporine-Induced Apoptosis, Indicating a Viral Specific Mechanism

The data in the previous chapter (Chapter 3) demonstrated that in response to poly(I:C) stimulation and RV infection (major and minor serotypes), both BEAS-2B cells and PBECs (from asthmatic and non-asthmatic patients) released TN-C into the supernatant, as measured by western blot and ELISA. These experiments have not, however, verified whether TN-C is actively secreted in a poly(I:C) / RV-dependent manner, or whether TN-C is being released indirectly due to cell death following stimulation / infection. To investigate this, AEC viability following poly(I:C) stimulation and RV infection was quantified, and TN-C release in response to non-viral mediated apoptosis was determined.

4.3.1. RV Reduces Cell Viability in BEAS-2B Cells but Poly(I:C) has no Cytotoxic Effect

BEAS-2B cell viability was imaged by light microscopy following poly(I:C) stimulation and RV infection. BEAS-2B cells were grown to confluence and stimulated with poly(I:C) (25 µg/ml) or infected with RV-1B (MOI 1.5) for up to 72 hours, and images of the cell cultures were taken at 40x magnification by an Olympus U-TVO-5XC-3 Lens (Olympus CKX41 microscope).

There was no change in cell viability at 24, 48 and 72 hours in the unstimulated media controls. Furthermore, although there was also no visible change in cell viability in response to poly(I:C) at 24, 48 and 72 hours, the cells underwent an elongated morphological change at 72 hours post stimulation. Finally, visible viral plaques (holes in the monolayer that indicate areas of cell death) in the cell monolayer were present in response to RV-1B at all-time points, indicating a loss in cell viability at 24, 48 and 72 hours. Cell viability appeared to decrease over time in response to RV-1B, with more visible plaques in the monolayer in the 72 hour samples (Figure 4.1.).

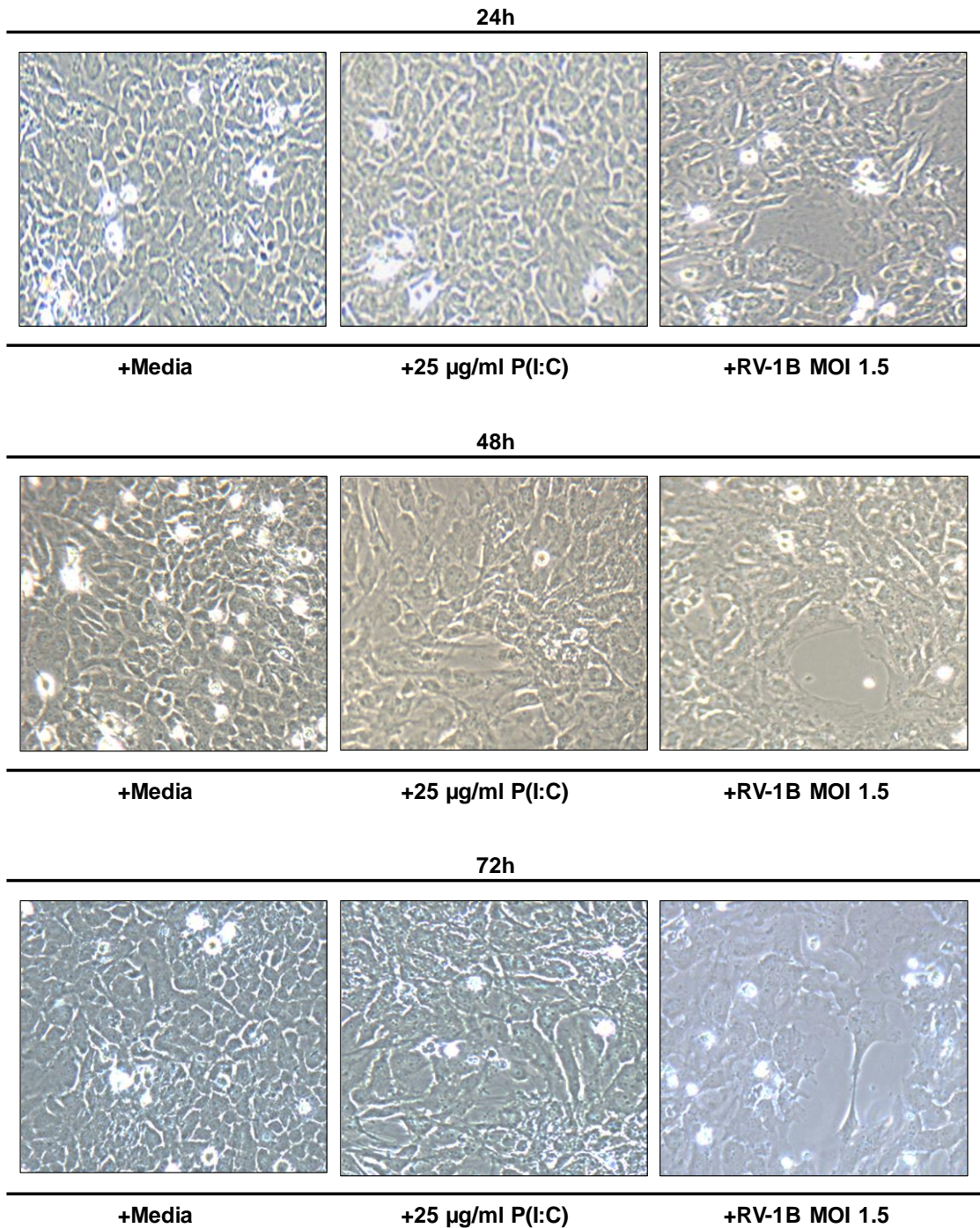


Figure 4.1. RV Reduces Cell Viability in BEAS-2B Cells but Poly(I:C) has no Cytotoxic Effect

BEAS-2B cells were grown to confluence and stimulated with poly(I:C) (25 µg/ml) or infected with RV-1B (MOI 1.5) for the indicated times. BEAS-2B cell viability was measured by imaging the cell cultures (40x magnification) with an Olympus U-TVO-5XC-3 Lens (Olympus CKX41 microscope). Images shown are a representative timeline (N=3) with each replicate representing a separate cell passage.

4.3.2. Poly(I:C) does not Affect BEAS-2B Cell Viability (as Measured by Cell Metabolic Activity) and Induces Significantly More TN-C Release than Staurosporine

To determine whether cell death contributes towards TN-C release or whether TN-C release is a virally-dependent mechanism, the next aim was to compare the amount of TN-C release induced by non-viral apoptosis to that induced by poly(I:C) and RV. To do this, TN-C release following stimulation with staurosporine, an inducer of apoptosis through both caspase independent and caspase dependent mechanisms (Belmokhtar et al. 2001), was compared to poly(I:C)-induced TN-C release in BEAS-2B cells. BEAS-2B cells were left unstimulated or stimulated with poly(I:C) (25 µg/ml) or staurosporine (4.6 µg/ml) or infected with RV-1B (MOI 1.5) for up to 72 hours. Cell metabolic activity was then determined by MTT assay as a measure of cell viability, and supernatant was collected and analysed for TN-C release as in Section 3.3.5. (staurosporine and poly(I:C) only).

In response to poly(I:C) stimulation of BEAS-2B cells, there was no change in cell metabolic activity compared to the unstimulated controls at 24, 48 and 72 hours (Figure 4.2A). A significant decrease in cell metabolic activity was observed in response to staurosporine at 24 (75% loss; $p < 0.05$), 48 (90% loss; $p < 0.0001$) and 72 hours (90% loss; $p < 0.001$) compared to the media control. The loss in cell metabolic activity was also significantly reduced in response to staurosporine, compared to the poly(I:C) cohort at 24 ($p < 0.05$), 48 ($p < 0.01$) and 72 hours ($p < 0.01$). Again, in response to poly(I:C), there was no loss in cell metabolic activity in BEAS-2B cells, but RV-1B infection caused a significant decrease in cell metabolic activity compared to both the media control and poly(I:C) cohort at 24 ($p < 0.05$ and $p < 0.05$), 48 ($p < 0.0001$ and $p < 0.0001$) and 72 hours ($p < 0.01$ and $p < 0.001$; Figure 4.2B). TN-C was detectable following western blot following stimulation with poly(I:C) and staurosporine (Figure 4.2C) and poly(I:C) induced significant TN-C release compared to both the media control and staurosporine at 48 ($p < 0.001$ and $p < 0.01$) and 72 hours ($p < 0.01$; Figure 4.2D). Notably, TN-C release following staurosporine stimulation was the same as the media control cells for all time points.

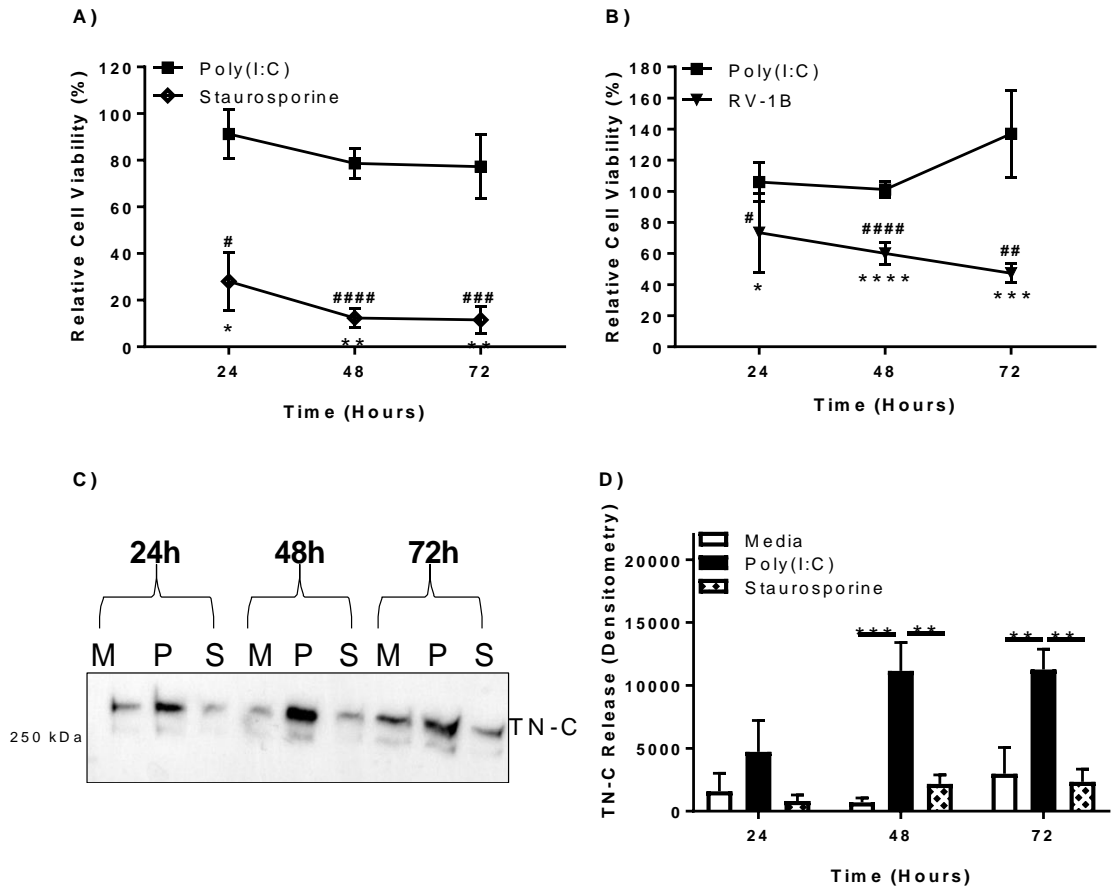


Figure 4.2. Poly(I:C) does not Affect BEAS-2B Cell Viability (as Measured by Cell Metabolic Activity) and Induces Significantly More TN-C Release than Staurosporine

BEAS-2B cells were grown to confluence and stimulated with poly(I:C) (25 $\mu\text{g}/\text{ml}$) or staurosporine (4.6 $\mu\text{g}/\text{ml}$), or infected with RV-1B (MOI 1.5) for the indicated times. BEAS-2B metabolic activity was measured by MTT assay in response to poly(I:C) and staurosporine **(A)** and poly(I:C) and RV-1B **(B)**. The presence of TN-C was analysed by western blotting (M for Media, P for poly(I:C) and S for staurosporine, one representative blot shown) **(C)** and densitometry of the top band was performed in ImageJ software **(D)**.

Values expressed as mean \pm SEM (N=3) with each replicate representing a separate cell passage. Significant differences in cell viability (# compared to media control and * compared to poly(I:C)) and TN-C release are indicated by, * $p < 0.05$; ** $p < 0.01$; *** $p < 0.001$; **** $p < 0.0001$, analysed by two way repeated measures ANOVA with Tukey's post hoc test.

4.3.3. Poly(I:C) does not Affect PBEC Cell Viability (as Measured by Cell Metabolic Activity) and Poly(I:C) and RV Induces Significantly More TN-C Release than Staurosporine

Next, PBECs were left unstimulated or stimulated with poly(I:C) (25 µg/ml) or staurosporine (4.6 µg/ml) or infected with RV-1B (MOI 1.5) for 72 hours and cell metabolic activity was then determined by MTT assay as in Section 4.3.2. as a measure of cell viability. Supernatant was collected and analysed for TN-C release as in Section 3.3.5 (24-72 hours in poly(I:C) experiment and 48 hours only RV experiment).

In response to poly(I:C), there was no statistically significant change in cell metabolic activity compared to the media control, with approximately only a 10% reduction at 24, 48 and 72 hours (Figure 4.3A). A significant decrease in cell metabolic activity was induced in response to staurosporine at 24 ($p < 0.0001$), 48 ($p < 0.0001$) and 72 hours ($p < 0.0001$) compared to the media control. The loss in cell metabolic activity was also reduced in response to staurosporine compared to the poly(I:C) cohort at 24 ($p < 0.01$), 48 ($p < 0.001$) and 72 hours ($p < 0.0001$). In the RV-1B infection experiment, staurosporine also caused a significant decrease in cell metabolic activity compared to the unstimulated control and RV-1B infection at all time points ($p < 0.0001$; Figure 4.3B). Interestingly, whilst cell metabolic activity was higher than the unstimulated media control in the RV-1B cohort at 24 hours (120%; $p < 0.01$), cell metabolic activity significantly decreased at 48 hours (20% loss; $p < 0.01$) and 72 hours (35% loss; $p < 0.0001$) post infection. TN-C was detectable following western blot following stimulation with poly(I:C) and RV infection (Figure 4.3C and 4.3E respectively) and poly(I:C) and RV induced significant TN-C release compared to staurosporine at 72 hours and 48 hours respectively ($p < 0.05$; Figure 4.3D and 4.3F). Again, TN-C release following staurosporine stimulation was the same as the media control cells for all time points ($p < 0.001$).

These results confirm that statistically significant increases in TN-C release occur in response to poly(I:C) and RV-1B, but not in response to staurosporine treatment. In contrast, staurosporine had the most significant impact on cell metabolic activity and thus cell viability. These results indicate that TN-C release is an active, virally-dependent mechanism upon infection rather than due to cell cytotoxicity following infection.

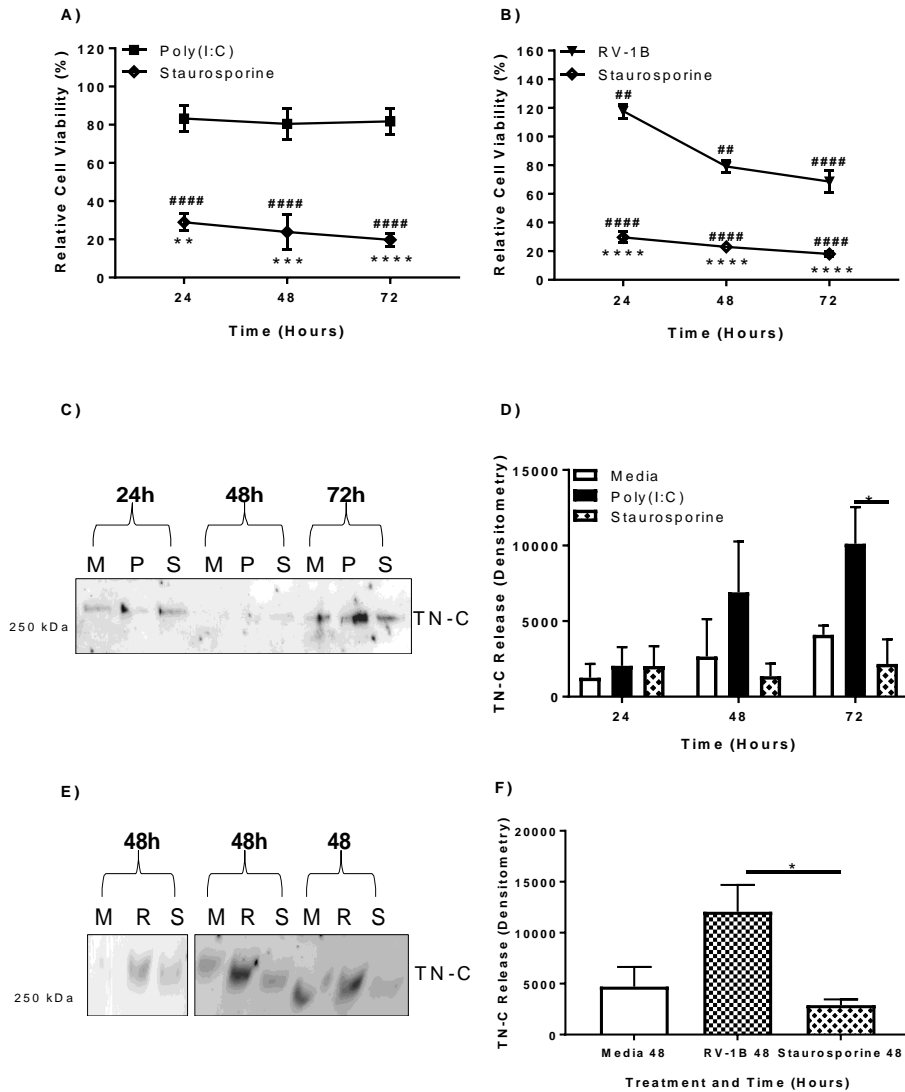


Figure 4.3. Poly(I:C) does not Affect PBEC Cell Viability (as Measured by Cell Metabolic Activity) and Poly(I:C) and RV Induces Significantly More TN-C Release than Staurosporine

PBECs cells were grown to confluence and stimulated with poly(I:C) (25 µg/ml) or staurosporine (4.6 µg/ml) or infected with RV-1B (MOI 1.5) for the indicated times. PBEC metabolic activity was measured by MTT assay in response to poly(I:C) and staurosporine (A) and staurosporine and RV-1B (B). The presence of TN-C was analysed by western blotting (M for Media, P for poly(I:C) and S for staurosporine, one representative blot shown) (C) and densitometry of the top band was performed in ImageJ software (D). The presence of TN-C was analysed by western blotting (M for Media, R for RV-1B and S for staurosporine (all three Ns shown on two blots) (E) and densitometry of the top band was performed in ImageJ software (F). Values expressed as mean ± SEM (N=3) with each replicate representing an independent PBEC donor. Significant differences in cell viability (# compared to media control and * compared to poly(I:C) / RV-1B) and TN-C release are indicated by, * p<0.05; ** p<0.01; *** p<0.001; **** p<0.0001, analysed by one way repeated measures ANOVA with Dunnet's post hoc test or two way repeated measures ANOVA with Tukey's post hoc test.

4.4. Poly(I:C) Stimulation and RV Infection of BEAS-2B Cells Induces Overall Exosome Release and Exosome-Associated TN-C Expression

With the results in Section 4.1. demonstrating that release of TN-C was a virally-dependent mechanism, the next aim was to further investigate the mechanisms behind RV-induced TN-C release. As EVs, and in particular exosomes, are implicated in viral infection, asthma pathogenesis and also play a role in the delivery of inflammatory mediators such as IL-1, the release of exosomes in response to poly(I:C) and RV in AECs was measured. For the purpose of this study, the term EV will be used when covering both exosomes and MVs.

4.4.1. AECs Grow and Respond to Poly(I:C) in EV-Depleted Media, Despite a Loss in Cell Viability

BEAS-2B Media is supplemented with FCS, which is known to contain bovine EVs that interfere with, and reduce the accuracy of, NTA analysis. Furthermore, the recipe for the PBEC media is not disclosed and thus it is not known if EVs are present. Thus, to remove bovine EVs from FCS, the FCS was spun in the ultracentrifuge overnight at 120,000 rcf. The EV-depleted FCS was then added to BEAS-2B Media to make EV-Depleted Media. For PBECs, PBEC Basal Media was spun in the ultracentrifuge overnight at 120,000 rcf and was made into EV-Depleted Media. The concentration of the EVs present in BEAS-2B Basal Media and EV-Depleted BEAS-2B Basal Media was then measured by NTA on the NanoSight NS300 instrument, and PBEC Basal Media and EV-Depleted PBEC Basal Media was measured by NTA on the ZetaView instrument. To confirm that BEAS-2B and PBEC cell growth was unaffected by EV-Depleted Basal Media, an MTT cell viability assay was performed. Finally, to confirm that the cells could respond as expected to poly(I:C) in EV-Depleted media, CXCL8 and CCL5 ELISAs were carried out.

EV removal from FCS prior to addition to BEAS-2B Basal Media was successful, as BEAS-2B EV-Depleted Basal Media had significantly less EVs ($p < 0.001$), with an almost undetectable level of EVs compared to 3×10^8 particles per ml in the standard media (Figure 4.4A). Furthermore, the amount of EVs in the PBEC Basal Media and PBEC EV-Depleted Basal media was below the limit of detection (4.1×10^6 ; Figure 4.4B). PBEC cell viability was unaffected throughout the stimulation time course and BEAS-2B cells grew to confluence with the same cell viability at 24 and 48 hours in EV-Depleted Basal Media (Figure 4.4C). Additionally, despite a statistically significant reduction in cell metabolic activity at 72 hours (20% loss; $p < 0.01$), cell number and morphology looked as expected when assessed by eye using a light microscope. Both BEAS-2B cells and PBECs responded to poly(I:C) stimulation in EV-Depleted Media, with significant CXCL8 induction at 24, 48 and 72 hours ($p < 0.0001$; Figure 4.4D; PBEC data not shown) and CCL5 at 48 hours ($p < 0.01$; Figure 4.4E; PBEC data not shown). These results indicate that BEAS-2B cells and PBECs can grow and respond to viral stimulation in EV-Depleted Basal Media and so can be used in future experiments, involving NTA.

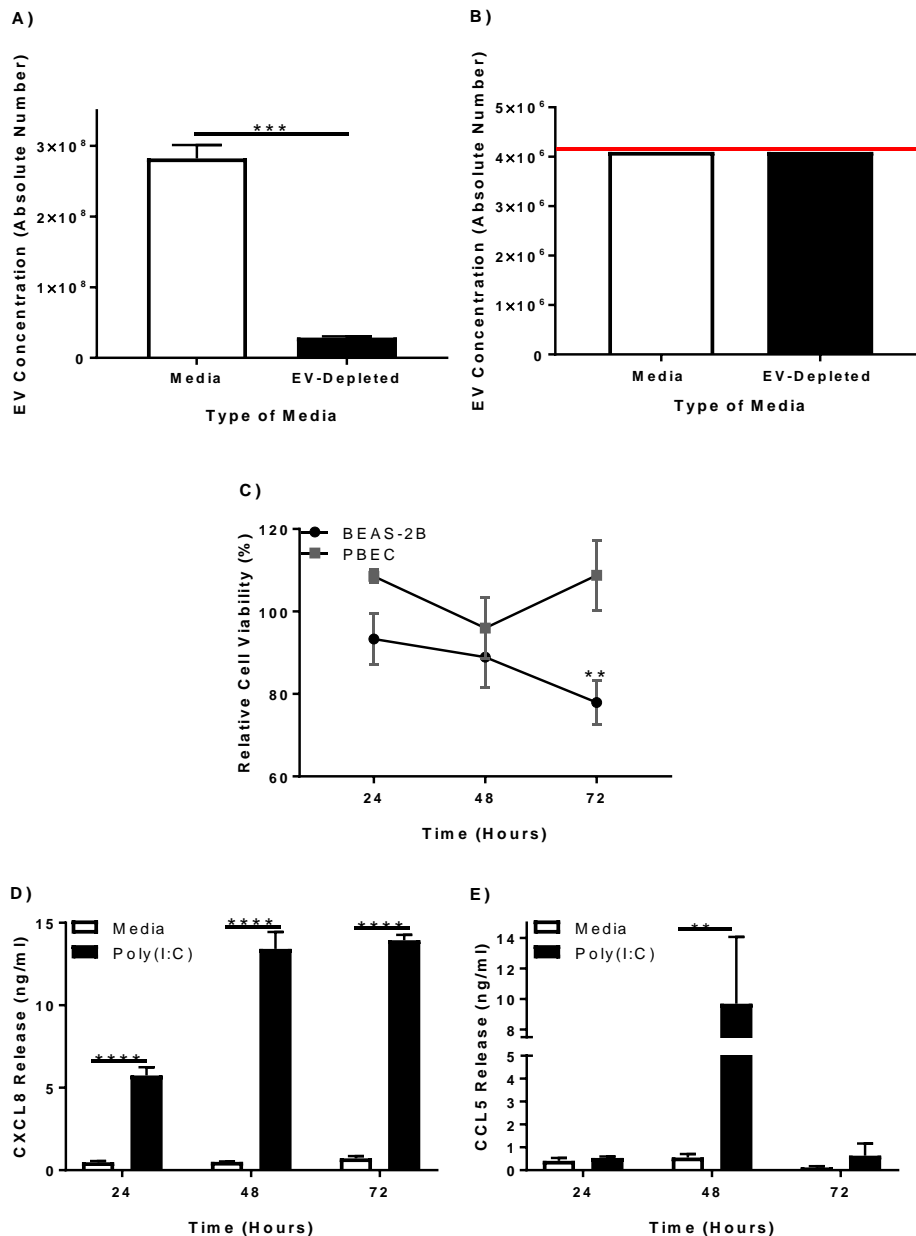


Figure 4.4. AECs Grow to Confluence and Respond to Poly(I:C) in EV-Depleted Media

FCS was centrifuged in an ultracentrifuge overnight at 120,000 rcf in order to remove bovine EVs, and was then added to BEAS-2B Media to make BEAS-2B EV-Depleted Media. PBEC Basal Media was centrifuged in an ultracentrifuge overnight at 120,000 rcf in order to remove EVs to make EV-Depleted PBEC Basal Media. The concentration of EVs present in BEAS-2B (A) and PBEC (B) Basal and EV-Depleted Basal was measured by NTA analysis. BEAS-2B cells and PBECs were cultured in Basal Media and EV-Depleted Basal Media for the indicated times and an MTT assay was performed to quantify cell metabolism as a measure of cell viability (C). BEAS-2B cells were grown to confluence in EV-Depleted media, stimulated with poly(I:C) (25 $\mu\text{g}/\text{ml}$) for the indicated times and a CXCL8 (D) and CCL5 (E) ELISA was performed. Values expressed as mean \pm SEM or mean only (N=3) with each replicate a separate cell passage or PBEC donor. Significance differences in EV concentration, cell viability and chemokine production are indicated by, ** $p < 0.01$; *** $p < 0.001$; **** $p < 0.0001$, analysed by paired T-test and two way ANOVA with Tukey's post hoc test.

4.4.2. Poly(I:C) Stimulation of BEAS-2B Cells and PBECs Induces the Release of EVs with the Size-Range and Protein Composition of Exosomes

BEAS-2B cells and PBECs were grown to confluence in EV-Depleted Basal Media and left unstimulated or stimulated with 25 µg/ml poly(I:C) for up to 72 hours. Exosomes were then isolated using the four spin ultracentrifugation isolation method as described in Figure 2.2. The BEAS-2B isolated exosomes were also analysed for the presence of exosome-enriched proteins CD9 and flotillin-1, EV-associated protein (depending on the EV type) β-actin and EV-deficient protein GRP94 by western blot. Finally, the concentration and size of BEAS-2B and PBEC EVs isolated following poly(I:C) stimulation was then measured by NTA on the ZetaView instrument.

As expected, CD9 and flotillin-1 were present in the BEAS-2B exosome isolated fraction at the unstimulated controls and poly(I:C) stimulated cohorts throughout the stimulation timeline (Figure 4.5A), but interestingly β-actin was not expressed. Furthermore, the EV negative control GRP94 was also not expressed in the exosome isolated fraction. Densitometry of CD9 and flotillin-1 revealed a significant increase in the exosome-enriched proteins at 72 hours post stimulation ($p < 0.0001$; Figure 4.5B and 4.5C). When the BEAS-2B exosome isolated fraction was measured by NTA analysis, poly(I:C) induced a significant release in exosomes at 72 hours post infection (correlating with the western blot expression of exosome-enriched proteins; $p < 0.05$; Figure 4.5D), with an increase from approximately 7×10^6 to 1.4×10^7 . The average exosome size was approximately 100 nm at all-time points, whilst 48-hour poly(I:C) stimulation also induced the release of EVs at approximately 150 nm. When the PBEC exosome isolated fraction was measured by NTA analysis, poly(I:C) again induced a release of exosomes with an average size of approximately 110 nm at 72 hours post-stimulation, with an increase from approximately 6×10^6 to 9×10^6 (not statistically significant; Figure 4.5E).

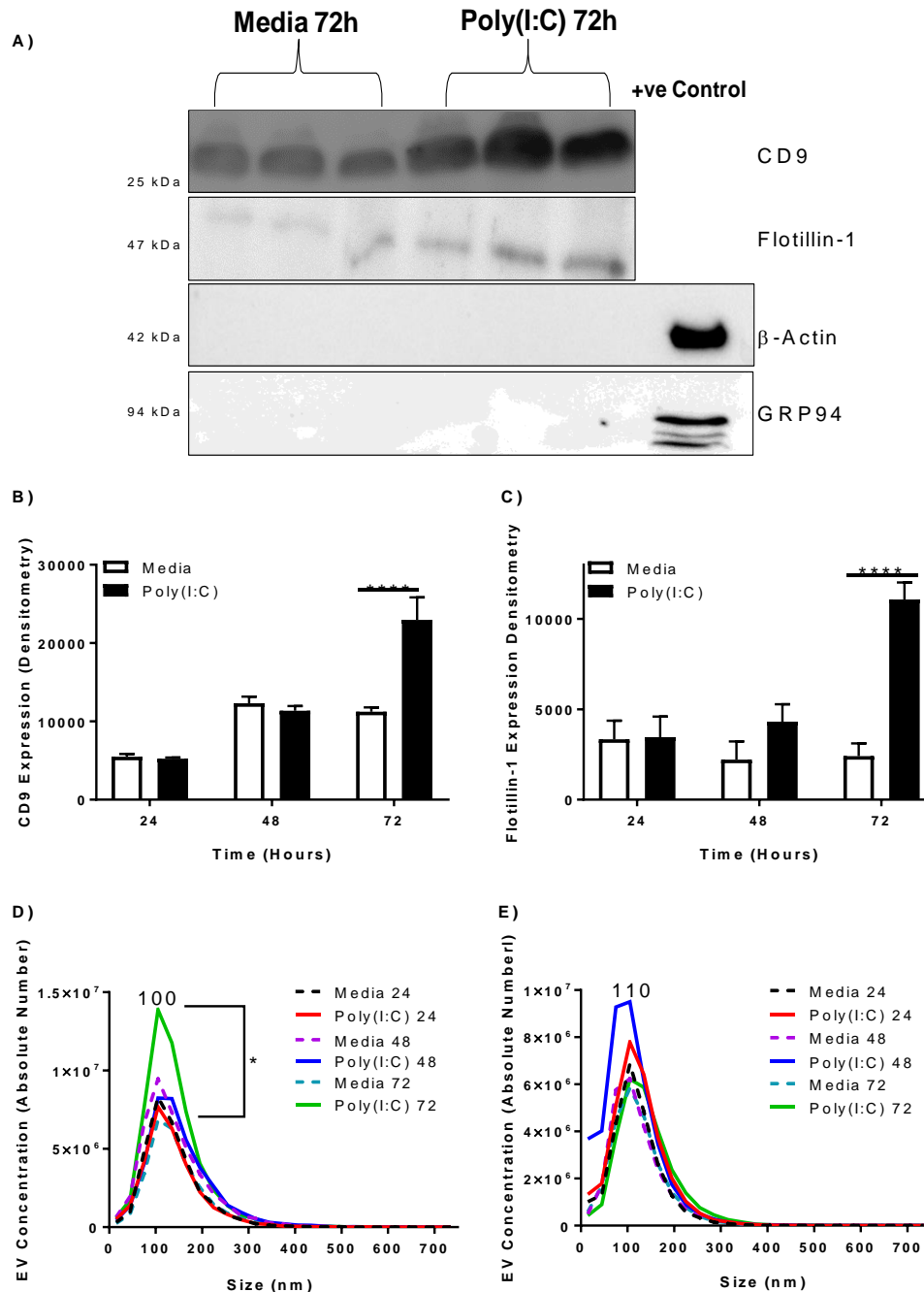


Figure 4.5. Poly(I:C) Stimulation of AECs Induces the Expression of Exosome-Enriched Proteins and EV Release Within the Size Range of Exosomes

BEAS-2B cells and PBECs were grown to confluence in EV-Depleted media and stimulated with poly(I:C) (25 µg/ml) for the indicated times. Exosomes were then isolated by the four spin ultracentrifugation isolation method, and re-suspended in 100 µl PBS. **(A)** CD9, flotillin-1, β-actin, and GRP94 expression in BEAS-2B exosome isolates were measured by western blot (one representative blot shown). BEAS-2B exosome CD9 **(B)** and flotillin-1 **(C)** expression was quantified by densitometry using ImageJ software. BEAS-2B **(D)** and PBEC **(E)** exosome concentration and size were quantified by Nanoparticle Tracking Analysis on ZetaView. Values expressed as mean ± SEM (N=3-7) with each replicate a different cell passage or PBEC donor. Significance differences in exosome-associated protein expression and exosome release are indicated by * p<0.05; **** p<0.0001, analysed by two way ANOVA with Tukey's post hoc test.

4.4.3. Poly(I:C) Stimulation of BEAS-2B Cells Induces Exosome-Associated-TN-C Expression

With the isolated EVs characterised by NTA and western blotting as primarily exosomes, the next aim was to analyse the exosomes for the presence of TN-C. Exosomes were isolated as per Figure 2.2. and 10 μ L of exosome sample was analysed by western blotting for TN-C expression as per section 3.4.2.

Western blot analysis determined that both the smaller (~250 kDa) and larger (>250 kDa) variants of TN-C were present in the exosomes isolated from poly(I:C) stimulated BEAS-2B cells (Figure 4.6A). Poly(I:C) stimulation significantly induced exosome-associated TN-C release at 72 hours post stimulation ($p < 0.05$; Figure 4.6B). When this was normalised to flotillin-1 expression (and thus exosome number), the increase in TN-C expression was not statistically significant (Figure 4.6C).

4.4.4. RV Infection of BEAS-2B Cells Induces Exosome-Enriched Protein Expression and Exosome-Associated-TN-C Expression

Next, exosomes following RV infection of BEAS-2B cells were characterised and exosome-associated TN-C expression was quantified by western blot. BEAS-2B cells were grown to confluence in EV-Depleted BEAS-2B Basal Media and left unstimulated or infected with RV-1B for up to 48 hours. Exosomes were then isolated using the four spin ultracentrifugation isolation method as detailed in Section 4.4.2. The isolated exosomes were analysed for the presence of exosome-enriched proteins CD9 and flotillin-1 and TN-C by western blot. Due to health and safety regulations, RV isolated exosomes could not be analysed by NTA.

In BEAS-2B cells, CD9, flotillin-1 and TN-C could all be detected by western blot and in response to RV-1B (Figure 4.7A). When measured by densitometry, there was approximately a 5-fold increase in CD9 (Figure 4.7B) and flotillin-1 (Figure 4.7C) expression and a 2-fold increase TN-C expression (Figure 4.7D). These increases were not statistically significant, with further experiments required to determine whether the increases in exosome-associated proteins occur following RV infection.

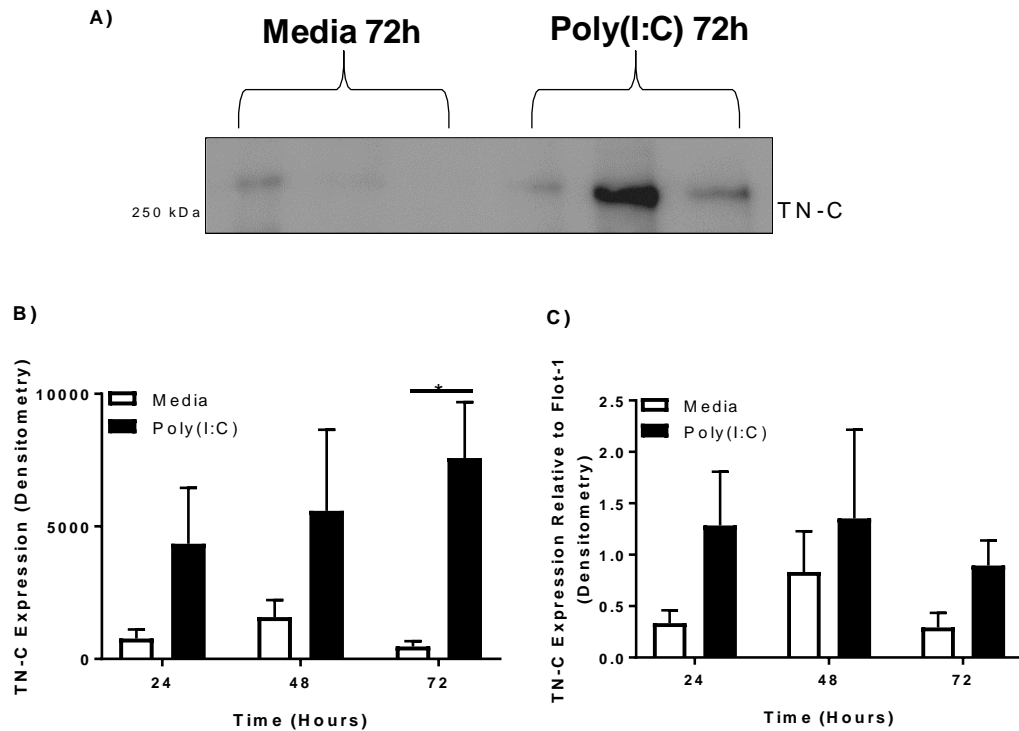
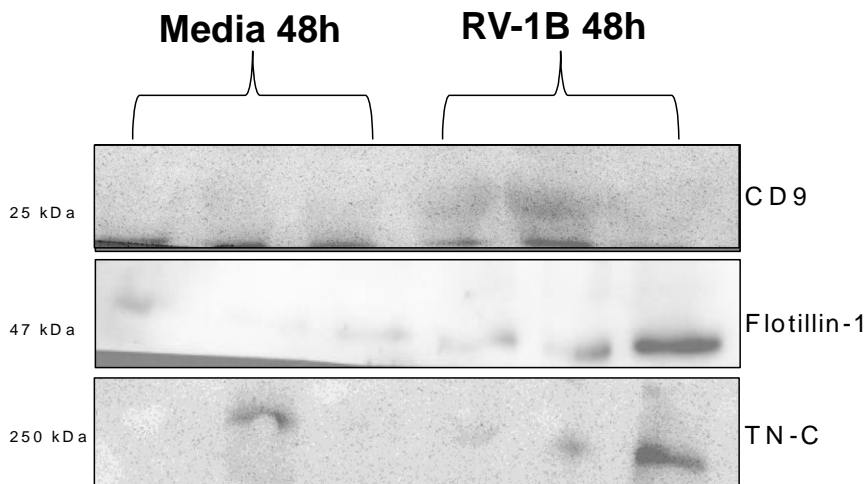


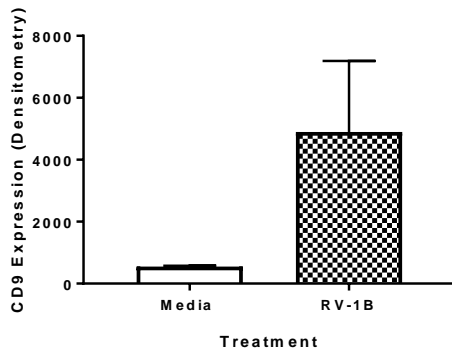
Figure 4.6. Poly(I:C) Stimulation of BEAS-2B Cells Induces Significant Exosome-Associated TN-C Release

BEAS-2B cells were grown to confluence in EV-Depleted media, and stimulated with poly(I:C) (25 $\mu\text{g}/\text{ml}$) for the indicated times. Exosomes were then isolated by the four spin purification method, and re-suspended in 100 μl PBS. **(A)** TN-C expression was measured by western blot (one representative blot shown). **(B)** TN-C expression only **(B)** and TN-C expression normalised to flotillin-1 expression from Figure 4.5E **(C)** was quantified by densitometry using ImageJ software. Values expressed as mean \pm SEM (N=7-9) with each replicate a different cell passage. Significance differences in TN-C expression are indicated by * $p < 0.05$, analysed by two way ANOVA with Tukey's post hoc test.

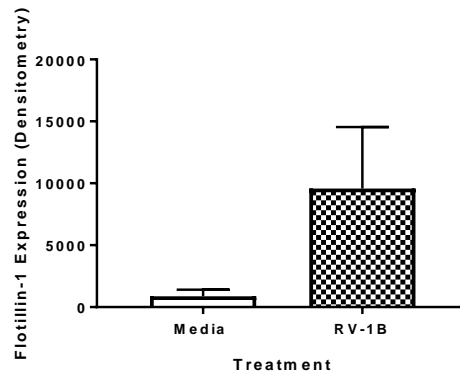
A)



B)



C)



D)

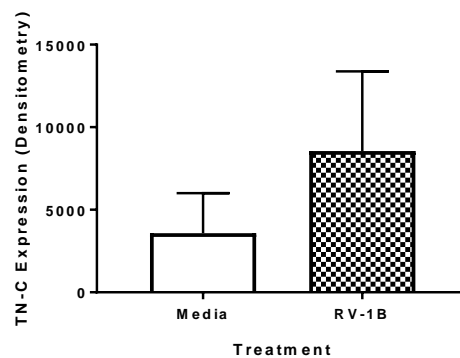


Figure 4.7. RV Infection of BEAS-2B Cells Induces Exosome-Associated Proteins and Exosome-Associated TN-C Release

BEAS-2B cells were grown to confluence in EV-Depleted media, and infected with RV-1B (MOI 1.5) for the indicated times. Exosomes were then isolated by the four spin purification method, and re-suspended in 100 μ l PBS. CD9, flotillin-1 and TN-C expression was measured by western blot (A; one representative blot shown). CD9 (B), flotillin-1 (C) and TN-C expression (D) was quantified by densitometry using ImageJ software. Values expressed as mean \pm SEM (N=3) with each replicate a different cell passage, analysed by paired T-test.

4.4.5. Exosome-Associated TN-C Release is an Abundant Pathway of Release Following Viral Stimulation / Infection

Following confirmation of the release of exosome-associated TN-C following poly(I:C) stimulation, the next aim was to distinguish whether this was a pathway of substantial release in AECs. To do this, BEAS-2B cells were left unstimulated or stimulated with 25 µg/ml poly(I:C) for up to 72 hours and EVs were isolated as per Section 4.4.2. TN-C expression was determined by western blotting in the 4 main fractions during the isolation process (see Section 2.11 for more information): 1. supernatant, 2. MV isolated fraction, 3. exosome isolated fraction and 4. remaining supernatant following removal of MVs and exosomes. The 72-hour time point of each fraction was analysed on the same gel.

Both the small and large isoforms of TN-C expression were visible in all isolation fractions (Figure 4.8A) and when measured by densitometry, TN-C expression was the highest in the supernatant, with almost no expression in the MV isolation fraction (Figure 4.8B). Furthermore, the expression of TN-C in both the exosome isolation fraction and supernatant after EV removal was approximately 50% of the supernatant TN-C expression. TN-C expression was significantly less compared to the supernatant in the MVs ($p < 0.001$), exosomes and supernatant after EV removal ($p < 0.05$).

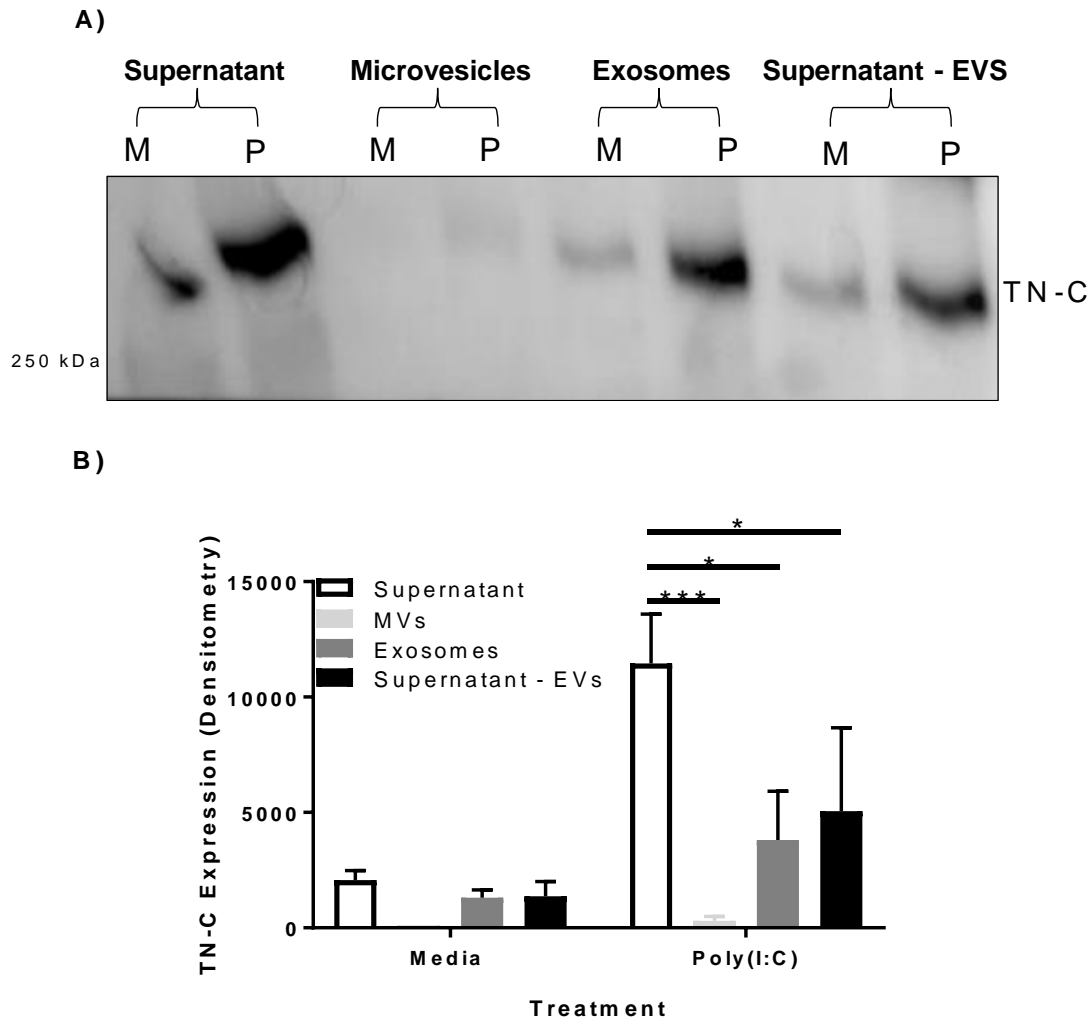


Figure 4.8. Exosome-Associated TN-C Release is an Abundant Pathway Following Viral Stimulation

BEAS-2B cells were grown to confluence in EV-Depleted media and stimulated with poly(I:C) (25 μ g/ml) for the indicated times. MVs and exosomes were then isolated by the four spin purification method, and re-suspended in 100 μ l PBS. TN-C expression in each of the four fractions (supernatant, MVs, exosomes and supernatant following EV isolation) was measured by western blot (**A**; one representative blot shown). TN-C expression (**B**) was quantified by densitometry using ImageJ software. Values expressed as mean \pm SEM (N=3) with each replicate a different cell passage. Significance differences in TN-C expression are indicated by * $p < 0.05$; *** $p < 0.001$), analysed by one way ANOVA with Dunnett's test.

4.5. Summary and Discussion

4.5.1. Summary

The results in this chapter confirm that AEC TN-C release in response to RV infection is viral specific and does not occur in response to non-viral cell cytotoxicity. The release of TN-C following RV infection was demonstrated for the first time to occur through the release of exosomes with an average size of 100-110 nm. Furthermore, this increase in released TN-C was determined to be partly due to an increase in exosome concentration following stimulation / infection. These results begin to reveal the mechanisms behind RV-induced TN-C release, and the association of TN-C with exosomes may have important implications in RV-induced exacerbations.

4.5.2. TN-C Release is Viral Specific and Not Induced in Response to Non-Viral Cell Death

The determination of whether TN-C release following RV infection is a virally-specific response is of importance, due to RV and poly(I:C) inducing cell cytotoxicity in AECs (Deszcz et al. 2005, Blaas and Fuchs 2016, Koizumi et al. 2016). Furthermore, when relating the pathway to *in vivo* RV infection, it is thought that alternative non-lytic pathways may also exist (Blaas and Fuchs 2016). Thus, if TN-C release following RV infection occurs due to non-specific cell cytotoxicity or viral-specific cell toxicity only (and not due, in some part, to virally-induced signalling pathways), then this pathway would be of less biological or clinical significance.

4.5.2.1. RV and Staurosporine Reduces Cell Viability in AECs, but Poly(I:C) Does Not

Poly(I:C) did not induce cell cytotoxicity during the stimulation time-course (as measured by microscopy; Figure 4.1.) or loss in cell metabolic activity (and thus cell viability, as measured by MTT assay) in BEAS-2B cells (Figure 4.2A), or any significant loss in cell metabolic activity in PBECS, with only approximately a loss of 20% (Figure 4.3A). RV infection, meanwhile, induced significant loss in cell metabolic activity in both BEAS-2B cells (Figure 4.1 and 4.2B) and PBECS (Figure 4.3B), with a loss of 20-40%, as did staurosporine (Figure 4.2A. 4.3A and 4.3B), inducing a loss of 75-90% cell metabolic activity.

Despite the lack of cell cytotoxicity observed by microscopy following poly(I:C) stimulation, elongation of the cells occurred at 72 hours post-stimulation. The reason for this morphological change is currently unknown, but it can be postulated that this is due to EMT. EMT (described in Section 1.1.2.) has been established to be important in asthma pathogenesis, with AECs reverting to myofibroblasts, driving fibrosis, and also occurs in response to RV infection and can be induced by TN-C (see Section 1.1.2). Alpha smooth muscle actin (α -SMA) is an indicator of EMT (Ding et al. 2014), and therefore future work can confirm this process by measuring α -SMA levels by western blot or immunofluorescence. Microscopy also demonstrated the formation of viral plaques in BEAS-2B cells following RV infection, alongside cell elongation, Viral plaques

are the areas formed in response to viral efflux following infection and this causes cell death and 'holes' in the monolayer form. The formation of viral plaques following RV infection has been demonstrated previously in our lab (Stokes et al. 2016).

The loss of cell metabolic activity following RV infection and staurosporine stimulation correlated with previous studies performed in the lab and with other literature (Bossios et al. 2005, Ismail et al. 2014). Interestingly, poly(I:C) had been previously demonstrated in other publications to induce cell cytotoxicity in BEAS-2B cells and PBECs (Koizumi et al. 2016) and thus the results in this study contradict with this. The Koizumi et al study demonstrated a reduction in live BEAS-2B cells through apoptosis at 72 hours post stimulation with 0.1 µg-100 µg/ml of poly(I:C) via annexin staining and through terminal deoxynucleotidyl transferase dUTP nick end labelling (TUNEL) staining in 50 and 100 µg/ml of poly(I:C). The lack of cell cytotoxicity following poly(I:C) stimulation demonstrated in this thesis (confirmed by microscopy and MTT assay) suggests that 25 µg/ml is a non-cytotoxic concentration in AECs, with higher concentrations capable of inducing cytotoxicity, whilst the cytotoxicity observed in other studies at smaller concentrations needs to be investigated further. Furthermore, due to donor variability in PBECs, it can be theorised that certain donors may be more susceptible to poly(I:C)-induced cell cytotoxicity, leading to variation in results in other studies.

4.5.2.2. RV and Poly(I:C) Induces Significant TN-C Release in AECs, but Staurosporine Does Not

Following poly(I:C) and staurosporine stimulation of BEAS-2B cells, poly(I:C) induced significant TN-C release compared to the media control and staurosporine stimulated cells at 48 and 72 hours (Figure 4.2D). Furthermore, both poly(I:C) and RV induced significant TN-C release in PBECs compared to staurosporine at 72 hours and 48 hours post stimulation / infection respectively (Figure 4.3D and 4.3F).

Staurosporine is an established inducer of apoptosis through multiple caspase dependent and independent mechanisms and thus was chosen as a positive control for regulated cell death (Belmokhtar et al. 2001), and importantly, RV-induced apoptosis also occurs via mechanisms known to be triggered by the compound. Staurosporine has been demonstrated to induce apoptosis from 3 hours through caspase 3 (and not through caspase 6, 7 or 8), as well as potentially through caspase independent mechanisms (Belmokhtar et al. 2001). RV-A, B and C have all been demonstrated to induce apoptosis through caspase 3 mechanisms (Nakagome et al. 2014, Croft, Walker and Ghildyal 2018) and also potentially through caspase-independent pathways due to viral protease inhibition of RIPK1 (Lotzerich et al. 2018). It should be noted that staurosporine is not a perfect mimic of RV-induced cell death, however, as staurosporine was demonstrated to induce much more caspase 3 activity compared to RV infection (Nakagome et al. 2014) and RV has also been demonstrated to induce caspase 7 and 9 dependent apoptosis (Deszcz et al. 2005, Nakagome et al. 2014).

These results are important as they demonstrate the viral specificity of the described pathway and determine that the release of TN-C in AECs does not occur in response to non-specific cell cytotoxicity only. If the TN-C release observed following RV infection was due to cell death allowing the 'leakage' of TN-C into the supernatant, then upregulation in TN-C release would also occur following staurosporine induced-cell cytotoxicity. To further confirm this point, poly(I:C) also induces significant TN-C release despite a lack of any significant cell cytotoxicity in BEAS-2B cells. These experiments do not confirm if viral-specific cell death is important for maximal TN-C release however (which could be likely, due to TN-C being upregulated during the wound healing response). The determination that TN-C release is viral-specific is an important one and validates the rest of the experiments in Chapter 4 which further investigates the mechanism of release.

4.5.3. Poly(I:C) and RV Induce Exosome Release in AECs

4.5.3.1. Characterisation of the EVs Released by AECs Following Viral Stimulation Allow the EV Population to be Defined as Primarily Containing Exosomes

NTA analysis of basally released EVs, and EVs released following poly(I:C) stimulation of BEAS-2B cells and PBECs, revealed an average size of approximately 100-110 nm (with some larger vesicles up to 150 nm also present; Figure 4.5D and 4.5E). When analysed by western blot, positive controls CD9 and flotillin-1 were present in the EV isolates, whilst β -actin and negative control GRP94 was not (Figure 4.5A). NTA was also deemed to be accurate due to the lack of EVs in the PBEC media and EV removal from FCS in the BEAS-2B cell media was successful prior to performing the experiments (Figure 4.4A and 4.4D). Additionally, CD9 and flotillin-1 expression was also induced by RV infection (Figure 4.7).

The characterisation of EVs, and distinguishing between MVs and exosomes, is a growing and fluid field that continues to change as further information is revealed. The characterisation of EVs in this study reflect the currently accepted characterisation methods of MVs and exosomes, and conform to the publishing guidelines set out by the Journal of Extracellular Vesicles (Lotvall et al. 2014) and responses from other scientists prominent in the field (Witwer et al. 2017). The size of exosomes are commonly accepted to be between 50-120 nm (Raposo and Stoorvogel 2013, Willms et al. 2016), whilst the size of MVs are between 100-1000 nm. This size crossover means that NTA analysis alone cannot determine what type of EVs are present in this study, but confirms that either exosomes, small MVs or both are present. It is important to note that these results can be considered to be accurate and free from poly(I:C) contamination for a number of reasons. Approximately 30% of the EVs measured by NTA analysis were within the estimated size range poly(I:C) (136-690 nm), however, there was no difference in the NTA size expression profiles between the media control and poly(I:C) samples and thus it was determined that poly(I:C) stimulation did not affect the accuracy of NTA. Poly(I:C) is also not expected to be secreted by the cells following internalisation and stimulation, and contaminant proteins are thought to be removed by the multiple wash and filter steps in the isolation protocol. Finally, the

size of RV virions are 20-30 nm (Winther 2011), so if NTA analysis was performed in the future following RV infection, the accuracy of the EV analysis would not be affected.

ExoCarta is a tool which collates studies on exosomes and ranks the exosomal markers used in differential cell types and species (Keerthikumar et al. 2016). CD9 was the most described exosomal marker (demonstrated in 98 studies), with β -actin 5th (93 studies), and flotillin-1 41st (56 studies). Furthermore, there were no studies that found GRP94 to be associated with exosomes, demonstrating that accurate markers were chosen in this study. Moreover, CD9 and flotillin-1 have also been demonstrated to be expressed specifically in exosomes derived from lung epithelial cells and AECs (Moon et al. 2015, Szul et al. 2016, Chahar et al. 2018). Confirmation of EVs by western blot is a topic under much debate, with no proteins determined to be able to confirm the presence of EVs and instead are said to be EV-enriched (Lotvall et al. 2014). Therefore it has to be noted that markers such as flotillin-1 and CD9 used in this study are exosome-enriched proteins and the presence of these in the isolates does not confirm the presence of exosomes, only suggests they have been isolated. The absence of GRP94, a protein located in the ER and not expressed in exosomes, demonstrates the lack of intracellular proteins in the isolates, confirming a lack of 'contamination' from cell debris or cell-associated proteins. β -actin is a protein that is incorporated into some cell-type specific EVs, but not others. β -actin was not expressed in bronchial epithelial cell exosomes in this study, despite having previously been demonstrated to be present in 3D tracheobronchial ciliated epithelium (Kesimer et al. 2009), indicating potential differential EV cargo proteins in different airway cell types. MVs have no commonly accepted marker, and thus whilst these western blots have determined the presence of exosomal enriched proteins (and thus exosomes) in the exosome isolated fraction, it cannot be confirmed whether MVs are also present. The ultracentrifugation isolation method should remove MVs and pellet exosomes only, but it has to be noted that the efficiency of this method is not 100% accurate (Tang et al. 2017) and thus some small MVs may still be present.

When the NTA and western blot data are analysed, they correlate and reveal the presence of exosomes released from AECs following poly(I:C) stimulation and RV infection. These results also cannot rule out the presence of small MVs, but for the purpose of this study, the isolated vesicles will still be defined as exosomes throughout this study, due to the likelihood this fraction is predominantly exosomes.

4.5.3.2. Poly(I:C) and RV Induces the Overall Concentration of Exosome Release in AECs

In BEAS-2B cells, the overall concentration of exosome release was significantly increased in response to poly(I:C) at 72 hours, with the concentration increasing from 0.8×10^6 to 1.4×10^6 as measured by ZetaView (Figure 4.5D). These results were reflected in the expression of exosome-enriched proteins, with significant induction in CD9 and flotillin-1 at 72 hours post stimulation (Figure 4.5B and Figure 4.5C). Although no NTA was carried out for the RV infection

exosome isolates, CD9 and flotillin-1 expression were induced at 72 hours post infection (Figure 4.7), in keeping with the poly(I:C) data.

These results confirm by two separate methods that exosomes are induced in response to viral stimulation / infection. Although EV release following RV infection has been studied previously, this is the first time that the concentration of exosomes following viral TLR3 stimulation has been quantified in AECs by NTA. AECs are the primary site of infection and replication for RV, and the amount of exosomes induced in response to poly(I:C) stimulation are much greater than was demonstrated in a previous study investigating RV-induced exosomes in nasal aspirates - 5-10 particles/ μ l (Gutierrez et al. 2016). The amount of exosomes induced by RV infection is less than that induced by RSV infection of AECs – approximately 3.68×10^8 particles/ml (Chahar et al. 2018). Also of note, RSV infection induced the release of exosomes at 24 hours post infection, whereas this thesis demonstrates increased exosome release at 72 hours post infection, revealing viral-specific differences in exosome release following AEC infection.

The mechanisms and functional reasons for RV-induced EV release are currently not fully understood, but a logical theory can be generated based on previous knowledge of viral infection and the ESCRT pathway. Exosomes originate from the endosomal pathway (Raposo and Stoorvogel 2013), and as RV virions are internalised into endosomes following initial binding through ICAM-1 and LDL receptors (Blaas and Fuchs 2016), it can be theorised that this increased endosomal traffic will lead to an increase in the ESCRT-pathway, leading to an increase in the formation and release of exosomes. Furthermore, RV protein VP2 has been shown to be present in HeLa cell release exosomes following infection, and exosomes following infection from other enteroviruses such as polio and CVB have been demonstrated to contain infectious virions (Chen et al. 2015), revealing that exosome-upregulation may be due to viral-specific modulation to aid viral infection. Furthermore, the initiation of the immune response following viral infection is vital for the effective removal of the virus (Alenquer and Amorim 2015), and therefore upregulation of exosomes allows rapid communication and delivery of contents between cells that are vital in this process.

It is clear from previous evidence that induction of exosomes can aid viral infection, viral replication, viral propagation and disease pathogenesis, and so the quantification and confirmation of substantial exosome release following RV infection of AECs is an important one. These results have determined the size, partial protein content and concentration of exosomes at basal levels and in response to poly(I:C) stimulation / RV infection, allowing for the important conclusion that RV infection has the ability to modulate exosome release in AECs. This could have important consequences for asthma pathogenesis, RV infection and RV-induced asthma exacerbations.

4.5.4. TN-C Release is Associated with Exosomes and is Induced in Response to Poly(I:C) Stimulation and RV Infection

Following the determination that exosome release was induced in response to poly(I:C) stimulation and RV infection, TN-C expression was then measured. TN-C was associated with exosomes at all time points both at unstimulated controls and in response to poly(I:C). Furthermore, BEAS-2B exosome-associated TN-C release was significantly induced at 72 hours post-stimulation (Figure 4.6B). When normalised to flotillin-1 expression, there was no change in overall TN-C release (Figure 4.6C), with a smaller, non-statistically significant increase in TN-C expression in response to poly(I:C). Furthermore, following poly(I:C) stimulation, exosome-associated TN-C release was measured by western blot and the release was compared in different fractions of the exosome isolation process, revealing that approximately 50% of TN-C released was associated with exosomes, with the rest present in the supernatant (Figure 4.8).

This reveals for the first time that significant exosome-associated TN-C release occurs in response to RV infection. The fact that this significance is lost when normalised to exosome number suggests that the increase in TN-C expression may be primarily due to the increase in overall exosome number, but as TN-C expression does not fall back to baseline, more TN-C may also be incorporated into existing exosomes too. The exosome isolates also appeared to contain almost half of the TN-C available in the supernatant, with little expression in the MVs. This result however, only indicates, rather than confirms, that approximately 50% of virally-induced TN-C release occurs via exosome-associated release. This could be due to a number of reasons. Firstly, exosome isolation by any method, including ultracentrifugation, does not have 100% isolation efficiency and so TN-C expression in the MV fraction, exosome fraction and in the supernatant cannot be accurately determined, with some exosomes and MVs potentially left in the supernatant following isolation. Secondly, despite the fact that 10 µl of each sample was loaded onto the western blot gel, the EVs in each fraction are diluted in differential amounts of media (1 ml in the two supernatant fractions and 100 µl in the MV and exosome isolates), which could further affect the accuracy of the result.

Despite widespread studies demonstrating TN-C release, evidence behind the mechanisms of release is scarce. Although TN-C has previously been established to be present within exosomes by proteomic analysis in cancerous cells (Ji et al. 2013, Greening et al. 2016) and kidney epithelial tubular cells in chronic kidney disease (Wang et al. 2017), this is the first time TN-C has been demonstrated to be associated with exosomes derived from AECs both at basal levels and upregulated in response to poly(I:C) / RV. Furthermore, this is the first time the association has been confirmed by western blotting, with the advantage of this technique (over proteomics) is that it allows the splice variants expressed to be analysed, thus revealing the large splice variant as the main variant released. This result therefore reveals a mechanism of release for the large variant of TN-C (that is associated with inflammation), something that has not been previously described in AECs or any other cell type. The fact that exosome-associated TN-C is detected by western blot is interesting, as the antibody binds to the N-terminal of the

protein (TA domain), suggesting that the whole molecule is being released, rather than the FNIII domain, which can be cleaved at different sites by MMPs and be released in soluble fragments, changing the function of the protein (Giblin and Midwood 2015, Midwood et al. 2016).

Exosome-associated TN-C release is the only well documented mechanistic description of TN-C release in the literature and the results in this study correlates with this, finding no TN-C release in the MV isolate. The fact that TN-C is associated with exosomes is important for a number of reasons. Firstly exosomes are synthesised and released quickly and allow recycling of intracellular cargo (Alenquer and Amorim 2015) and as TN-C is a large and complex protein, this mechanism of release can be theorised to aid with the relatively quick response observed following infection. Secondly, exosomes can 'travel' quite large distances overall several cell diameters (Panakova et al. 2005, Lakkaraju and Rodriguez-Boulan 2008) and therefore this gives TN-C the potential to signal and exert the protein's function further afield. Finally, as exosomes are internalised following binding with the target cell, allowing the delivery of its cargo, the association of TN-C with exosomes will therefore allow internalisation of the protein and TN-C may have the ability to bind to intracellular receptors as well as external ones. This could be particularly important in AECs, where the expression profile of TLR4 (one of the main receptors involved in TN-C-induced inflammation) may be expressed primarily intracellularly, rather than on the surface membrane (Guillot et al. 2004).

4.5.5. Conclusion

The results in this chapter reveal that the pathway of RV-induced AEC TN-C release described in Chapter 3 is viral-specific, does not require virally-induced cell death to occur and does not occur in response to non-viral specific cell death. Furthermore, the results in this chapter reveal for the first time that RV-induced TN-C release is associated with the large upregulation of AEC exosomes, with the average size of exosomes at 100-110 nm.

The fact that TN-C release is associated with exosomes following viral infection has wide implications for the function of the protein, both in the non-asthmatic and asthmatic airway. Furthermore, independently of TN-C release, the fact that exosomes are induced following RV infection in large quantities is also an important finding that may impact on asthma pathogenesis. Therefore, the function of TN-C, exosomes and exosomal-associated TN-C will be investigated in Chapter 5.

Chapter 5 – Results: The Function of TN-C and Exosomes in the Airway Following RV Infection

5.1. Introduction

The results in this study have so far revealed a novel pathway in which TN-C is released in response to RV infection, and furthermore, this release occurs in a viral specific manner and is associated with exosome release. Next, the consequences of this pathway were investigated by examining the function of TN-C, exosomes and exosomal-associated TN-C.

It is well established that TN-C is upregulated and can contribute to inflammation and pathogenesis in a number of diseases. For example, TN-C is increased and has been demonstrated to act as a DAMP in the synovia of patients with RA (Midwood et al. 2009, Page et al. 2012). TN-C^{-/-} mice in a RA model are protected from tissue destruction, and addition of full-length TN-C and recombinant FBG domain to human synovial fibroblasts and macrophages induced the production of IL-6, CXCL8 and TNF α . Furthermore, FBG was demonstrated to act through the TLR4-MyD88 pathway, as neutralising antibodies towards TLR4 significantly inhibited FBG-induced IL-6, CXCL8 and TNF α synthesis (Midwood et al. 2009). TN-C induced inflammation is also potentiated further through autocrine transcriptional regulation of the protein, in which inflammation in the synovia or tumour-matrix environment induces the expression of TN-C, which subsequently induces additional inflammatory cytokine release and further TN-C expression (Goh et al. 2010). TN-C has also been demonstrated to be required for the polarisation of dendritic cells towards a Th17 phenotype. In a RA mouse model, TN-C^{-/-} mice had significantly less IL-17 in the synovia compared to TN-C^{+/+} controls and dendritic cells taken from TN-C^{-/-} mice also produced less IL-17 in response to LPS stimulation (Ruhmann et al. 2012). TN-C is integral for the proinflammatory response of primary mouse bone marrow derived macrophages (BMDMs) to LPS. BMDMs from TN-C^{-/-} mice stimulated with LPS produced significantly less TNF α , IL-6 and CXCL1, and more IL-10, compared to BMDMs from TN-C^{+/+} mice; with TN-C-induced mir-155 production found to be vital for the expression of inflammatory cytokines (Piccinini and Midwood 2012).

Despite evidence of TN-C being involved in the production of inflammatory cytokines in the synovia of RA patients, evidence of TN-C contributing towards the inflammatory phenotype of the airway in asthmatics is sparse. In a Ova-sensitised allergic airway mouse model, TN-C^{-/-} mice had significantly less MCP-1, MMP-9, IL-5, IL-13 and IgE in their BALF in response to Ova challenge, compared to TN-C^{+/+} Ova treated controls. TN-C was also added exogenously to mouse splenocytes and induced significant IL-5, IL-13, IFN γ and IgE production (Nakahara et al. 2006). Despite this, it has yet to be directly investigated if TN-C is an inducer of inflammation in human bronchial epithelial cells and / or inflammatory cells in the airway of asthmatics, and which TN-C domains and receptors are involved.

Additionally, EVs (both exosomes and MVs) have been demonstrated to play a vital role in delivering inflammatory mediators to surrounding cells in the asthmatic airway. For example, IL-1 β is readily packaged and released via EVs (Qu et al. 2007, Lopez-Castejon and Brough 2011, Verderio et al. 2012), and has roles in the pathogenesis of asthma, inducing neutrophil and macrophage infiltration, airway remodelling and mucus production (Lappalainen et al. 2005). Exosomes from asthmatic patients have increased concentration of enzymes which are important in bronchoconstriction and mucus secretion, and stimulation of an AEC line with exosomes from asthmatic patients induced significant CXCL8 compared to exosomes from healthy controls. Other studies have demonstrated differences in the miRNA composition of exosomes between asthmatics and non-asthmatics, with miRNA found in asthmatic exosomes postulated to induce inflammatory cytokine release, leading to eosinophil migration and activation (Mazzeo et al. 2015). MVs have also recently been implicated in lung epithelial inflammation, most notably with AEC MVs isolated following hyperoxia damage inducing TNF α and IL-1 β in macrophages (Lee et al. 2016).

TN-C is a potent driver of inflammation, with the majority of the inflammatory potential demonstrated in the synovium of RA patients. The ability of TN-C to induce inflammation in the airway however, is an area that requires further research. Furthermore, the effects of EVs on the pathogenesis of asthma is a dynamic field, with it becoming clear that EVs, particularly exosomes, have an important role in potentiating airway inflammation in asthmatic patients. Investigation into the function of TN-C (with and without exosomes) will reveal to what extent TN-C and virally-induced exosomes play a role in RV-induced airway inflammation, and whether this could be a therapeutic target in the future.

5.2. Hypothesis

It was hypothesised that TN-C and virally induced exosomes have the ability to induce inflammatory cytokine and chemokine expression from AECs and MDMs. Furthermore, it was hypothesised that siRNA knockdown of TN-C in exosomes following poly(I:C) stimulation would reduce the inflammatory potential of these EVs.

The specific aims of this chapter were to investigate:

1. The effect of TN-C knockdown by siRNA on CXCL8 and CCL5 release following poly(I:C) stimulation and RV infection of AECs.
2. The ability of purified recombinant TN-C and FBG to induce inflammatory CXCL8 release from AECs and MDMs.
3. The ability of virally-induced exosomes to induce CXCL8, IL-6 and CCL5 release from AECs and MDMs.
4. The ability of virally-induced exosomes high and low in TN-C expression to induce CXCL8 release from AECs.

5.3. Knockdown of TN-C by siRNA Prior to Poly(I:C) Stimulation of AECs may Modulate the Inflammatory and Anti-Viral Response

5.3.1. No Significant Changes in CXCL8 and CCL5 Release were Observed in BEAS-2B Cells Following TN-C siRNA Knockdown and Poly(I:C) Stimulation

First, the efficacy of TN-C siRNA on TN-C expression and CXCL8 and CCL5 release prior to poly(I:C) stimulation in BEAS-2B cells was investigated. BEAS-2B cells were treated with either 100 nM TN-C siRNA, 100 nM scrambled siRNA, water (mock control) or Opti-Mem only (untransfected control) with lipofectamine for 24 hours. The cells were then left unstimulated or stimulated with poly(I:C) (25 µg/ml) for 48 hours. Cells were lysed and the protein lysate extracted and analysed for TN-C and β -actin by western blot. Cell free supernatant was also collected and TN-C release analysed by western blot, and CXCL8 and CCL5 release analysed by ELISA.

In BEAS-2B cells, TN-C siRNA reduced cell-associated TN-C and released TN-C by approximately 50% (not statistically significant; Figure 5.1A, 5.1B and 5.1C) in the media control and poly(I:C) treated cells. Whilst a trend of decreased CXCL8 release (Figure 5.1D) and increased CCL5 release (Figure 5.1E) was observed in the TN-C knockdown samples in response to poly(I:C) stimulation, this did not reach statistical significance, with further experimental repeats required to observe any potential differences..

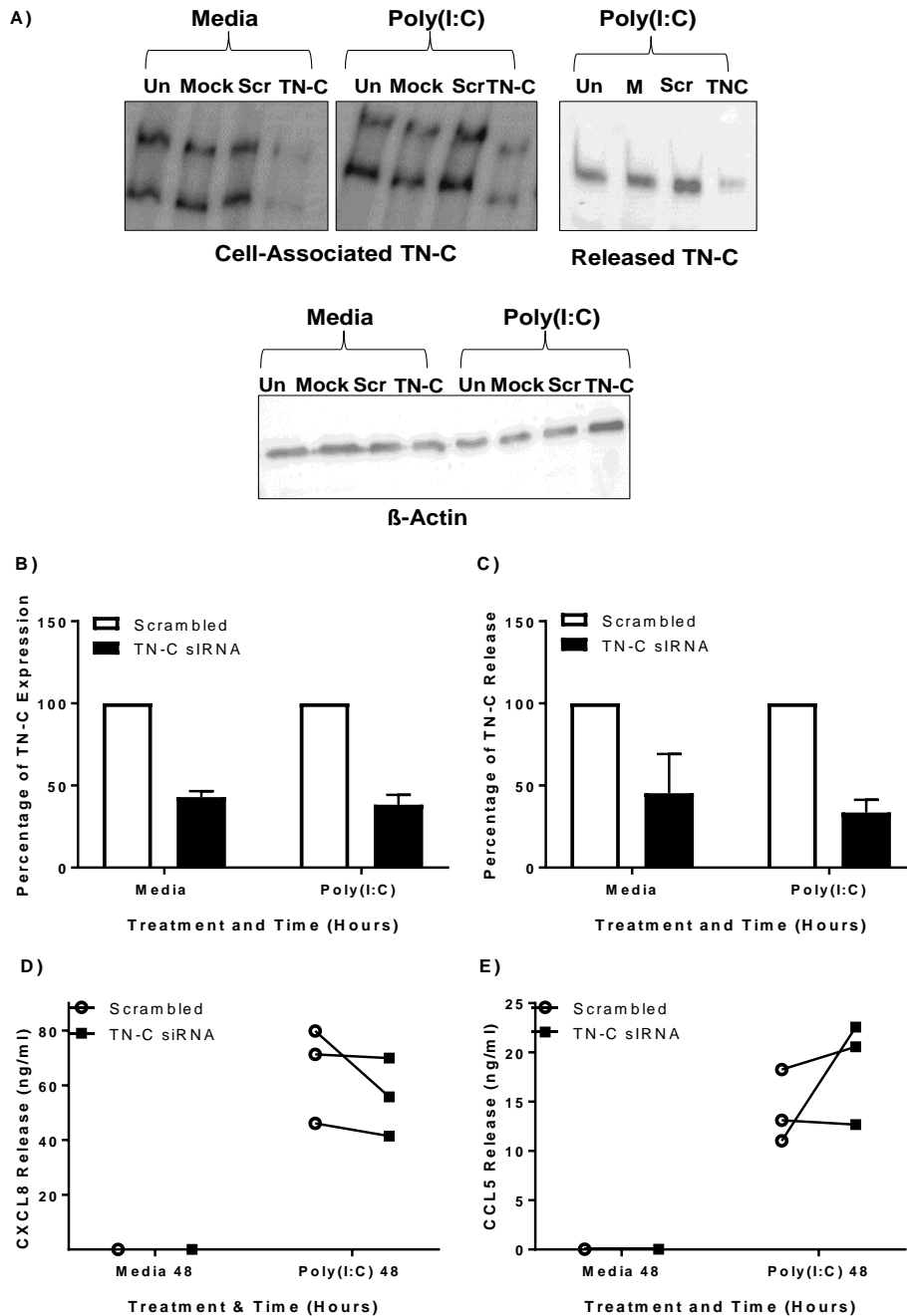


Figure 5.1. No Significant Changes in CXCL8 and CCL5 Release Occurred in BEAS-2B Cells Following TN-C siRNA Knockdown and Poly(I:C) Stimulation

BEAS-2B were pre-treated with 100 nM TN-C siRNA (TN-C), 100 nM scrambled siRNA (Scr), water (mock control; M) or Opti-mem (untransfected control; Un) with lipofectamine for 24 hours, and then stimulated with poly(I:C) (25 µg/ml) for 48 hours. **(A)** Cell lysate and supernatant samples were measured for cell-associated TN-C, released TN-C and β-actin expression via western blot (one representative blot shown). Densitometry of the top band of scrambled and TN-C siRNA was performed in ImageJ software with poly(I:C) cell associated TN-C normalised to β-actin control **(B)** and released TN-C **(C)**. Cell free supernatants were analysed for CXCL8 **(D)** and CCL5 **(E)** by ELISA. Values expressed as mean ± SEM (N=3) with each replicate representing an independent cell passage. Data analysed by determined using Repeated Measures Two-Way ANOVA with Tukey's post hoc test or paired T-test. Analysis was performed on absolute TN-C expression values.

5.3.2. Knockdown of TN-C by siRNA Prior to Poly(I:C) Stimulation of PBECs Successfully Reduced TN-C Expression, but the Knockdown of TN-C Prior to RV-1B Infection of PBECs was Unable to be Measured

The efficacy of TN-C siRNA on TN-C expression in PBECs was then investigated. PBECs were treated with either 100 nM TN-C siRNA, 100 nM scrambled siRNA, water (mock control) or Opti-Mem only (untransfected control) with lipofectamine for 24 hours. The cells were then left unstimulated or stimulated with poly(I:C) (25 µg/ml) or infected with RV-1B (MOI 1.5) for 24 and 48 hours. Cells were lysed and then the protein lysate was extracted and analysed for TN-C and β-actin by western blot. Cell free supernatant was also collected and TN-C release was analysed by western blot.

TN-C knockdown by TN-C siRNA was successful, with visible knockdown in cell-associated and released TN-C samples at both 24 and 48 hours post stimulation (48 hour western blot shown; Figure 5.2A). Furthermore, TN-C siRNA treatment reduced the expression of both the small and large splice variants. TN-C expression following TN-C siRNA treatment was reduced by approximately 65% and 75% ($p < 0.01$) in the unstimulated 24 and 48-hour cell-associated samples compared to scrambled siRNA (Figure 5.2B). Additionally, following poly(I:C) stimulation, TN-C siRNA reduced cell-associated TN-C expression by 65% and 75% at 24 and 48 hours respectively ($p < 0.01$). Released TN-C was also reduced by 90% ($p < 0.01$) and 80% at 24 and 48 hours respectively in response to poly(I:C) ($p < 0.05$; Figure 5.2C). Knockdown could not be measured in the unstimulated released cohort, as TN-C release was not visible.

Despite the fact that PBEC TN-C siRNA treatment successfully reduced intracellular TN-C in untreated cells and in cells infected with RV-1B, there was no visible TN-C release at 24 hours in 3 of the 5 donors. Of note, TN-C release is usually quantified by western blot at 48 hours (Figure 5.2D), and thus the knockdown of released TN-C could not be accurately quantified at the earlier timepoint of 24 hours. However, knockdown could not be accurately measured at 48 hours post RV-1B infection, as the combination of 24 hours siRNA treatment and 48 hours RV-1B infection induced cell cytotoxicity, resulting in inconsistent β-actin expression and the lack of measurable cell-associated and released TN-C expression (Figure 5.2E).

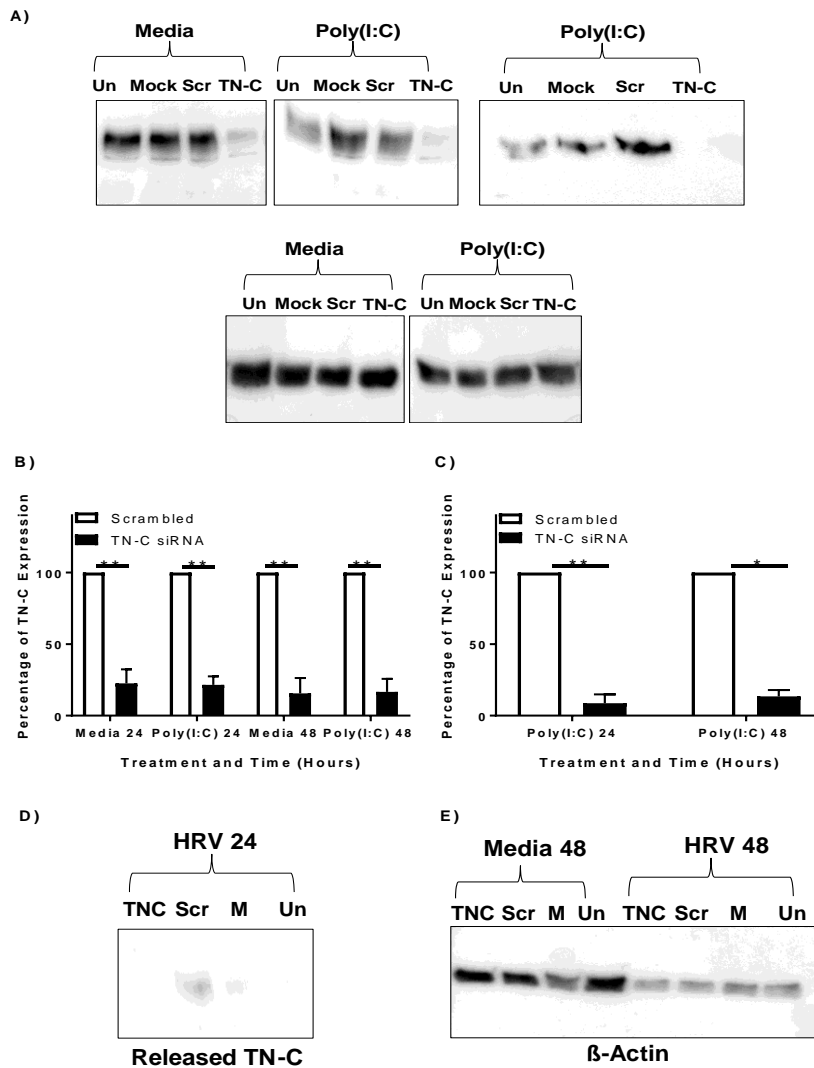


Figure 5.2. siRNA Knockdown of TN-C Reduced Cell-Associated TN-C Expression and TN-C Release in PBECS

PBECs were pre-treated with 100 nM TN-C siRNA (TN-C), 100 nM scrambled siRNA (Scr), water (mock control; M) or Opti-mem (untransfected control; Un) with lipofectamine for 24 hours, and then stimulated with poly(I:C) (25 µg/ml) or infected with RV-1B (MOI 1.5) for 24 and 48 hours. **(A)** Poly(I:C) cell lysate and supernatant samples were measured for cell-associated TN-C, released TN-C and β-actin expression via western blot (one 48 hour representative blot shown). Densitometry of the top band of scrambled and TN-C siRNA was performed in ImageJ software for poly(I:C) cell associated TN-C normalised to β-actin control **(B)** and released TN-C **(C)**. RV-1B 24 hours **(D)** and 48 hours **(E)** cell lysate and supernatant samples were measured for cell-associated TN-C, released TN-C and β-actin expression via western blot (one representative blot of the lack of TN-C release following RV-1B 24 hour infection and lack of consistent β-actin expression after 48 hours infection shown). Values expressed as mean ± SEM (N=5 for 24 hours and N=3 for 48 hours) with each replicate representing an independent PBEC donor. Significance differences in TN-C expression indicated by * p<0.05; ** p<0.01, determined using Repeated Measures Two-Way ANOVA with Tukey's post hoc test. Analysis was performed on absolute TN-C expression values.

5.3.3. Knockdown of TN-C by siRNA Prior to Poly(I:C) Stimulation of PBECs has No Impact on CXCL8 Release but may Modulate the Initial CCL5 Response

After successful knockdown of cell-associated TN-C expression and TN-C release, the next aim was to compare CXCL8 production in the TN-C siRNA samples and controls. Cell free supernatants (from the same experiment as Section 5.3.2) following siRNA transfection and poly(I:C) stimulation were prepared and analysed for CXCL8, CCL5, TNF α and IL-5 production by ELISA.

Although there was significant TN-C knockdown in response to siRNA transfection and poly(I:C) stimulation, there was no difference in CXCL8 (Figure 5.3A), CCL5 (Figure 5.3B), TNF α (Figure 5.3C) or IL-5 (Figure 5.3D) release at 24 or 48 hours post stimulation

5.4. Recombinant TN-C Induced CXCL8 Release from Primary Human MDMs

5.4.1. Recombinant Full-Length TN-C was Purified from HEK-293 Supernatant

In order to investigate the effects of TN-C on AECs and MDMs, the next aim was to purify active full-length recombinant TN-C to be used in the experiments. HEK-293 cells transfected with the pCEP-huTNChis plasmid (full-length TN-C, with all FNIII domains and a his-tag attached to the N-terminal; Lange et al. 2008) were obtained from University of Strasbourg. Recombinant full-length TN-C was then purified from HEK-293 supernatant by Ni²⁺-his-tag purification as per Section 2.15. The presence of TN-C following purification was confirmed by Coomassie staining, dialysed against TN-Tween (0.01%), aliquoted and stored at -80°C. Next, the presence of LPS was measured by a LAL test, CDS was used to determine whether the protein was folded, and the concentration of the purified TN-C was quantified by a BSA standard curve quantification assay. Finally, the samples that had been successfully purified, were folded, and were LPS free were analysed for the presence of TN-C and his-tag by western blot.

Purification and concentration of TN-C by Ni²⁺-his-tag purification was successful with six elution fractions containing TN-C, determined as the only visible band was above 250 kDa, (representative gel shown; Figure 5.4A). There was less than 10 pg/ml of LPS present in three of the six TN-C fractions as measured by LAL assay (Figure 5.4B), so these fractions were acceptable for use. The recombinant TN-C was folded correctly, which was also demonstrated through denaturation of the tertiary structure of the protein by boiling (Figure 5.4C). Quantification of the TN-C fractions revealed concentrations between 0.6 μ M and 1.0 μ M as measured by BSA standard curve (Figure 5.4D) and this concentration was confirmed by a BCA assay (data not shown). TN-C and his-tag expression were identified by western blot, confirming the specificity of the purification (Figure 5.4E).

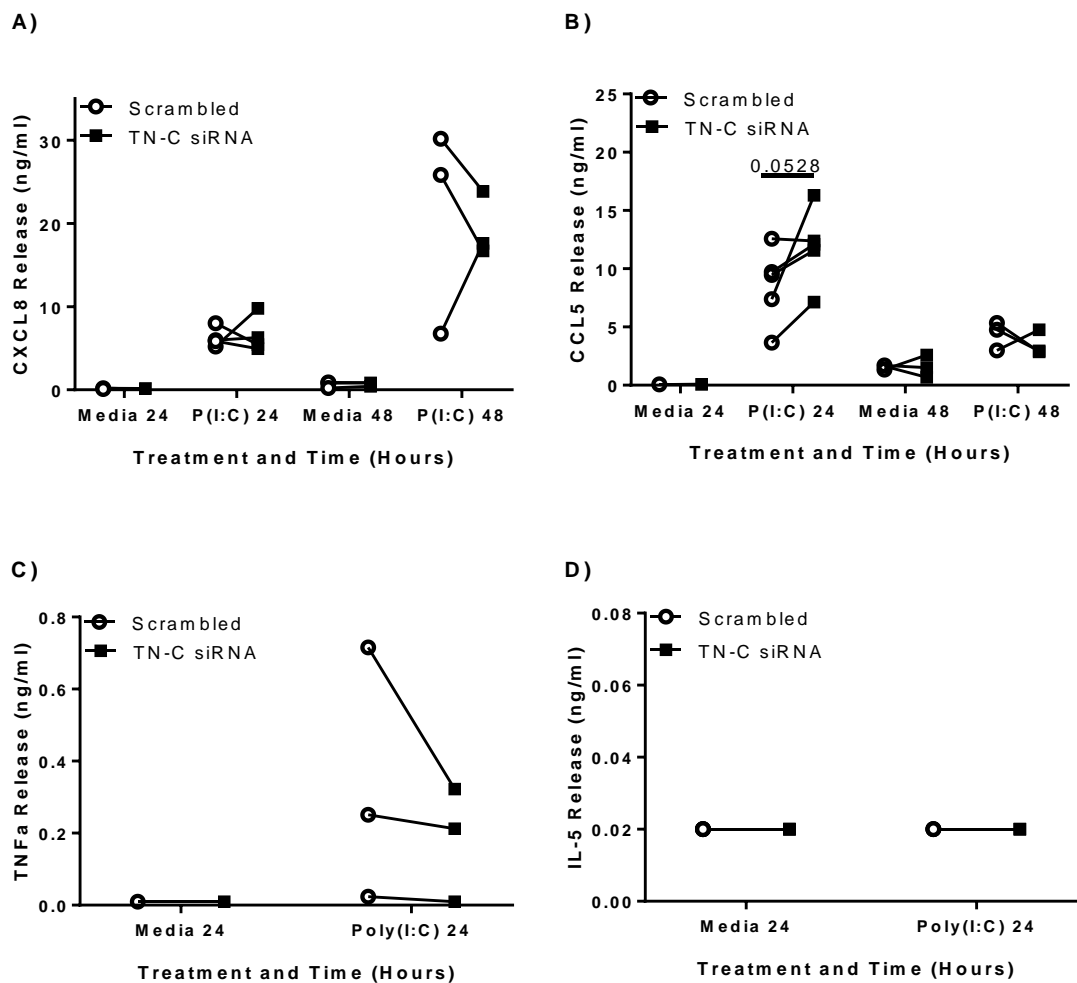


Figure 5.3. Knockdown of TN-C by siRNA Prior to Poly(I:C) Stimulation of PBECs did not Affect Inflammatory CXCL8 Release but may Modulate the Initial CCL5 Response

PBECs were pre-treated with 100 nM TN-C siRNA, 100 nM scrambled siRNA, water (mock control) or media only (untransfected control) with lipofectamine for 24 hours, and then stimulated with poly(I:C) (25 μ g/ml) for 24 and 48 hours. Cell free supernatants were prepared and analysed for 24 and 48 hour CXCL8 (A) and CCL5 (B) release by ELISA and 24 hour TNF α (C) and IL-5 release (D) release by cytometric bead array, with scrambled and TN-C siRNA values displayed. Values expressed as mean \pm SEM (N=3-5) with each replicate an individual PBEC donor. Significance determined using two-way ANOVA with repeated measures Tukey's post hoc test.

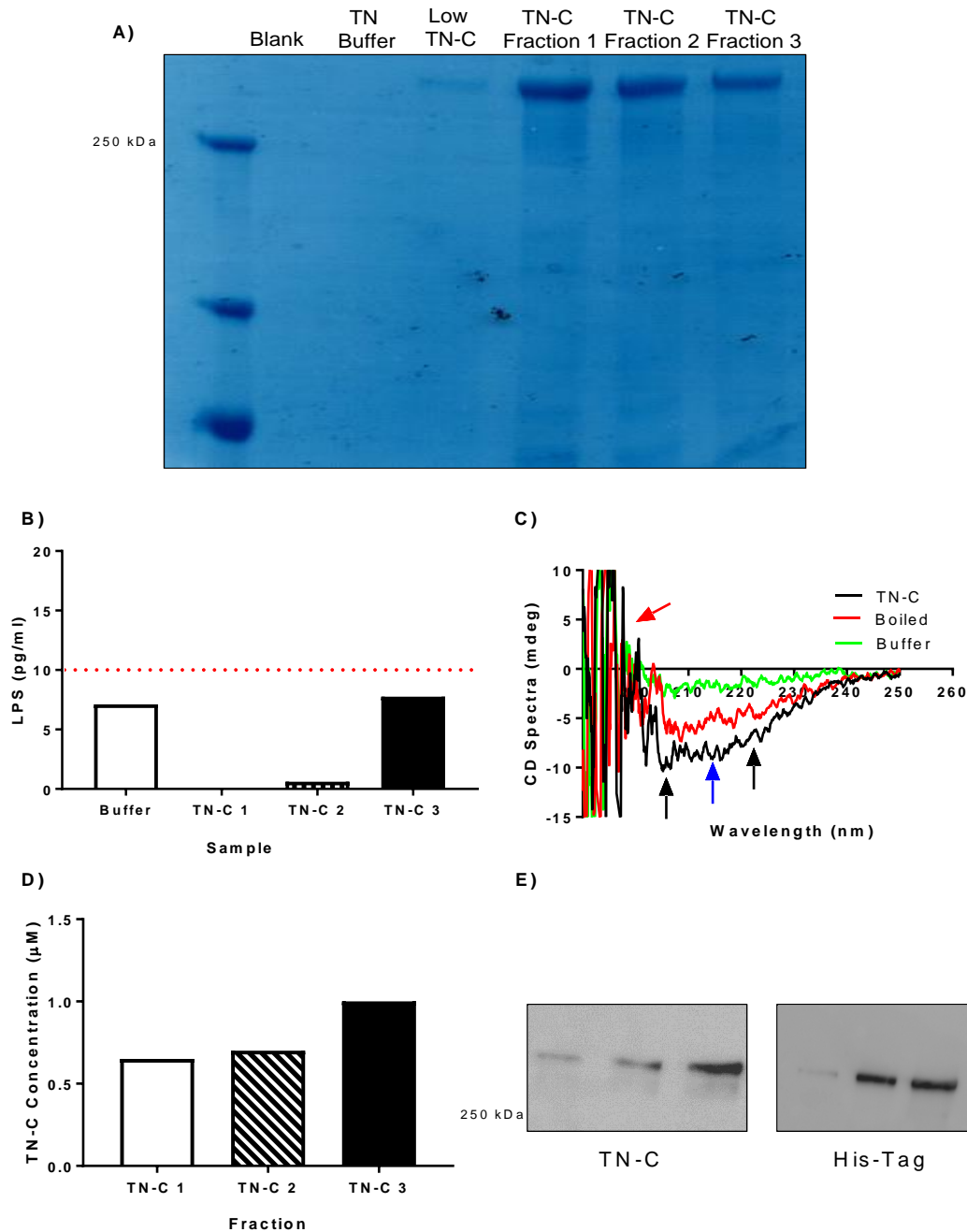


Figure 5.4. LPS-Free Full-Length Recombinant TN-C with His-tag was Purified, Concentrated and Quantified from HEK-293-pCEP-huTNChis Cells

(A) Full-length TN-C with his-tag was purified and concentrated from HEK-293-pCEP-huTNChis cells by Ni^{2+} -his-tag purification, and fractions were analysed for protein expression by Coomassie staining (representative gel shown). The presence of LPS was measured by an LAL test **(B)** and circular dichroism spectra was used to determine whether the protein was folded correctly **(C)**; representative graph shown). The negative peak at 195 nm (red arrow) indicates the random coil, the peaks at 208 nm and 220 nm (black arrow) indicates the alpha helix and the peak at 215 nm (blue arrow) indicates the beta sheet of the protein. TN-C expression was quantified by a Coomassie stain BSA standard curve **(D)** and TN-C fractions were analysed for TN-C and his-tag expression by western blot **(E)**. Data displayed as individual TN-C fractions (N=3).

5.4.2. Recombinant Full-Length TN-C, Recombinant FBG-TN-C and LPS Induce CXCL8 Release from MDMs

Following the purification of LPS-free full-length TN-C, next, the ability of the protein to induce inflammatory CXCL8 release from MDMs was investigated. Primary human MDMs were left unstimulated or stimulated with smooth LPS strain 0111:B4 (0.1 µg/ml), 0.1 µM recombinant full-length TN-C or 1 µM purified recombinant TN-C FBG domain (donated by Anja Schwenzer, University of Oxford; Section 2.14.6) for 24 hours. The concentrations of TN-C, FBG and LPS used were chosen due to previous work in our lab (Midwood et al. 2009, Schwenzer et al 2016, Zuliani-Alvarez et al. 2017). Supernatant was then collected and analysed for CXCL8 by ELISA.

Recombinant full-length TN-C and FBG-TN-C stimulation of MDMs induced significant CXCL8 release at 24 hours compared to the unstimulated media control ($p < 0.05$ and $p < 0.01$ respectively; Figure 5.5). The amount of CXCL8 induced was comparable to that induced by LPS, which also induced significant release compared to the media control ($p < 0.05$).

5.5. LPS and Recombinant TN-C-FBG Induced Moderate CXCL8 Release from BEAS-2B Cells

5.5.1. Smooth (but not Rough) LPS Induce CXCL8 Release from BEAS-2B Cells

Prior to AEC stimulation with purified recombinant TN-C and TN-C-FBG, it was first important to determine whether BEAS-2B cells could respond to TLR4 stimulation (the main inflammatory pathway induced by TN-C through FBG), with evidence currently unclear as to whether AECs can respond to LPS (Zanini et al. 2010, Stokes et al. 2011). BEAS-2B cells were left unstimulated or stimulated with 0.1 or 10 µg/ml LPS EH100 (rough strain) or LPS 0111:B4 (smooth strain), with and without 1 µg/ml PMB (an LPS inhibitor) for 24 hours. Supernatant was then collected and analysed for CXCL8 expression by ELISA.

Smooth LPS 0111:B4 induced CXCL8 expression at 24 hours, with both concentrations inducing significant release ($p < 0.0001$; Figure 5.6A). Furthermore, PMB significantly reduced CXCL8 release induced by smooth LPS ($p < 0.0001$). Notably, rough LPS did not induce CXCL8 release at either concentration and smooth LPS did not induce CCL5 release in BEAS-2B cells (Figure 5.6B).

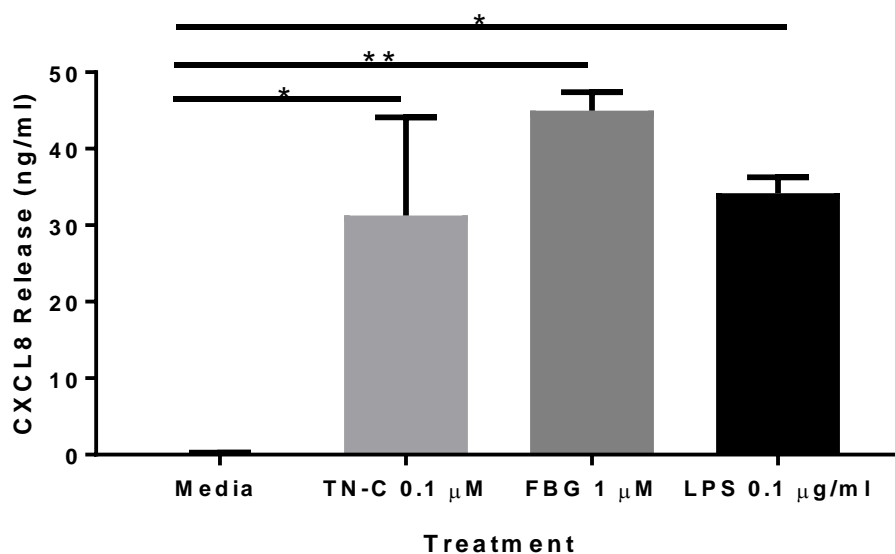


Figure 5.5. Recombinant Full-Length TN-C and Recombinant FBG-TN-C Stimulation of Primary Human MDMs Induces CXCL8 Expression

Primary human MDMs were treated with recombinant full-length TN-C (0.1 μ M), recombinant FBG-TN-C (1 μ M) or smooth LPS strain 0111:B4 (0.1 μ g/ml) for 24 hours and cell free supernatants collected and analysed for CXCL8 by ELISA. Values expressed as mean \pm SEM (N=3) with each replicate an independent MDM donor. Significance differences in CXCL8 release indicated by * $p < 0.05$; ** $p < 0.01$, analysed by one way ANOVA with Dunnett's post hoc test.

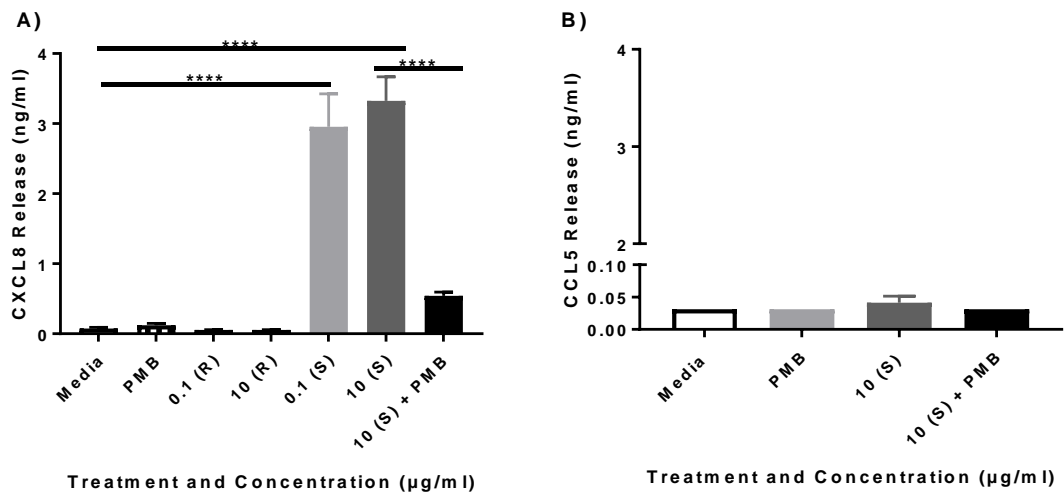


Figure 5.6. Smooth LPS Stimulation of BEAS-2B Cells Induces CXCL8 Release

BEAS-2B cells were treated with Rough (R) LPS strain EH100 and Smooth (S) strain 0111:B4 (0.1 and 10 µg/ml), with or without PMB LPS inhibitor (1 µg/ml) for 24 hours. Cell-free supernatants were prepared and levels of CXCL8 (A) and CCL5 (B) measured by ELISA. Data shown are mean ± SEM, with each replicate representing a separate cell passage (N=3). Significant differences in CXCL8 production are indicated by **** p<0.0001, analysed by one way ANOVA with Tukey's post hoc test.

5.5.2. Recombinant FBG-TN-C Induces Moderate CXCL8 Release from BEAS-2B Cells

Next, BEAS-2B cells were left unstimulated or stimulated with 0.1 μM of recombinant TN-C or 1-2 μM of purified recombinant FBG domain for 24 hours, and supernatant was collected and analysed for CXCL8, IL-6 and TNF α by ELISA.

Recombinant TN-C stimulation of BEAS-2B cells did not induce CXCL8 release (Figure 5.7A), however FBG stimulation induced statistically significant, but moderate, CXCL8 expression at 2 μM ($p < 0.05$; Figure 5.7B). IL-6 (Figure 5.7C) or TNF α (Figure 5.7D) was not induced at any of the concentrations used.

5.6. Exosomes from Virally Stimulated BEAS-2B Cells Induces Inflammatory Cytokine and Chemokine Release from BEAS-2B Cells

Next, the ability of virally-induced exosomes to induce cytokine and chemokine release from BEAS-2B cells and MDMs was measured. BEAS-2B cells were grown to confluence in EV-Depleted Basal Media and left unstimulated or stimulated with 25 $\mu\text{g/ml}$ poly(I:C) for 72 hours. Exosomes were then isolated using the four spin ultracentrifugation isolation method described in Figure 2.2. Following isolation, exosome concentration was calculated by NTA and added to new BEAS-2B cells or MDMs at 10,000 and 20,000 exosomes per μl . Cell free supernatants were collected at 24 hours post stimulation and analysed for CXCL8, IL-6 and CCL5 by ELISA. A zero hour poly(I:C) stimulated control was also included to determine whether poly(I:C) was carried over into the exosome fraction during isolation. To generate this, supernatant was collected and exosomes isolated immediately after BEAS-2B poly(I:C) stimulation.

In BEAS-2B cells, significant CXCL8 was released in response to exosomes from poly(I:C) stimulated cells at 10,000 and 20,000 exosomes per μl ($p < 0.01$ and $p < 0.001$ respectively; Figure 5.8A). Of note, the zero hour poly(I:C) control did not induce any CXCL8 release in BEAS-2B cells. Furthermore, exosomes isolated from poly(I:C) stimulated cells induced significantly more IL-6 release than exosomes isolated from unstimulated media control cells, with significant induction observed at 20,000 exosomes per μl ($p < 0.05$; Figure 5.8B). Significant CCL5 release was also induced in response to poly(I:C) derived exosomes at 20,000 exosomes per μl ($p < 0.01$; Figure 5.8C). Interestingly, in MDMs, exosomes isolated from both the unstimulated media and poly(I:C) stimulated BEAS-2B cells induced CXCL8 release, and although the amount of CXCL8 release induced by poly(I:C)-derived exosomes was higher than the media control equivalents, this was not statistically significant (Figure 5.8D). The amount of CXCL8 induced by the media control and poly(I:C) exosomes at 20,000 per μl was significantly greater than the CXCL8 at media (basal) levels ($p < 0.05$ and $p < 0.01$ respectively).

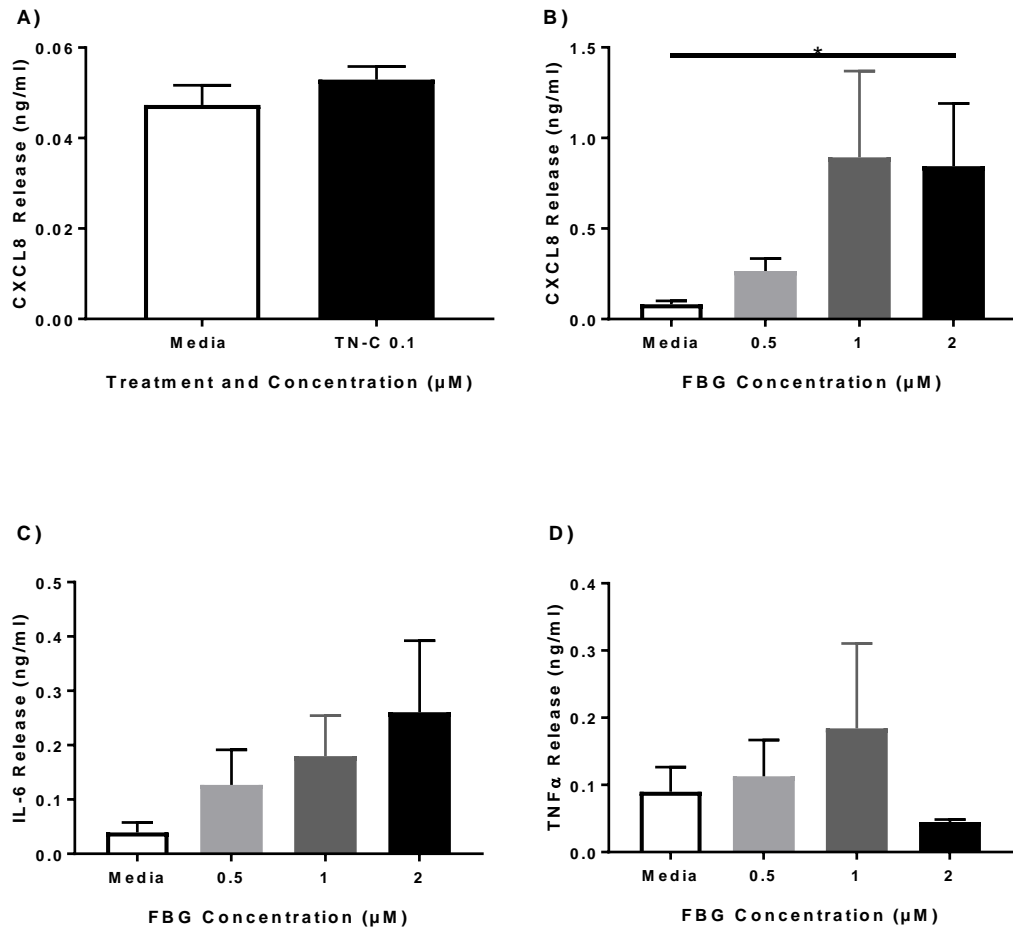


Figure 5.7. Recombinant FBG-TN-C Stimulation of BEAS-2B Cells Induces CXCL8 Release

BEAS-2B cells were stimulated with purified recombinant full-length TN-C and levels of CXCL8 were assayed by ELISA (A) and BEAS-2B were also stimulated with recombinant FBG-TN-C and CXCL8 (B), IL-6 (C) and TNFα (D) were analysed by ELISA. Data shown are mean ± SEM, with each replicate representing a separate cell passage (N=3). Significant differences in cytokine / chemokine production are indicated by * p<0.05, analysed by one way ANOVA with Tukey's post hoc test.

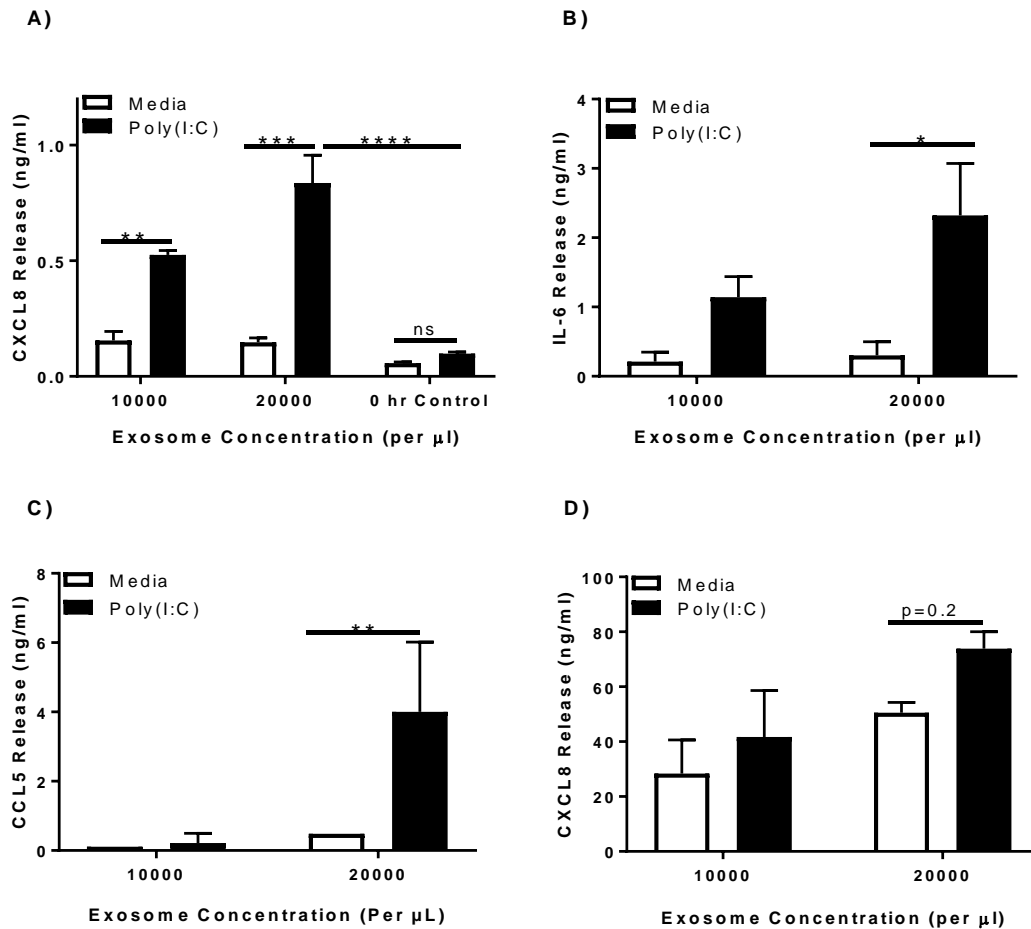


Figure 5.8. Exosomes Isolated from Virally-Stimulated BEAS-2B Cells Induce BEAS-2B Cell Cytokine and Chemokine Release

BEAS-2B cells were grown to confluence in exosome-depleted media, and stimulated with poly(I:C) (25 μg/ml) for 72 hours. Exosomes were then isolated by the four spin purification method, re-suspended in 100 μl PBS and concentration measured by NTA. Exosomes were added to fresh BEAS-2B cells at the designated concentrations and cell free supernatants were collected at 24 hours. CXCL8 with a zero hour poly(I:C) control (**A**), IL-6 (**B**) and CCL5 (**C**) were measured by ELISA. MDMs were stimulated with BEAS-2B derived exosomes and CXCL8 measured by ELISA (**D**). Values expressed as mean ± SEM (N=3) with each replicate a different cell passage or MDM donor, analysed by two way ANOVA with Tukey's post hoc test.

5.7. TN-C Induces a Greater Fold-Induction of CXCL8 Release from MDMs, Whilst Exosomes Induce Greater CXCL8 Release from BEAS-2B Cells

As MDMs are an immune cell, they invariably release greater amounts of cytokines and chemokines than AECs. Therefore, in order to determine and compare the relative potency of TN-C and exosomes in these two cell types, the fold increase of CXCL8 induced was calculated. To do this, CXCL8 release values obtained in the LPS stimulation experiments (Figure 5.5 and 5.6), TN-C and FBG stimulation experiments (Figure 5.5 and 5.7) and exosome stimulation experiments (5.8) were converted into CXCL8 fold change induction.

LPS (Figure 5.9A), full-length TN-C (Figure 5.9B) and TN-C-FBG (Figure 5.9C) all induced a greater fold induction of CXCL8 release from MDMs (approximately 350-500 fold) compared to BEAS-2B cells (approximately 10-40 fold). In response to poly(I:C) stimulated BEAS-2B derived exosomes (20,000 per μL) stimulation, the fold increase of CXCL8 release from BEAS-2Bs was significantly greater than from MDMs, with a 6 fold increase compared to a 2 fold increase ($p < 0.01$; Figure 5.9D).

5.8. TN-C Knockdown in BEAS-2B Isolated Exosomes did not Affect Exosome-Induced CXCL8 Release from AECs

5.8.1. Knockdown of TN-C in BEAS-2B Exosomes Was Successful Following Poly(I:C) Stimulation

To investigate whether TN-C has a role in virally-stimulated exosome-induced inflammation, first, TN-C expression was knocked down in BEAS-2B exosomes by siRNA treatment. BEAS-2B cells were grown in EV-depleted media and treated with either 100 nM TN-C siRNA, 100 nM scrambled siRNA, or a mock water control with lipofectamine for 24 hours. The cells were then left unstimulated or stimulated with poly(I:C) (25 $\mu\text{g}/\text{ml}$) for 72 hours and exosomes were isolated as per Figure 2.2. Cell-associated TN-C expression, TN-C release in the supernatant, exosome-associated TN-C expression and β -actin expression was then measured by western blotting.

TN-C expression was detectable in the cell-associated samples, cell supernatant samples and exosome isolated fractions, with consistent cell associated β -actin expression also present (Figure 5.10A). Significant TN-C knockdown occurred in response to TN-C siRNA treatment in the cell-associated (normalised to β -actin; $p < 0.05$; Figure 5.10B), released TN-C ($p < 0.001$; Figure 5.10C) and exosome-associated ($p < 0.001$; Figure 5.10D) poly(I:C) samples compared to the scrambled control, as determined using densitometrical analysis.

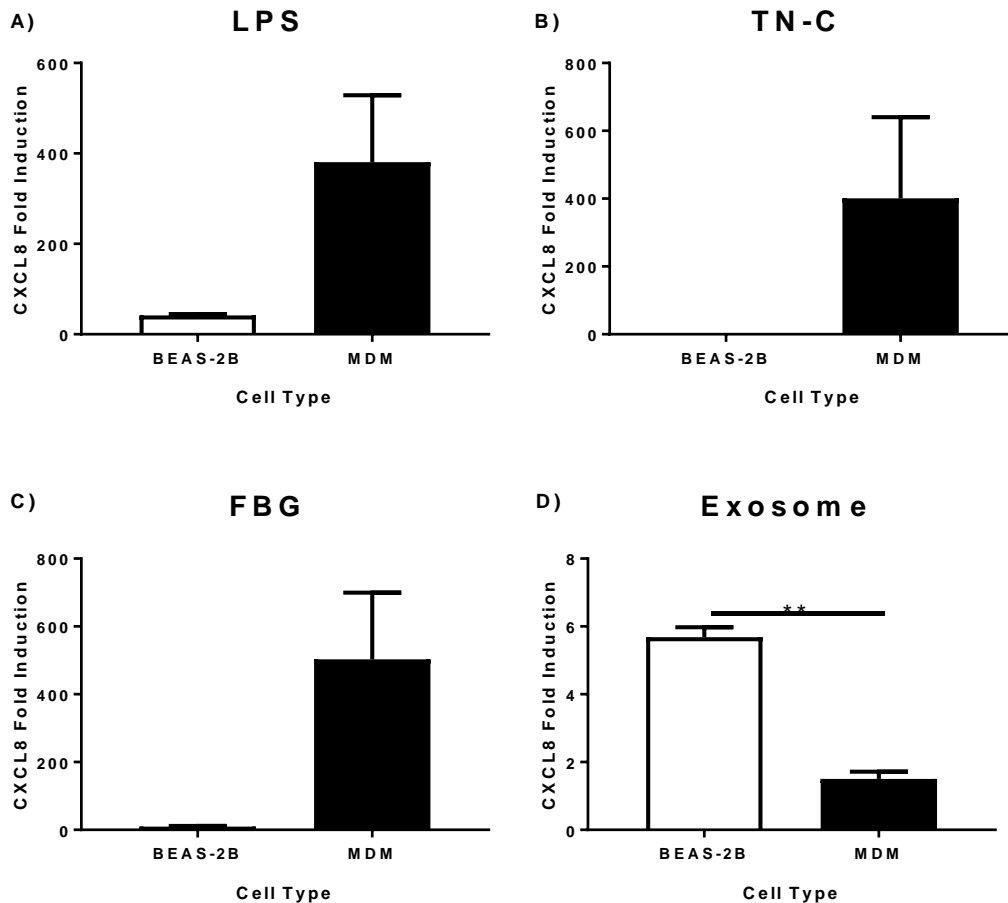


Figure 5.9. LPS, TN-C and TN-C-FBG Induce Greater CXCL8 Release from Primary Human MDMs, Whilst Poly(I:C) Stimulated BEAS-2B Derived Exosomes Induce Greater CXCL8 Release from BEAS-2B Cells

The results of the BEAS-2B and MDM stimulation CXCL8 experiments were converted to fold change in order to directly compare between the two cell types. The experiments compared were: LPS BEAS-2B and MDM stimulations (Figure 5.6A and 5.5; **A**), full-length TN-C BEAS-2B and MDM stimulations (Figure 5.7A and 5.5; **B**), FBG-TN-C BEAS-2B and MDM stimulations (Figure 5.7B and 5.5; **C**) and poly(I:C) derived AEC exosomes BEAS-2B and MDM stimulations (Figure 5.8A and 5.8D; **D**). Values expressed as mean \pm SEM (N=3) with each replicate representing a separate cell passage or independent MDM donor. Significance differences in CXCL8 release indicated by ** p<0.01, analysed using paired T-test.

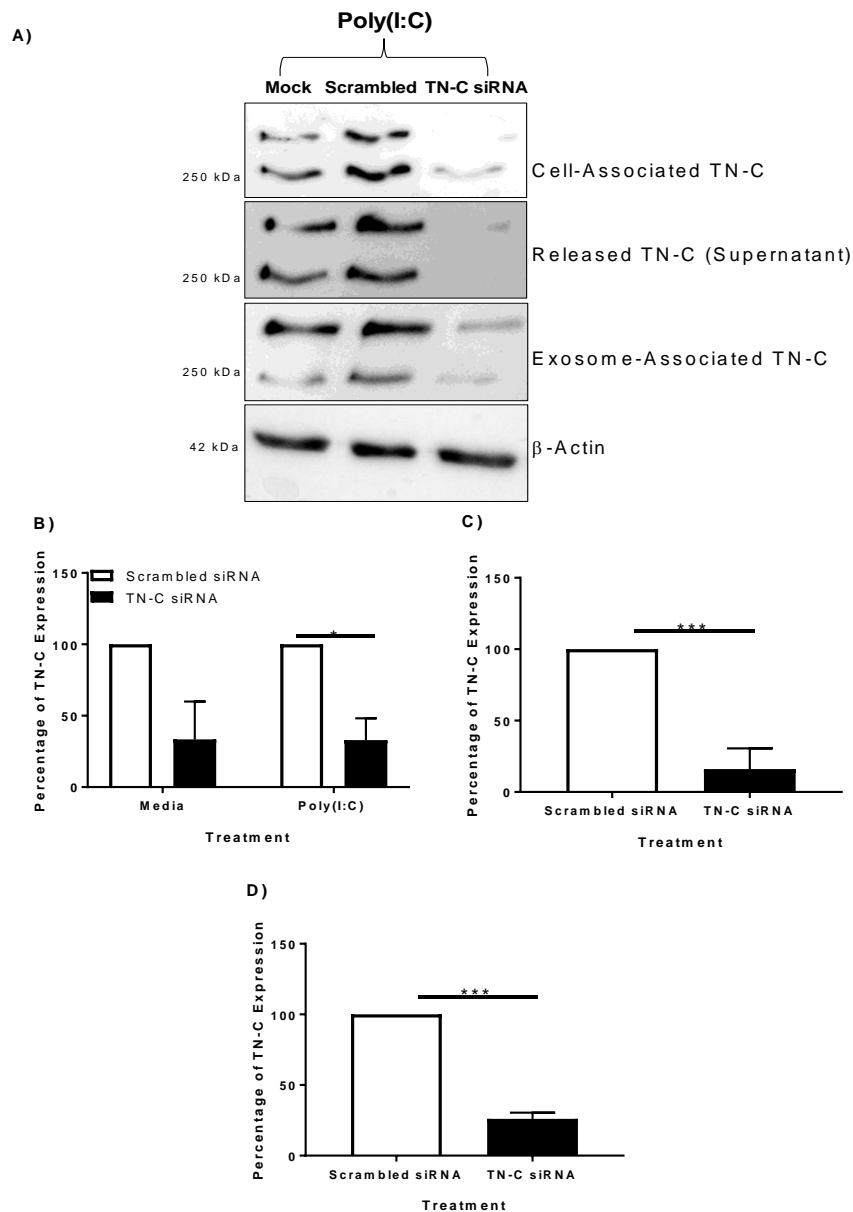


Figure 5.10. siRNA Knockdown of TN-C Reduced Cell-Associated TN-C Expression, TN-C Release and Exosome-Associated TN-C in BEAS-2B Cells Following Poly(I:C) Stimulation

BEAS-2B were pre-treated with 100 nM TN-C siRNA, 100 nM scrambled siRNA or water (mock control) with lipofectamine for 24 hours, and then stimulated with poly(I:C) (25 µg/ml) for 72 hours. **(A)** Cell lysate, supernatant samples and EVs were measured for cell-associated TN-C, released TN-C, EV-associated TN-C and β -actin expression via western blot (one representative blot for each shown). Densitometry of the top band of scrambled and TN-C siRNA was performed in ImageJ software with poly(I:C) cell associated TN-C normalised to β -actin control **(B)**, released TN-C **(C)** and EV-associated TN-C **(D)**. Values expressed as mean \pm SEM (N=3) with each replicate representing a separate cell passage. Significance differences in TN-C expression indicated by * $p < 0.05$; *** $p < 0.001$, determined using Two-Way ANOVA with Tukey's post hoc test. Analysis was performed on absolute TN-C expression values.

5.8.2. TN-C Knockdown did not Impact Exosome-Induced CXCL8 Release from AECs

Finally, the BEAS-2B poly(I:C) derived exosomes isolated in Section 5.7.1. that were low in TN-C expression (TN-C siRNA treated) or high in TN-C expression (scrambled siRNA treated), were added to separate BEAS-2B cells at approximately 10,000 and 20,000 exosomes per μ l for 24 hours. For this experiment, exosome concentration could not be calculated due to technical problems with the ZetaView NTA machine and thus exosome concentration was estimated based on previous calculations. Cell free supernatants were collected and analysed for CXCL8 and CCL5 by ELISA.

In response to poly(I:C), CXCL8 release was significantly increased at 24 hours ($p < 0.05$; Figure 5.11A). There was no significant difference between the amount of CXCL8 release induced by TN-C siRNA treated and scrambled siRNA treated exosomes at both 10,000 and 20,000 exosomes per μ l. Furthermore, there was no difference between the amount of CCL5 release induced by TN-C siRNA and scrambled siRNA treated exosomes at both concentrations (Figure 5.11B).

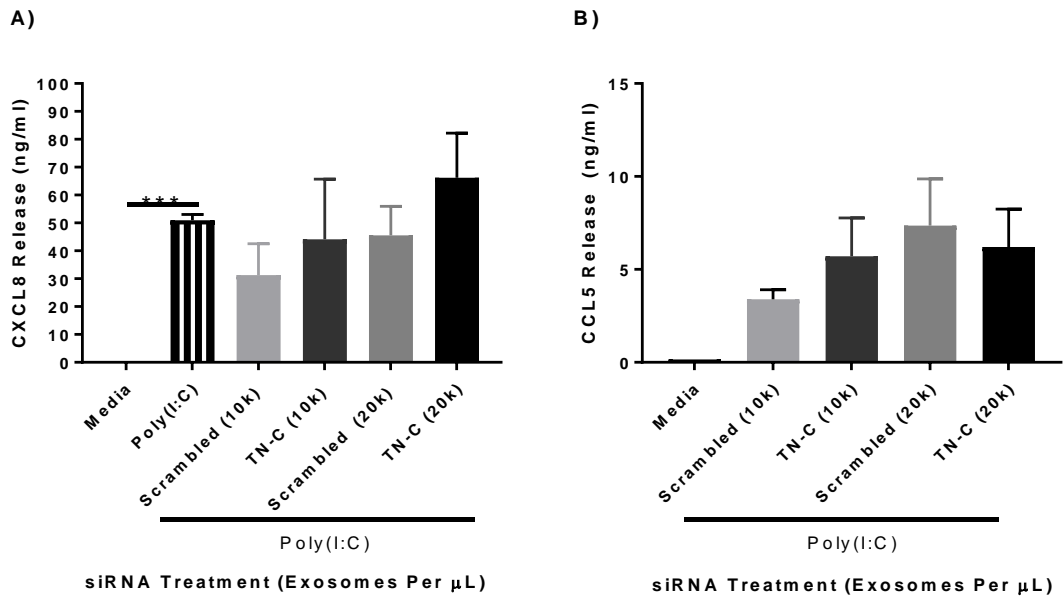


Figure 5.11. TN-C Knockdown did not Impact on Exosome-Induced BEAS-2B Cell CXCL8 and CCL5 Release

BEAS-2B were pre-treated with 100 nM TN-C siRNA or 100 nM scrambled siRNA for 24 hours, and then stimulated with poly(I:C) (25 $\mu\text{g/ml}$) for 72 hours. Exosomes were next isolated by the four-step ultracentrifugation method and TN-C expression was determined by western blotting. Fresh BEAS-2B cells were next stimulated with poly(I:C) (25 $\mu\text{g/ml}$), poly(I:C) BEAS-2B-derived TN-C siRNA treated exosomes or poly(I:C) BEAS-2B-derived scrambled siRNA treated exosomes for 24 hours. Cell free supernatants were collected and analysed for CXCL8 (**A**) and CCL5 (**B**) release by ELISA. Values expressed as mean \pm SEM (N=3) with each replicate representing a separate cell passage stimulated with a separate exosome population. Significance differences in chemokine expression indicated by *** $p < 0.001$, determined using One-Way ANOVA with Dunnett's post hoc test.

5.9. Summary and Discussion

5.9.1. Summary

The results in this chapter revealed that AECs can respond to a smooth LPS strain, but not to a rough LPS strain. This establishes the ability of the AECs used in this study to respond to TLR4 stimulation, and revealing one potential reason why contradictory evidence regarding the ability of AECs to respond to LPS currently exists. Data was also generated that correlated with previous work in the Midwood group (and wider afield), with purified recombinant TN-C and TN-C-FBG having the ability to induce CXCL8 release from MDMs. The findings also revealed that FBG-TN-C had the ability to induce moderate CXCL8 release from AECs, with this theorised to occur through the TLR4 receptor. Furthermore, the results in this chapter also confirm for the first time the ability of virally stimulated BEAS-2B cell-derived exosomes to induce specific release of inflammatory cytokines and chemokines from BEAS-2B cells and MDMs. The role of TN-C in this exosome-induced cytokine / chemokine release is yet to be fully elucidated, with initial siRNA knockdown results showing that TN-C was not required for exosomes to induce inflammatory responses.

5.9.2. TN-C Induces Inflammatory CXCL8 Release from MDMs

In response to stimulation of MDMs with purified full-length-recombinant TN-C (0.1 μM) and purified TN-C FBG (1 μM), a significant release of CXCL8 occurred (Figure 5.5). Furthermore, the fold upregulation of CXCL8 was approximately 375 and 400 fold respectively (Figure 5.9B and C). Notably, the total amount and fold upregulation of CXCL8 induced by TN-C and TN-C-FBG was equivalent to that induced by LPS (Figure 5.5 and 5.9A) – a potent inductor of TLR4 inflammation in MDMs. The TN-C used for stimulation was demonstrated to be pure, folded and LPS free (Figure 5.4).

The results in Figure 5.5. correlate closely with a number of studies demonstrating the inflammatory effect of TN-C on macrophages. Stimulation of primary human macrophages with 1 μM of FBG, for example, induced a 200 fold increase in CXCL8 expression (Midwood et al. 2009). In this study, full-length TN-C and TN-C-FBG also induced significant amounts of TNF α and IL-6 from primary human macrophages and synovial fibroblasts, mediated through the FBG domain of TN-C. Furthermore, in another study, stimulation of primary human macrophages with 1 μM of TN-C-FBG induced 500 ng/ml of CXCL8 release (Zuliani-Alvarez et al. 2017), revealing TN-C may have an even greater inflammatory effect on macrophages than demonstrated in this thesis. The induction of CXCL8 in response to TN-C in this thesis also correlates with the association of high TN-C expression and enhanced CXCL8 in the synovia of RA patients (Page et al. 2012).

TN-C induces a potent inflammatory effect on MDMs, which has important implications as macrophage recruitment to the airway is increased in RV infection and allergic airway

inflammation. Human lung macrophages (HLM) are one of the most prominent cells isolated in BALF, and lavage of specific airway sections has determined the large presence of macrophages in the alveoli and the wider airway (Hamid et al. 2003). HLMs are further recruited following respiratory viral infections, including RV (Laza-Stanca et al. 2006), RSV (Goritzka et al. 2015) and influenza (Duan, Hibbs and Chen 2017). The recruitment of these cells can produce anti-viral IFN (Goritzka et al. 2015) and inflammatory cytokine release such as TNF α (Duan et al. 2017), to aid the removal of the pathogen and resolution of the infection. It is also established that RV is able to infect these macrophages and replicate, inducing further TNF α release (Laza-Stanca et al. 2006). Furthermore, allergic airway inflammation in asthma, independent of viral infection, recruits HLMs to the airway (Lumeng 2016), and HLMs from asthmatic patients have been determined to have enhanced IgE Fc receptor expression, leading to increased cytokine release and phagocytosis (Melewick et al. 1982). Macrophages in asthma may also skew towards an M2 phenotype, which produces IL-4, IL-10 and IL-13 to induce airway inflammation, wound healing and remodelling (Lee et al. 2015).

It must also be noted that whilst human MDMs are a good model to study the effects of TN-C on airway inflammation, and airway macrophages (including alveolar and lung) are derived from monocytes (Misharin et al. 2017), differential responses between HLMs and MDMs do occur. These differences are important as they suggest that TN-C may have an even greater inflammatory effect on HLMs, with LPS inducing significantly more TNF α , IL-6 and IL-1 β release from this macrophage subset compared to MDMs (Victoni et al. 2017). This, therefore, indicates HLMs may have a more pronounced response to TLR4-induced inflammation. Furthermore, HLMs do not express β_2 adrenergic receptors and so do not respond to two forms of asthma treatment, formoterol or salmeterol (Victoni et al. 2017), whilst MDMs do, further demonstrating that HLMs are more resistant to suppression of inflammatory cytokine release.

TN-C has the ability to induce CXCL8, IL-6 and TNF α from MDMs, all which play important roles in viral infection, airway inflammation and asthma pathogenesis. CXCL8 is a neutrophil and mast cell chemoattractant, which is vital for the immune response to viral infection. CXCL8 is also increased in the airway and BALF of asthmatics, and can promote angiogenesis, important in airway remodelling and the degeneration in lung function (Ordonez et al. 2000, John et al. 2009, Tang et al. 2016). Mast cells play a vital role in IgE dependent inflammation during allergic asthma (Reuter, Stassen and Taube 2010), whilst neutrophils are increased in the airway of asthmatics and correlate with asthma exacerbations (Fahy et al. 1995, John et al. 2009). Neutrophils release a large number of cytokines and chemokines, including CXCL8, IL-6 and IL-9 (which is vital for the regulation of Th2 cells and integral in the pathogenesis of asthma), as well as TNF α , IFN γ and TGF- β , which among other things, are transcriptional regulators of TN-C (Foley and Hamid 2007). IL-6 has been demonstrated to be vital for the immune clearance of respiratory viruses (Yang et al. 2017) and is significantly higher in the serum of asthmatics compared to non-asthmatics (Yokoyama et al. 1995, Yokoyama et al. 1997). IL-6 also induces MAPK signalling through the C/EBP arm of the

pathway (Figure 1.5.) leading to further inflammatory cytokine release (Rincon and Irvin 2012) and correlates inversely with lung function, as measured by forced expiratory volume (FEV₁; Morjaria et al. 2011). Meanwhile TNF α has been demonstrated to potentiate RV infection, (Berg, Andersen and Owen 2004), is increased in asthmatics (Bradding et al. 1994), is a chemoattractant for other inflammatory cells and induces inflammatory cytokine release (Berry et al. 2007). Additionally, TNF α also plays a role in AHR induction through LT release in airway smooth muscle (Menard and Bissonnette 2000), induces further ICAM-1 expression for RV infection (Krunbosky et al. 2000) and is a transcriptional regulator for further TN-C expression (Nakamura et al. 2004).

Whilst the ability of the purified recombinant TN-C and TN-C FBG to induce CXCL8 release from MDMs has previously been demonstrated, the findings of this thesis are important for two reasons. First, the results confirmed the activity of the purified full-length TN-C and TN-C-FBG used in this work, which was important for the subsequent studies of BEAS-2B stimulation. Secondly, these results demonstrate the large inflammatory effect that TN-C has on MDMs (with the molecule as potent an inducer as LPS), and it can be theorised that this inflammation will be heightened in an asthmatic setting, with the increased concentration of macrophages and the skew towards an inflammatory macrophage phenotype, in RV infection and asthma. This implicates RV-induced TN-C release and subsequent TN-C-induced MDM inflammation in RV-induced asthma exacerbations.

5.9.3. AECs Have the Ability to Respond to Smooth-LPS Stimulation

Following LPS stimulation, BEAS-2B cells produced a statistically significant CXCL8 response to smooth LPS serotype 0111:B4 (0.1 and 10 μ g/ml), but did not respond to rough LPS strain EH100 at the same concentrations (Figure 5.6A.). CXCL8 upregulation in response to LPS 0111:B4 stimulation was approximately 30 fold (Figure 5.9A); but in contrast smooth LPS stimulation did not induce CCL5 release (Figure 5.6B).

LPS stimulation of BEAS-2B cells was used to investigate the ability of these cells to respond to TLR4 inflammation, due to contradictory evidence in previous studies. Smooth LPS is made up of three main parts: lipid A, rough core oligosaccharide and the O-antigenic side chain, whilst rough LPS lacks this side chain (Zanini et al. 2010). Other cell types have also been established to have differential responses to different strains of LPS. For example, in mouse dendritic cells, smooth LPS required the CD14 co-receptor for stimulation at a low concentration (0.01 μ g/ml) and could induce an inflammatory response independent of CD14 at 0.1 μ g/ml. Moreover, rough LPS was able to induce cytokine release at even low concentrations independent of CD14 (Zanini et al. 2010). These responses differed from the AEC responses in this thesis, indicating cell-specific responses to LPS strains, potentially due to differing expression of TLR4 and TLR4 co-receptors. The BEAS-2B response to (low concentration) smooth LPS has previously been determined to be dependent on CD14, and the response to LPS was greater in A549 cells (Schulz et al. 2002), and so the results in this thesis suggest that this dependence on CD14 can

potentially be overcome with an increased concentration of smooth LPS. In a separate study, it was determined that monocytes (which express CD14) were required in a co-culture for a substantial BEAS-2B response to rough LPS, with rough LPS stimulation alone not enough to induce CXCL8 release (Stokes et al. 2011). Of note, another study demonstrated that BEAS-2B cells can express and secrete CD14 and are vital in the LPS response, whilst other studies found no CD14 expression in BEAS-2B cells and other epithelial cell lines (Pugin et al. 1993, Schulz et al. 2002). BEAS-2B cells were also demonstrated to express less MD2 (another important co-receptor) in smaller quantities than A549 cells (Guillot et al. 2004).

The above evidence seems to suggest that LPS-TLR4 stimulation is dependent on a number of factors, including the type of cell stimulated, the dose of LPS stimulation, the rough or smooth phenotype used and even the specific LPS strain used. This may be important in regards to TN-C stimulation of airway epithelial cells, discussed in the next section (Section 5.9.4.)

5.9.4. TN-C Induces Moderate Inflammatory CXCL8 Release from AECs and May Help Dampen the Initial Anti-Viral Response

5.9.4.1. FBG-TN-C Stimulation of AECs Induces CXCL8 Release

In response to stimulation of BEAS-2B cells with purified full-length-recombinant TN-C (0.1 μM), there was no induction of CXCL8 release (Figure 5.7A). In response to purified TN-C FBG (1 μM) stimulation, however, there was a moderate but statistically significant release of CXCL8 (Figure 5.7B), despite no induction of IL-6 (Figure 5.7C) or TNF α (Figure 5.7D). The fold upregulation of CXCL8 in response to TN-C-FBG was approximately 10-fold (Figure 5.9C) and the TN-C used in the experiments was the same as was purified and validated for the MDM stimulation experiments (Figure 5.4).

The important roles of CXCL8 in viral infection, inflammation and asthma are described in Section 5.9.2. The fact that TN-C-FBG induced CXCL8 release from BEAS-2B cells, whilst full-length TN-C did not, is most likely to be due to the limitations of the experiment, rather than any physiological difference between the molecules. Due to only small amounts of recombinant-TN-C being purified, the maximum amount of full-length TN-C that could be used for the triplicate stimulation experiments was 0.1 μM , whilst up to 2 μM of TN-C-FBG could be used due to a more plentiful purification yield. FBG-TN-C had the ability to induce CXCL8 release at larger concentrations from BEAS-2B cells, and 0.1 μM of full-length TN-C is enough to induce inflammatory cytokine release from MDMs and fibroblasts (Midwood et al. 2009). Despite this, it can be theorised that 0.1 μM of full-length TN-C is an insufficient concentration to induce a response from BEAS-2B cells. The response of BEAS-2B cells to full-length TN-C and TN-C-FBG also revealed a different and cellular specific response, compared to MDMs. In this thesis, TN-C elicited a much greater CXCL8 release from MDMs than from BEAS-2B cells, in keeping with other studies that had established TN-C as a potent inducer of CXCL8, IL-6 and TNF α from MDMs (Midwood et al. 2009, Zuliani-Alvarez et al. 2017). In contrast, no release of IL-6 or TNF α

was observed from BEAS-2B cells in response to TN-C. One of the main reasons for this can be theorised to be due to the differential TLR4 expression. In BEAS-2B cells, TLR3 has been determined to be the dominant receptor expressed by RT-PCR, with TLR2, TLR6, TLR5 and TLR1 all expressed in higher quantities than TLR4, which has levels of expression similar to TLR7/8 (Sha et al. 2004). On the other hand, monocytes and macrophages express high levels of TLR4 mRNA and membrane TLR4 protein (Vaure and Liu 2014) and in addition, TLR4 stimulation of MDMs by LPS can lead to the rapid upregulation of further TLR4 expression (Schroder et al. 2012). This upregulation could also potentially occur in response to TN-C stimulation, further potentiating the response. Meanwhile, BEAS-2B cells do express TLR4, as determined by western blot, but flow cytometry in a number of AEC types, including PBECs and BEAS-2Bs, demonstrated that the majority of TLR4 is localised intracellularly and not on the surface of the cell (Guillot et al. 2004). This has important implications for TN-C-FBG AEC stimulation, as although TLR4 receptors can be recycled to and from the PM (Kagan 2010), low membrane TLR4 expression on the surface of BEAS-2B cells may be responsible for this decreased response compared to MDMs. RSV infection of AECs has been demonstrated to upregulate TLR4 membrane expression and subsequently enhance AEC susceptibility to LPS stimulation. Therefore, viral infection itself may result in a greater susceptibility to AEC virally-induced-TN-C release and the consequential TLR4 dependent inflammation (Monick et al. 2003).

TN-C-FBG was also a less potent inducer of CXCL8 release from BEAS-2B cells than LPS. As the co-receptors, dose and phenotype of LPS has an effect on the potency of BEAS-2B cell LPS-induced inflammation (Section 5.9.3), it can be theorised this is also important for response to TN-C-FBG. Currently, the co-receptors required (if any) for TN-C-FBG induced inflammation are not known, however previous evidence has demonstrated that co-receptors CD14 and MD2 (which are required for the induction of LPS-induced TLR4 inflammation) are not required for cytokine release in response to TN-C-FBG in MDMs (Midwood et al. 2009). Any co-receptors required for TN-C-FBG-induced TLR4 inflammation may therefore, be present in lower quantities in BEAS-2B cells, compared to MDMs. Furthermore, it may be possible that the reliance of co-receptors for the induction of the TN-C-FBG response could be overcome with an increase in concentration of TN-C-FBG (as happens with smooth LPS stimulation of BEAS-2B cells), but more investigation is needed to clarify this. Whilst hydrophobic interactions seem to be integral for both TN-C-FBG and LPS binding to TLR4 (Park et al. 2009, Zuliani-Alvarez et al. 2017), there are also structural differences that may account for the differential BEAS-2B responses to stimulation with the molecules. TN-C-FBG has three sites important for activity and receptor binding: the positively charged residues from loops 5, 6, and 7, hydrophobic/polar residues in loop 7 and cationic residues in loop 10 (Zuliani-Alvarez et al. 2017). On the other hand, LPS is extracted from the bacteria and transferred to the MD2 complex by Lipid-A-LPS binding protein-CD14 interactions, allowing TLR4 to form both hydrophobic and hydrophilic bonds with LPS and the F126 and L87 loops of MD2.

Despite only moderate inflammation being induced in response to TN-C-FBG stimulation, this is still a result of potential importance. Asthma is underlined by a chronic inflammation in the airway leading to AHR (Murdoch and Lloyd 2010) and thus RV-induced TN-C release and induction of CXCL8 release in AECs could play a role in this. Due to the MOI used in this study, AECs were viable for approximately 72-96 hours. In response to a lower MOI, however, AECs *in vitro* are viable for much longer (multiple weeks / months), and *in vivo*, RV infection can persist up to 2 weeks (Greenberg 2003), with multiple cycles of RV infection, replication and virion release. This could lead to increased TN-C release and subsequent TN-C-induced AEC inflammatory release. Furthermore, TN-C is usually broken down into soluble fragments by MMP9, but large isoforms are more resistant to MMP9 degradation (Siri et al. 1995). Therefore, large TN-C variant release induced by RV-infection, and released in higher quantities in asthmatics, is more likely to persist in the airway and exert the inflammatory effects described in this study. MMP9 levels are increased in asthmatics and correlate with the severity of asthma exacerbations (Oshita et al. 2003), which may suggest upregulation is partly in order to help combat the increased release of large isoform TN-C in the airway.

The results in this study demonstrate that RV-induced TN-C release occurs, which subsequently induces CXCL8 release in AECs. Albeit this release is moderate, concentrations of TN-C release in the airway may build up over time due to persistent RV infection, increased large isoform TN-C release and resistance to MMP9 degradation. Therefore, this could be an important feature in asthma pathogenesis, with the increased recruitment of inflammatory cells to the airway contributing towards the pathogenesis of the disease. This may also result in a TN-C expression feedback loop (described previously in RA; Goh et al. 2010), through the induction of TN-C transcriptional regulators.

5.9.4.2. Knockdown of TN-C Prior to RV Infection has no Significant Effect on CXCL8 Release but may Affect the Initial Anti-Viral Response

Approximately 50% knockdown of TN-C expression and release in BEAS-2B cells (by siRNA treatment alongside following viral stimulation; Figure 5.1B and 5.1C) had no significant effect on CXCL8 or CCL5 release (Figure 5.2D). Despite this, there was a trend towards decreased CXCL8 release and increased CCL5 release in the poly(I:C) TN-C siRNA cohorts. In PBECs, siRNA knockdown and poly(I:C) stimulation achieved approximately 70-90% knockdown in TN-C expression and release (Figure 5.2), but there was no effect on CXCL8, TNF α and IL-5 release (Figure 5.2A, 5.2C and 5.2D). There was also increased CCL5 release in the poly(I:C) TN-C treated samples at 24 hours post stimulation, ($p=0.0528$), although further experimental repeats are required to see if this trend is real or not.

The lack of statistical significance in CXCL8 and CCL5 release in the siRNA experiments can be explained due to a number of reasons. Firstly, TN-C has only been demonstrated to induce moderate CXCL8 release in BEAS-2B cells through FBG-stimulation, and therefore as only

approximately 50-80% of TN-C was knocked down by siRNA treatment, this might not be sufficient enough to observe significant differences. Small changes could also be masked further due to the relatively small sample sizes used in this study (n=3-5). This moderate difference in the inflammatory response may also be masked by the large upregulation of cytokines and chemokines following RV infection, or may be compensated for, by other inflammatory molecules having the ability to induce inflammation in the absence of TN-C. It can be theorised, therefore, that a greater number of sample numbers may be required to tease out these differences following siRNA treatment. siRNA can also induce inflammation in target cells itself (Jackson and Linsley 2010), which could mask any TN-C dependent changes. This is demonstrated in this study, with greater chemokine release in response to siRNA and poly(I:C) stimulation in PBECs (Figure 5.3) compared to poly(I:C) stimulation only (Figure 3.11). Additionally, this inflammation can lead to cell cytotoxicity (Fedorov et al. 2006), demonstrated by the increase in cell death following siRNA treatment and viral stimulation / infection (Figure 5.2), which could further influence the experimental results.

The decrease (but not statistically significant) in AEC CXCL8 release in response to TN-C siRNA treatment and poly(I:C) stimulation appeared to follow the same trend in both BEAS-2B cells and PBECs. The results also correlates with Figure 5.7A (see previous Section 5.9.4.2.), which established that TN-C-FBG stimulation can induce CXCL8 release in BEAS-2Bs. If it is confirmed through further work that TN-C knockdown increases the CCL5 response at 24 hours post stimulation in PBECs, this would be an observation of note. There is currently no evidence of TN-C-induced CCL5 down-regulation in any cell type, and indeed LPS (and thus TLR4) stimulation of macrophages has been demonstrated to induce a moderate production of CCL5 mRNA expression (Bandow et al. 2012, Kong et al. 2014). CCL5 (among other factors) has also been demonstrated to be required in tumour cells for increased TN-C expression and enhanced metastasis (Mi et al. 2011). This suggests that TN-C knockdown in airway epithelial cells may invoke a similar system of increased airway epithelial cell CCL5 release following RV infection, potentially in order to induce TN-C expression that would be required in the wound healing response. Additionally, it could also be theorised that as TN-C induces inflammatory cytokine release through the TLR4 pathway, this may 'skew' the response to a more inflammatory phenotype, which may also dampen the initial anti-virus response. Removal of TN-C from this system may then allow the cells to mount an appropriate anti-viral response to infection; however, more investigation is needed to study this further. Unfortunately, CCL5 release following stimulation of BEAS-2B cells with TN-C-FBG was not examined in this study due to time constraints, which could have helped to correlate the CCL5 siRNA results.

5.9.5. Exosomes from Virally Stimulated AECs Induce Inflammatory and Anti-Viral Cytokine / Chemokine Release from BEAS-2B Cells

In response to stimulation of BEAS-2B cells with BEAS-2B cell derived exosomes, significant CXCL8 (Figure 5.8A), IL-6 (Figure 5.8B) and CCL5 (Figure 5.8C) was induced in response to virally-induced exosomes (72 hours post stimulation and high in TN-C expression) compared to

that induced by media control exosomes (72 hours post stimulation and low in TN-C expression). Furthermore, it was determined that poly(I:C) was not carried over in the poly(I:C) stimulated vesicles, as the 0 hour poly(I:C) control did not induce CXCL8 release (Figure 5.8A), and the fold induction of CXCL8 release was approximately 6 fold (Figure 5.9D).

This is the first time that exosomes derived from TLR3 / viral stimulated BEAS-2Bs have been shown to have the ability to induce CXCL8 and IL-6 inflammatory release from AECs. These results also correlate with another recent study, that demonstrated that exosomes isolated from A549 cells following RSV infection (which is recognised by TLR3) could induce the anti-viral chemokine CCL5 (Chahar et al. 2018). The Chahar study also demonstrated these EVs had the ability to induce CXCL10 and TNF α release. Furthermore, the control exosomes both in this thesis and the Chahar study did not induce any inflammatory or anti-viral cytokine / chemokine release from AECs. The CCL5 release induced by poly(I:C) stimulated EVs in this study was approximately 6 fold greater than reported in the Chahar study, insinuating there may be a differential response in different types of AECs and in response to different stimuli. Therefore, the next aim will be to stimulate AECs with RV-induced AEC exosomes, in order to elucidate whether viral specific differences exist. The effects of CXCL8, TNF α and IL-6 in the airway have been described in Sections 5.9.3. and 5.9.5., whilst CCL5 also plays an important role in both viral infection and the pathogenesis of asthma. CCL5 is an effective recruiter of monocytes, eosinophil and T-cells, which are vital in the removal of the virus (Schall et al. 1990, Culley et al. 2006). Furthermore, CCL5 levels correlate with both T-cell localisation in the lung and asthma exacerbations (Castro et al. 2004), probably due to large CCL5 upregulation following viral infection. The result in this thesis also correlates with *in silico* screening of exosomes isolated from NLF following RV infection, which were predicted to have anti-viral functions (Gutierrez et al. 2016).

Exosomes are vital in the communication between cells and once released, exosomes can travel over several cell lengths in order to reach target cells (Panakova et al. 2005, Lakkaraju and Rodriguez-Boulan 2008). Once this occurs, they are internalised by macropinocytosis and clathrin-independent endocytosis in order to deliver their contents (Verdera et al. 2017). Following RV infection, it is vital that the immune response is initiated rapidly, and can reach a large number of target cells. AECs are the barrier to infection and so exosome release can allow this to occur. RV-induced exosomal inflammation may have important consequences for airway inflammation and asthma exacerbations, especially as exosomes in the airway of asthmatics are already more plentiful and predisposed towards a more inflammatory phenotype. For example, exosome release is increased in some cell types in asthmatics, such as eosinophils (Mazzeo et al. 2015). BALF exosomes from asthmatic patients also induced significant CXCL8 compared to the exosomes from healthy controls in a 16HB14o- bronchial epithelial cell line (Paredes et al. 2012), and addition of exosomes isolated from the NLF of healthy subjects have been demonstrated to induce the significant migration of monocytes, neutrophils and NK cells *in vitro* (Lasser et al. 2016). This thesis demonstrates that the amount

of inflammatory exosomes can be increased following viral challenge, delivering its cargo to AECs and increasing inflammatory cytokine / chemokine release such as CXCL8 and TNF α , which drives further release and immune cell recruitment, as well as potential further TN-C expression. This is a mechanism that can be theorised to provide a link between RV infection of the airway, heightened airway inflammation following infection and ultimately the initiation of an asthma exacerbation.

5.9.6. Exosomes from Control and Virally Stimulated AECs Induce CXCL8 Release from MDMs

In response to stimulation of MDM with BEAS-2B cell derived exosomes, moderate CXCL8 release was induced in response to virally stimulated vesicles compared to media control vesicles (Figure 5.8D), with an approximate 1.5 fold increase (Figure 5.9D), but this was not statistically significant ($p=0.2$). The amount of CXCL8 induced by the media control exosomes in Figure 5.8D was also much greater than CXCL8 release at basal levels from MDMs, which were taken from previous MDM stimulation experiments (Figure 5.5). The fold upregulation of CXCL8 in poly(I:C) exosomes compared to media control exosomes was approximately two-fold (Figure 5.9D).

These results correlate with results from the Chahar study, that demonstrated both control and RSV-derived AEC exosomes had the ability to induce inflammatory chemokine release from MDMs, with MCP-1 and IP-10 induced (Chahar et al. 2018). Interestingly, this study also demonstrated that CCL5 could be induced in response to both control and RSV-derived exosomes, which was not investigated in this thesis. The fact that AEC-induced exosomes elicit differential responses in MDMs and BEAS-2Bs suggests cellular specific responses to EVs. First, media control exosomes do not induce a response from BEAS-2B cells but do in MDMs, suggesting a heightened sensitivity to exosome stimulation. This is to be expected, due to the numerous differences between the two cell type described in this study (such as TLR composition, susceptibility to pathogens, cytokine release etc.), however, LPS contamination may also account for these differences. Exosomes cannot be isolated in a sterile manner and as BEAS-2B cells do not respond to media control exosomes (with CXCL8, IL-6 and CCL5 release at basal levels), it can be determined that either LPS is not present, or does not induce a response. Conversely, as media control exosomes do induce CXCL8 release from MDMs, it cannot be ruled out that LPS may be contributing to this observed CXCL8 release, especially due to their heightened sensitivity to LPS stimulation (Figure 5.5). The differences between media control and poly(I:C)-derived exosomes can be determined to be independent of LPS, however, with the fold upregulation of CXCL8 3 times greater from BEAS-2Bs than MDMs. The reasons for a greater AEC response to exosomes over MDMs are currently unknown. One potential theory is that as MDMs are already activated by the basal exosomes, the inflammatory response may be already close to maximal levels, and thus the additional inflammatory mediators present in the virally-stimulated exosomes may not have much of an additive effect.

Furthermore, AECs have been established to be more sensitive to TLR3 stimulation than MDMs, whilst MDMs are more sensitive to TLR4 stimulation (Al Mubarak et al. 2018), so it is possible AECs may be more susceptible to the inflammatory mediators present in virally stimulated exosomes, which may potentially include RV proteins, RNA and virions.

The results have demonstrated that exosomes from virally stimulated AECs (and potentially media control exosomes) have an inflammatory effect on AECs and MDMs that may drive airway inflammatory and anti-viral cytokine / chemokine production following infection. Moreover, this inflammation may also be heightened in asthma. These results however, do not establish to what extent RV-induced TN-C plays a role in this pathway.

5.9.7. Initial Results Indicate TN-C May Not Play a Role in Exosome-Induced AEC CXCL8 and CCL5 Release, but Further Investigation is Required

Significant TN-C knockdown in BEAS-2B cell-associated TN-C (60% knockdown; Figure 5.10A), released TN-C (80% knockdown; Figure 5.10B) and exosomal associated TN-C (70% knockdown; Figure 5.10D) was achieved in response to TN-C siRNA treatment and 72 hours poly(I:C) stimulation. There was no significant difference in CXCL8 (Figure 5.11A) and CCL5 (Figure 5.11B) release in response to BEAS-2B cell stimulation with TN-C siRNA treated exosomes, however, compared to stimulation with scrambled siRNA treated exosomes. Despite this, there was however a trend of CXCL8 increase in cells stimulated with the siRNA treated exosomes at 20,000 exosomes per μ l.

Despite no significant differences in BEAS-2B chemokine release following stimulation with poly(I:C)-TN-C siRNA treated and poly(I:C)-scrambled siRNA treated exosomes, it is still not clear whether TN-C plays a role in exosome-induced inflammation following viral infection. This is due to a number of limitations within the final experiments. For example, despite statistically significant TN-C knockdown, TN-C expression in the exosomes was not ablated 100%, with approximately 30% TN-C expression remaining, and this may be sufficient to still induce responses in target cells.

Most significantly, the amount of CXCL8 and CCL5 release in these cells following stimulation with the poly(I:C)-siRNA treated exosomes (Figure 5.11A) is greater (approximately 40-fold and 2-fold, respectively) than that induced by poly(I:C)-non-siRNA treated exosomes (Figure 5.8A). There are a number of reasons that could explain this. The BEAS-2B cells used in the siRNA experiments in Figure 5.11. (both in the BEAS-2B cells treated with poly(I:C)-siRNA and the BEAS-2B cells stimulated with the exosomes) were separate batches to those used in the first exosome stimulation experiments in Figure 5.8, and as batch-specific differences have been determined previously in BEAS-2B cells (Zhao and Klimecki 2015), there may be some differential responses to exosome-induced inflammation. Despite this, it is unlikely that the large differences in CXCL8 induction following exosome stimulation would be as profound, especially as BEAS-2Bs cells are a cell line. The other theories behind this increased chemokine release

following stimulation with siRNA treated exosomes regard the siRNA pre-treatment. These results seem to suggest that siRNA is being incorporated into the exosomes itself and having a direct inflammatory effect following stimulation. siRNA has been previously demonstrated to induce inflammation in a number of cell types (as detailed in Section 5.9.4.2.; Jackson and Linsley 2010) and this was potentially demonstrated in the earlier siRNA experiments in this study (Figure 5.1, 5.2. and 5.3.). It is also theorised that siRNA treatment could indirectly affect the composition of the exosomes released by the cells, as siRNA treatment of cells have been previously been demonstrated to have a number of off target effects (i.e. independent of knockdown of the target protein; mentioned in Section 5.9.4.2.), including cell cytotoxicity (Fedorov et al. 2006). Although evidence of siRNA having off target effects in exosome composition has not currently been evidenced, the modulation of exosomal content has previously been demonstrated with exosomes isolated following chemotherapy (Bandari et al. 2018), apoptosis (Lynch, Panagopoulou and Gregory 2017) and necrosis (Jelonek, Widlak and Pietrowska 2016). Therefore, the greater cell cytotoxicity induced by siRNA treatment and viral stimulation observed in this study could potentially change the composition of the exosomes released by the cell. This may lead to the packaging of more inflammatory mediators into the vesicles, and therefore these exosomes would have a greater inflammatory effect on the target cell following stimulation. Furthermore, another important off target effect of siRNA treatment is the modulation of the miRNA composition of cells, through the modulation of the RNA interference machinery (Jackson and Linsley 2010, Liang, Hart and Crooke 2013). This is an important observation, as changes in miRNA composition have previously been demonstrated to modulate the inflammatory potential of exosomes. For example asthmatic patients had a different exosomal miRNA profile compared to non-asthmatics, with 24 differentially regulated miRNAs identified, and this was demonstrated to enhance the inflammatory potential of these exosomes (Levanen et al. 2013). It is therefore feasible that siRNA treatment of BEAS-2B cells modulates the miRNA profile of the exosomes, leading to more inflammatory mediators being packaged into the vesicles and to induction of greater inflammatory cytokine / chemokine release following stimulation, masking any potential effects of TN-C knockdown.

It is also important to note that TN-C may have alternative roles in RV-induced exosome inflammation, rather than being a direct inducer of inflammation itself. For example, in response to HIV-1 infection of T-cells and DCs, DC exosomes containing HIV were demonstrated to be internalised at a greater rate than T-cell exosomes (Kulkarni and Prasad 2017), due to FN (an ECM protein that closely associates with TN-C) and galectin-3 (a lectin molecule involved in cell adhesion) being present in DC exosomes and absent in T-cell exosomes. As TN-C is important in cell adhesion, it may play a similar role to FN and galectin-3, allowing exosomes to bind to target cells and internalise.

Due to the number of limitations with this final experiment, it is currently not clear whether TN-C plays a role in exosome-induced inflammation. What is clear, however, is that the two pathways described in this study, RV-induced TN-C release and RV-induced exosome release, seem to

have important roles in airway inflammation, and furthermore, the capability of TN-C and exosomes to induce inflammation may be increased in the asthmatic airway. Chapter 6 will summarise and explain the wider implications of the pathway, as well as explain how the role of TN-C in virally-derived exosome release can be researched in further detail.

Chapter 6 – Overall Discussion and Conclusions

6.1. A Proposed Model of RV-Induced TN-C and Exosome Release in AECs Leading to Increased Airway Inflammation

The results in this thesis demonstrate novel pathways of RV-induced TN-C and exosome release. It is proposed that TN-C is initially upregulated in response to RV infection in order to contribute to the wound healing response and to recruit immune cells into the lungs to help clear infection, whilst exosomes are released in order to communicate with the surrounding cells to help coordinate an appropriate inflammatory and anti-viral response. However, the TN-C and exosomal response to RV infection becomes exaggerated in the asthmatic airway, and this pronounced response, combined with a number of other factors, leads to a more potent increase in airway inflammation following infection. The pathway of TN-C and exosome release is summarised in Figure 6.1, whilst the inflammatory effects of TN-C and exosome release are summarised in Figure 6.2.

6.1.1. RV-Induced TN-C Expression and Release is TLR3 Dependent, TLR7 Independent and a Viral Specific Mechanism

RV infection of AECs (both major and minor serotypes), through initial binding to ICAM-1 or LDL receptors, leads to the trafficking of the virus to the early endosome where the low pH leads to viral uncoating and replication (Fuchs and Blaas 2012). During this replication, the ssRNA forms a temporary dsRNA intermediate, which activates TLR3 (but not TLR7) and induces the release of cytokines and chemokines such as TNF α , TGF- β , CXCL8 and CCL5. TGF- β 1 and TNF α are known transcriptional regulators of TN-C through the MAPK/ERK and NF- κ B/p65 pathways (Vollmer et al. 1997, Nakamura et al. 2004, Makinde et al. 2007, Goh et al. 2010) and TNF α has been demonstrated in preliminary results in this study to induce TN-C release. Therefore, it is postulated that it is the activation of these pathways following RV infection that triggers the signalling cascade required for the expression and release of TN-C in AECs. Other receptors such as TLR2, MDA5 and RIG-I may play a role in this pathway and so further investigation is required. This process is also independent of non-specific cell death and can occur without large amounts of virally-induced cell cytotoxicity. Finally, this pathway was also validated using an *in vivo* model, with intranasal poly(I:C) stimulation of adult C57BL/6 mice inducing the expression of TN-C in the BALF.

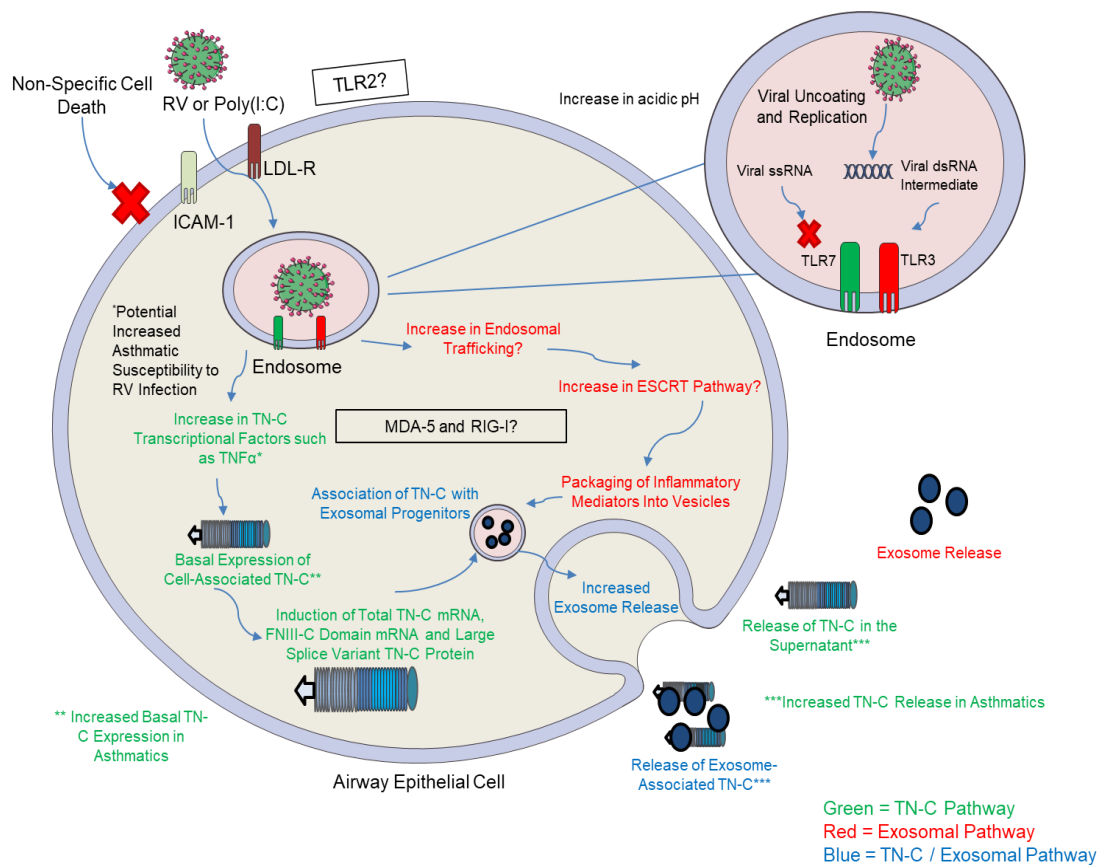


Figure 6.1. The Proposed Mechanism of TN-C and Exosome Release Following RV Infection in AECs

Upon AEC RV infection (by major or minor serotypes through ICAM-1 or LDL receptors), the virus is trafficked to the endosome. The low pH in the endosome leads to the uncoating of the virus and viral replication, through which temporary viral dsRNA is synthesised from ssRNA, which is recognised by TLR3. TLR7 does not seem to play a role in this process and the role of TLR2, MDA5 and RIG-I in this pathway are yet to be elucidated. The TLR3-dependent pathway induces the expression of TN-C transcriptional regulators, which are postulated to result in the expression of large splice variant TN-C isoform expression. This is thought to occur by alternative splicing, potentially from an already available pool of basal TN-C and through moderate TN-C mRNA upregulation. The change to the TN-C structure by alternative splicing may provide the trigger for the protein to migrate from the cytoplasm to the membrane, where the protein is then released into the supernatant. The large isoform of TN-C is also the main isoform released and this isoform is more resistant to MMP9 degradation. TN-C release is more pronounced in asthmatics, with greater expression and release at basal levels and in response to RV. Furthermore, a substantial proportion of TN-C release in AECs is associated with EVs, with significant TN-C release associating and correlating with the increase in exosome release following infection. It can be postulated that increased endosomal trafficking following RV infection induces increased exosome production and release, as the ESCRT exosomal formation pathway originates from the endosomal pathway, however the pathway behind RV-induced exosome release is yet to be elucidated. The green pathway indicates TN-C upregulation pathway, the red pathway indicates exosome upregulation pathway and the blue pathway indicates where both pathways merge.

6.1.2. Intracellular TN-C Expression Following RV Infection is Dependent on a Number of Factors, can be Controlled by Alternative Splicing and may be More Pronounced in Asthmatics

The results in this study indicate that the type of TN-C regulation that occurs in response RV-induced signalling, and in response to transcriptional regulators such as TNF α , is not the mass intracellular upregulation of the protein as originally hypothesised. In fact, the upregulation in TN-C mRNA and cell-associated expression seems to be more nuanced and tightly controlled, with a number of factors affecting the type of expression. In cells with low levels of basal TN-C mRNA, upregulation of overall TN-C mRNA occurs, as well as potential changes to FNIII splice domain expression. However, in cells with higher levels of basal TN-C mRNA expression, intracellular upregulation is not observed and instead, changes to the alternatively spliced FNIII domains occur. The upregulation of TN-C cell-associated protein expression also correlates with this, with large TN-C upregulation in cells with low basal expression and low upregulation in cells with high expression. The modification of TN-C splice variants and the upregulation of TN-C FNIII mRNA seem to correlate at the protein level, with RV infection increasing the ratio of large:small variants, independent of a lack of increase in overall expression. Furthermore, the type of stimulus may have an effect on the type of expression, with RV infection being the only stimulus to induce overall TN-C and FNIII specific mRNA expression in PBECs. This may indicate that TLR2, MDA5 and RIG-I could also play a role in this pathway, alongside TLR3. Donor specific differences in PBECs to RV induced TN-C expression may also occur, which is feasible as PBECs from different donors show variability to viral titre, cytokines and chemokines produced to RV infection and RV-induced cytotoxicity (Stokes et al. 2016).

It is well established that cell associated TN-C expression in the RBM of asthmatics is increased over that of non-asthmatics (Laitinen et al. 1997). Work demonstrated in this thesis correlates with this, with AA PBECs having increased basal levels of TN-C mRNA compared to NANA PBECs at 6 and 24 hours. In response to RV infection, upregulation of TN-C mRNA is also greater at 6 hours in the AA PBECs, but then NANA PBECs reach the same level of expression by 24 hours, demonstrating the higher basal expression may allow a more pronounced initial upregulation following RV infection in asthmatics.

6.1.3. RV Infection Induces Exosome Release in AECs

RV infection of AECs also induces the release of EVs, with a large induction of exosomes with an average size of 100-110 nm. This again is TLR3 dependent, TLR7 independent and it is not yet determined whether TLR2, RIG-I and MDA5 have a role in RV-induced exosome release. The mechanisms and functional reasons for RV-induced EV release are not yet revealed, but as exosomes originate from the endosomal pathway (Raposo and Stoorvogel 2013), and as RV is processed into the endosomal pathway following infection (Fuchs and Blaas 2012), it can be theorised that RV infection leads to an excess of endosomes inside the cell. This would result in some endosomes being re-cycled back to the membrane to deal with further infection (Maxfield

and McGraw 2004) and other endosomes entering the ESCRT pathway leading to increased exosome release.

6.1.4. RV Infection Induces TN-C Release in AECs, is More Pronounced in Asthmatics and a Large Proportion is Associated with Exosomes

Following RV-induced upregulation of cell-associated TN-C expression and / or the upregulation in large splice variant expression, next, TN-C is released. The results in this study indicate that TN-C is released in two main ways following RV-infection, release of the protein into the supernatant (Figure 3.6, 3.10, 3.14 and 3.15) and release of exosomal-associated TN-C (Figure 4.6). This release is again dependent on TLR3 stimulation and is independent of cell death and TLR7 stimulation. Based on preliminary experiments, it was determined that approximately 50% of released TN-C was released in the supernatant and 50% was associated with exosomes, but further investigation is required to determine the accuracy of this. The function of TN-C changes depending on the size of the protein, as incorporation of more FNIII domains and glycosylation allows the protein to bind to more target proteins and exert different functions (Zisch et al. 1992, Ghert et al. 2001b, Giblin and Midwood 2015). Therefore, the upregulation of larger TN-C transcripts following RV infection allows the protein to interact with more molecules, and it can be postulated that this may allow the protein to be incorporated into exosomes or bind to other targets (such as membrane proteins) that allows the protein to be released. Importantly, TN-C release is also increased in AA PBECs compared to NANA PBECs in response to RV infection and at basal levels. Preliminary experiments seem to indicate it is this higher basal level of expression in AA PBECs (rather than increased susceptibility to prolonged RV infection etc.) that contributes to the increase in overall TN-C release in response to RV infection, compared to NANA PBECs.

6.1.5. The Proposed Functional Reasons for RV-Induced Tenascin-C and Exosomal Release

This study has focused on the contributory role that RV-induced TN-C and exosomes may have on airway inflammation and ultimately asthma exacerbations, as this is the most pertinent to the study aim. However, it is not yet known if TN-C has an initial functional role in the biological response to RV infection, which can over time have a detrimental effect (either through multiple viral infection cycles or continual asthma pathogenesis), or whether TN-C is only harmful when expressed during asthma or in response to RV infection. Furthermore, it has not yet been determined why RV infection modulates exosome release, leading to exosomes that that increases the inflammatory potential of these vesicles.

The majority of research into TN-C release has been carried out in the area of cancer biology, with the increased release in metastatic cells determined to increase metastasis and the oncogenic phenotype of the tumour (Hancox et al. 2009, Ferrari and Calvo 2014), and this release can also be associated with exosomes (Ji et al. 2013, Greening et al. 2016). TN-C is

also implicit in the wound healing response (Forsberg et al. 1996, Latijnhouwers et al. 1997), where it is demonstrated to be released from cells such as epidermal keratinocytes and is vital in signalling and cellular recruitment to resolve the damaged epithelium. It can therefore be theorised that airway epithelium damage due to RV infection and increased inflammation in asthma leads to the upregulation of TN-C release (both independent of exosome release and also exosome associated). This TN-C upregulation is then vital in helping to modulate the adhesion of target cells and recruit cells such as fibroblasts, macrophages and neutrophils required for the wound healing process (Latijnhouwers et al. 1997, Patel, Maheshwari and Chandra 2016), and the recruitment of immune cells required for the innate immune response to viral infection (Takeuchi and Akira 2009). This theory is supported by TN-C induced CXCL8 and IL-6 release in either MDMs and / or AECs (Figure 5.5 and 5.7), which are potent immune cell recruiters.

Exosomes are important to the propagation of virulence and pathogenesis following viral infection. As RV protein VP2 has been demonstrated to be present in RV-induced exosomes in HeLa cells (Chen et al. 2015), it can be theorised that RV may upregulate exosomal release and utilise exosomes to exit the cell in a non-lytic manner, delivering proteins such as virions to the surrounding cells and thus aiding transmission; a mechanism described in other enterovirus infections, such as CVB (Inal and Jorfi 2013). Furthermore, exosomes derived from virally infected cells can induce cell death, increase the speed and efficiency of infection and allow evasion of the innate immune response (Zhang et al. 2018), therefore RV may also utilise exosomes to aid pathogenesis. In contrast, exosomes can also assist the innate immune response to viral infection by enhancing TLR expression on macrophages and promoting the function of NK cells, T-cells and B-cells (Zhang et al. 2018), thus, the modulation of exosomal contents following RV infection may be an AEC response, in order to initiate the removal of the virus. This theory is supported by the results in this study, with RV-induced AEC release inducing CCL5 expression in stimulated AECs (Figure 5.8C). Exosomes have also been demonstrated to play a role in the wound healing response by delivering contents such as EGF which are vital for angiogenesis and other wound healing mechanisms (Golchin, Hosseinzadeh and Ardeshiryajimi 2018). It can be theorised, therefore, that RV-induced exosome release may occur in order to resolve airway epithelial cell damage. This theory is supported by RV-induced AEC release inducing CXCL8 and IL-6 expression in stimulated AECs, which recruit immune cells among other functions (Figure 5.8).

Whilst TN-C and exosome release following infection may be important for resolving RV infection and initiating the wound healing response to viral infection and asthma, TN-C and exosomes can also have a detrimental effect in the airway (especially in diseased airways, such as asthma), which is explained in the next section.

6.1.6. The Proposed Detrimental Inflammatory Implications of RV-Induced TN-C and Exosome Release in the Airway

RV infection induces the release of the large isoform of TN-C, >250 kDa in size, potentially to recruit immune cells required for viral clearance and the initiation of the wound healing response (Section 6.1.5). The TN-C released following RV infection has been demonstrated to induce high levels of CXCL8 (Figure 5.5), IL-6 and TNF α (Midwood et al. 2009) release from MDMs and moderate CXCL8 release from AECs (Figure 5.7), with TN-C-FBG stimulation demonstrating that this is TLR4-dependent. MDMs have high levels of TLR4 expression (Vaure and Liu 2014) whilst in comparison, AEC TLR4 expression is low (Sha et al. 2004) and may be not be localised to the membrane (Guillot et al. 2004). This could therefore explain the differential response to TN-C. CXCL8, IL-6 and TNF α release will lead to increased infiltration of immune cells in the airway (Ordonez et al. 2000, John et al. 2009, Tang et al. 2016), potentiation of viral infection (Berg et al. 2004) and loss in lung function contributing to AHR (Menard and Bissonnette 2000). TNF α is also a transcriptional regulator of TN-C and so could form an autocrine-feedback loop in the airway, leading to increased TN-C expression (Goh et al. 2010). The size of the isoform is important, as large isoforms of TN-C are more resistant to MMP9 degradation (Siri et al. 1995) and have a greater capacity to induce inflammation than smaller isoforms (Ghert et al. 2001a, Midwood et al. 2009, Goh et al. 2010, Page et al. 2012). TN-C expression, with an enhanced ability to induce inflammation will, therefore, persist in the airway after the clearance of viral infection or the completion of the wound healing response, potentially being incorporated in the RBM of cells (Laitinen et al. 1997) or in the ECM. Furthermore, TN-C expression is also higher in the RBM of asthmatics compared to non-asthmatics (Laitinen et al. 1997) and the release of TN-C (also the large isoform) is also greater in asthmatics compared to non-asthmatics following RV infection (Figure 3.18C).

RV infection of AECs also induces the release of exosomes, potentially in order to help initiate the response to viral infection and to help wound healing responses (Alenquer and Amorim 2015, Golchin et al. 2018). These exosomes may also be hijacked by the virus, and used to deliver viral proteins, RNA and virions to surrounding cells (Chen et al. 2015). Exosomes are internalised and contents are delivered once they reach the target cell, and these RV-induced AEC-derived exosome are able to induce greater cytokine and chemokine release than non-infected AEC-derived exosomes, inducing significant CXCL8, IL-6 and CCL5 in BEAS-2Bs and moderate CXCL8 release in MDMs (Figure 5.8). Additionally, asthmatic EVs contain are able to induce greater inflammation than non-asthmatic derived exosomes, with changes to protein cargo (such as TN-C; Figure 4.6) and miRNAs (Paredes et al. 2012, Kulshreshtha et al. 2013, Mazzeo et al. 2015, Lasser et al. 2016).

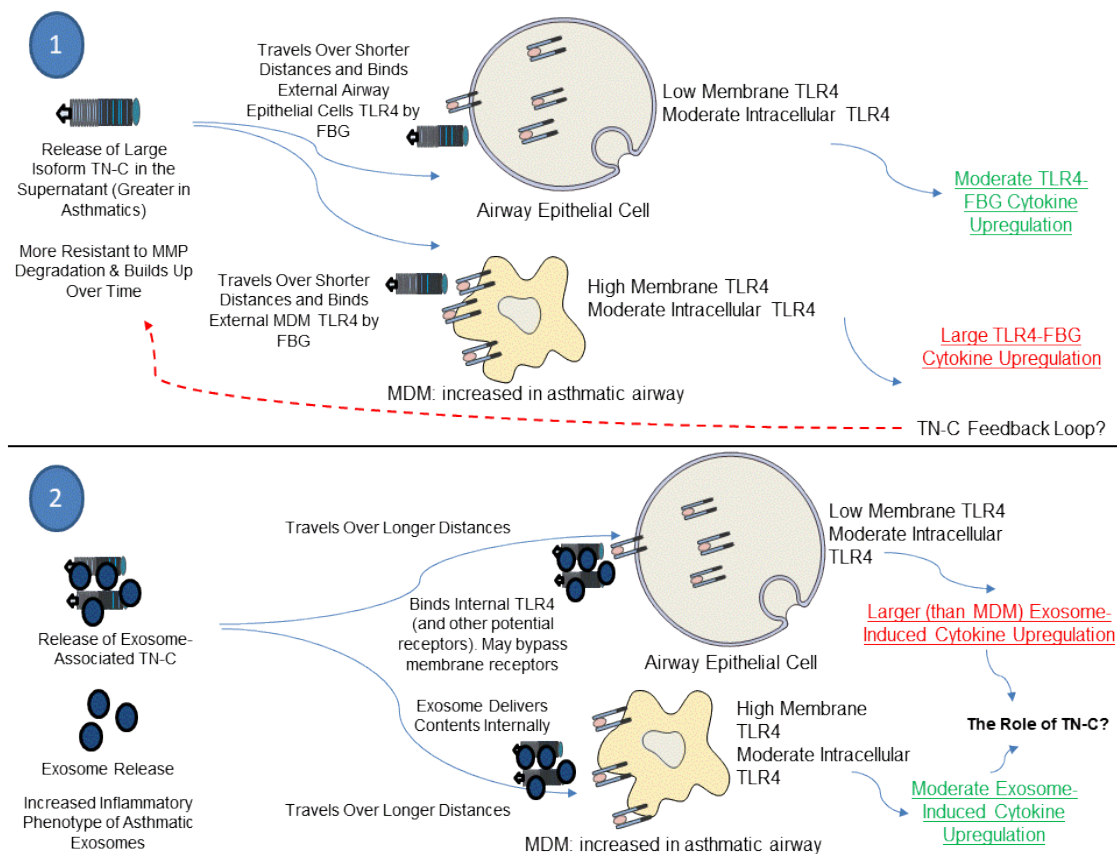


Figure 6.2. The Proposed Inflammatory and Anti-Viral Implications of RV-Induced TN-C and Exosome Release in the Airway

(1) Following RV-induced AEC TN-C release, the protein can migrate over short distances and has been demonstrated to be able to bind to AECs and MDMs via the FBG domain. The natural receptor of the FBG domain is TLR4, and AECs have low PM TLR4 and moderate levels of intracellular TLR4, whilst macrophages have high levels of membrane TLR4. Due to this, TN-C can induce large upregulation of inflammatory cytokine / chemokine release from MDMs and moderate cytokine / chemokine release from AECs. The large TN-C isoform released by AECs following RV-infection is more resistant to MMP9 degradation and the inflammatory response induced by TN-C may form a transcriptional feedback loop, promoting more TN-C expression and delivering a prolonged chronic airway inflammatory effect. **(2)** Following RV-induced AEC exosome and exosomal-associated TN-C release, the exosomes can travel over longer distance and once they encounter target cells (in this case, AECs and MDMs), they will internalise and deliver the inflammatory cargo (including TN-C). This induces a moderate inflammatory response from MDMs and a larger inflammatory and anti-viral response from AECs. Exosomes from asthmatic AECs have been previously been demonstrated to induced greater inflammation than exosomes from non-asthmatic AECs, however, the extent to which TN-C plays a role, the other inflammatory and anti-viral mediators involved and the receptors involved are yet to be elucidated.

To summarise the pathway described in this study, the release of the large inflammatory isoform TN-C is induced in response to RV is increased in asthmatics, this will persist in the airway and induce cytokine / chemokine release from MDMs and moderate but chronic AEC CXCL8 release, which could contribute to AHR. Furthermore, RV induces the release of exosomes in airway epithelial cells, which are able to induce greater inflammation than non-infected AEC exosomes. This could be potentiated further in asthma, with asthmatic exosomes containing more inflammatory mediators such as certain miRNAs. Although TN-C is associated with exosomes following RV infection and is upregulated alongside exosomal release, the role TN-C has on exosome-induced inflammation is not yet elucidated. TN-C could also act on other targets in the airways such as fibroblasts, and exosomes has been demonstrated to induce inflammation in a number of cell types such as neutrophils and dendritic cells, which could potentiate inflammation even further (Midwood et al. 2009).

6.1.7. Clinical Implications of RV-Induced TN-C and Exosome Release

The two pathways described have a number of important potential therapeutic implications. TN-C is a protein that can be targeted therapeutically by TLR4 inhibitors, with TLR4 inhibitor treatment reducing cytokine release *in vitro* in synovial fibroblasts and macrophages (Midwood et al. 2009), and thus this type of therapeutic intervention may be successful in helping to dampen the excessive local immune response to TN-C following RV-dependent release. Moreover, as the FNIII and EGF domains are important in the wound healing response (Midwood and Orend 2009), the targeting of TLR4 may reduce inflammation, but not affect the important wound healing response following airway epithelial damage in response to infection.

The revelation of exosome-induced inflammation following RV infection (which will have components independent of TN-C, such as potential changes to miRNA profile), demonstrates the need for a multi-targeted approach to fully address RV-mediated inflammation following infection. Current work investigating exosomes as therapeutics has focused on utilising exosomes as drug delivery vesicles, which has been shown to be more effective than liposomes or synthetic vesicles (Ha et al. 2016). Drugs or proteins are either modified to be targeted towards the ESCRT pathway, or by isolating the vesicles, inserting the drug and re-administration of the exosomes into the target tissues. Anti-virals, anti-inflammatories and other drugs, therefore, could be incorporated into airway epithelial cells vesicles, which may help to dampen the immune response in asthmatics following viral infection. It would be important however, that these changes do not dampen the immune response enough to allow RV infection to continue.

Moreover, as TN-C has been demonstrated to be an accurate biomarker of RA diagnosis (Schwenzer et al. 2016) and RV can be difficult to culture (Johnston et al. 1995b), the association of soluble or exosome-associated TN-C expression could be utilised as a quickly defined and accurate biomarker of virally-induced asthma exacerbations following

hospitalisation. This could help with quicker diagnosis and suitable treatment of patients, and aid studies investigating the causes of respiratory / asthma-associated hospitalisations.

Further investigation of the mechanisms behind RV-induced TN-C and exosomal release, as well as the consequences of this pathway, will enable the role of RV-induced airway inflammation and asthma exacerbations to be understood in more detail. This future work could be crucial, as it could potentially lead to the development of therapeutic interventions in the future.

6.2. Limitations and Future Plans

There are a number of future experiments that can be conducted in order to improve and further elucidate information about the results in this study. Airway epithelial cell TN-C release has been demonstrated to be TLR3 dependent and TLR7 independent, however it is not known what other receptors, if any, are involved in this process during RV infection. An important future experiment is to utilise siRNA to knockdown the expression of receptors involved in RV signalling, such as TLR2, TLR3, RIG-I, MDA5, ICAM-1 and LDLs, in order to reveal which are required for the induction of TN-C release. The results obtained following differential knockdown of receptors will provide definitive evidence of the signalling pathways involved in the pathway, and it will be interesting to determine whether the process is mainly TLR3 dependent, or whether further receptors are required to be activated for maximal protein release. A further technique to uncover the mechanisms behind this process is to treat the cells with differential TN-C transcriptional regulators involved in RV infection, in order to define which cytokines determine TN-C release. Preliminary results in this study have determined TNF α may play a role in TN-C release following RV infection, but further investigation is required for a definitive answer. Cytokines and chemokines such as TGF- β , CCL5 and IL-4 may also play a role, and should be investigated.

Another important experiment would be to investigate the apical-basal axis of TN-C release in airway epithelial cells and this could be completed through ALI cell culture. Currently, the model used in this study uses a submerged culture of epithelial cells, that whilst are the most commonly used method for modelling the respiratory tract; they are not the most biologically relevant method available. Submerged epithelial cell cultures (that are bought from suppliers) allow the epithelial cells to form tight junctions, but these cells do not differentiate and become ciliated and mucus producing. A number of cells taken from biopsies and cultured in this way may differentiate in this way, but these cells seem to be lost in supplier bought batches. In order to differentiate airway epithelial cells into mucus producing, ciliated cells, ALI cultures need to be used. ALI's are epithelial cell transwell cultures that differentiate over a 30-day period to form a pseudostratified mucocilliary epithelium that closely models the respiratory epithelium (Pezzulo et al. 2011). ALI cultures have epithelial cells submerged in cell media and ciliated goblet cells (which produce mucus) which are exposed to air. The current drawbacks of these methods include the expensive nature of the assay, the length the assay takes, and they fact

that these cells produce large amounts of mucus, that can make viral infection of these models difficult. RV infection of ALI cultures would allow the collection of two distinct supernatants, basal supernatants from the epithelial cells and apical washes from the ciliated cells, allowing the apical-basal orientation of TN-C release to be determined. This could further help to determine the function of the protein following release, as the apical and basal sides of the epithelium are exposed to different cells, proteins and pathogens.

This study has focused on the expression of TN-C in exosomes following RV infection, as it is most pertinent to the research aim. It is important in the future to perform full proteomics of the exosome composition of AEC at basal levels and in response to RV infection, in order to reveal what other cargo is modulated. Further analysis also needs to be carried out on asthmatic samples, to investigate whether the TN-C structure and exosomal composition differs in AA PBECs following RV infection, Analysis of TN-C mRNA splice expression in asthmatic samples would reveal whether certain FNIII domains are implicated in the disease and whether RV can further induce these domains. Further analysis of cell-associated TN-C in AA cells would also allow confirmation as to if intracellular protein expression correlates with the observed increased mRNA and released TN-C. Exosomes isolated from AA PBECs would allow the determination as to whether exosomes from AA PBECs have a greater inflammatory phenotype and whether this is potentiated further by RV infection.

Currently, the siRNA experiments performed in this study do not provide definitive evidence as to whether TN-C knockdown, alongside RV infection, modulates cytokine / chemokine release, and as to whether TN-C knockdown in exosomes modulates the amount of inflammation induced in RV-induced AEC-derived exosome stimulation. Co-culture experiments with AECs and MDMs, or AECs and other cells may help with this, as MDMs are more sensitive to TN-C stimulation and this may allow any potential differences to be distinguished. Moreover, siRNA treatment may be inducing inflammatory cytokine / chemokine release in the cells, either through direct stimulation or by inducing exosome compositional changes. Thus using clustered regularly interspaced short palindromic repeats (CRISPR) to create TN-C^{-/-} PBECs, and subsequent TN-C^{-/-} exosomes, would allow greater control over TN-C expression and avoid siRNA off target effects, such as cell cytotoxicity.

A number of further exosome stimulation experiments could be performed to elucidate the role of these vesicles in RV-induced inflammation. First, stimulation experiments with exosomes from AECs following RV infection needs to be completed, as these may produce differential responses from poly(I:C)-derived exosomes demonstrated in this study and the RSV-derived exosome stimulation study (Chahar et al. 2018). The rate of exosomal uptake can also be measured by EV internalisation assays, and if exosomes are internalised at a greater rate following RV infection, this may help determine whether TN-C plays a role in exosome target cell attachment, like FN and galectin-3 (Kulkarni and Prasad 2017). Transmission electron microscopy can also be used to image RV capsid or TN-C stained with an immunofluorescent dye. This would allow determination as to whether RV virions are present in AEC exosomes

following infection, and whether TN-C is present inside the vesicles or on the surface, helping to further clarify the composition and role of the exosomes following infection. A CBA assay could also be performed on supernatants of cells following TN-C and EV stimulation of AECs, in order to reveal the full profile of cytokines and chemokines released, and importantly, the exosome and TN-C stimulation experiments should be conducted on PBECs also, in order to determine whether there are cellular differences between the cell line and primary cells.

6.3. Conclusion

In conclusion, this study has revealed a novel pathway whereby RV-infection of AECs induces both the expression and release of TN-C, and the release of exosomes. TN-C and exosomes produced upon viral infection are able to induce the release of inflammatory cytokines and chemokines from a number of cells in the airway, which may have important implication for asthma exacerbations.

It was demonstrated that overall TN-C mRNA expression, TN-C-FNIII-specific splice domain mRNA expression and cell-associated TN-C expression could be modulated in response to RV infection, ultimately leading to the significant release of TN-C from the cell. This pathway was demonstrated to be TLR3-dependent and independent of TLR7 and cell cytotoxicity. One of the most significant findings in this study is that TN-C release following RV infection was demonstrated to be more pronounced in asthmatics, potentially revealing why TN-C has been previously been demonstrated to be expressed in higher quantities in the asthmatic airway. The study also revealed for the first time, that AEC viral TLR3-dependent stimulation induced significant exosomal release and TN-C was associated with these exosomes, with expression correlating with exosome number.

RV-induced TN-C release was demonstrated to induce large inflammatory CXCL8 release from MDMs (correlating with previous work in the Midwood lab), whilst it was revealed for the first time that TN-C-FBG had the ability to induce moderate CXCL8 release from AECs. The main isoform released in response to RV infection was a large isoform >250 kDa in size, which has previously been demonstrated to induce greater amounts of inflammation and is more resistant to degradation, and thus RV-induced TN-C may persist in the airway, inducing chronic inflammation in the airway. Perhaps most importantly, exosomes from RV-infected AECs induced significant inflammatory and anti-viral cytokine / chemokines release from AECs, whilst exosomes from non-virally cells did not, and both types of exosomes induced CXCL8 release from MDMs. The role of TN-C in RV-induced exosomal inflammation, however, is yet to be elucidated.

The results in this study therefore, reveal two novel pathways of RV infection that have the ability to induce substantial inflammation in the airway. Both of these pathways also have the capacity to be potentiated further in asthma, and therefore may play roles in RV-induced exacerbations of asthma. Further investigation will reveal whether TN-C and exosomes can be

targeted for therapeutic effect, in order to dampen the overactive inflammatory response in the airway of asthmatics.

References

Papers

- Accordini, S., A. G. Corsico, M. Braggion, M. W. Gerbase, D. Gislason, A. Gulsvik, J. Heinrich, C. Janson, D. Jarvis, R. Jogi, I. Pin, Y. Schoefer, M. Bugiani, L. Cazzoletti, I. Cerveri, A. Marcon, R. de Marco, G. Therapy Hlth Economics Working & S. European Community Resp Hlth (2013) The Cost of Persistent Asthma in Europe: An International Population-Based Study in Adults. *International Archives of Allergy and Immunology*, 160, 93-101.
- Afsar, F. S., S. Aktas & G. Diniz (2011) Tenascin-C Expression in Papulosquamous Disorders Other than Psoriasis in Pediatric Patients: An Epiphenomenon? *Journal of Cutaneous Medicine and Surgery*, 15, 1-7.
- Aggarwal, S. & A. L. Gurney (2002) IL-17: Prototype Member of an Emerging Cytokine Family. *Journal of Leukocyte Biology*, 71, 1-8.
- Aihara, M., L. D. Truong, J. K. Dunn, T. M. Wheeler, P. T. Scardino & T. C. Thompson (1994) Frequency of Apoptotic Bodies Positively Correlates with Gleason Grade in Prostate-Cancer. *Human Pathology*, 25, 797-801.
- Aikawa, T., S. Shimura, H. Sasaki, M. Ebina & T. Takishima (1992) Marked Goblet Cell Hyperplasia with Mucus Accumulation in the Airways of Patients Who Died of Severe Acute Asthma Attack. *Chest*, 101, 916-921.
- Akhurst, R. J., S. A. Lehnert, A. Faissner & E. Duffie (1990) TGF-beta in Murine Morphogenetic Processes - the Early Embryo and Cardiogenesis. *Development*, 108, 645-656.
- Al-Muhsen, S., S. Letuve, A. Vazquez-Tello, M. A. Pureza, H. Al-Jahdali, A. S. Bahammam, Q. Hamid & R. Halwani (2013) Th17 Cytokines Induce Pro-Fibrotic Cytokines Release From Human Eosinophils. *Respiratory Research*, 14.
- Al Mubarak, R., N. Roberts, R. J. Mason, S. Alper & H. W. Chu (2018) Comparison of Pro- and Anti-Inflammatory Responses in Paired Human Primary Airway Epithelial Cells and Alveolar Macrophages. *Respiratory Research*, 19.
- Al-Nedawi, K., B. Meehan, R. S. Kerbel, A. C. Allison & J. Rak (2009) Endothelial Expression of Autocrine VEGF Upon the Uptake Of Tumor-Derived Microvesicles Containing Oncogenic EGFR. *Proceedings of the National Academy of Sciences of the United States of America*, 106, 3794-3799.
- Alenquer, M. & M. J. Amorim (2015) Exosome Biogenesis, Regulation, and Function in Viral Infection. *Viruses-Basel*, 7, 5066-5083.
- Alexopoulou, L., A. C. Holt, R. Medzhitov & R. A. Flavell (2001) Recognition of Double-Stranded RNA and Activation of NF-kappa B by Toll-Like Receptor 3. *Nature*, 413, 732-738.
- Altan-Bonnet, N. (2016) Extracellular Vesicles are the Trojan Horses of Viral Infection. *Current Opinion in Microbiology*, 32, 77-81.
- Amin, K., D. Ludviksdottir, C. Janson, O. Nettelbladt, E. Bjornsson, G. M. Roomans, G. Boman, L. Seveus, P. Venge & B. H. R. Grp (2000) Inflammation and Structural Changes in the Airways of Patients with Atopic and Nonatopic Asthma. *American Journal of Respiratory and Critical Care Medicine*, 162, 2295-2301.
- Araki, Y., K. I. Mukaisyo, H. Sugihara, Y. Fujiyama & T. Hattori (2010) Increased Apoptosis and Decreased Proliferation of Colonic Epithelium in Dextran Sulfate Sodium-Induced Colitis in Mice. *Oncology Reports*, 24, 869-874.
- Asano, T., N. Iwasaki, S. Kon, M. Kanayama, J. Morimoto, A. Minami & T. Uede (2014) alpha 9 beta 1 Integrin Acts as a Critical Intrinsic Regulator of Human Rheumatoid Arthritis. *Rheumatology*, 53, 415-424.
- Bailey, S. R., S. Boustany, J. K. Burgess, S. J. Hirst, H. S. Sharma, D. E. Simcock, P. R. Suravaram & M. Weckmann (2009) Airway Vascular Reactivity and Vascularisation in Human Chronic Airway Disease. *Pulmonary Pharmacology & Therapeutics*, 22, 417-425.
- Bakhti, M., C. Winter & M. Simons (2011) Inhibition of Myelin Membrane Sheath Formation by Oligodendrocyte-Derived Exosome-Like Vesicles. *Journal of Biological Chemistry*, 286, 787-796.

- Bandari, S. K., A. Purushothaman, V. C. Ramani, G. J. Brinkley, D. S. Chandrashekar, S. Varambally, J. A. Mobley, Y. Zhang, E. E. Brown, I. Vlodaysky & R. D. Sanderson (2018) Chemotherapy Induces Secretion of Exosomes Loaded With Heparanase that Degrades Extracellular Matrix and Impacts Tumor and Host Cell Behavior. *Matrix Biology*, 65, 104-118.
- Bandow, K., J. Kusuyama, M. Shamoto, K. Kakimoto, T. Ohnishi & T. Matsuguchi (2012) LPS-Induced Chemokine Expression in Both MyD88-Dependent and -Independent Manners is Regulated By Cot/Tp12-ERK Axis in Macrophages. *Febs Letters*, 586, 1540-1546.
- Barnett, S. B. L. & T. A. Nurmagambetov (2011) Costs of Asthma in the United States: 2002-2007. *Journal of Allergy and Clinical Immunology*, 127, 145-152.
- Bartlett, N. W., R. P. Walton, M. R. Edwards, J. Aniscenko, G. Caramori, J. Zhu, N. Glanville, K. J. Choy, P. Jourdan, J. Burnet, T. J. Tuthill, M. S. Pedrick, M. J. Hurle, C. Plumpton, N. A. Sharp, J. N. Bussell, D. M. Swallow, J. Schwarze, B. Guy, J. Walmond, P. K. Jeffery, C. M. Lloyd, A. Papi, R. A. Killington, D. J. Rowlands, E. D. Blair, N. J. Clarke & S. L. Johnston (2008) Mouse Models of Rhinovirus-Induced Disease and Exacerbation of Allergic Airway Inflammation. *Nature Medicine*, 14, 199-204.
- Becker, A. B. & E. M. Abrams (2017) Asthma Guidelines: the Global Initiative for Asthma in Relation to National Guidelines. *Current Opinion in Allergy and Clinical Immunology*, 17, 99-103.
- Belmokhtar, C. A., J. Hillion & E. Segal-Bendirdjian (2001) Staurosporine Induces Apoptosis Through Both Caspase-Dependent and Caspase-Independent Mechanisms. *Oncogene*, 20, 3354-3362.
- Bennett, J. A., L. R. Prince, L. C. Parker, C. A. Stokes, H. G. de Bruin, M. van den Berge, I. H. Heijink, M. K. Whyte & I. Sabroe (2012) Pellino-1 Selectively Regulates Epithelial Cell Responses to Rhinovirus. *Journal of Virology*, 86, 6595-6604.
- Berg, K., H. Andersen & T. C. Owen (2004) The Regulation of Rhinovirus Infection In Vitro by IL-8, HIF1 α , and TNF- α . *Apmis*, 112, 172-182.
- Bergeron, C., M. K. Tulic & Q. Hamid (2010) Airway Remodelling in Asthma: From Benchside to Clinical Practice. *Canadian Respiratory Journal*, 17, E85-E93.
- Berry, M., C. Brightling, I. Pavord & A. J. Wardlaw (2007) TNF- α in Asthma. *Current Opinion in Pharmacology*, 7, 279-282.
- Berube, K., Z. Prytherch, C. Job & T. Hughes (2010) Human Primary Bronchial Lung Cell Constructs: the New Respiratory Models. *Toxicology*, 278, 311-318.
- Bizzintino, J., W. M. Lee, I. A. Laing, F. Vang, T. Pappas, G. Zhang, A. C. Martin, S. K. Khoo, D. W. Cox, G. C. Geelhoed, P. C. McMinne, J. Goldblatt, J. E. Gern & P. N. Le Soue (2011) Association Between Human Rhinovirus C and Severity of Acute Asthma in Children. *European Respiratory Journal*, 37, 1037-1042.
- Blaas, D. & R. Fuchs (2016) Mechanism of Human Rhinovirus Infections. *Mol Cell Pediatr*, 3, 21.
- Bloom, C. I., F. Nissen, I. J. Douglas, L. Smeeth, P. Cullinan & J. K. Quint (2018) Exacerbation Risk and Characterisation of the UK's Asthma Population from Infants to Old Age. *Thorax*, 73, 313-320.
- Bochkov, Y. A., K. M. Hanson, S. Keles, R. A. Brockman-Schneider, N. N. Jarjour & J. E. Gern (2010) Rhinovirus-Induced Modulation of Gene Expression in Bronchial Epithelial Cells from Subjects with Asthma. *Mucosal Immunology*, 3, 69-80.
- Bochkov, Y. A., K. Watters, S. Ashraf, T. F. Griggs, M. K. Devries, D. J. Jackson, A. C. Palmenberg & J. E. Gern (2015) Cadherin-Related Family Member 3, a Childhood Asthma Susceptibility Gene Product, Mediates Rhinovirus C Binding and Replication. *Proceedings of the National Academy of Sciences of the United States of America*, 112, 5485-5490.
- Bonizzi, G. & M. Karin (2004) The Two NF- κ B Activation Pathways and Their Role in Innate and Adaptive Immunity. *Trends in Immunology*, 25, 280-288.
- Border, W. A. & N. A. Noble (1994) Transforming Growth-Factor- β in Tissue Fibrosis. *New England Journal of Medicine*, 331, 1286-1292.
- Borsi, L., B. Carnemolla, G. Nicolo, B. Spina, G. Tanara & L. Zardi (1992) Expression of Different Tenascin Isoforms in Normal, Hyperplastic and Neoplastic Human Breast Tissues. *International Journal of Cancer*, 52, 688-692.
- Borthwick, L. A., T. A. Wynn & A. J. Fisher (2013) Cytokine Mediated Tissue Fibrosis. *Biochim Biophys Acta*, 1832, 1049-60.

- Bossios, A., S. Psarras, D. Gourgiotis, C. L. Skevaki, A. G. Constantopoulos, P. Saxoni-Papageorgiou & N. G. Papadopoulos (2005) Rhinovirus Infection Induces Cytotoxicity and Delays Wound Healing in Bronchial Epithelial Cells. *Respiratory Research*, 6.
- Bourdon, M. A., C. J. Wikstrand, H. Furthmayr, T. J. Matthews & D. D. Bigner (1983) Human Glioma-Mesenchymal Extracellular-Matrix Antigen Defined by Monoclonal-Antibody. *Cancer Research*, 43, 2796-2805.
- Bousquet, J., E. Mantzouranis, A. A. Cruz, N. Ait-Khaled, C. E. Baena-Cagnani, E. R. Bleeker, C. E. Brightling, P. Burney, A. Bush, W. W. Busse, T. B. Casale, M. Chan-Yeung, R. C. Chen, B. Chowdhury, K. F. Chung, R. Dahl, J. M. Drazen, L. M. Fabbri, S. T. Holgate, F. Kauffmann, T. Haahtela, N. Khaltaev, J. P. Kiley, M. R. Masjedi, Y. Mohammad, P. O'Byrne, M. R. Partridge, K. F. Rabe, A. Togias, C. van Weel, S. Wenzel, N. S. Zhong & T. Zuberbier (2010) Uniform Definition of Asthma Severity, Control, and Exacerbations: Document Presented for the World Health Organization Consultation on Severe Asthma. *Journal of Allergy and Clinical Immunology*, 126, 926-938.
- Bradding, P., J. A. Roberts, K. M. Britten, S. Montefort, R. Djukanovic, R. Mueller, C. H. Heusser, P. H. Howarth & S. T. Holgate (1994) Interleukin-4, Interleukin-5, and Interleukin-6 And Tumor-Necrosis-Factor-alpha in Normal and Asthmatic Airways - Evidence for the Human Mast-Cell as a Source of These Cytokines. *American Journal of Respiratory Cell and Molecular Biology*, 10, 471-480.
- Branton, M. H. & J. B. Kopp (1999) TGF-beta and Fibrosis. *Microbes and Infection*, 1, 1349-1365.
- Brellier, F., K. Hostettler, H.-R. Hotz, C. Ozcakir, S. A. Cologlu, D. Togbe, B. Ryffel, M. Roth & R. Chiquet-Ehrismann (2011) Tenascin-C triggers fibrin accumulation by downregulation of tissue plasminogen activator. *Febs Letters*, 585, 913-920.
- Brewster, C. E. P., P. H. Howarth, R. Djukanovic, J. Wilson, S. T. Holgate & W. R. Roche (1990) Myofibroblasts and Subepithelial Fibrosis in Bronchial-Asthma. *American Journal of Respiratory Cell and Molecular Biology*, 3, 507-511.
- Brunner, A., C. Mayerl, A. Tzankov, I. Verdorfer, I. Tschorner, H. Rogatsch & G. Mikuz (2004) Prognostic Significance of Tenascin-C Expression in Superficial and Invasive Bladder Cancer. *Journal of Clinical Pathology*, 57, 927-931.
- Budnik, V., C. Ruiz-Canada & F. Wendler (2016) Extracellular Vesicles Round Off Communication in the Nervous System. *Nature Reviews Neuroscience*, 17, 160-172.
- Cakebread, J. A., Y. Xu, C. Grainge, V. Kehagia, P. H. Howarth, S. T. Holgate & D. E. Davies (2011) Exogenous IFN-beta has Antiviral and Anti-Inflammatory Properties in Primary Bronchial Epithelial Cells from Asthmatic Subjects Exposed to Rhinovirus. *Journal of Allergy and Clinical Immunology*, 127, 1148-U416.
- Cantaluppi, V., S. Gatti, D. Medica, F. Figliolini, S. Bruno, M. C. Deregibus, A. Sordi, L. Biancone, C. Tetta & G. Camussi (2012) Microvesicles Derived from Endothelial Progenitor Cells Protect the Kidney from Ischemia-Reperfusion Injury by MicroRNA-Dependent Reprogramming of Resident Renal Cells. *Kidney International*, 82, 412-427.
- Carmeliet, P. (2000) Mechanisms of Angiogenesis and Arteriogenesis. *Nature Medicine*, 6, 389-395.
- Carnemolla, B., P. Castellani, M. Ponassi, L. Borsi, S. Urbini, G. Nicolo, A. Dorcaratto, G. Viale, G. Winter, D. Neri & L. Zardi (1999) Identification of a Glioblastoma-Associated Tenascin-C Isoform by a High Affinity Recombinant Antibody. *American Journal of Pathology*, 154, 1345-1352.
- Castro, M., S. R. Bloch, M. V. Jenkerson, S. DeMartino, D. L. Hamilos, R. B. Cochran, X. P. E, L. A. Zhang, H. C. Wang, J. P. Bradley, K. B. Schechtman & M. J. Holtzman (2004) Asthma Exacerbations After Glucocorticoid Withdrawal Reflects T Cell Recruitment to the Airway. *American Journal of Respiratory and Critical Care Medicine*, 169, 842-849.
- Chahar, H. S., T. Corsello, A. S. Kudlicki, N. Komaravelli & A. Casola (2018) Respiratory Syncytial Virus Infection Changes Cargo Composition of Exosome Released from Airway Epithelial Cells. *Scientific Reports*, 8.
- Chang, M., W. Jin & S. C. Sun (2009) Peli1 Facilitates TRIF-dependent Toll-Like Receptor Signaling and Proinflammatory Cytokine Production. *Nature Immunology*, 10, 1089-U66.
- Chauhan, A. J., H. M. Inskip, C. H. Linaker, S. Smith, J. Schreiber, S. L. Johnston & S. T. Holgate (2003) Personal Exposure to Nitrogen Dioxide (NO₂) and the Severity of Virus-Induced Asthma in Children. *Lancet*, 361, 1939-1944.

- Chen, Y. H., W. L. Du, M. C. Hagemeijer, P. M. Takvorian, C. Pau, A. Cali, C. A. Brantner, E. S. Stempinski, P. S. Connelly, H. C. Ma, P. Jiang, E. Wimmer, G. Altan-Bonnet & N. Altan-Bonnet (2015) Phosphatidylserine Vesicles Enable Efficient En Bloc Transmission of Enteroviruses. *Cell*, 160, 619-630.
- Chiquet-Ehrismann, R. & R. P. Tucker (2004) Connective Tissues: Signalling by Tenascins. *International Journal of Biochemistry & Cell Biology*, 36, 1085-1089.
- Chiquet-Ehrismann, R., E. J. Mackie, C. A. Pearson & T. Sakakura (1986) Tenascin - An Extracellular-Matrix Protein Involved in Tissue Interactions During Fetal Development and Oncogenesis. *Cell*, 47, 131-139.
- Chiquet-Ehrismann, R., M. Tannheimer, M. Koch, A. Brunner, J. Spring, D. Martin, S. Baumgartner & M. Chiquet (1994) Tenascin-C Expression by Fibroblasts is Elevated in Stressed Collagen Gels. *Journal of Cell Biology*, 127, 2093-2101.
- Choi, U. Y., J. S. Kang, Y. S. Hwang & Y. J. Kim (2015) Oligoadenylate Synthase-Like (OASL) Proteins: Dual Functions and Associations with Diseases. *Experimental and Molecular Medicine*, 47.
- Chun, Y. H., J. Y. Park, H. Lee, H. S. Kim, S. Won, H. J. Joe, W. J. Chung, J.-s. Yoon, H. H. Kim, J. T. Kim & J. S. Lee (2013) Rhinovirus-Infected Epithelial Cells Produce More IL-8 and RANTES Compared with Other Respiratory Viruses. *Allergy Asthma & Immunology Research*, 5, 216-223.
- Chung, C. Y., J. E. Murphy-Ullrich & H. P. Erickson (1996) Mitogenesis, Cell Migration, and Loss of Focal Adhesions Induced by Tenascin-C Interacting with its Cell Surface Receptor, Annexin II. *Molecular Biology of the Cell*, 7, 883-892.
- Cifuentes-Diaz, C., E. Velasco, F. A. Meunier, D. Goudou, L. Belkadi, L. Faille, M. Murawsky, D. Angaut-Petit, J. Molgo, M. Schachner, Y. Saga, S. Aizawa & F. Rieger (1998) The Peripheral Nerve and the Neuromuscular Junction are Affected in the Tenascin-C-Deficient Mouse. *Cellular and Molecular Biology*, 44, 357-379.
- Clarke, C. J. P., A. Hales, A. Hunt & B. M. J. Foxwell (1998) IL-10-Mediated Suppression of TNF-alpha Production is Independent of its Ability to Inhibit NF Chi B Activity. *European Journal of Immunology*, 28, 1719-1726.
- Conde-Vancells, J., E. Rodriguez-Suarez, N. Embade, D. Gil, R. Matthiesen, M. Valle, F. Elortza, S. C. Lu, J. M. Mato & J. M. Falcon-Perez (2008) Characterization and Comprehensive Proteome Profiling of Exosomes Secreted by Hepatocytes. *Journal of Proteome Research*, 7, 5157-5166.
- Contoli, M., S. D. Message, V. Laza-Stanca, M. R. Edwards, P. A. B. Wark, N. W. Bartlett, T. Kebabdz, P. Mallia, L. A. Stanciu, H. L. Parker, L. Slater, A. Lewis-Antes, O. M. Kon, S. T. Holgate, D. E. Davies, S. V. Kolenko, A. Papi & S. L. Johnston (2006) Role of Deficient Type III Interferon-Lambda Production in Asthma Exacerbations. *Nature Medicine*, 12, 1023-1026.
- Conway, J. F. & D. A. D. Parry (1991) 3-Stranded Alpha-Fibrous Proteins - the Heptad Repeat and its Implications for Structure. *International Journal of Biological Macromolecules*, 13, 14-16.
- Corne, J. M., C. Marshall, S. Smith, J. Schreiber, G. Sanderson, S. T. Holgate & S. L. Johnston (2002) Frequency, Severity, and Duration of Rhinovirus Infections in Asthmatic and Non-Asthmatic Individuals: a Longitudinal Cohort Study. *Lancet*, 359, 831-834.
- Corry, D. B., G. Grunig, H. Hadeiba, V. P. Kurup, M. L. Warnock, D. Sheppard, D. M. Rennick & R. M. Locksley (1998) Requirements for Allergen-Induced Airway Hyperreactivity in T and B Cell-Deficient Mice. *Molecular Medicine*, 4, 344-355.
- Croft, S. N., E. J. Walker & R. Ghildyal (2018) Human Rhinovirus 3C Protease Cleaves RIPK1, Concurrent with Caspase 8 Activation. *Scientific Reports*, 8.
- Culley, F. J., A. A. J. Pennycook, J. S. Tregoning, J. S. Dodd, G. Walzl, T. N. Wells, T. Hussell & P. J. M. Openshaw (2006) Role of CCL5 (RANTES) in Viral Lung Disease. *Journal of Virology*, 80, 8151-8157.
- Denlinger, L. C., R. L. Sorkness, W. M. Lee, M. D. Evans, M. J. Wolff, S. K. Mathur, G. M. Crisafi, K. L. Gaworski, T. E. Pappas, R. F. Vrtis, E. A. Kelly, J. E. Gern & N. N. Jarjour (2011) Lower Airway Rhinovirus Burden and the Seasonal Risk of Asthma Exacerbation. *American Journal of Respiratory and Critical Care Medicine*, 184, 1007-1014.
- Denlinger, L. C., Engle, L., King, T. S., Avila, P., Krishnan, J. A., Sorkness, R. L. & Sorkness, C. (2014). Risk Factors For Delayed Recovery From Asthma Exacerbations. *American Journal Of Respiratory And Critical Care Medicine*, 189.

- Deszcz, L., E. Gaudernak, E. Kuechler & J. Seipelt (2005) Apoptotic Events Induced by Human Rhinovirus Infection. *Journal of General Virology*, 86, 1379-1389.
- Diebold, S. S., T. Kaisho, H. Hemmi, S. Akira & C. R. E. Sousa (2004) Innate Antiviral Responses by Means of TLR7-Mediated Recognition of Single-Stranded RNA. *Science*, 303, 1529-1531.
- Ding, L., Zhang, Z. W., Shang, D., Cheng, J., Yuan, H., Wu, Y. N., Song, X. L. & Jiang, H. B. (2014) Alpha-Smooth Muscle Actin-Positive Myofibroblasts, In Association With Epithelial-Mesenchymal Transition And Lymphogenesis, Is A Critical Prognostic Parameter In Patients With Oral Tongue Squamous Cell Carcinoma. *Journal Of Oral Pathology & Medicine*, 43, 335-343.
- Doeing, D. C. & Solway, J. (2013). Airway Smooth Muscle In The Pathophysiology And Treatment Of Asthma. *Journal Of Applied Physiology*, 114, 834-843.
- Duan, M. B., M. L. Hibbs & W. S. Chen (2017) The Contributions of Lung Macrophage and Monocyte Heterogeneity to Influenza Pathogenesis. *Immunology and Cell Biology*, 95, 225-235.
- Duncan, E. M. & J. V. Fahy (2017) Asthma and Corticosteroids: Time for a More Precise Approach to Treatment. *European Respiratory Journal*, 49.
- Dunnill, M. S. (1960) The Pathology of Asthma, with Special Reference to Changes in the Bronchial Mucosa. *Journal of Clinical Pathology*, 13, 27-33.
- DUVERNELLE, C., FREUND, V. & FROSSARD, N. (2003). Transforming growth factor-beta and its role in asthma. *Pulmonary Pharmacology & Therapeutics*, 16, 181-196
- Edlmayr, J., K. Niespodziana, T. Popow-Kraupp, V. Krzyzanek, M. Focke-Tejkl, D. Blaas, M. Grote & R. Valenta (2011) Antibodies Induced with Recombinant VP1 from Human Rhinovirus Exhibit Cross-Neutralisation. *European Respiratory Journal*, 37, 44-52.
- Edwards, M. R., N. W. Bartlett, D. Clarke, M. Birrell, M. Belvisi & S. L. Johnston (2009) Targeting the NF-kappa B Pathway in Asthma and Chronic Obstructive Pulmonary Disease. *Pharmacology & Therapeutics*, 121, 1-13.
- Edwards, M. R., C. A. Hewson, V. Laza-Stanca, H. T. H. Lau, N. Mukaida, M. B. Hershenson & S. L. Johnston (2007) Protein Kinase R, I Kappa B Kinase-beta and NF-kappa B are Required for Human Rhinovirus Induced Pro-Inflammatory Cytokine Production in Bronchial Epithelial Cells. *Molecular Immunology*, 44, 1587-1597.
- El Andaloussi, S., I. Maeger, X. O. Breakefield & M. J. A. Wood (2013) Extracellular Vesicles: Biology and Emerging Therapeutic Opportunities. *Nature Reviews Drug Discovery*, 12, 348-358.
- Emori, T., J. Hirose, K. Ise, J. Yomoda, M. Kasahara, T. Shinkuma, H. Yoshitomi, H. Ito, M. Hashimoto, S. Sugahara, H. Fujita, N. Yamamoto, Y. Morita, S. Narumiya & I. Aramori (2017) Constitutive Activation of Integrin alpha 9 Augments Self-Directed Hyperplastic and Proinflammatory Properties of Fibroblast-like Synoviocytes of Rheumatoid Arthritis. *Journal of Immunology*, 199, 3427-3436.
- Erickson, H. P. (1994) Reversible Unfolding of Fibronectin Type-III and Immunoglobulin Domains Provides the Structural Basis for Stretch and Elasticity of Titin and Fibronectin. *Proceedings of the National Academy of Sciences of the United States of America*, 91, 10114-10118.
- Estany, S., V. Vicens-Zygmunt, R. Llatjos, A. Montes, R. Penin, I. Escobar, A. Xaubet, S. Santos, F. Manresa, J. Dorca & M. Molina-Molina (2014) Lung Fibrotic Tenascin-C Upregulation is Associated with Other Extracellular Matrix Proteins and Induced by TGF beta 1. *Bmc Pulmonary Medicine*, 14.
- Etemadi, M. R., K. H. Ling, S. Z. Abidin, H. Y. Chee & Z. Sekawi (2017) Gene Expression Patterns Induced at Different Stages of Rhinovirus Infection in Human Alveolar Epithelial Cells. *Plos One*, 12.
- Fahy, J. V., K. W. Kim, J. Liu & H. A. Boushey (1995) Prominent Neutrophilic Inflammation in Sputum from Subjects with Asthma Exacerbation. *Journal of Allergy and Clinical Immunology*, 95, 843-852.
- Fedorov, Y., E. M. Anderson, A. Birmingham, A. Reynolds, J. Karpilow, K. Robinson, D. Leake, W. S. Marshall & A. Khvorova (2006) Off-Target Effects by siRNA Can Induce Toxic Phenotype. *Rna-a Publication of the Rna Society*, 12, 1188-1196.
- Ferrari, N. & F. Calvo (2014) Tumor Microenvironment: Unleashing Metalloproteinases to Induce a CAF Phenotype. *Current Biology*, 24, R1009-R1011.
- Fischer, D., M. BrownLudi, T. Schulthess & R. ChiquetEhrismann (1997) Concerted Action of Tenascin-C Domains in Cell Adhesion, Anti-Adhesion and Promotion of Neurite Outgrowth. *Journal of Cell Science*, 110, 1513-1522.

- Fluck, M., S. I. Mund, J. C. Schittny, S. Klossner, A. C. Durieux & M. N. Giraud (2008) Mechano-Regulated Tenascin-C Orchestrates Muscle Repair. *Proceedings of the National Academy of Sciences of the United States of America*, 105, 13662-13667.
- Foley, S. C. & Q. Hamid (2007) Images in Allergy and Immunology: Neutrophils in Asthma. *Journal of Allergy and Clinical Immunology*, 119, 1282-1286.
- Forsberg, E., E. Hirsch, L. Frohlich, M. Meyer, P. Ekblom, A. Aszodi, S. Werner & R. Fassler (1996) Skin Wounds and Severed nerves Heal Normally in Mice Lacking Tenascin-C. *Proceedings of the National Academy of Sciences of the United States of America*, 93, 6594-6599.
- Fouda, G. G., F. H. Jaeger, J. D. Amos, C. Ho, E. L. Kunz, K. Anasti, L. W. Stamper, B. E. Liebl, K. H. Barbas, T. Ohashi, M. A. Moseley, H.-X. Liao, H. P. Erickson, S. M. Alam & S. R. Permar (2013) Tenascin-C is an Innate Broad-Spectrum, HIV-1-Neutralizing Protein in Breast Milk. *Proceedings of the National Academy of Sciences of the United States of America*, 110, 18220-18225.
- Franchi, L., Wamer, N., Viani, K. & Nunez, G. (2009). Function Of Nod-Like Receptors In Microbial Recognition And Host Defense. *Immunological Reviews*, 227, 106-128.
- Francisco-Cruz, A., M. Aguilar-Santelises, O. Ramos-Espinosa, D. Mata-Espinosa, B. Marquina-Castillo, J. Barrios-Payan & R. Hernandez-Pando (2014) Granulocyte-Macrophage Colony-Stimulating Factor: Not Just Another Haematopoietic Growth Factor. *Medical Oncology*, 31.
- Freytmuth, F., A. Vabret, J. Brouard, F. Toutain, R. Verdon, J. Petitjean, S. Gouarin, J. F. Duhamel & B. Guillois (1999) Detection of Viral, Chlamydia Pneumoniae and Mycoplasma Pneumoniae Infections in Exacerbations of Asthma in Children. *Journal of Clinical Virology*, 13, 131-139.
- Fuchs, R. & D. Blaas (2012) Productive Entry Pathways of Human Rhinoviruses. *Advances in virology*, 2012, 826301-826301.
- Gagliardo, R., P. Chanez, M. Mathieu, A. Bruno, G. Costanzo, C. Gougat, I. Vachier, L. Bousquet, G. Bonsignore & A. M. Vignola (2003) Persistent Activation of Nuclear Factor-kappa B Signaling Pathway in Severe Uncontrolled Asthma. *American Journal of Respiratory and Critical Care Medicine*, 168, 1190-1198.
- Gale, M. & M. G. Katze (1998) Molecular mechanisms of Interferon Resistance Mediated by Viral-Directed Inhibition of PKR, the Interferon-Induced Protein Kinase. *Pharmacology & Therapeutics*, 78, 29-46.
- Galli, S. J. & M. Tsai (2012) IgE and Mast Cells in Allergic Disease. *Nature Medicine*, 18, 693-704.
- Garbino, J., M. W. Gerbase, W. Wunderli, L. Kolarova, L. P. Nicod, T. Rochat & L. Kaiser (2004) Respiratory Viruses and Severe Lower Respiratory Tract Complications in Hospitalized Patients. *Chest*, 125, 1033-1039.
- Garwood, J., U. Theodoridis, V. Calco, A. Dobbertin & A. Faissner (2012) Existence of Tenascin-C Isoforms in Rat that Contain the Alternatively Spliced AD1 Domain are Developmentally Regulated During Hippocampal Development. *Cellular and Molecular Neurobiology*, 32, 279-287.
- Gauchat, J. F., S. Henchoz, G. Mazzei, J. P. Aubry, T. Brunner, H. Blasey, P. Life, D. Talabot, L. Floresromo, J. Thompson, K. Kishi, J. Butterfield, C. Dahinden & J. Y. Bonnefoy (1993) Induction of Human IgE Synthesis in B-Cells by Mast-Cells and Basophils. *Nature*, 365, 340-343.
- GharaeeKermani, M. & S. H. Phan (1997) Lung Interleukin-5 Expression in Murine Bleomycin-Induced Pulmonary Fibrosis. *American Journal of Respiratory Cell and Molecular Biology*, 16, 438-447.
- Ghert, M. A., S. T. Jung, W. N. Qi, J. M. Harrelson, H. P. Erickson, J. A. Block & S. P. Scully (2001a) The Clinical Significance of Tenascin-C Splice Variant Expression in Chondrosarcoma. *Oncology*, 61, 306-314.
- Ghert, M. A., W. N. Qi, H. P. Erickson, J. A. Block & S. P. Scully (2001b) Tenascin-C Splice Variant Adhesive/Anti-Adhesive Effects on Chondrosarcoma Cell Attachment to Fibronectin. *Cell Structure and Function*, 26, 179-187.
- Giblin, S. P. & K. S. Midwood (2015) Tenascin-C: Form Versus Function. *Cell Adhesion & Migration*, 9, 48-82.
- Goh, F. G., A. M. Piccinini, T. Krausgruber, I. A. Udalova & K. S. Midwood (2010) Transcriptional Regulation of the Endogenous Danger Signal Tenascin-C: A Novel Autocrine Loop in Inflammation. *Journal of Immunology*, 184, 2655-2662.

- Golchin, A., S. Hosseinzadeh & A. Ardeshiryajimi (2018) The Exosomes Released from Different Cell Types and Their Effects in Wound Healing. *Journal of Cellular Biochemistry*, 119, 5043-5052.
- Golledge, J., P. Clancy, J. Maguire, L. Lincz & S. Koblar (2011) The Role of Tenascin-C in Cardiovascular Disease. *Cardiovascular Research*, 92, 19-28.
- Goritzka, M., S. Makris, F. Kausar, L. R. Durant, C. Pereira, Y. Kumagai, F. J. Culley, M. Mack, S. Akira & C. Johansson (2015) Alveolar Macrophage-Derived Type I Interferons Orchestrate Innate Immunity to RSV Through Recruitment of Antiviral Monocytes. *Journal of Experimental Medicine*, 212, 699-714.
- Graser, A., A. B. Ekici, N. Sopel, V. O. Melichar, T. Zimmermann, N. G. Papadopoulos, S. Taka, F. Ferrazzi, T. Vuorinen & S. Finotto (2016) Rhinovirus Inhibits IL-17A and the Downstream Immune Responses in Allergic Asthma. *Mucosal Immunology*, 9, 1183-1192.
- Greenberg, S. B. (2003) Respiratory Consequences of Rhinovirus Infection. *Archives of Internal Medicine*, 163, 278-284.
- Greening, D. W., H. Ji, M. S. Chen, B. W. S. Robinson, I. M. Dick, J. Creaney & R. J. Simpson (2016) Secreted Primary Human Malignant Mesothelioma Exosome Signature Reflects Oncogenic Cargo. *Scientific Reports*, 6.
- Gregory, P. A., A. G. Bert, E. L. Paterson, S. C. Barry, A. Tsykin, G. Farshid, M. A. Vadas, Y. Khew-Goodall & G. J. Goodall (2008) The mir-200 family and mir-205 Regulate Epithelial to Mesenchymal Transition by Targeting ZEB1 and SIP1. *Nature Cell Biology*, 10, 593-601.
- Greve, J. M., G. Davis, A. M. Meyer, C. P. Forte, S. C. Yost, C. W. Marior, M. E. Kamarck & A. McClelland (1989) The Major Human Rhinovirus Receptor is ICAM-1. *Cell*, 56, 839-847.
- Guillot, L., S. Medjane, K. Le-Barillec, V. Balloy, C. Danel, M. Chignard & M. Si-Tahar (2004) Response of Human Pulmonary Epithelial Cells to Lipopolysaccharide Involves Toll-like Receptor 4 (TLR4)-Dependent Signaling Pathways - Evidence for an Intracellular Compartmentalization of TLR4. *Journal of Biological Chemistry*, 279, 2712-2718.
- Gulcher, J. R., M. J. Alexakos, M. M. Lebeau, R. S. Lemons & K. Stefansson (1990) Chromosomal Localization of the Human Hexabrachion (Tenascin) Gene and Evidence for Recent Reduplication within the Gene. *Genomics*, 6, 616-622.
- Gulcher, J. R., D. E. Nies, L. S. Marton & K. Stefansson (1989) An Alternatively Spliced Region of the Human Hexabrachion Contains a Repeat of Potential N-Glycosylation Sites. *Proceedings of the National Academy of Sciences of the United States of America*, 86, 1588-1592.
- Gutierrez, M. J., J. L. Gomez, G. F. Perez, K. Pancham, S. Val, D. K. Pillai, M. Giri, S. Ferrante, R. Freishtat, M. C. Rose, D. Preciado & G. Nino (2016) Airway Secretory microRNAome Changes during Rhinovirus Infection in Early Childhood. *Plos One*, 11.
- Guttery, D. S., R. A. Hancox, K. T. Mulligan, S. Hughes, S. M. Lambe, J. H. Pringle, R. A. Walker, J. L. Jones & J. A. Shaw (2010) Association of Invasion-Promoting Tenascin-C Additional Domains with Breast Cancers in Young Women. *Breast Cancer Research*, 12.
- Ha, D., Yang, N. N. & Nadithe, V. (2016). Exosomes As Therapeutic Drug Carriers And Delivery Vehicles Across Biological Membranes: Current Perspectives And Future Challenges. *Acta Pharmaceutica Sinica B*, 6, 287-296.
- Hackett, T. L., S. M. Warner, D. Stefanowicz, F. Shaheen, D. V. Pechkovsky, L. A. Murray, R. Argentieri, A. Kicic, S. M. Stick, T. R. Bai & D. A. Knight (2009) Induction of Epithelial-Mesenchymal Transition in Primary Airway Epithelial Cells from Patients with Asthma by Transforming Growth Factor-beta 1. *American Journal of Respiratory and Critical Care Medicine*, 180, 122-133.
- Hall, I. P. (2000) Second Messengers, Ion Channels and Pharmacology of Airway Smooth Muscle. *European Respiratory Journal*, 15, 1120-1127.
- Halwani, R., A. Vazquez-Tello, Y. Sumi, M. A. Pureza, A. Bahammam, H. Al-Jahdali, A. Soussi-Gounni, B. Mahboub, S. Al-Muhsen & Q. Hamid (2013) Eosinophils Induce Airway Smooth Muscle Cell Proliferation. *Journal of Clinical Immunology*, 33, 595-604.
- Hamid, Q., M. K. Tulic, M. C. Liu & R. Moqbel (2003) Inflammatory Cells in Asthma: Mechanisms and Implications for Therapy. *Journal of Allergy and Clinical Immunology*, 111, S5-S17.
- Hancox, R. A., M. D. Allen, D. L. Holliday, D. R. Edwards, C. J. Pennington, D. S. Guttery, J. A. Shaw, R. A. Walker, J. H. Pringle & J. L. Jones (2009) Tumour-Associated Tenascin-C

- Isoforms Promote Breast Cancer Cell Invasion and Growth by Matrix Metalloproteinase-Dependent and Independent Mechanisms. *Breast Cancer Research*, 11.
- Harvala, H., C. L. McIntyre, N. J. McLeish, J. Kondracka, J. Palmer, P. Molyneaux, R. Gunson, S. Bennett, K. Templeton & P. Simmonds (2012) High Detection Frequency and Viral Loads of Human Rhinovirus Species A to C in Fecal Samples; Diagnostic and Clinical Implications. *Journal of Medical Virology*, 84, 536-542.
- Hasegawa, M., Y. Nakoshi, M. Muraki, A. Sudo, N. Kinoshita, T. Yoshida & A. Uchida (2007) Expression of Large Tenascin-C Splice variants in Synovial Fluid of Patients with Rheumatoid Arthritis. *Journal of Orthopaedic Research*, 25, 563-568.
- Hata, A. N. & R. M. Breyer (2004) Pharmacology and Signaling of Prostaglandin Receptors: Multiple Roles in Inflammation and Immune Modulation. *Pharmacology & Therapeutics*, 103, 147-166.
- Hatchwell, L., A. Collison, J. Girkin, K. Parsons, J. Y. Li, J. Zhang, S. Phipps, D. Knight, N. W. Bartlett, S. L. Johnston, P. S. Foster, P. A. B. Wark & J. Mattes (2015) Toll-Like Receptor 7 Governs Interferon and Inflammatory Responses to Rhinovirus and is Suppressed by IL-5-Induced Lung Eosinophilia. *Thorax*, 70, 854-861.
- Hauptmann, S., L. Zardi, A. Siri, B. Carnemolla, L. Borsi, N. Castellucci, B. Klosterhalfen, P. Hartung, J. Weis, G. Stocker, H. D. Haubeck & C. J. Kirkpatrick (1995) Extracellular-Matrix Proteins in Colorectal Carcinomas - Expression of Tenascin and Fibronectin Isoforms. *Laboratory Investigation*, 73, 172-182.
- Hauzenberger, D., P. Olivier, D. Gundersen & C. Ruegg (1999) Tenascin-C Inhibits beta 1 Integrin-Dependent T Lymphocyte Adhesion to Fibronectin Through the Binding of its FNIII 1-5 Repeats to Fibronectin. *European Journal of Immunology*, 29, 1435-1447.
- Heil, F., H. Hemmi, H. Hochrein, F. Ampenberger, C. Kirschning, S. Akira, G. Lipford, H. Wagner & S. Bauer (2004) Species-Specific Recognition of Single-Stranded RNA via Toll-Like Receptor 7 and 8. *Science*, 303, 1526-1529.
- Hemmings, B. A. & D. F. Restuccia (2015) The PI3K-PKB/Akt Pathway (vol 4, a011189, 2012). *Cold Spring Harbor Perspectives in Biology*, 7.
- Hewson, C. A., A. Jardine, M. R. Edwards, V. Laza-Stanca & S. L. Johnston (2005) Toll-Like Receptor 3 is Induced by and Mediates Antiviral Activity Against Rhinovirus Infection of Human Bronchial Epithelial Cells. *Journal of Virology*, 79, 12273-12279.
- Hofer, F., M. Gruenberger, H. Kowalski, H. Machat, M. Huettinger, E. Kuechler & D. Blaas (1994) Members of the Low-Density-Lipoprotein Receptor Family Mediate Cell Entry of a Minor-Group Common Cold Virus. *Proceedings of the National Academy of Sciences of the United States of America*, 91, 1839-1842.
- Hsia, H. C. & J. E. Schwarzbauer (2005) Meet The Tenascins: Multifunctional and Mysterious. *Journal of Biological Chemistry*, 280, 26641-26644.
- Hsu, C., Y. Morohashi, S. Yoshimura, N. Manrique-Hoyos, S. Y. Jung, M. A. Lauterbach, M. Bakhti, M. Gronborg, W. Mobius, J. Rhee, F. A. Barr & M. Simons (2010) Regulation of Exosome Secretion by Rab35 and its GTPase-Activating Proteins TBC1D10A-C. *Journal of Cell Biology*, 189, 223-232.
- Huang, W. T., Chiquet-Ehrismann, R., Moyano, J. V., Garcia-Pardo, A. & Orend, G. (2001). Interference Of Tenascin-C With Syndecan-4 Binding To Fibronectin Blocks Cell Adhesion And Stimulates Tumor Cell Proliferation. *Cancer Research*, 61, 8586-8594.
- Imaizumi, T., T. Aizawa, R. Hayakari, F. Xing, P. F. Meng, K. Tsuruga, T. Matsumiya, H. Yoshida, L. Wang, T. Tatsuta & H. Tanaka (2015) Tumor Necrosis Factor-alpha Synergistically Enhances Polyinosinic-Polycytidylic Acid-Induced Toll-Like Receptor 3 Signaling in Cultured Normal Human Mesangial Cells: Possible Involvement in the Pathogenesis of Lupus Nephritis. *Clinical and Experimental Nephrology*, 19, 75-81.
- Imanaka-Yoshida, K. & H. Aoki (2014) Tenascin-C and Mechanotransduction in the Development and Diseases of Cardiovascular System. *Frontiers in Physiology*, 5.
- Inal, J. M. & S. Jorfi (2013) Coxsackievirus B Transmission and Possible New Roles for Extracellular Vesicles. *Biochemical Society Transactions*, 41, 299-302.
- Ismail, S., C. A. Stokes, E. C. Prestwich, R. L. Roberts, J. K. Juss, I. Sabroe & L. C. Parker (2014) Phosphoinositide-3 Kinase Inhibition Modulates Responses to Rhinovirus by Mechanisms that Are Predominantly Independent of Autophagy. *Plos One*, 9.
- Ivanoff, L. A., J. W. Dubay, J. F. Morris, S. J. Roberts, L. Gutshall, E. J. Sternberg, E. Hunter, T. J. Matthews & S. R. Petteway (1992) V3 Loop Region of the HIV-1 GP120 Envelope Protein is Essential for Virus Infectivity. *Virology*, 187, 423-432.

- Jackson, A. L. & P. S. Linsley (2010) Recognizing and Avoiding siRNA Off-Target Effects for Target Identification and Therapeutic Application. *Nature Reviews Drug Discovery*, 9, 57-67.
- Jackson, D. J., R. E. Gangnon, M. D. Evans, K. A. Roberg, E. L. Anderson, T. E. Pappas, M. C. Printz, W. M. Lee, P. A. Shult, E. Reisdorf, K. T. Carlson-Dakes, L. P. Salazar, D. F. DaSilva, C. J. Tisler, J. E. Gern & R. F. Lemanske (2008) Wheezing Rhinovirus Illnesses in Early Life Predict Asthma Development in High-Risk Children. *American Journal of Respiratory and Critical Care Medicine*, 178, 667-672.
- Jackson, D. J., Rana B.M., Shamji B.W., Trujillo-Torralbo M.B., Footitt J., Del-Rosario J., Telcian A.G., Nikonova A., Zhu J., Aniscenko J., Gogsadze L., Bakhsoliani E., Traub S., Dhariwal J., Porter J., Hunt D., Hunt T., Hunt T., Stanciu LA, Khaitov M, Bartlett NW, Edwards MR, Kon OM, Mallia P, Papadopoulos NG, Akdis CA, Westwick J, Edwards MJ, Cousins DJ, Walton RP, Johnston SI. 2014. IL-33-Dependent Type 2 Inflammation During Rhinovirus-Induced Asthma Exacerbations In Vivo. 1373-1382.: *Am J Respir Crit Care Med*, .
- Jackson, W. T., T. H. Giddings, M. P. Taylor, S. Mulinyawe, M. Rabinovitch, R. R. Kopito & K. Kirkegaard (2005) Subversion of Cellular Autophagosomal Machinery by RNA Viruses. *Plos Biology*, 3, 861-871.
- Jacobs, S. E., D. M. Lamson, K. St George & T. J. Walsh (2013) Human Rhinoviruses. *Clinical Microbiology Reviews*, 26, 135-162.
- Jansen, F., X. Y. Yang, S. Proebsting, M. Hoelscher, D. Przybilla, K. Baumann, T. Schmitz, A. Dolf, E. Endl, B. S. Franklin, J. M. Sinning, M. Vasa-Nicotera, G. Nickenig & N. Werner (2014) MicroRNA Expression in Circulating Microvesicles Predicts Cardiovascular Events in Patients with Coronary Artery Disease. *Journal of the American Heart Association*, 3.
- Jelonek, K., P. Widlak & M. Pietrowska (2016) The Influence of Ionizing Radiation on Exosome Composition, Secretion and Intercellular Communication. *Protein and Peptide Letters*, 23, 656-663.
- Ji, H., D. W. Greening, T. W. Barnes, J. W. Lim, B. J. Tauro, A. Rai, R. Xu, C. Adda, S. Mathivanan, W. Zhao, Y. H. Xue, T. Xu, H. J. Zhu & R. J. Simpson (2013) Proteome Profiling of Exosomes Derived from Human Primary and Metastatic Colorectal Cancer Cells Reveal Differential Expression of Key Metastatic Factors and Signal Transduction Components. *Proteomics*, 13, 1672-1686.
- Jinnin, M., H. Ihn, Y. Asano, K. Yamane, M. Trojanowska & K. Tamaki (2004) Tenascin-C Upregulation by Transforming Growth Factor-beta in Human Dermal Fibroblasts Involves Smad3, Sp1, and Ets1. *Oncogene*, 23, 1656-1667.
- Jinnin, M., H. Ihn, Y. Asano, K. Yamane, M. Trojanowska & K. Tamaki (2006) Upregulation of Tenascin-C Expression by IL-13 in Human Dermal Fibroblasts via the Phosphoinositide 3-Kinase/Akt and the Protein Kinase C Signaling Pathways. *Journal of Investigative Dermatology*, 126, 551-560.
- Joester, A. & A. Faissner (1999) Evidence for Combinatorial Variability of Tenascin-C Isoforms and Developmental Regulation in the Mouse Central Nervous System. *Journal of Biological Chemistry*, 274, 17144-17151.
- Joester, A. & A. Faissner (2001) The Structure and Function of Tenascins in the Nervous System. *Matrix Biology*, 20, 13-22.
- John, A. E., Y. M. Zhu, C. E. Brightling, L. H. Pang & A. J. Knox (2009) Human Airway Smooth Muscle Cells from Asthmatic Individuals Have CXCL8 Hypersecretion Due to Increased NF-kappa B p65, C/EBP beta, and RNA Polymerase II Binding to the CXCL8 Promoter. *Journal of Immunology*, 183, 4682-4692.
- Johnston, S. L. (2005) Overview of Virus-Induced Airway Disease. *Proceedings of the American Thoracic Society*, 2, 150-6.
- Johnston, S. L., N. J. Freezer, W. Ritter, S. O'Toole & P. H. Howarth (1995a) Prostaglandin D2-Induced Bronchoconstriction is Mediated Only in Part by the Thromboxane Prostanoid Receptor. *Eur Respir J*, 8, 411-5.
- Johnston, S. L., A. Papi, M. M. Monick & G. W. Hunninghake (1997) Rhinoviruses Induce Interleukin-8 mRNA and Protein Production in Human Monocytes. *Journal of Infectious Diseases*, 175, 323-329.
- Johnston, S. L., P. K. Pattemore, G. Sanderson, S. Smith, F. Lampe, L. Josephs, P. Symington, S. Otoole, S. H. Myint, D. A. J. Tyrrell & S. T. Holgate (1995b) Community Study of Role

- of Viral-Infections in Exacerbations of Asthma in 9-11 Year-Old Children. *British Medical Journal*, 310, 1225-1229.
- Jones, F. S., M. P. Burgoon, S. Hoffman, K. L. Crossin, B. A. Cunningham & G. M. Edelman (1988) A CDNA Clone for Cytotactin Contains Sequences Similar to Epidermal Growth Factor-Like Repeats and Segments of Fibronectin and Fibrinogen. *Proceedings of the National Academy of Sciences of the United States of America*, 85, 2186-2190.
- Jones, F. S. & P. L. Jones (2000a) The Tenascin Family of ECM Glycoproteins: Structure, Function, and Regulation During Embryonic Development and Tissue Remodeling. *Developmental Dynamics*, 218, 235-259.
- Jones, P. L. & F. S. Jones (2000b) Tenascin-C in Development and Disease: Gene Regulation and Cell Function. *Matrix Biology*, 19, 581-596.
- Joyce, D. A., D. P. Gibbons, P. Green, J. H. Steer, M. Feldmann & F. M. Brennan (1994) 2 Inhibitors of Pro-Inflammatory Cytokine Release, Interleukin-10 and Interleukin-4, Have Contrasting Effects on Release of Soluble P75 Tumor-Necrosis-Factor Receptor by Cultured Monocytes. *European Journal of Immunology*, 24, 2699-2705.
- Kagan, J. C. (2010) Recycling Endosomes and TLR Signaling-The Rab11 GTPase Leads the Way. *Immunity*, 33, 578-580.
- Kanayama, M., D. Kurotaki, J. Morimoto, T. Asano, Y. Matsui, Y. Nakayama, Y. Saito, K. Ito, C. Kimura, N. Iwasaki, K. Suzuki, T. Harada, H. M. Li, J. Uehara, T. Miyazaki, A. Minami, S. Kon & T. Uede (2009) alpha(9) Integrin and Its Ligands Constitute Critical Joint Microenvironments for Development of Autoimmune Arthritis. *Journal of Immunology*, 182, 8015-8025.
- Kanayama, M., J. Morimoto, Y. Matsui, M. Ikesue, K. Danzaki, D. Kurotaki, K. Ito, T. Yoshida & T. Uede (2011) alpha(9)beta(1) Integrin-Mediated Signaling Serves as an Intrinsic Regulator of Pathogenic Th17 Cell Generation. *Journal of Immunology*, 187, 5851-5864.
- Kariyawasam, H. H., M. Aizen, J. Barkans, D. S. Robinson & A. B. Kay (2007) Remodeling and Airway Hyperresponsiveness but not Cellular Inflammation Persist After Allergen Challenge in Asthma. *American Journal of Respiratory and Critical Care Medicine*, 175, 896-904.
- Karjalainen, E. M., A. Lindqvist, L. A. Laitinen, T. Kava, A. Altraja, M. Halme & A. Laitinen (2003) Airway Inflammation and Basement Membrane Tenascin in Newly Diagnosed Atopic and Nonatopic Asthma. *Respiratory Medicine*, 97, 1045-1051.
- Karupiah, G., Q. W. Xie, R. M. L. Buller, C. Nathan, C. Duarte & J. D. Macmicking (1993) Inhibition of Viral Replication by Interferon-Gamma-Induced Nitric-Oxide Synthase. *Science*, 261, 1445-1448.
- Katpally, U., T. M. Fu, D. C. Freed, D. R. Casimiro & T. J. Smith (2009) Antibodies to the Buried N Terminus of Rhinovirus VP4 Exhibit Cross-Serotypic Neutralization. *Journal of Virology*, 83, 7040-7048.
- Kawai, T. & S. Akira (2010) The Role of Pattern-Recognition Receptors in Innate Immunity: Update on Toll-Like Receptors. *Nature Immunology*, 11, 373-384.
- Keerthikumar, S., D. Chisanga, D. Ariyaratne, H. Saffar, S. Anand, K. N. Zhao, M. Samuel, M. Pathan, M. Jois, N. Chilamkurti, L. Gangoda & S. Mathivanan (2016) ExoCarta: A Web-Based Compendium of Exosomal Cargo. *Journal of Molecular Biology*, 428, 688-692.
- Kesimer, M., M. Scull, B. Brighton, G. DeMaria, K. Burns, W. O'Neal, R. J. Pickles & J. K. Sheehan (2009) Characterization of Exosome-Like Vesicles Released from Human Tracheobronchial Ciliated Epithelium: a Possible Role in Innate Defense. *Faseb Journal*, 23, 1858-1868.
- Khan, M. A. (2013) Inflammation Signals Airway Smooth Muscle Cell Proliferation in Asthma Pathogenesis. *Multidisciplinary Respiratory Medicine*, 8.
- Kim, J., S. P. Sanders, E. S. Siekierski, V. Casolaro & D. Proud (2000) Role of NF-kappa B in Cytokine Production Induced from Human Airway Epithelial Cells by Rhinovirus Infection. *Journal of Immunology*, 165, 3384-3392.
- Kips, J. C. (2001). Cytokines in asthma. *European Respiratory Journal*, 18, 24S-33S.
- Kleckner, I. R. & M. P. Foster (2011) An introduction to NMR-based approaches for measuring protein dynamics. *Biochimica Et Biophysica Acta-Proteins and Proteomics*, 1814, 942-968.
- Klein, K. A. & W. T. Jackson (2011) Human Rhinovirus 2 Induces the Autophagic Pathway and Replicates More Efficiently in Autophagic Cells. *Journal of Virology*, 85, 9651-9654.

- Koizumi, Y., H. Nagase, T. Nakajima, M. Kawamura & K. Ohta (2016) Toll-Like Receptor 3 Ligand Specifically Induced Bronchial Epithelial Cell Death in Caspase Dependent Manner and Functionally Upregulated Fas Expression. *Allergol Int*, 65 Suppl, S30-7.
- Kong, S. M. Y., B. K. K. Chan, J. S. Park, K. J. Hill, J. B. Aitken, L. Cottle, H. Farghaian, A. R. Cole, P. A. Lay, C. M. Sue & A. A. Cooper (2014) Parkinson's Disease-Linked Human PARK9/ATP13A2 Maintains Zinc Homeostasis and Promotes alpha-Synuclein Externalization via Exosomes. *Human Molecular Genetics*, 23, 2816-2833.
- Konoshenko, M. Y., Lekchnov, E. A., Vlassov, A. V. & Laktionov, P. P. (2018). Isolation Of Extracellular Vesicles: General Methodologies And Latest Trends. *Biomed Research International*.
- Koyama, E., Leatherman, J. L., Shimazu, A., Nah, H. D. & Pacifici, M. (1995) Syndecan-3, Tenascin-C, And The Development Of Cartilaginous Skeletal Elements And Joints In Chick Limbs. *Developmental Dynamics*, 203, 152-162.
- Krishnan, V., Diette, G. B., Rand, C. S., Bilderback, A. L., Merriman, B., Hansel, N. N. & Krishnan, J. A. (2006). Mortality In Patients Hospitalized For Asthma Exacerbations In The United States. *American Journal Of Respiratory And Critical Care Medicine*, 174, 633-638.
- Krunkosky, T. M., B. M. Fischer, L. D. Martin, N. Jones, N. J. Akley & K. B. Adler (2000) Effects of TNF-alpha on Expression of ICAM-1 in Human Airway Epithelial Cells in vitro - Signaling Pathways Controlling Surface and Gene Expression. *American Journal of Respiratory Cell and Molecular Biology*, 22, 685-692.
- Kuhen, K. L. & C. E. Samuel (1999) Mechanism of Interferon Action: Functional Characterization of Positive and Negative Regulatory Domains that Modulate Transcriptional Activation of the Human RNA-Dependent Protein Kinase PKR Promoter. *Virology*, 254, 182-195.
- Kulkarni, R. & A. Prasad (2017) Exosomes Derived from HIV-1 Infected DCs Mediate Viral Trans-Infection via Fibronectin and Galectin-3. *Scientific Reports*, 7.
- Kulshreshtha, A., T. Ahmad, A. Agrawal & B. Ghosh (2013) Proinflammatory Role of Epithelial Cell-Derived Exosomes in Allergic Airway Inflammation. *Journal of Allergy and Clinical Immunology*, 131, 1194-+.
- Kumar, M., T. Ahmad, A. Sharma, U. Mabalirajan, A. Kulshreshtha, A. Agrawal & B. Ghosh (2011) Let-7 microRNA-Mediated Regulation of IL-13 and Allergic Airway Inflammation. *Journal of Allergy and Clinical Immunology*, 128, 1077-U545.
- Kuo, C., S. Lim, N. J. C. King, N. W. Bartlett, R. P. Walton, J. Zhu, N. Glanville, J. Aniscenko, S. L. Johnston, J. K. Burgess, J. L. Black & B. G. Oliver (2012) Rhinovirus Infection Induces Expression of Airway Remodelling Factors In Vitro and In Vivo (vol 16, pg 367, 2011). *Respirology*, 17, 192-192.
- Kuo, C., S. Lim, N. J. C. King, S. L. Johnston, J. K. Burgess, J. L. Black & B. G. Oliver (2011) Rhinovirus Infection Induces Extracellular Matrix Protein Deposition in Asthmatic and Non-Asthmatic Airway Smooth Muscle Cells. *American Journal of Physiology-Lung Cellular and Molecular Physiology*, 300, L951-L957.
- Kusagawa, H., K. Onoda, S. Namikawa, I. Yada, A. Okada, T. Yoshida & T. Sakakura (1998) Expression and Degeneration of Tenascin-C in Human Lung Cancers. *British Journal of Cancer*, 77, 98-102.
- L'Huillier, A. G., L. Kaiser, T. J. Petty, M. Kilowoko, E. Kyungu, P. Hongoa, G. Vieille, L. Turin, B. Genton, V. D'Acromont & C. Tapparel (2015) Molecular Epidemiology of Human Rhinoviruses and Enteroviruses Highlights Their Diversity in Sub-Saharan Africa. *Viruses-Basel*, 7, 6412-6423.
- Laitinen, A., A. Altraja, M. Kampe, M. Linden, I. Virtanen & L. A. Laitinen (1997) Tenascin is Increased in Airway Basement Membrane of Asthmatics and Decreased by an Inhaled Steroid. *American Journal of Respiratory and Critical Care Medicine*, 156, 951-958.
- Lakkaraju, A. & E. Rodriguez-Boulan (2008) Itinerant Exosomes: Emerging Roles in Cell and Tissue Polarity. *Trends in Cell Biology*, 18, 199-209.
- Lambert, K. A., L. A. Prendergast, S. C. Dharmage, M. Tang, M. O'Sullivan, T. Tran, J. Druce, P. Bardin, M. J. Abramson & B. Erbas (2017) The Role of Human Rhinovirus (HRV) Species on Asthma Exacerbation Severity in Children and Adolescents. *J Asthma*, 1-7.
- Lambrecht, B. N. & H. Hammad (2012) The Airway Epithelium in Asthma. *Nat Med*, 18, 684-92.
- Lange, K., M. Kammerer, M. E. Hegi, S. Grotegut, A. Dittmann, W. Huang, G. W. Yip, M. Gotte, C. Ruiz & G. Orend (2008) Endothelin Receptor Type B Counteracts Tenascin-C-

- Induced Endothelin Receptor Type A-Dependent Focal Adhesion and Actin Stress Fiber Disorganization. *European Journal of Cell Biology*, 87, 44-44.
- Lappalainen, U., J. A. Whitsett, S. E. Wert, J. W. Tichelaar & K. Bry (2005) Interleukin-1 beta Causes Pulmonary Inflammation, Emphysema, and Airway Remodeling in the Adult Murine Lung. *American Journal of Respiratory Cell and Molecular Biology*, 32, 311-318.
- Lasser, C., S. E. O'Neil, G. V. Shelke, C. Sihlbom, S. F. Hansson, Y. S. Gho, B. Lundback & J. Lotvall (2016) Exosomes in the Nose Induce Immune Cell Trafficking and Harbour an Altered Protein Cargo in Chronic Airway Inflammation. *Journal of Translational Medicine*, 14.
- Latijnhouwers, M., M. Bergers, M. Ponc, H. Dijkman, M. Andriessen & J. Schalkwijk (1997) Human Epidermal Keratinocytes are a Source of Tenascin-C During Wound Healing. *Journal of Investigative Dermatology*, 108, 776-783.
- Latijnhouwers, M., G. J. de Jongh, M. Bergers, M. J. M. de Rooij & J. Schalkwijk (2000) Expression of Tenascin-C Splice Variants by Human Skin Cells. *Archives of Dermatological Research*, 292, 446-454.
- Lau, C., X. Wang, L. Song, M. North, S. Wiehler, D. Proud & C. W. Chow (2008) Syk Associates with Clathrin and Mediates Phosphatidylinositol 3-Kinase Activation During Human Rhinovirus Internalization. *Journal of Immunology*, 180, 870-880.
- Lawrence, T. (2009) The Nuclear Factor NF-kappaB Pathway in Inflammation. *Cold Spring Harb Perspect Biol*, 1, a001651.
- Laza-Stanca, V., L. A. Stanciu, S. D. Message, M. R. Edwards, J. E. Gern & S. L. Johnston (2006) Rhinovirus Replication in Human Macrophages Induces NF-kappa B-Dependent Tumor Necrosis Factor alpha Production. *Journal of Virology*, 80, 8248-8258.
- Lee, H. D., D. Zhang, Z. W. Zhu, C. S. Dela Cruz & Y. Jin (2016) Epithelial Cell-Derived Microvesicles Activate Macrophages and Promote Inflammation via Microvesicle-Containing microRNAs. *Scientific Reports*, 6.
- Lee, Y. G., J. J. Jeong, S. Nyenhuis, E. Berdyshev, S. Chung, R. Ranjan, M. Karpurapu, J. Deng, F. Qian, E. A. B. Kelly, N. N. Jarjour, S. J. Ackerman, V. Natarajan, J. W. Christman & G. Y. Park (2015) Recruited Alveolar Macrophages, in Response to Airway Epithelial-Derived Monocyte Chemoattractant Protein 1/CCL2, Regulate Airway Inflammation and Remodeling in Allergic Asthma. *American Journal of Respiratory Cell and Molecular Biology*, 52, 772-784.
- Levanen, B., N. R. Bhakta, P. T. Paredes, R. Barbeau, S. Hiltbrunner, J. L. Pollack, C. M. Skold, M. Svartengren, J. Grunewald, S. Gabrielsson, A. Eklund, B. M. Larsson, P. G. Woodruff, D. J. Erle & A. M. Wheelock (2013) Altered microRNA Profiles in Bronchoalveolar Lavage Fluid Exosomes in Asthmatic Patients. *Journal of Allergy and Clinical Immunology*, 131, 894-+.
- Levy, D. E., I. J. Marie & J. E. Durbin (2011) Induction and Function of Type I and III Interferon in Response to Viral Infection. *Current Opinion in Virology*, 1, 476-486.
- Leynaert, B., J. Sunyer, R. Garcia-Esteban, C. Svanes, D. Jarvis, I. Cerveri, J. Draetva, T. Gislason, J. Heinrich, C. Janson, N. Kuenzli, R. de Marco, E. Omenaas, C. Raherison, F. G. Real, M. Wjst, E. Zemp, M. Zureik, P. G. J. Burney, J. M. Anto & F. Neukirch (2012) Gender Differences in Prevalence, Diagnosis and Incidence of Allergic and Non-Allergic Asthma: a Population-Based Cohort. *Thorax*, 67, 625-631.
- Liang, X. H., C. E. Hart & S. T. Croke (2013) Transfection of siRNAs can Alter miRNA levels and Trigger Non-Specific Protein Degradation in Mammalian Cells. *Biochimica Et Biophysica Acta-Gene Regulatory Mechanisms*, 1829, 455-468.
- Libert, C., N. Takahashi, A. Cauwels, P. Brouckaert, H. Bluethmann & W. Fiers (1994) Response of Interleukin-6-Deficient Mice to Tumor Necrosis Factor-Induced Metabolic Changes and Lethality. *European Journal of Immunology*, 24, 2237-2242.
- Lommatzsch, M. (2016) Severe Asthma: Definition, Diagnosis and Treatment. *Allergologie*, 39, 206-207.
- Loo, Y. M. & Gale, M. (2011). Immune Signaling By Rig-I-Like Receptors. *Immunity*, 34, 680-692.
- Lopez-Castejon, G. & D. Brough (2011) Understanding the Mechanism of IL-1 beta Secretion. *Cytokine & Growth Factor Reviews*, 22, 189-195.
- Lopez-Souza, N., S. Favoreto, H. Wong, T. Ward, S. Yagi, D. Schnurr, W. E. Finkbeiner, G. M. Dolganov, J. H. Widdicombe, H. A. Boushey & P. C. Avila (2009) In Vitro Susceptibility to Rhinovirus Infection is Greater for Bronchial than for Nasal Airway Epithelial Cells in Human Subjects. *Journal of Allergy and Clinical Immunology*, 123, 1384-1390.

- Lotvall, J., A. F. Hill, F. Hochberg, E. I. Buzas, D. Di Vizio, C. Gardiner, Y. S. Gho, I. V. Kurochkin, S. Mathivanan, P. Quesenberry, S. Sahoo, H. Tahara, M. H. Wauben, K. W. Witwer & C. Thery (2014) Minimal Experimental Requirements for Definition of Extracellular Vesicles and their Functions: a Position Statement from the International Society for Extracellular Vesicles. *J Extracell Vesicles*, 3, 26913.
- Lotzerich, M., P. S. Roulin, K. Boucke, R. Witte, O. Georgiev & U. F. Greber (2018) Rhinovirus 3C Protease Suppresses Apoptosis and Triggers Caspase-Independent Cell Death. *Cell Death & Disease*, 9.
- Lukacs, N. W., R. M. Strieter, S. W. Chensue, M. Widmer & S. L. Kunkel (1995) TNF-alpha Mediates Recruitment of Neutrophils and Eosinophils During Airway Inflammation. *Journal of Immunology*, 154, 5411-5417.
- Lumeng, C. N. (2016) Lung Macrophage Diversity and Asthma. *Annals of the American Thoracic Society*, 13, S31-S34.
- Lynch, C., M. Panagopoulou & C. D. Gregory (2017) Extracellular Vesicles Arising from Apoptotic Cells in Tumors: Roles in Cancer Pathogenesis and Potential Clinical Applications. *Frontiers in Immunology*, 8.
- Machino-Ohtsuka, T., K. Tajiri, T. Kimura, S. Sakai, A. Sato, T. Yoshida, M. Hiroe, Y. Yasutomi, K. Aonuma & K. Imanaka-Yoshida (2014) Tenascin-C Aggravates Autoimmune Myocarditis via Dendritic Cell Activation and Th17 Cell Differentiation. *Journal of the American Heart Association*, 3.
- Mackie, E. J., W. Halfter & D. Liverani (1988) Induction of Tenascin in Healing Wounds. *Journal of Cell Biology*, 107, 2757-2767.
- Maier, S., R. Lutz, L. Gelman, A. Sarasa-Renedo, S. Schenk, C. Grashoff & M. Chiquet (2008) Tenascin-C Induction by Cyclic Strain Requires Integrin-Linked Kinase. *Biochimica Et Biophysica Acta-Molecular Cell Research*, 1783, 1150-1162.
- Makinde, T., R. F. Murphy & D. K. Agrawal (2007) The Regulatory Role of TGF-beta in Airway Remodeling in Asthma. *Immunology and Cell Biology*, 85, 348-356.
- Matei, I., C. M. Ghajar & D. Lyden (2011) A Tenascin-C Foundation for the Metastatic Niche. *Cancer Cell*, 20, 139-141.
- Matsuda, A., T. Hirota, M. Akahoshi, M. Shimizu, M. Tamari, A. Miyatake, A. Takahashi, K. Nakashima, N. Takahashi, K. Obara, N. Yuyama, S. Doi, Y. Kamogawa, T. Enomoto, K. Ohshima, T. Tsunoda, S. Miyatake, K. Fujita, M. Kusakabe, K. Izuhara, Y. Nakamura, J. Hopkin & T. Shirakawa (2005) Coding SNP in Tenascin-C FNIII-D Domain Associates with Adult Asthma. *Human Molecular Genetics*, 14, 2779-2786.
- Matsuda, A., A. Yoshiki, Y. Tagawa, H. Matsuda & M. Kusakabe (1999) Corneal Wound Healing in Tenascin Knockout Mouse. *Investigative Ophthalmology & Visual Science*, 40, 1071-1080.
- Matsumoto, M. & T. Seya (2008) TLR3: Interferon Induction by Double-Stranded RNA Including Poly(I : C). *Advanced Drug Delivery Reviews*, 60, 805-812.
- Matsuzaki, H., Y. Mikami, K. Makita, H. Takeshima, M. Horie, S. Noguchi, T. Jo, O. Narumoto, T. Kohyama, H. Takizawa, T. Nagase & Y. Yamauchi (2015) Interleukin-17A and Toll-Like Receptor 3 Ligand Poly(I:C) Synergistically Induced Neutrophil Chemoattractant Production by Bronchial Epithelial Cells. *Plos One*, 10.
- Maxfield, F. R. & T. E. McGraw (2004) Endocytic Recycling. *Nature Reviews Molecular Cell Biology*, 5, 121-132.
- Mayer, A. K., M. Muehmer, J. Mages, K. Gueinzus, C. Hess, K. Heeg, R. Bals, R. Lang & A. H. Dalpke (2007) Differential Recognition of TLR-Dependent Microbial Ligands in Human Bronchial Epithelial Cells. *Journal of Immunology*, 178, 3134-3142.
- Mazzeo, C., J. A. Canas, M. P. Zafra, A. R. Marco, M. Fernandez-Nieto, V. Sanz, M. Mittelbrunn, M. Izquierdo, F. Baixauli, J. Sastre & V. del Pozo (2015) Exosome Secretion by Eosinophils: A Possible Role in Asthma Pathogenesis. *Journal of Allergy and Clinical Immunology*, 135, 1603-1613.
- McGraw, D. W., K. F. Almoosa, R. J. Paul, B. K. Kobilka & S. B. Liggett (2003) Antithetic Regulation by beta-Adrenergic Receptors of G(q) Receptor Signaling via Phospholipase C Underlies the Airway beta-Agonist Paradox. *Journal of Clinical Investigation*, 112, 619-626.
- McIntyre, C. L., N. J. Knowles & P. Simmonds (2013) Proposals for the Classification of Human Rhinovirus Species A, B and C into Genotypically Assigned Types. *Journal of General Virology*, 94, 1791-1806.

- McKenzie, A. N. J., J. A. Culpepper, R. D. Malefyt, F. Briere, J. Punnonen, G. Aversa, A. Sato, W. Dang, B. G. Cocks, S. Menon, J. E. Devries, J. Banchereau & G. Zurawski (1993) Interleukin-13, a T-Cell-Derived Cytokine that Regulates Human Monocyte And B-Cell Function. *Proceedings of the National Academy of Sciences of the United States of America*, 90, 3735-3739.
- McLean, G. R. (2014) Developing a Vaccine for Human Rhinoviruses. *J Vaccines Immun*, 2, 16-20.
- Melewicz, F. M., L. E. Kline, A. B. Cohen & H. L. Spiegelberg (1982) Characterization of FC-Receptors for IgE on Human Alveolar Macrophages. *Clinical and Experimental Immunology*, 49, 364-370.
- Menard, G. & E. Y. Bissonnette (2000) Priming of Alveolar Macrophages by Leukotriene D-4 - Potentiation of Inflammation. *American Journal of Respiratory Cell and Molecular Biology*, 23, 572-577.
- Merke, D. P., W. Chen, R. Morissette, Z. Xu, C. Van Ryzin, V. Sachdev, H. Hannoush, S. M. Shanbhag, A. T. Acevedo, M. Nishitani, A. E. Arai & N. B. McDonnell (2013) Tenascin-X Haploinsufficiency Associated with Ehlers-Danlos Syndrome in Patients with Congenital Adrenal Hyperplasia. *Journal of Clinical Endocrinology & Metabolism*, 98, E379-E387.
- Meuronen, A., P. Karisola, M. Leino, T. Savinko, K. Sirola, M. L. Majuri, P. Piirila, I. Virtanen, M. Makela, A. Laitinen, L. A. Laitinen & H. Alenius (2011) Attenuated Expression of Tenascin-C in Ovalbumin-Challenged STAT4^{-/-} mice. *Respiratory Research*, 12.
- Mi, Z. Y., S. D. Bhattacharya, V. M. Kim, H. T. Guo, L. J. Talbot & P. C. Kuo (2011) Osteopontin Promotes CCL5-Mesenchymal Stromal Cell-Mediated Breast Cancer Metastasis. *Carcinogenesis*, 32, 477-487.
- Michele, M. & A. Faissner (2009) Tenascin-C Stimulates Contactin-Dependent Neurite Outgrowth via Activation of Phospholipase C. *Molecular and Cellular Neuroscience*, 41, 397-408.
- Midwood, K., S. Sacre, A. M. Piccinini, J. Inglis, A. Trebault, E. Chan, S. Drexler, N. Sofat, M. Kashiwagi, G. Orend, F. Brennan & B. Foxwell (2009) Tenascin-C is an Endogenous Activator of Toll-Like Receptor 4 that is Essential for Maintaining Inflammation in Arthritic Joint Disease. *Nature Medicine*, 15, 774-U11.
- Midwood, K. S., M. Chiquet, R. P. Tucker & G. Orend (2016) Tenascin-C at a Glance. *Journal of Cell Science*, 129, 4321-4327.
- Midwood, K. S. & G. Orend (2009) The Role of Tenascin-C in Tissue Injury and Tumorigenesis. *Journal of Cell Communication and Signaling*, 3, 287-310.
- Mighell, A. J., J. Thompson, W. J. Hume, A. F. Markham & P. A. Robinson (1997) Human Tenascin-C: Identification of a Novel Type III Repeat in Oral Cancer and of Novel Splice Variants in Normal, Malignant and Reactive Oral Mucosae. *International Journal of Cancer*, 72, 236-240.
- Miller, E. K., N. Khuri-Bulos, J. V. Williams, A. A. Shehabi, S. Faouri, I. Al Jundi, Q. X. Chen, L. Heil, Y. Mohamed, L. L. Morin, A. Ali & N. B. Halasa (2009) Human Rhinovirus C Associated with Wheezing in Hospitalised Children in the Middle East. *Journal of Clinical Virology*, 46, 85-89.
- Minear, M. A., D. R. Crosslin, B. S. Sutton, J. J. Connelly, S. C. Nelson, S. Gadson-Watson, T. Y. Wang, D. Seo, J. M. Vance, M. H. Sketch, C. Haynes, P. J. Goldschmidt-Clermont, S. H. Shah, W. E. Kraus, E. R. Hauser & S. G. Gregory (2011) Polymorphic Variants in Tenascin-C (TNC) are Associated with Atherosclerosis and Coronary Artery Disease. *Human Genetics*, 129, 641-654.
- Minn, A. J., G. P. Gupta, P. M. Siegel, P. D. Bos, W. P. Shu, D. D. Giri, A. Viale, A. B. Olshen, W. L. Gerald & J. Massague (2005) Genes that Mediate Breast Cancer Metastasis to Lung. *Nature*, 436, 518-524.
- Misharin, A. V., L. Morales-Nebreda, P. A. Reyfman, C. M. Cuda, J. M. Walter, A. C. McQuattie-Pimentel, C. I. Chen, K. R. Anekalla, N. Joshi, K. J. N. Williams, H. Abdala-Valencia, T. J. Yacoub, M. Chi, S. Chiu, F. J. Gonzalez-Gonzalez, K. Gates, A. P. Lam, T. T. Nicholson, P. J. Homan, S. Soberanes, S. Dominguez, V. K. Morgan, R. Saber, A. Shaffer, M. Hinchcliff, S. A. Marshall, A. Bharat, S. Berdnikovs, S. M. Bhorade, E. T. Bartom, R. I. Morimoto, W. E. Balch, J. I. Sznajder, N. S. Chandel, G. M. Mutlu, M. Jain, C. J. Gottardi, B. D. Singer, K. M. Ridge, N. Bagheri, A. Shilatifard, G. R. S. Budinger & H. Perlman (2017) Monocyte-Derived Alveolar Macrophages Drive Lung Fibrosis and Persist in the Lung Over the life Span. *Journal of Experimental Medicine*, 214, 2387-2404.

- Monick, M. M., T. O. Yarovinsky, L. S. Powers, N. S. Butler, A. B. Carter, G. Gudmundsson & G. W. Hunninghake (2003) Respiratory Syncytial Virus Upregulates TLR4 and Sensitizes Airway Epithelial Cells to Endotoxin. *Journal of Biological Chemistry*, 278, 53035-53044.
- Moon, H. G., Y. Cao, J. Yang, J. H. Lee, H. S. Choi & Y. Jin (2015) Lung Epithelial Cell-Derived Extracellular Vesicles Activate Macrophage-Mediated Inflammatory Responses via ROCK1 Pathway. *Cell Death & Disease*, 6.
- Morawski, M., A. Dityatev, M. Hartlage-Ruebsamen, M. Blosa, M. Holzer, K. Flach, S. Pavlica, G. Dityateva, J. Grosche, G. Brueckner & M. Schachner (2014) Tenascin-R Promotes Assembly of the Extracellular Matrix of Perineuronal Nets via Clustering of Aggrecan. *Philosophical Transactions of the Royal Society B-Biological Sciences*, 369.
- Morjaria, J. B., K. S. Babu, P. Vijayanand, A. J. Chauhan, D. E. Davies & S. T. Holgate (2011) Sputum IL-6 Concentrations in Severe Asthma and its Relationship with FEV1. *Thorax*, 66, 537-537.
- Morris, G. E., L. C. Parker, J. R. Ward, E. C. Jones, M. K. B. Whyte, C. E. Brightling, P. Bradding, S. K. Dower & I. Sabroe (2006) Cooperative Molecular and Cellular networks Regulate Toll-Like Receptor-Dependent Inflammatory Responses. *Faseb Journal*, 20, 2153-+.
- Mosser, A. G., R. Brockman-Schneider, S. Amineva, L. Burchell, J. B. Sedgwick, W. W. Busse & J. E. Gern (2002) Similar Frequency of Rhinovirus-Infectible Cells in Upper and Lower Airway Epithelium. *Journal of Infectious Diseases*, 185, 734-743.
- Mukherjee, M., A. Stoddart, R. P. Gupta, B. I. Nwaru, A. Farr, M. Heaven, D. Fitzsimmons, A. Bandyopadhyay, C. Aftab, C. R. Simpson, R. A. Lyons, C. Fischbacher, C. Dibben, M. D. Shields, C. J. Phillips, D. P. Strachan, G. A. Davies, B. McKinstry & A. Sheikh (2016) The Epidemiology, Healthcare and Societal Burden and Costs of Asthma in the UK and its Member Nations: Analyses of Standalone and Linked National Databases. *BMC Med*, 14, 113.
- Muralidharan-Chari, V., J. Clancy, C. Plou, M. Romao, P. Chavrier, G. Raposo & C. D'Souza-Schorey (2009) ARF6-Regulated Shedding of Tumor Cell-Derived Plasma Membrane Microvesicles. *Current Biology*, 19, 1875-1885.
- Murdoch, J. R. & C. M. Lloyd (2010) Chronic Inflammation and Asthma. *Mutation Research-Fundamental and Molecular Mechanisms of Mutagenesis*, 690, 24-39.
- Nagarkar, D. R., E. R. Bowman, D. Schneider, Q. O. Wang, J. Shim, Y. Zhao, M. J. Linn, C. L. McHenry, B. Gosangi, J. K. Bentley, W. C. Tsai, U. S. Sajjan, N. W. Lukacs & M. B. Hershenson (2010) Rhinovirus Infection of Allergen-Sensitized and -Challenged Mice Induces Eotaxin Release from Functionally Polarized Macrophages. *Journal of Immunology*, 185, 2525-2535.
- Nakagome, K., Y. A. Bochkov, S. Ashraf, R. A. Brockman-Schneider, M. D. Evans, T. R. Pasic & J. E. Gern (2014) Effects of Rhinovirus Species on Viral Replication and Cytokine Production. *Journal of Allergy and Clinical Immunology*, 134, 332-+.
- Nakahara, H., E. C. Gabazza, H. Fujimoto, Y. Nishii, C. N. D'Alessandro-Gabazza, N. E. Bruno, T. Takagi, T. Hayashi, J. Maruyama, K. Maruyama, K. Imanaka-Yoshida, K. Suzuki, T. Yoshida, Y. Adachi & O. Taguchi (2006) Deficiency of Tenascin C Attenuates Allergen-Induced Bronchial Asthma in the Mouse. *European Journal of Immunology*, 36, 3334-3345.
- Nakamura, Y., S. Esnault, T. Maeda, E. A. B. Kelly, J. S. Malter & N. N. Jarjour (2004) Ets-1 Regulates TNF-alpha-Induced Matrix Metalloproteinase-9 and Tenascin Expression in Primary Bronchial Fibroblasts. *Journal of Immunology*, 172, 1945-1952.
- Nakamura-Ishizu, A., Y. Okuno, Y. Omatsu, K. Okabe, J. Morimoto, T. Uede, T. Nagasawa, T. Suda & Y. Kubota (2012) Extracellular Matrix Protein Tenascin-C is Required in the Bone Marrow Microenvironment Primed for Hematopoietic Regeneration. *Blood*, 119, 5429-5437.
- Nakoshi, Y., M. Hasegawa, A. Sudo, T. Yoshida & A. Uchida (2008) Regulation of Tenascin-C Expression by Tumor Necrosis Factor-alpha in Cultured Human Osteoarthritis Chondrocytes. *Journal of Rheumatology*, 35, 147-152.
- Narayanan, A., S. Iordanskiy, R. Das, R. Van Duyne, S. Santos, E. Jaworski, I. Guendel, G. Sampey, E. Dalby, M. Iglesias-Ussel, A. Popratiloff, R. Hakami, K. Kehn-Hall, M. Young, C. Subra, C. Gilbert, C. Bailey, F. Romerio & F. Kashanchi (2013) Exosomes Derived from HIV-1-infected Cells Contain Trans-Activation Response Element RNA. *Journal of Biological Chemistry*, 288, 20014-20033.

- Newcomb, D. C., U. S. Sajjan, D. R. Nagarkar, Q. Wang, S. Nanua, Y. Zhou, C. L. McHenry, K. T. Hennrick, W. C. Tsai, J. K. Bentley, N. W. Lukacs, S. L. Johnston & M. B. Hershenson (2008) Human Rhinovirus 1B Exposure Induces Phosphatidylinositol 3-Kinase-Dependent Airway Inflammation in Mice. *American Journal of Respiratory and Critical Care Medicine*, 177, 1111-1121.
- Nicholson, K. G., J. Kent & D. C. Ireland (1993) Respiratory Viruses and Exacerbations of Asthma in Adults. *British Medical Journal*, 307, 982-986.
- Nishio, T., S. Kawaguchi, T. Iseda, T. Kawasaki & T. Hase (2003) Secretion of Tenascin-C by Cultured Astrocytes: Regulation of Cell Proliferation and Process Elongation. *Brain Research*, 990, 129-140.
- Noah, T. L., J. R. Yankaskas, J. L. Carson, T. M. Gambling, L. H. Cazares, K. P. McKinnon & R. B. Devlin (1995) Tight Junctions and Mucin Messenger-RNA in BEAS-2B Cells. *In Vitro Cellular & Developmental Biology-Animal*, 31, 738-740.
- O'Byrne, P. M. & M. D. Inman (2003) Airway Hyperresponsiveness. *Chest*, 123, 411S-416S.
- Oberhauser, A. F., P. E. Marszalek, H. P. Erickson & J. M. Fernandez (1998) The Molecular Elasticity of the Extracellular Matrix Protein Tenascin. *Nature*, 393, 181-185.
- Ocklind, G., J. Talts, R. Fassler, A. Mattsson & P. Ekblom (1993) Expression of Tenascin in Developing and Adult-Mouse Lymphoid Organs. *Journal of Histochemistry & Cytochemistry*, 41, 1163-1169.
- Opal, S. M. & V. A. DePalo (2000) Anti-Inflammatory Cytokines. *Chest*, 117, 1162-1172.
- Ordonez, C. L., R. Khashayar, H. H. Wong, R. Ferrando, R. Wu, D. M. Hyde, J. A. Hotchkiss, Y. Zhang, A. Novikov, G. Dolganov & J. V. Fahy (2001) Mild and Moderate Asthma is associated with Airway Goblet Cell Hyperplasia and Abnormalities in Mucin Gene Expression. *American Journal of Respiratory and Critical Care Medicine*, 163, 517-523.
- Ordonez, C. L., T. E. Shaughnessy, M. A. Matthay & J. V. Fahy (2000) Increased Neutrophil Numbers and IL-8 levels in Airway Secretions in Acute Severe Asthma Clinical and Biologic Significance. *American Journal of Respiratory and Critical Care Medicine*, 161, 1185-1190.
- Oshita, Y., T. Koga, T. Kamimura, K. Matsuo, T. Rikimaru & H. Aizawa (2003) Increased Circulating 92 kDa Matrix Metalloproteinase (MMP-9) Activity in Exacerbations of Asthma. *Thorax*, 58, 757-760.
- Page, T. H., P. J. Charles, A. M. Piccinini, V. Nicolaidou, P. C. Taylor & K. S. Midwood (2012) Raised Circulating Tenascin-C in Rheumatoid Arthritis. *Arthritis Research & Therapy*, 14.
- Panakova, D., H. Sprong, E. Marois, C. Thiele & S. Eaton (2005) Lipoprotein Particles are Required for Hedgehog and Wingless Signalling. *Nature*, 435, 58-65.
- Papi, A. & S. L. Johnston (1999) Rhinovirus Infection Induces Expression of its Own Receptor Inter Cellular Adhesion Molecule 1 (ICAM-1) via Increased NF-kappa B-Mediated Transcription. *Journal of Biological Chemistry*, 274, 9707-9720.
- Paredes, P. T., J. Esser, C. Admyre, M. Nord, Q. K. Rahman, A. Lukic, O. Radmark, R. Gronneberg, J. Grunewald, A. Eklund, A. Scheynius & S. Gabrielsson (2012) Bronchoalveolar Lavage Fluid Exosomes Contribute to Cytokine and Leukotriene Production in Allergic Asthma. *Allergy*, 67, 911-919.
- Park, B. S., D. H. Song, H. M. Kim, B. S. Choi, H. Lee & J. O. Lee (2009) The Structural Basis of Lipopolysaccharide Recognition by the TLR4-MD-2 Complex. *Nature*, 458, 1191-U130.
- Parker, L. C., E. C. Prestwich, J. R. Ward, E. Smythe, A. Berry, M. Triantafilou, K. Triantafilou & I. Sabroe (2008) A Phosphatidylserine Species Inhibits a Range of TLR- but not IL-1 beta-Induced Inflammatory Responses by Disruption of Membrane Microdomains. *Journal of Immunology*, 181, 5606-5617.
- Parker, L. C., C. A. Stokes & I. Sabroe (2014) Rhinoviral Infection and Asthma: The Detection and Management of Rhinoviruses by Airway Epithelial Cells. *Clinical and Experimental Allergy*, 44, 20-28.
- Patel, S., A. Maheshwari & A. Chandra (2016) Biomarkers for Wound Healing and their Evaluation. *Journal of Wound Care*, 25, 46-55.
- Pearce, N., N. Ait-Khaled, R. Beasley, J. Mallol, U. Keil, E. Mitchell, C. Robertson & I. P. T. S. Grp (2007) Worldwide Trends in the Prevalence of Asthma Symptoms: Phase III of the International Study of Asthma and Allergies in Childhood (ISAAC). *Thorax*, 62, 758-766.
- Petrik, J. (2016) Immunomodulatory Effects of Exosomes Produced by Virus-Infected Cells. *Transfusion and Apheresis Science*, 55, 84-91.

- Pezzulo, A. A., T. D. Starner, T. E. Scheetz, G. L. Traver, A. E. Tilley, B. G. Harvey, R. G. Crystal, P. B. McCray & J. Zabner (2011) The Air-Liquid Interface and Use of Primary Cell Cultures are Important to Recapitulate the Transcriptional Profile of In Vivo Airway Epithelia. *American Journal of Physiology-Lung Cellular and Molecular Physiology*, 300, L25-L31.
- Piccinini, A. M. & K. S. Midwood (2012) Endogenous Control of Immunity Against Infection: Tenascin-C Regulates TLR4-Mediated Inflammation via MicroRNA-155. *Cell Reports*, 2, 914-926.
- Piccinini, A. M., L. Zuliani-Alvarez, J. M. P. Lim & K. S. Midwood (2016) Distinct Microenvironmental Cues Stimulate Divergent TLR4-Mediated Signaling Pathways in Macrophages. *Science Signaling*, 9.
- Pillai, P., C. J. Corrigan & S. Ying (2011) Airway Epithelium in Atopic and Non-Atopic Asthma: Similarities and Differences. *ISRN allergy*, 2011, 195846-195846.
- Piper, S. C., J. Ferguson, L. Kay, L. C. Parker, I. Sabroe, M. A. Sleeman, E. Briend & D. K. Finch (2013) The Role of Interleukin-1 and Interleukin-18 in Pro-Inflammatory and Anti-Viral Responses to Rhinovirus in Primary Bronchial Epithelial Cells. *Plos One*, 8.
- Pollart, S. M., R. M. Compton & K. S. Elward (2011) Management of Acute Asthma Exacerbations. *American Family Physician*, 84, 40-47.
- Poynter, M. E., C. G. Irvin & Y. M. W. Janssen-Heininger (2002) Rapid Activation of Nuclear Factor-kappa B in Airway Epithelium in a Murine Model of Allergic Airway Inflammation. *American Journal of Pathology*, 160, 1325-1334.
- Prieto, A. L., C. Anderssonfison & K. L. Crossin (1992) Characterization of Multiple Adhesive and Counteradhesive Domains in the Extracellular-Matrix Protein Cytotactin. *Journal of Cell Biology*, 119, 663-678.
- Proud, D., R. B. Turner, B. Winther, S. Wiehler, J. P. Tiesman, T. D. Reichling, K. D. Juhlin, A. W. Fulmer, B. Y. Ho, A. A. Walanski, C. L. Poore, H. Mizoguchi, L. Jump, M. L. Moore, C. K. Zukowski & J. W. Clymer (2008) Gene Expression Profiles During In Vivo Human Rhinovirus Infection Insights into the Host Response. *American Journal of Respiratory and Critical Care Medicine*, 178, 962-968.
- Pugin, J., C. C. Schurermaly, D. Leturcq, A. Moriarty, R. J. Ulevitch & P. S. Tobias (1993) Lipopolysaccharide Activation of Human Endothelial and Epithelial-Cells is Mediated by Lipopolysaccharide-Binding Protein and Soluble CD14. *Proceedings of the National Academy of Sciences of the United States of America*, 90, 2744-2748.
- Qu, Y., L. Franchi, G. Nunez & G. R. Dubyak (2007) Nonclassical IL-1 beta Secretion Stimulated by P2X7 Receptors is Dependent on Inflammasome Activation and Correlated with Exosome Release in Murine Macrophages. *Journal of Immunology*, 179, 1913-1925.
- Raab-Traub, N. & D. P. Dittmer (2017) Viral Effects on the Content and Function of Extracellular Vesicles. *Nature Reviews Microbiology*, 15, 559-572.
- Ramakrishnaiah, V., C. Thumann, I. Fofana, F. Habersetzer, Q. W. Pan, P. E. de Ruyter, R. Willemsen, J. A. A. Demmers, V. S. Raj, G. Jenster, J. Kwekkeboom, H. W. Tilanus, B. L. Haagsma, T. F. Baumert & L. J. W. van der Laan (2013) Exosome-Mediated Transmission of Hepatitis C Virus Between Human Hepatoma Huh7.5 cells. *Proceedings of the National Academy of Sciences of the United States of America*, 110, 13109-13113.
- Raposo, G., H. W. Nijman, W. Stoorvogel, R. Leijendekker, C. V. Harding, C. J. M. Melief & H. J. Geuze (1996) B Lymphocytes Secrete Antigen-Presenting Vesicles. *Journal of Experimental Medicine*, 183, 1161-1172.
- Raposo, G. & W. Stoorvogel (2013) Extracellular Vesicles: Exosomes, Microvesicles, and Friends. *Journal of Cell Biology*, 200, 373-383.
- Rawlinson, W. D., Z. Waliuzzaman, I. W. Carter, Y. C. Belessis, K. M. Gilbert & J. R. Morton (2003) Asthma Exacerbations in Children Associated with Rhinovirus but not Human Metapneumovirus Infection. *J Infect Dis*, 187, 1314-8.
- Raza, K., A. Schwenzer, M. Juarez, P. Venables, A. Filer, C. D. Buckley & K. S. Midwood (2016) Detection of Antibodies To Citrullinated Tenascin-C In Patients with Early Synovitis is Associated with the Development of Rheumatoid Arthritis. *RMD Open*, 2, e000318.
- Reddel, R. R., Y. Ke, B. I. Gerwin, M. G. McMenamin, J. F. Lechner, R. T. Su, D. E. Brash, J. B. Park, J. S. Rhim & C. C. Harris (1988) Transformation of Human Bronchial Epithelial-Cells by Infection with SV40 or Adenovirus-12 SV40 Hybrid Virus, or Transfection Via

- Strontium Phosphate Coprecipitation with a Plasmid Containing SV40 Early Region Genes. *Cancer Research*, 48, 1904-1909.
- Redington, A. E., Madden, J., Frew, A. J., Djukanovic, R., Roche, W. R., Holgate, S. T. & Howarth, P. H. (1997). Transforming Growth Factor-Beta 1 In Asthma - Measurement In Bronchoalveolar Lavage Fluid. *American Journal Of Respiratory And Critical Care Medicine*, 156, 642-647.
- Reuter, S., M. Stassen & C. Taube (2010) Mast Cells in Allergic Asthma and Beyond. *Yonsei Medical Journal*, 51, 797-807.
- Riedl, S., A. Tandara, M. Reinshagen, U. Hinz, A. Faissner, H. Bodenmuller, H. J. Buhr, C. Herfarth & P. Moller (2001) Serum Tenascin-C is an Indicator of Inflammatory Bowel Disease Activity. *International Journal of Colorectal Disease*, 16, 285-291.
- Rincon, M. & C. G. Irvin (2012) Role of IL-6 in Asthma and Other Inflammatory Pulmonary Diseases. *International Journal of Biological Sciences*, 8, 1281-1290.
- Robinson, S. M., G. Tsueng, J. Sin, V. Mangale, S. Rahawi, L. L. McIntyre, W. Williams, N. Kha, C. Cruz, B. M. Hancock, D. P. Nguyen, M. R. Sayen, B. J. Hilton, K. S. Doran, A. M. Segall, R. Wolkowicz, C. T. Cornell, J. L. Whitton, R. A. Gottlieb & R. Feuer (2014) Coxsackievirus B Exits the Host Cell in Shed Microvesicles Displaying Autophagosomal Markers. *Plos Pathogens*, 10.
- Roche, W. R., R. Beasley, J. H. Williams & S. T. Holgate (1989) Subepithelial Fibrosis in the Bronchi of Asthmatics. *Lancet*, 1, 520-524.
- Rogers, D. F. (2002) Airway Goblet Cell Hyperplasia in Asthma: Hypersecretory and Anti-Inflammatory? *Clinical and Experimental Allergy*, 32, 1124-1127.
- Royce, S. G., V. Cheng, C. S. Samuel & M. L. K. Tang (2012) The Regulation of Fibrosis in Airway Remodeling in Asthma. *Molecular and Cellular Endocrinology*, 351, 167-175.
- Ruhmann, M., A. M. Piccinini, P. L. Kong & K. S. Midwood (2012) Endogenous Activation of Adaptive Immunity: Tenascin-C Drives Interleukin-17 Synthesis in Murine Arthritic Joint Disease. *Arthritis and Rheumatism*, 64, 2179-2190.
- Rutherford, M. N., G. E. Hannigan & B. R. G. Williams (1988) Interferon-Induced Binding of Nuclear Factors to Promoter Elements of the 2-5a Synthetase Gene. *Embo Journal*, 7, 751-759.
- Saga, Y., T. Tsukamoto, N. H. Jing, M. Kusakabe & T. Sakakura (1991) Murine Tenascin - CDNA Cloning, Structure and Temporal Expression of Isoforms. *Gene*, 104, 177-185.
- Saharinen, J., Hyytiainen, M., Taipale, J. & Keski-Oja, J. (1999). Latent Transforming Growth Factor-Beta Binding Proteins (Ltbps) - Structural Extracellular Matrix Proteins For Targeting Tgf-Beta Action. *Cytokine & Growth Factor Reviews*, 10, 99-117.
- Saito, H., H. Morikawa, K. Howie, L. Crawford, A. J. Baatjes, E. Denburg, M. M. Cyr & J. A. Denburg (2004) Effects of a Cysteinyl Leukotriene Receptor Antagonist on Eosinophil Recruitment in Experimental Allergic Rhinitis. *Immunology*, 113, 246-252.
- Samuel, C. E. (2001) Antiviral Actions of Interferons. *Clinical Microbiology Reviews*, 14, 778-809.
- Sanders, S. P., E. S. Siekierski, J. D. Porter, S. M. Richards & D. Proud (1998) Nitric Oxide Inhibits Rhinovirus-Induced Cytokine Production and Viral Replication in a Human Respiratory Epithelial Cell Line. *Journal of Virology*, 72, 934-942.
- Sano, K., K. Asanuma-Date, F. Arisaka, S. Hattori & H. Ogawa (2007) Changes in Glycosylation of Vitronectin Modulate Multimerization and Collagen Binding During Liver Regeneration. *Glycobiology*, 17, 784-794.
- Sastre, B., J. A. Canas, J. M. Rodrigo-Munoz & V. del Pozo (2017) Novel Modulators of Asthma and Allergy: Exosomes and microRNAs. *Frontiers in Immunology*, 8.
- Saura, M., C. Zaragoza, A. McMillan, R. A. Quick, C. Hohenadl, J. M. Lowenstein & C. J. Lowenstein (1999) An Antiviral Mechanism of Nitric Oxide: Inhibition of a Viral Protease. *Immunity*, 10, 21-28.
- Schall, T. J., K. Bacon, K. J. Toy & D. V. Goeddel (1990) Selective Attraction of Monocytes and Lymphocytes-T of the Memory Phenotype by Cytokine RANTES. *Nature*, 347, 669-671.
- Schroder, K., K. M. Irvine, M. S. Taylor, N. J. Bokil, K. A. L. Cao, K. A. Masterman, L. I. Labzin, C. A. Semple, R. Kapetanovic, L. Fairbairn, A. Akalin, G. J. Faulkner, J. K. Baillie, M. Gongora, C. O. Daub, H. Kawaji, G. J. McLachlan, N. Goldman, S. M. Grimmond, P. Carninci, H. Suzuki, Y. Hayashizaki, B. Lenhard, D. A. Hume & M. J. Sweet (2012) Conservation and Divergence in Toll-Like Receptor 4-Regulated Gene Expression in Primary Human Versus Mouse Macrophages. *Proceedings of the National Academy of Sciences of the United States of America*, 109, E944-E953.

- Schuler, B. A., M. T. Schreiber, L. Li, M. Mokry, M. L. Kingdon, D. N. Raugi, C. Smith, C. Hameister, V. R. Racaniello & D. J. Hall (2014) Major and Minor Group Rhinoviruses Elicit Differential Signaling and Cytokine Responses as a Function of Receptor-Mediated Signal Transduction. *Plos One*, 9.
- Schulz, C., L. Farkas, K. Wolf, K. Kratzel, G. Eissner & M. Pfeifer (2002) Differences in LPS-Induced Activation of Bronchial Epithelial Cells (BEAS-2B) and Type II-Like Pneumocytes (A-549). *Scandinavian Journal of Immunology*, 56, 294-302.
- Schulz, O., A. Pichlmair, J. Rehwinkel, N. C. Rogers, D. Scheuner, H. Kato, O. Takeuchi, S. Akira, R. J. Kaufman & C. R. E. Sousa (2010) Protein Kinase R Contributes to Immunity against Specific Viruses by Regulating Interferon mRNA Integrity. *Cell Host & Microbe*, 7, 354-361.
- Schwenzer, A., X. Jiang, T. R. Mikuls, J. B. Payne, H. R. Sayles, A. M. Quirke, B. M. Kessler, R. Fischer, P. J. Venables, K. Lundberg & K. S. Midwood (2016) Identification of an Immunodominant Peptide from Citrullinated Tenascin-C as a Major Target for Autoantibodies in Rheumatoid Arthritis. *Annals of the Rheumatic Diseases*, 75, 1876-1883.
- Scudieri, P., E. Caci, S. Bruno, L. Ferrera, M. Schiavon, E. Sondo, V. Tomati, A. Gianotti, O. Zegarra-Moran, N. Pedemonte, F. Rea, R. Ravazzolo & L. J. V. Galletta (2012) Association of TMEM16A Chloride Channel Overexpression with Airway Goblet Cell Metaplasia. *Journal of Physiology-London*, 590, 6141-6155.
- Sears, M. R. (2014) Trends in the Prevalence of Asthma. *Chest*, 145, 219-225.
- Senftleben, U., Y. X. Cao, G. T. Xiao, F. R. Greten, G. Krahn, G. Bonizzi, Y. Chen, Y. L. Hu, A. Fong, S. C. Sun & M. Karin (2001) Activation by IKK alpha of a Second, Evolutionary Conserved, NF-kappa B Signaling Pathway. *Science*, 293, 1495-1499.
- Seth, R. B., L. Sun, C. K. Ea & Z. J. Chen (2005) Identification and Characterization of MAVS, a Mitochondrial Antiviral Signaling Protein that Activates NF-kappaB and IRF3. *Cell*, 122, 669-82.
- Sha, Q., A. Q. Truong-Tran, J. R. Plitt, L. A. Beck & R. P. Schleimer (2004) Activation of Airway Epithelial Cells by Toll-Like Receptor Agonists. *American Journal of Respiratory Cell and Molecular Biology*, 31, 358-364.
- Shao, H. S., J. M. Kirkwood & A. Wells (2015) Tenascin-C Signaling in Melanoma. *Cell Adhesion & Migration*, 9, 125-130.
- Shimojo, N., R. Hashizume, K. Kanayama, M. Hara, Y. Suzuki, T. Nishioka, M. Hiroe, T. Yoshida & K. Imanaka-Yoshida (2015) Tenascin-C May Accelerate Cardiac Fibrosis by Activating Macrophages via the Integrin alpha V beta 3/NuclearFactor-kappa B/Interleukin-6 Axis. *Hypertension*, 66, 757-766.
- Silacci, M., S. S. Brack, N. Spath, A. Buck, S. Hillinger, S. Arni, W. Weder, L. Zardi & D. Neri (2006) Human Monoclonal Antibodies to Domain C of Tenascin-C Selectively Target Solid Tumors In Vivo. *Protein Engineering Design & Selection*, 19, 471-478.
- Singeton, R. J., L. R. Bulkow, K. Miernyk, C. DeByle, L. Pruitt, K. B. Hummel, D. Bruden, J. A. Englund, L. J. Anderson, L. Lucher, R. C. Holman & T. W. Hennessy (2010) Viral Respiratory Infections in Hospitalized and Community Control Children in Alaska. *Journal of Medical Virology*, 82, 1282-1290.
- Siri, A., V. Knauper, N. Veirana, F. Caocci, G. Murphy & L. Zardi (1995) Different Susceptibility of Small and Large Human Tenascin-C Isoforms to Degradation by Matrix Metalloproteinases. *Journal of Biological Chemistry*, 270, 8650-8654.
- Slater, L., N. W. Bartlett, J. J. Haas, J. Zhu, S. D. Message, R. P. Walton, A. Sykes, S. Dahdaleh, D. L. Clarke, M. G. Belvisi, O. M. Kon, T. Fujita, P. K. Jeffery, S. L. Johnston & M. R. Edwards (2010) Co-Ordinated Role of TLR3, RIG-I and MDA5 in the Innate Response to Rhinovirus in Bronchial Epithelium. *Plos Pathogens*, 6.
- Snyers, L., H. Zwickl & D. Blaas (2003) Human Rhinovirus Type 2 is Internalized by Clathrin-Mediated Endocytosis. *Journal of Virology*, 77, 5360-5369.
- Soini, Y., D. Kamel, M. Apajasarkkinen, I. Virtanen & V. P. Lehto (1993) Tenascin Immunoreactivity in Normal and Pathological Bone-Marrow. *Journal of Clinical Pathology*, 46, 218-221.
- Stack, J., S. L. Doyle, D. J. Connolly, L. S. Reinert, K. M. O'Keeffe, R. M. McLoughlin, S. R. Paludan & A. G. Bowie (2014) TRAM Is Required for TLR2 Endosomal Signaling to Type I IFN Induction. *Journal of Immunology*, 193, 6090-6102.
- Steentoft, C., S. Y. Vakhrushev, H. J. Joshi, Y. Kong, M. B. Vester-Christensen, K. Schjoldager, K. Lavrsen, S. Dabelsteen, N. B. Pedersen, L. Marcos-Silva, R. Gupta, E. P. Bennett,

- U. Mandel, S. Brunak, H. H. Wandall, S. B. Lavery & H. Clausen (2013) Precision Mapping of the Human O-GalNAc Glycoproteome Through SimpleCell Technology. *Embo Journal*, 32, 1478-1488.
- Stewart, C. E., E. E. Torr, N. H. Mohd Jamili, C. Bosquillon & I. Sayers (2012) Evaluation of Differentiated Human Bronchial Epithelial Cell Culture Systems for Asthma Research. *Journal of allergy*, 2012, 943982-943982.
- Stokes, C. A., S. Ismail, E. P. Dick, J. A. Bennett, S. L. Johnston, M. R. Edwards, I. Sabroe & L. C. Parker (2011) Role of Interleukin-1 and MyD88-Dependent Signaling in Rhinovirus Infection. *Journal of Virology*, 85, 7912-7921.
- Stokes, C. A., R. Kaur, M. R. Edwards, M. Mondhe, D. Robinson, E. C. Prestwich, R. D. Hume, C. A. Marshall, Y. Perrie, V. B. O'Donnell, J. L. Harwood, I. Sabroe & L. C. Parker (2016) Human Rhinovirus-Induced Inflammatory Responses are Inhibited by Phosphatidylserine Containing Liposomes. *Mucosal Immunology*, 9, 1303-1316.
- Subbarao, P. & F. Ratjen (2006) beta(2)-Agonists for Asthma - The Pediatric Perspective. *Clinical Reviews in Allergy & Immunology*, 31, 209-218.
- Sykes, A., M. R. Edwards, J. Macintyre, A. del Rosario, E. Bakhsoliani, M. B. Trujillo-Torralbo, O. M. Kon, P. Mallia, M. McHale & S. L. Johnston (2012) Rhinovirus 16-Induced IFN-alpha and IFN-beta are Deficient in Bronchoalveolar Lavage Cells in Asthmatic Patients. *Journal of Allergy and Clinical Immunology*, 129, 1506-+.
- Sykes, A., J. Macintyre, M. R. Edwards, A. del Rosario, J. Haas, V. Gielen, O. M. Kon, M. McHale & S. L. Johnston (2014) Rhinovirus-Induced Interferon Production is not Deficient in Well Controlled Asthma. *Thorax*, 69, 240-246.
- Szatanek, R., Baj-Krzyworzeka, M., Zimoch, J., Lekka, M., Siedlar, M. & Baran, J. (2017). The Methods Of Choice For Extracellular Vesicles (Evs) Characterization. *International Journal Of Molecular Sciences*, 18.
- Szul, T., P. E. Bratcher, K. B. Fraser, M. Kong, R. Tirouvanziam, S. Ingersoll, E. Sztul, S. Rangarajan, J. E. Blalock, X. Xu & A. Gaggar (2016) Toll-Like Receptor 4 Engagement Mediates Prolyl Endopeptidase Release from Airway Epithelia via Exosomes. *American Journal of Respiratory Cell and Molecular Biology*, 54, 359-369.
- Takei, K. & V. Haucke (2001) Clathrin-Mediated Endocytosis: Membrane Factors Pull the Trigger. *Trends in Cell Biology*, 11, 385-391.
- Takeuchi, O. & S. Akira (2009) Innate Immunity to Virus Infection. *Immunological Reviews*, 227, 75-86.
- Tan, S. S., K. L. Crossin, S. Hoffman & G. M. Edelman (1987) Asymmetric Expression in Somites of Cytotactin and its Proteoglycan Ligand is Correlated with Neural Crest Cell Distribution. *Proceedings of the National Academy of Sciences of the United States of America*, 84, 7977-7981.
- Tang, F. S. M., D. Van Ly, K. Spann, P. C. Reading, J. K. Burgess, D. Hartl, K. J. Baines & B. G. Oliver (2016) Differential Neutrophil Activation in Viral Infections: Enhanced TLR-7/8-Mediated CXCL8 Release in Asthma. *Respirology*, 21, 172-179.
- Tang, Y. T., Y. Y. Huang, L. Zheng, S. H. Qin, X. P. Xu, T. X. An, Y. Xu, Y. S. Wu, X. M. Hu, B. H. Ping & Q. Wang (2017) Comparison of Isolation Methods of Exosomes and Exosomal RNA from Cell Culture Medium and Serum. *International Journal of Molecular Medicine*, 40, 834-844.
- Taylor, H. C., V. A. Lightner, W. F. Beyer, D. McCaslin, G. Briscoe & H. P. Erickson (1989) Biochemical and Structural Studies of Tenascin Hexabrachion Proteins. *Journal of Cellular Biochemistry*, 41, 71-90.
- Thomas, P. S. & G. Heywood (2002) Effects of Inhaled Tumour Necrosis Factor alpha in Subjects with Mild Asthma. *Thorax*, 57, 774-778.
- Tian, Y. X., M. V. Kuzimenkova, J. Halle, M. Wojdyr, A. D. D. Mendaza, P. O. Larsson, C. Muller & I. G. Scheblykin (2015) Molecular Weight Determination by Counting Molecules. *Journal of Physical Chemistry Letters*, 6, 923-927.
- To, T., S. Stanojevic, G. Moores, A. S. Gershon, E. D. Bateman, A. A. Cruz & L.-P. Boulet (2012) Global Asthma Prevalence in Adults: Findings from the Cross-Sectional World Health Survey. *Bmc Public Health*, 12.
- Triantafilou, K., E. Vakakis, E. A. J. Richer, G. L. Evans, J. P. Villiers & M. Triantafilou (2011) Human Rhinovirus Recognition in Non-Immune Cells is Mediated by Toll-Like Receptors and MDA-5, which Trigger a Synergetic Pro-Inflammatory Immune Response. *Virulence*, 2, 22-29.

- Tseloni-Balafouta, S., H. Gakiopoulou, G. Fanourakis, G. Voutsinas, D. Balafoutas & E. Patsouris (2006) Tenascin-C Protein Expression and mRNA Splice Variants in Thyroid Carcinoma. *Experimental and Molecular Pathology*, 80, 177-182.
- Tsunoda, T., H. Inada, I. Kalembeyi, K. Imanaka-Yoshida, M. Sakakibara, R. Okada, K. Katsuta, T. Sakakura, Y. Majima & T. Yoshida (2003) Involvement of Large Tenascin-C Splice Variants in Breast Cancer Progression. *American Journal of Pathology*, 162, 1857-1867.
- Tucker, R. P. (2001) Abnormal Neural Crest Cell Migration After the in Vivo Knockdown of Tenascin-C Expression with Morpholino Antisense Oligonucleotides. *Developmental Dynamics*, 222, 115-119.
- Tucker, R. P. & R. Chiquet-Ehrismann (2009) The Regulation of Tenascin Expression by Tissue Microenvironments. *Biochimica Et Biophysica Acta-Molecular Cell Research*, 1793, 888-892.
- Tucker, R. P., J. A. Hammarback, D. A. Jenrath, E. J. Mackie & Y. Xu (1993) Tenascin Expression in the Mouse: In Situ Localization and Induction In Vitro by bFGF. *J Cell Sci*, 104 (Pt 1), 69-76.
- Valadi, H., K. Ekstrom, A. Bossios, M. Sjostrand, J. J. Lee & J. O. Lotvall (2007) Exosome-Mediated Transfer of mRNAs and microRNAs is a Novel Mechanism of Genetic Exchange Between Cells. *Nature Cell Biology*, 9, 654-U72.
- Vanoverveld, F. J., P. G. Jorens, M. Rampart, W. Debacker & P. A. Vermeiere (1991) Tumor-Necrosis-Factor Stimulates Human Skin Mast-Cells to Release Histamine and Tryptase. *Clinical and Experimental Allergy*, 21, 711-714.
- Vareille, M., E. Kieninger, M. R. Edwards & N. Regamey (2011) The Airway Epithelium: Soldier in the Fight Against Respiratory Viruses (vol 24, pg 210, 2011). *Clinical Microbiology Reviews*, 24, 631-631.
- Vaure, C. & Y. Q. Liu (2014) A Comparative Review of Toll-Like Receptor 4 Expression and Functionality in Different Animal Species. *Frontiers in Immunology*, 5.
- Verdera, H. C., J. J. Gitz-Francois, R. M. Schiffelers & P. Vader (2017) Cellular Uptake of Extracellular Vesicles is Mediated by Clathrin-Independent Endocytosis and Macropinocytosis. *Journal of Controlled Release*, 266, 100-108.
- Verderio, C., L. Muzio, E. Turola, A. Bergami, L. Novellino, F. Ruffini, L. Riganti, I. Corradini, M. Francolini, L. Garzetti, C. Maiorino, F. Servida, A. Vercelli, M. Rocca, D. Dalla Libera, V. Martinelli, G. Comi, G. Martino, M. Matteoli & R. Furlan (2012) Myeloid Microvesicles are a Marker and Therapeutic Target for Neuroinflammation. *Annals of Neurology*, 72, 610-624.
- Vermeer, P. D., R. Harson, L. A. Einwalter, T. Moninger & J. Zabner (2003) Interleukin-9 Induces Goblet Cell Hyperplasia During Repair of Human Airway Epithelia. *American Journal of Respiratory Cell and Molecular Biology*, 28, 286-295.
- Victoni, T., H. Salvator, C. Abrial, M. Brollo, L. C. S. Porto, V. Lagente, E. Naline, S. Grassin-Delyle & P. Devillier (2017) Human Lung and Monocyte-Derived Macrophages Differ with Regard to the Effects of beta(2)-Adrenoceptor Agonists on Cytokine Release. *Respiratory Research*, 18.
- Vlassov, A. V., S. Magdaleno, R. Setterquist & R. Conrad (2012) Exosomes: Current Knowledge of their Composition, Biological Functions, and Diagnostic and Therapeutic Potentials. *Biochimica Et Biophysica Acta-General Subjects*, 1820, 940-948.
- Vollmer, G., M. I. Tan, W. Wunsche & K. Frank (1997) Expression of Tenascin-C by Human Endometrial Adenocarcinoma and Stroma Cells: Heterogeneity of Splice Variants and Induction by TGF-beta. *Biochemistry and Cell Biology-Biochimie Et Biologie Cellulaire*, 75, 759-769.
- Wallner, K., C. Li, P. K. Shah, K. J. Wu, S. M. Schwartz & B. G. Sharifi (2004) EGF-Like Domain of Tenascin-C is Proapoptotic for Cultured Smooth Muscle Cells. *Arteriosclerosis Thrombosis and Vascular Biology*, 24, 1416-1421.
- Wang, H. Y., T. Elston, A. Mogilner & G. Oster (1998) Force Generation in RNA Polymerase. *Biophysical Journal*, 74, 1186-1202.
- Wang, P., P. Wu, M. I. Siegel, R. W. Egan & M. M. Billah (1995) Interleukin (IL)-10 Inhibits Nuclear Factor kappa-B (Nf-Kappa-B) Activation in Human Monocytes - IL-10 And IL-4 Suppress Cytokine Synthesis by Different Mechanisms. *Journal of Biological Chemistry*, 270, 9558-9563.
- Wang, Q., D. R. Nagarkar, E. R. Bowman, D. Schneider, B. Gosangi, J. Lei, Y. Zhao, C. L. McHenry, R. V. Burgens, D. J. Miller, U. Sajjan & M. B. Hershenson (2009) Role of

- Double-Stranded RNA Pattern Recognition Receptors in Rhinovirus-Induced Airway Epithelial Cell Responses. *Journal of Immunology*, 183, 6989-6997.
- Wang, Y., Liu, J., Huang, B., Xu, Y. M., Li, J., Huang, L. F., Lin, J., Zhang, J., Min, Q. H., Yang, W. M. & Wang, X. Z. (2015). Mechanism Of Alternative Splicing And Its Regulation. *Biomedical Reports*, 3, 152-158.
- Wang, X. J., R. Wilkinson, K. Kildey, J. Potriquet, J. Mulvenna, R. J. Lobb, A. Moller, N. Cloonan, P. Mukhopadhyay, A. J. Kassianos & H. Healy (2017) Unique Molecular Profile of Exosomes Derived from Primary Human Proximal Tubular Epithelial Cells Under Diseased Conditions. *Journal of Extracellular Vesicles*, 6.
- Wark, P. A. B., S. L. Johnston, F. Bucchieri, R. Powell, S. Puddicombe, V. Laza-Stanca, S. T. Holgate & D. E. Davies (2005) Asthmatic Bronchial Epithelial Cells have a Deficient Innate Immune Response to Infection with Rhinovirus. *Journal of Experimental Medicine*, 201, 937-947.
- Wark, P. A. B., S. L. Johnston, I. Moric, J. L. Simpson, M. J. Hensley & P. G. Gibson (2002) Neutrophil Degranulation and Cell Lysis is Associated with Clinical Severity in Virus-Induced Asthma. *European Respiratory Journal*, 19, 68-75.
- Watanabe, G., H. Nishimori, H. Irifune, Y. Sasaki, S. Ishida, H. Zembutsu, T. Tanaka, S. Kawaguchi, T. Wada, J. Hata, M. Kusakabe, K. Yoshida, Y. Nakamura & T. Tokino (2003) Induction of Tenascin-C by Tumor-Specific EWS-ETS Fusion Genes. *Genes Chromosomes & Cancer*, 36, 224-232.
- Wenzel, S. E. (2012) Asthma Phenotypes: the Evolution from Clinical to Molecular Approaches. *Nature Medicine*, 18, 716-725.
- White, M. V. (1990) The Role of Histamine in Allergic Diseases. *Journal of Allergy and Clinical Immunology*, 86, 599-605.
- Whitton, J. L., C. T. Cornell & R. Feuer (2005) Host and Virus Determinants of Picornavirus Pathogenesis and Tropism. *Nature Reviews Microbiology*, 3, 765-776.
- Williams, B. R. (2001) Signal Integration via PKR. *Sci STKE*, 2001, re2.
- Williams, B. R. G. (1999) PKR; a Sentinel Kinase for Cellular Stress. *Oncogene*, 18, 6112-6120.
- Willms, E., H. J. Johansson, I. Mager, Y. Lee, K. E. M. Blomberg, M. Sadik, A. Alaarg, C. I. E. Smith, J. Lehtio, S. E. L. Andaloussi, M. J. A. Wood & P. Vader (2016) Cells Release Subpopulations of Exosomes with Distinct Molecular and Biological Properties. *Scientific Reports*, 6.
- Winther, B. (2011) Rhinovirus Infections in the Upper Airway. *Proc Am Thorac Soc*, 8, 79-89.
- Witwer, K. W., C. Soekmadji, A. F. Hill, M. H. Wauben, E. I. Buzas, D. Di Vizio, J. M. Falcon-Perez, C. Gardiner, F. Hochberg, I. V. Kurochkin, J. Lotvall, S. Mathivanan, R. Nieuwland, S. Sahoo, H. Tahara, A. C. Torrecilhas, A. M. Weaver, H. Yin, L. Zheng, Y. S. Ghossein, P. Quesenberry & C. Thery (2017) Updating the MISEV Minimal Requirements for Extracellular Vesicle Studies: Building Bridges to Reproducibility. *Journal of Extracellular Vesicles*, 6.
- Wu, Q., D. Jiang, C. J. Huang, L. F. van Dyk, L. W. Li & H. W. Chu (2015) Trehalose-Mediated Autophagy Impairs the Anti-Viral Function of Human Primary Airway Epithelial Cells. *Plos One*, 10.
- Wu, Q., L. F. van Dyk, D. Jiang, A. Dakhama, L. W. Li, S. R. White, A. Gross & H. W. Chu (2013) Interleukin-1 Receptor-Associated Kinase M (IRAK-M) Promotes Human Rhinovirus Infection in Lung Epithelial Cells via the Autophagic Pathway. *Virology*, 446, 199-206.
- Yagi, H., M. Yanagisawa, Y. Suzuki, Y. Nakatani, T. Ariga, K. Kato & R. K. Yu (2010) HNK-1 Epitope-Carrying Tenascin-C Spliced Variant Regulates the Proliferation of Mouse Embryonic Neural Stem Cells. *Journal of Biological Chemistry*, 285, 37293-37301.
- Yamashita, M., H. Fukui, K. Sugama, Y. Horio, S. Ito, H. Mizuguchi & H. Wada (1991) Expression Cloning of a cDNA-Encoding the Bovine Histamine-H1 Receptor. *Proceedings of the National Academy of Sciences of the United States of America*, 88, 11515-11519.
- Yang, M. L., C. T. Wang, S. J. Yang, C. H. Leu, S. H. Chen, C. L. Wu & A. L. Shiau (2017) IL-6 Ameliorates Acute Lung Injury in Influenza Virus Infection. *Scientific Reports*, 7.
- Yang, Z. T., S. Y. Yeo, Y. X. Yin, Z. H. Lin, H. M. Lee, Y. H. Xuan, Y. Cui & S. H. Kim (2016) Tenascin-C, a Prognostic Determinant of Esophageal Squamous Cell Carcinoma. *Plos One*, 11.

- Yoffe, A. M., P. Prinsen, A. Gopal, C. M. Knobler, W. M. Gelbart & A. Ben-Shaul (2008) Predicting the Sizes of Large RNA Molecules. *Proceedings of the National Academy of Sciences of the United States of America*, 105, 16153-16158.
- Yokoyama, A., N. Kohno, S. Fujino, H. Hamada, Y. Inoue, S. Fujioka, S. Ishida & K. Hiwada (1995) Circulating Interleukin-6 Levels in Patients with Bronchial-Asthma. *American Journal of Respiratory and Critical Care Medicine*, 151, 1354-1358.
- Yokoyama, A., N. Kohno, K. Sakai, K. I. Kondo, Y. Hirasawa & K. Hiwada (1997) Circulating Levels of Soluble Interleukin-6 Receptor in Patients with Bronchial Asthma. *American Journal of Respiratory and Critical Care Medicine*, 156, 1688-1691.
- Yue, F., Y. Cheng, A. Breschi, J. Vierstra, W. S. Wu, T. Ryba, R. Sandstrom, Z. H. Ma, C. Davis, B. D. Pope, Y. Shen, D. D. Pervouchine, S. Djebali, R. E. Thurman, R. Kaul, E. Rynes, A. Kirilusha, G. K. Marinov, B. A. Williams, D. Trout, H. Amrhein, K. Fisher-Aylor, I. Antoshechkin, G. DeSalvo, L. H. See, M. Fastuca, J. Drenkow, C. Zaleski, A. Dobin, P. Prieto, J. Lagarde, G. Bussotti, A. Tanzer, O. Denas, K. W. Li, M. A. Bender, M. H. Zhang, R. Byron, M. T. Groudine, D. McCleary, L. Pham, Z. Ye, S. Kuan, L. Edsall, Y. C. Wu, M. D. Rasmussen, M. S. Bansal, M. Kellis, C. A. Keller, C. S. Morrissey, T. Mishra, D. Jain, N. Dogan, R. S. Harris, P. Cayting, T. Kawli, A. P. Boyle, G. Euskirchen, A. Kundaje, S. Lin, Y. Lin, C. Jansen, V. S. Malladi, M. S. Cline, D. T. Erickson, V. M. Kirkup, K. Learned, C. A. Sloan, K. R. Rosenbloom, B. L. De Sousa, K. Beal, M. Pignatelli, P. Flicek, J. Lian, T. Kahveci, D. Lee, W. J. Kent, M. R. Santos, J. Herrero, C. Notredame, A. Johnson, S. Vong, K. Lee, D. Bates, F. Neri, M. Diegel, T. Canfield, P. J. Sabo, M. S. Wilken, T. A. Reh, E. Giste, A. Shafer, T. Kutayavin, E. Haugen, D. Dunn, A. P. Reynolds, S. Neph, R. Humbert, R. S. Hansen, M. De Bruijn, et al. (2014) A Comparative Encyclopedia of DNA Elements in the Mouse Genome. *Nature*, 515, 355-+.
- Zanini, A., A. Chetta, A. S. Imperatori, A. Spanevello & D. Olivieri (2010) The Role of the Bronchial Microvasculature in the Airway Remodelling in Asthma and COPD. *Respiratory Research*, 11.
- Zhang, W. C., X. F. Jiang, J. H. Bao, Y. Wang, H. X. Liu & L. J. Tang (2018) Exosomes in Pathogen Infections: A Bridge to Deliver Molecules and Link Functions. *Frontiers in Immunology*, 9.
- Zhao, F. & W. T. Klimecki (2015) Culture Conditions Profoundly Impact Phenotype in BEAS-2B, a Human Pulmonary Epithelial Model. *Journal of Applied Toxicology*, 35, 945-951.
- Zhao, Y. & S. L. Young (1995) TGF-beta Regulates Expression of Tenascin Alternative-Splicing Isoforms in Fetal-Rat Lung. *American Journal of Physiology-Lung Cellular and Molecular Physiology*, 268, L173-L180.
- Zhu, Z., W. L. Tang, A. Ray, Y. Wu, O. Einarsson, M. L. Landry, J. Gwaltney & J. A. Elias (1996) Rhinovirus Stimulation of Interleukin-6 In Vivo and In Vitro - Evidence for Nuclear Factor KB-Dependent Transcriptional Activation. *Journal of Clinical Investigation*, 97, 421-430.
- Zisch, A. H., L. Dalessandri, B. Ranscht, R. Falchetto, K. H. Winterhalter & L. Vaughan (1992) Neuronal Cell-Adhesion Molecule Contactin F11 Binds to Tenascin Via its Immunoglobulin-Like Domains. *Journal of Cell Biology*, 119, 203-213.
- Zuliani-Alvarez, L., A. M. Marzeda, C. Deligne, A. Schwenger, F. E. McCann, B. D. Marsden, A. M. Piccinini & K. S. Midwood (2017) Mapping Tenascin-C Interaction with Toll-Like Receptor 4 Reveals a New Subset of Endogenous Inflammatory Triggers. *Nature Communications*, 8.

Websites

Truman, D., Woodcock, F., Hancock, E., (2017) Estimating the Economic Burden of Respiratory Illness in the UK, last viewed 31/08/2018, <https://www.blf.org.uk/policy/economic-burden>

TNC tenascin C [*Homo sapiens* (human)] homologene, last viewed 31/08/18 www.ncbi.nlm.nih.gov/homologene